Carotenoid biosynthesis and metabolism in potato tubers

Adriana Stefania Pasare

A Thesis Submitted for the Degree of Doctor of Philosophy

Royal Holloway College, University of London

November 2012

Declaration of Authorship

I hereby declare that the present thesis is of my own composition and based on the results of work conducted by myself. The results reported here have not, in whole or in part, been previously presented for a higher degree or qualification. For investigations other than my own, there is a clear indication in the text by reference to the relevant workers or their publications.

Adriana Stefania Pasare

Acknowledgements

I would like to start by quoting Marie Curie, who said ‘I am among those who think that science has great beauty. A scientist in his laboratory is not only a technician: he is also a child placed before natural phenomena which impress him like a fairy tale’. It is a pleasure to thank all of those who made this thesis possible, thus giving me the opportunity to scientifically explore cellular processes and be humbly impressed with the correlations established by nature. I am heartily thankful to my supervisors, Mark Taylor, Alison Roberts, Paul Fraser and Peter Bramley, whose encouragement, guidance and support from the initial to the final level enabled me to develop a subject I am passionate about. Also, I would like to thank Kath Wright, Ray Campbell, Wayne Morris and Sean Chapman, for their constant support and helpful technical advice, but also all other JHI collaborating staff.

Lastly, I can but offer my love and blessings to all my family, who have always believed in me, encouraging me through my years of study. Thank you, Mami, Oana, George, Johnny and my dear loving husband, Ionut.

Abstract

Potato tuber flesh colour is a quality trait dependent on the types and levels of carotenoids. These, together with many plant growth regulators, sterols and terpenes, are isoprenoid derived compounds. Even though carotenoids have been extensively studied due to their importance in photosynthesis and nutrition, a clear understanding concerning the regulation of their accumulation and localisation in plant storage organs is lacking. The present study describes two strategies to investigate the regulation of carotenoid biosynthesis in potato. Firstly, in order to localise the site of synthesis of tuber carotenoids, stable transgenic potato plants were generated. These expressed two key carotenoid biosynthetic genes, *PHYTOENE SYNTHASE 2* (*PSY2*) and *β-CAROTENE HYDROXYLASE 2* (*CrtRb2*), fused to red fluorescent protein (RFP). The expression and carotenoid levels were significantly increased, confirming functionality of the protein-RFP ensembles. Confocal microscopy on developing tuber tissue made it possible to obtain images of PSY2-RFP and CrtRb2-RFP localisation into amyloplasts. Secondly, the effect of carotenoid degradation was addressed as a potential regulator of accumulation, based on the recent discovery that a *CAROTENOID CLEAVAGE DIOXYGENASE 4* (*CCD4*) reduces carotenoid levels in potato tubers. *CCD8* is another important member of the *CCD* gene family, with a role in strigolactone biosynthesis. In this study, *CCD8*-RNAi knock out lines were characterised. Although *CCD8* down-regulation did not significantly affect carotenoid content, a range of interesting above and below ground phenotypes was observed. Importantly, the study showed that the *CCD8* gene product impacts on stolon branching, tuber development and tuber dormancy.

Table of contents

List of figures

List of tables

List of abbreviations

%	percent
α	alpha
β	beta
Δ	delta
ε	epsilon
Ω	Ohms (electrical resistance)
ζ	zeta
°C	degrees centigrade
µF	microfarad
µl	microlitre
µm	micrometre
µM	micromolar
µmol	micromol
3D	three dimensional
A	absorbance
ABA	abscisic acid
ABRE-CE	ABA Response Element–Coupling Element
AcCCD8	*Actinidia chinensis* CCD8
AM	arbuscular mycorrhizal
Amp	ampicillin
Ant	antheraxanthin
AtCCD8	*Arabidopsis thaliana* CCD8

AtPSY	*Arabidopsis thaliana* PSY
AtRAP2.2	*Arabidopsis thaliana* APETALA2.2 ethylene responsive gene
AVI	anthocyanin vacuolar inclusion
BCH	beta carotene hydroxylase
BdCCD8	*Brachypodium distanchyon* CCD8
bkt1	algal ketolase
Bluo-gal	halogenated indolyl-β-galactosidase
bp	base pairs
B-B33-pK7R	*CrtRb2* under control of B33 prmoter, in pK7RWG2
B-pGEN	*CrtRb2* in pGENTR1a
B-pK7F	*CrtRb2* in pK7FWG2
B-pK7R	*CrtRb2* in pK7RWG2
ca.	*circa*
CaMV	*Cauliflower Mosaic Virus*
CCD	carotenoid cleavage dioxygenase
ccdB	control of cell death, cytotoxic gene
cDNA	complementary DNA
*Cr*GGPS	*Catharanthus rosa* GGPS
CHY	non heme β-ring hydroxylase
CK	cytokinin
CLSM	confocal laser scanning microscope
COP1	*CONSTITUTIVE PHOTOMORPHOGENESIS1*

cm	centimetre
CmCCD	*Chysanthemum moriflorium CCD*
crtB	*Erwinia uredovora* PSY
crtI	*Erwinia uredovora* PDS
CrtRb2	beta carotene hydroxylase 2
CRTISO	carotenoid isomerase
CRTL-b	beta carotene hydroxylase
CRTL-e	ε-ring hydroxylase
crtY	lycopene cyclase
crtZ	*Erwinia uredovora* β-carotene hydroxylase
cTP	length is the predicted length of the presequence
CsCCD	*Crocus sativus CCD*
CsZCD	*Crocus sativus* zeaxanthin-specific cleavage dioxygenase
cv.	cultivar
CYP	cytochrome P450 type enzymes
dad	*decreased apical dominance*
DDB1	UV-damaged DNA binding protein 1
DET1	de-etiolated 1
$DiOC_6$	dihexyloxacarbocyanine iodide
DMAPP	dimethylallyl pyrophosphate
DMSO	dimethylsulphoxide
DNA	deoxyribonucleic acid
DNase	deoxyribonuclease

dNTP	deoxyribonucleotide triphosphate
dpi	days post inoculation
DTT	dithiothreitol
DW	dry weight
DXP	1-deoxy D-xylulose 5-phosphate
DXR	1-deoxy D-xylulose 5-phosphate reductoisomerase
DXS	1-deoxyxylulose-5-phosphate synthase
E	extinction coefficient
E. coli	*Escherichia coli*
EF1α	*Elongation factor 1 alpha*
EDTA	ethylenediaminetetra acetic acid
eOH	ε-hydroxylase
EST	expressed sequence tag
et al.	and others
EV	empty vector
FAO	Food and Agriculture Organisation of the United Nations
FT	*Flowering locus T*
FW	fresh weight
g	acceleration due to gravity
g	gram
GA	gibberellin
gen	gentamycin

GFP	green fluorescent protein
GGPP	geranylgeranyl diphosphate
GGPS	geranylgeranyl diphosphate synthase
GmCCD8	*Glycine max* CCD8
GR24	growth response factor 24
h	hour
H_2O	water
hp	*high pigment*
HPLC	high performance liquid chromatography
htd	*high tillering dwarf*
HYD	non-heme di-iron beta-carotene hydroxylase
HY5	elongated hypocotyl 5
IAA	indole acetic acid
IDI	IPP isomerase
IPP	isopentenyl pyrophosphate
IPTG	isopropyl-β-D-thiogalactopyranoside
JHI	James Hutton Institute
kan	kanamycin
kb	kilobase pairs
KCl	potassium chloride
kg	kilogram
kV	kilovolts

l	litre
LB	Luria Bertani
LCY	lycopene cylase
LiCl	lithium chloride
LHC	light-harvesting complex
lut	lutein
m	metre
M	molar
max	*more axillary growth*
MCS	multi cloning site
MEP	2-C-methyl-D-erythritol 4-phosphate
mg	milligram
$MgCl_2$	magnesium chloride
$MgSO_4$	magnesium sulphate
min	minute
mm	milimetre
MOPS	3-morpholinopropane-1-sulfonic acid
mRNA	messenger RNA
MS	Murashige Skoog
MtCCD8	*Medicago truncatula* CCD8
MVA	mevalonic acid
n	number of replicates

NAA	naphthalene acetic acid
NaCl	sodium chloride
NaOAc	sodium acetate
NaOH	sodium hydroxide
NCED	9-*cis*-epoxycarotenoid dioxygenase
neo	neoxanthin
ng	nanogram
nm	nanometre
NPQ	non-photochemical quenching
NXS	neoxanthin synthase
OD	optical density
OEM	outer envelope membrane
Or	cauliflower *orange* mutant
ori	*origin of replication*
OsCCD8	*Oryza sativa* CCD8
P450	phytochrome 450
PAT	polar auxin transport
PB33	patatin B33 promoter
P-B33-pK7R	*PSY2* under control of B33 promoter, in pK7RWG2
PCR	polymerase chain reaction
PDS	phytoene desaturase
PG	plastoglobules

PTGS	post-transcriptional gene silencing
pH	-log [H^+]
PhCCD8	*Petunia hybrida CCD8*
PIFs	phytochrome-interaction factors
PIN	PIN-FORMED efflux carrier
P-pGEN	PSY in pGENTR1a
P-pK7F	PSY in pK7FWG2
P-pK7R	PSY in pK7RWG2
PsCCD8	*Pisum sativum* CCD8
PSY2	phytoene synthase 2
PtCCD8	*Populus trichocarpa* CCD8
qRT-PCR	quantitative reverse transcriptase polymerase chain reaction
QTL	quantitative trait loci
RFP	red fluorescent protein
rms	*ramosus*
RNAi	ribonucleic acid
RNAi	ribonucleic acid interference
rpm	revolutions *per* minute
RT-PCR	reverse transcriptase polymerase chain reaction
s	second
SAAT	Sonication-Assisted *Agrobacterium*-mediated Transformation
SAP	shrimp alkaline phosphatase

SASA	Science and Advice for Scottish Agriculture
SbCCD8	*Sorghum bicolor* CCD8
SDG	set domain group
SDS	sodium dodecyl sulphate
SDW	sterile distilled water
SL	strigolactone
SlCCD8	*Solanum lycopersicum CCD8*
SOC	super optimal catabolite repression
SRA	sprout release assay
StCCD8	*Solanum tuberosum* CCD8
Taq	*Thermus aquaticus*
TCP	*TEOSINTE BRANCHED1-CYCLOIDEA and PCF transcription factor*
T-DNA	transferred DNA
Ti	tumour inducing
TBE	tris-borate EDTA
tBLASTx	translated nucleotide search, with translated nucleotide query
TBSV	*Tomato bushy stunt virus*
TE	tris-EDTA
Tm	melting temperature
U	unit
UPL	Universal Probe Library

UV	ultraviolet
VDE	violaxanthin de-epoxidase
VIB	Flanders Interuniversity Institute for Biotechnology
vio	violaxanthin
vir	*virulence* region
VP14	*viviparous 14*
v/v	volume per volume
VvCCD8	*Vitis vinifera* CCD8
WT	wild type
WUR	Wageningen Universitat
w/v	weight per volume
X-gal	5-bromo-4-chloro-3-indoyl-β-D-galactopyranoside
Y	*yellow fleshed*
ZDS	carotene desaturase
ZEP	zeaxanthin epoxidase
Z-ISO	carotene isomerase
ZmCCD8	*Zea mays* CCD8
ZR	zeatin riboside

Chapter 1 Introduction

1.1 Potato and characteristics

1.1.1 Origins and diversity

Common potato, or *Solanum tuberosum* L., is a member of the *Solanaceae* botanical family, amongst other important plant species such as tomato (*Solanum lycopersicum* L.), sweet pepper (*Capsicum annuum*) and eggplant (*Solanum melongena*). Potatoes are recognized as a world-wide staple crop, constituting an excellent source of energy, fibre and vitamins (Section 1.1.3). However, it is estimated that only half of the cultivated potatoes are consumed fresh (http://www.potato2008.org/en/potato/utilization.html, accessed April 2012), with the rest being used in various forms such as potato food products, animal feed and as a source of starch (Wadsworth and McKenzie, 1963).

The cultivation of potato as a crop is dated circa 7000 years ago, originating in the Titicaca Plateau, a high region of the Andean Mountains of South America (Spooner *et al.*, 2005). It was in this region, which now covers Peru and Bolivia, the Aymara Indians developed and grew more than 200 varieties of potato (Salaman, 1985). Considering that potatoes were thought to be the main basis of the Aymara Indian and Incan diet, it was not surprising to find proof of their influence into the native culture, with excavation sites reporting potato shaped pottery (Hawkes, 1972).

The introduction of potatoes in Europe occurred in the late 1400s and 1500s, by the Spanish Conquistadors (Hawkes and Francisco-Ortega, 1992). A reliable and easy-to-grow crop, potatoes became a standard supply item on the Spanish ships, as a means to overcome scurvy, a disease associated with vitamin C deficiency. However, potato cultivation expanded at a slow rate in Europe, due to its reputation as a food for the underprivileged and its relationship to poisonous plants.

It was only at the end of the 18th century, when its cultivation spread across England and Ireland, that potato was widely accepted as a staple crop in Europe (Hawkes, 1947). Next, the migration of European settlers expanded the area of potato cultivation into North America, increasing the popularity of potatoes and establishing it as a staple crop for the world.

There are more than 4000 varieties of native potatoes, of different shapes and sizes, predominantly found in the Andes. From these, around 180 are wild potato species (Burlingame *et al.*, 2009), too bitter to eat, but good as a source of germplasm with natural resistances to pests, diseases or challenging climatic conditions (Spooner and Bamberg, 1994). Also, there are several sub-groups of the cultivated *Solanum tuberosum* species, selected through domestication. The most important ones are the diploid groups *Phureja* and *Stenotomum* and the tetraploid groups *Tuberosum* and *Andigena* (Dodds, 1962). The commonly cultivated potato, *Solanum tuberosum* spp. *tuberosum,* is tetraploid and was domesticated throughout centuries of extensive breeding across Europe and North America, to obtain potato plants adapted to tuberisation under long days (Douches *et al.*, 1996).

The potato genome is composed of sets of 12 chromosomes, which can vary in number to produce diploid, triploid, tetraploid, pentaploid and hexaploid potato plants (Knapp *et al.*, 2004). In order to cope with the current environmental and economic challenges, it is important to develop new varieties of pest and disease resistant, high productivity potato. The potential of potato genetic improvement depends on the quality of the gene pool. Moreover, breeders have access to over 220 tuber bearing varieties from the *Petota* section, which includes the commonly cultivated potato, and the close outgroup section *Etuberosa*, as a source of germplasm (Hanneman, 1989).

1.1.1 Morphology and growth characteristics of potato plants

Herbaceous plants with a height of 0.5 to 1 metre, potatoes are perennial plants, surviving *via* underground stems or stolons which swell into tubers (Figure 1). The plants have odd-pinnate compound leaves and an upright leading stem, with white to pale blue or lavender bisexual flowers, arranged in compact racemes (Cutter, 1978). In order to obtain the edible tubers, potato plants are grown as annuals, from seed tubers, and rarely grown from seed, as the commonly cultivated tetraploid potatoes are bred to be propagated as vegetative tubers. Potato fruits, stems and leaves also contain toxic substances named glycoalkaloids, such as solanine and chaconine (Zitnak and Johnston, 1970). The tubers of potato plants are composed of mainly vascular storage tissue or parenchyma. The cells in these tissues contain starch grain filled plastids known as amyloplasts (Figure 2). The starch granules are made up of a mixture of an essentially unbranched α-1,4-linked D-glucose polymer (amylose) and of a larger component (amylopectin) with the same basic structure, but with frequent α-1,6-branch points, that can be associated with lipids and proteins (Davies *et al.*, 1990).

1.1.2 Production and economic importance

Out of the five most cultivated tuber and root crops (potato, sweet potato, cassava, yams and taro), potato is the most economically important crop and the staple food of many countries. The cultivation of potato covers more than 100 countries and a variety of climates, from temperate to subtropical and tropical conditions. Potatoes are the world's major non-grain food crop with China, India and USA as the major producers in 2010 (http://faostat.fao.org/site/339/default.aspx, accessed March 2012). Production in developing countries is increasing, and in 2005, the Food and Agriculture Organisation of the United Nations (FAO) showed a rise in the potato cultivation for these regions of the world (http://www.potato2008.org/en/world/index.html, accessed in March 2012).

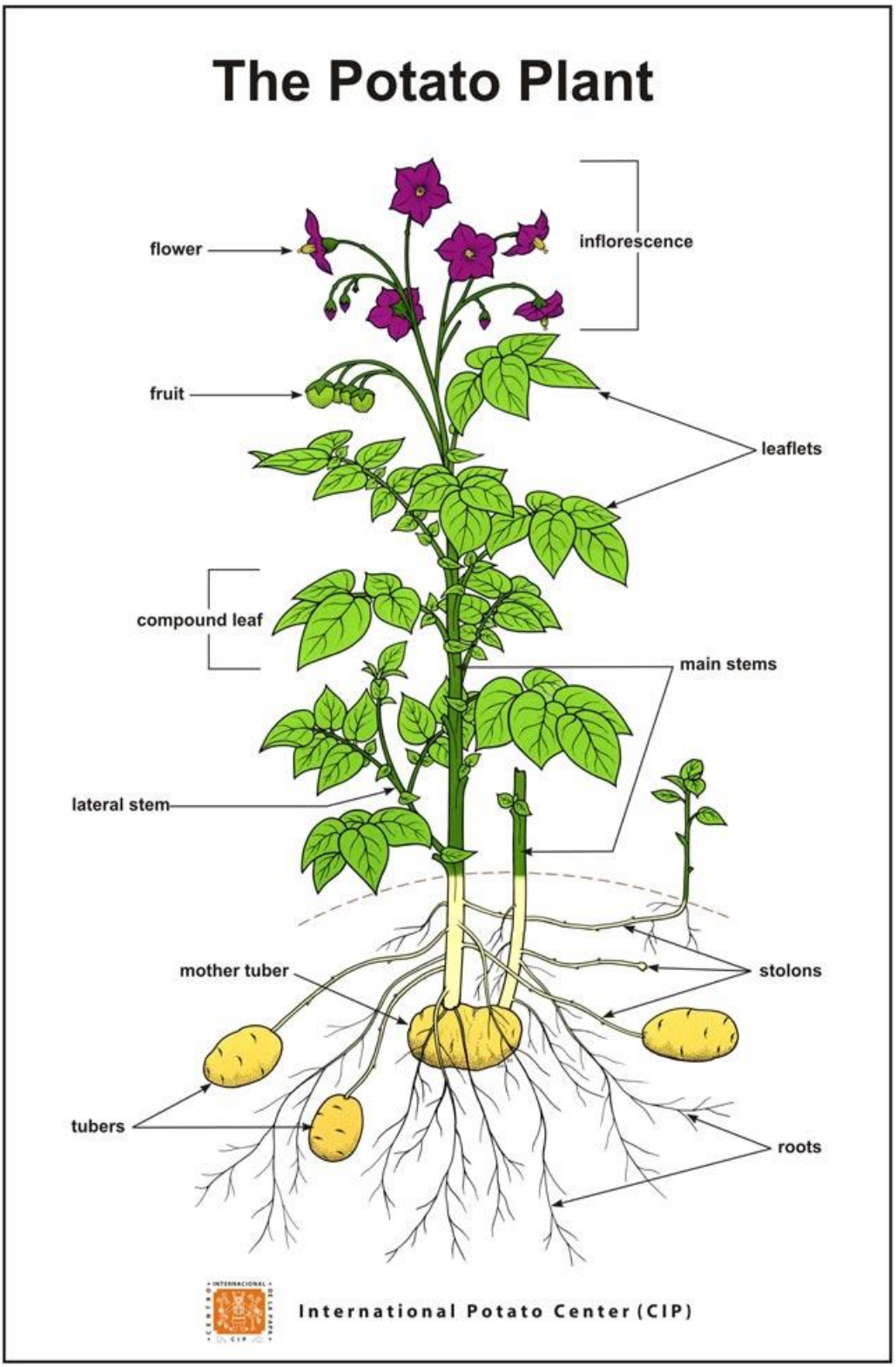

Figure 1. Diagram of the potato plant, describing aerial and underground elements of the plant. Source: http://cipotato.org/potato/how-potato-grows, accessed March 2012.

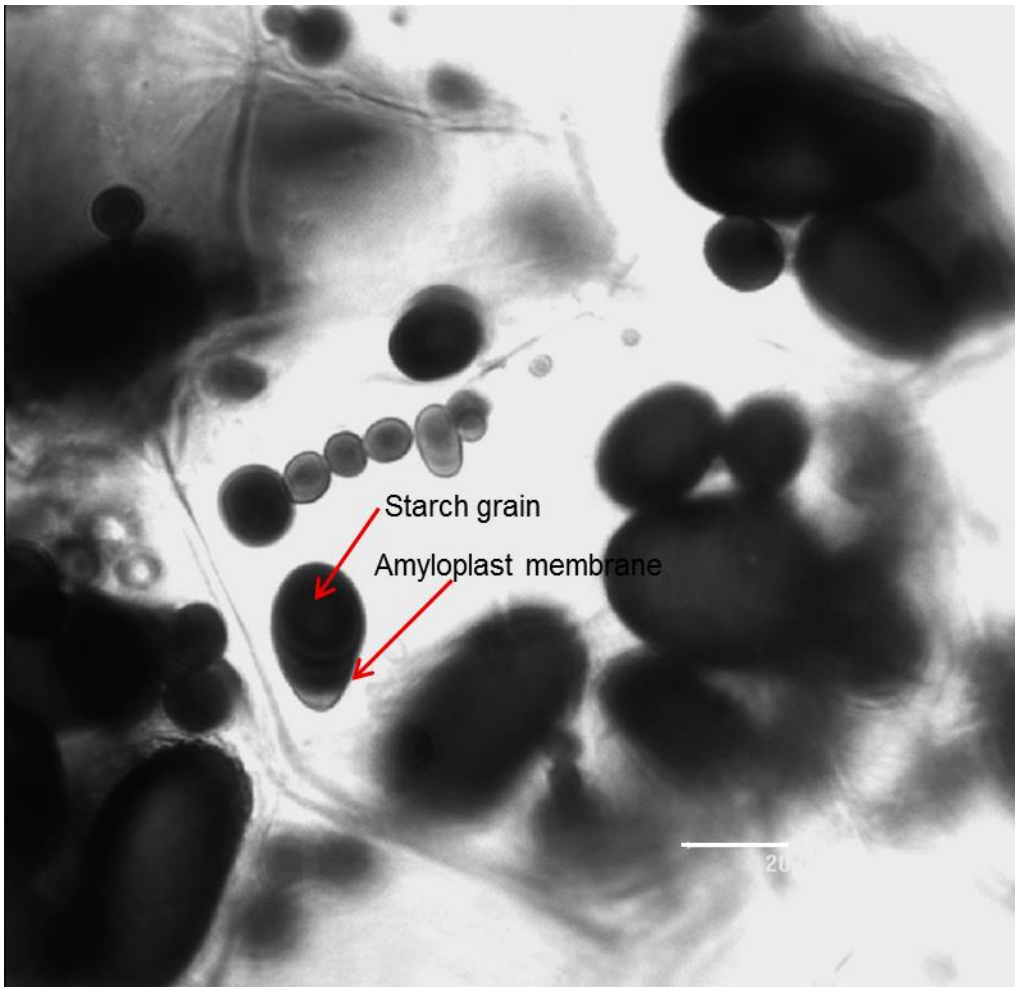

Figure 2. Image of the potato parenchyma, taken with the light microscope (Section 2.8.4) and stained with Lugol's solution. The presented cell contains a wide population of plastids with starch grains (amyloplasts). Red arrows mark the clear outline of a starch grain-containing amyloplast, encircled by a membrane and stroma. Bar size is 20 μm.

1.1.3 Consumption and nutritional value

The potato's high content of carbohydrates, proteins and fibres make it an excellent source of energy and an alternative to the cereal staple crops. Recent statistics by Kantar World Panel showed that, in UK, potatoes are eaten as part of ~10.3 billion meals made at home each year, which is an average of 3.3 meals a week for each member of the population (http://www.potato.org.uk/market-information/consumers, accessed March 2012).

More than an excellent, low-fat source of carbohydrates, potato tubers contain high quality proteins and notably high vitamin C, vitamin B3 (niacin), vitamin B5 (pantothenic acid), vitamin B6 (pyridoxine), potassium, phosphorus, and magnesium levels (Camire *et al.,* 2009). Recognized as an important source of health-promoting antioxidants in the human diet (Brown *et al.*, 2005), it was found that an average serving of skin-on potatoes provides roughly 10% of the recommended daily intake of fibre (http://cipotato.org/potato/nutrition, accessed April 2012; Figure 3 for more information and values). Very interestingly, it was found that there is a wide variability in the levels of health-promoting micronutrients within the native potato germplasm (Andre *et al.*, 2007), suggesting new possibilities for crop improvement programmes.

The flesh colour of potato tuber can range from white, yellow, pink, red, purple to even blue, depending on the type and levels of carotenoids (Section 1.2.3) or anthocyanins present. Nowadays, there is a great amount of interest in the yellowness or purpleness of tuber flesh, probably due to perceived benefits of higher antioxidant content (Brown et *al.* 2005), as shown in a study by Seefeldt *et al.* (2011), in which the yellow colour of tuber flesh influenced purchasing decisions for consumers.

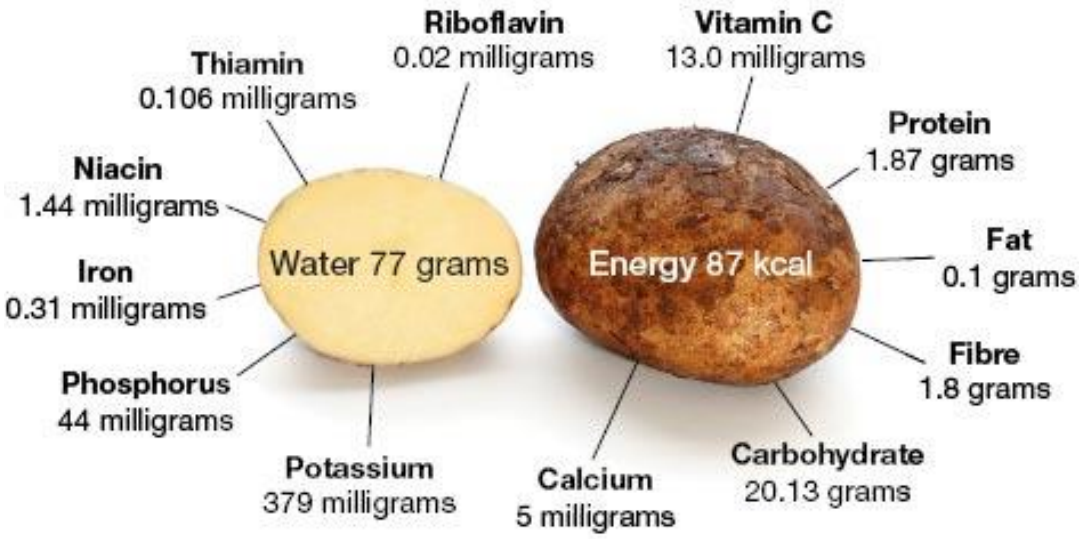

Figure 3. The nutrient content of potatoes, based on 100 g, after boiling in skin (Source: United States Department of Agriculture, National Nutrient Database, http://www.potato2008.org/en/potato/factsheets.html, accessed April 2012).

1.2 Carotenoids

1.2.1 Chemical structure and types of carotenoids

Carotenoids are isoprenoid-derived pigments widely found in nature. Reports on the naturally occurring pigments that we now know as carotenoids date as early as 1817, mentioning their presence in red peppers (Braconnot, 1817). Real progress in researching the nature of carotenoids came in the first part of the 20th century, with the invention of column chromatography by Tswett, detailed in Berezkin (2001). This new technology has greatly aided advances in establishing the correct molecular formulae of several carotenoids (reviewed in Willstatter, 1933). In the 1930s, the laboratories of Kuhn and Karrer deduced the isoprenoid nature of carotenoids, followed by the correct formulation of the end groups of lycopene, β-carotene, α-carotene, zeaxanthin and lutein by Karrer and his colleagues, reviewed in Britton *et al.* (2004). In that time, it was also established that carotenoids with an un-substituted β-ring can be metabolized into vitamin A or retinol (Karrer and Ruckstuhl, 1945).

Nowadays, more than 600 types of carotenoids are known, exclusive of *cis/trans* isomers (Fraser and Bramley, 2004). Carotenoids are lipophilic substances with distinctive light absorbing properties derived from their polyene chain, a long chromophore of conjugated double bonds, also responsible for the chemical reactivity of carotenoids toward oxidizing agents and free radicals (Britton, 1995). Carotenoids are constituted from two C_{20} geranylgeranyl diphosphate (GGPP) molecules. The resulting C_{40} carbon skeleton (Figure 4A) can then be modified to yield the diverse types of carotenoids, by three mechanisms: 1) cyclization at one terminus or both termini of the molecule to give the seven different end groups (illustrated in Figure 4B; detailed in Table 1), 2) by changes in hydrogenation level or 3) by addition of oxygen containing functional groups (Britton, 1991, 1995). Carotenoids that contain only the parent hydrocarbons are known as carotenes and the ones that contain one or more oxygen functions are known as xanthophylls.

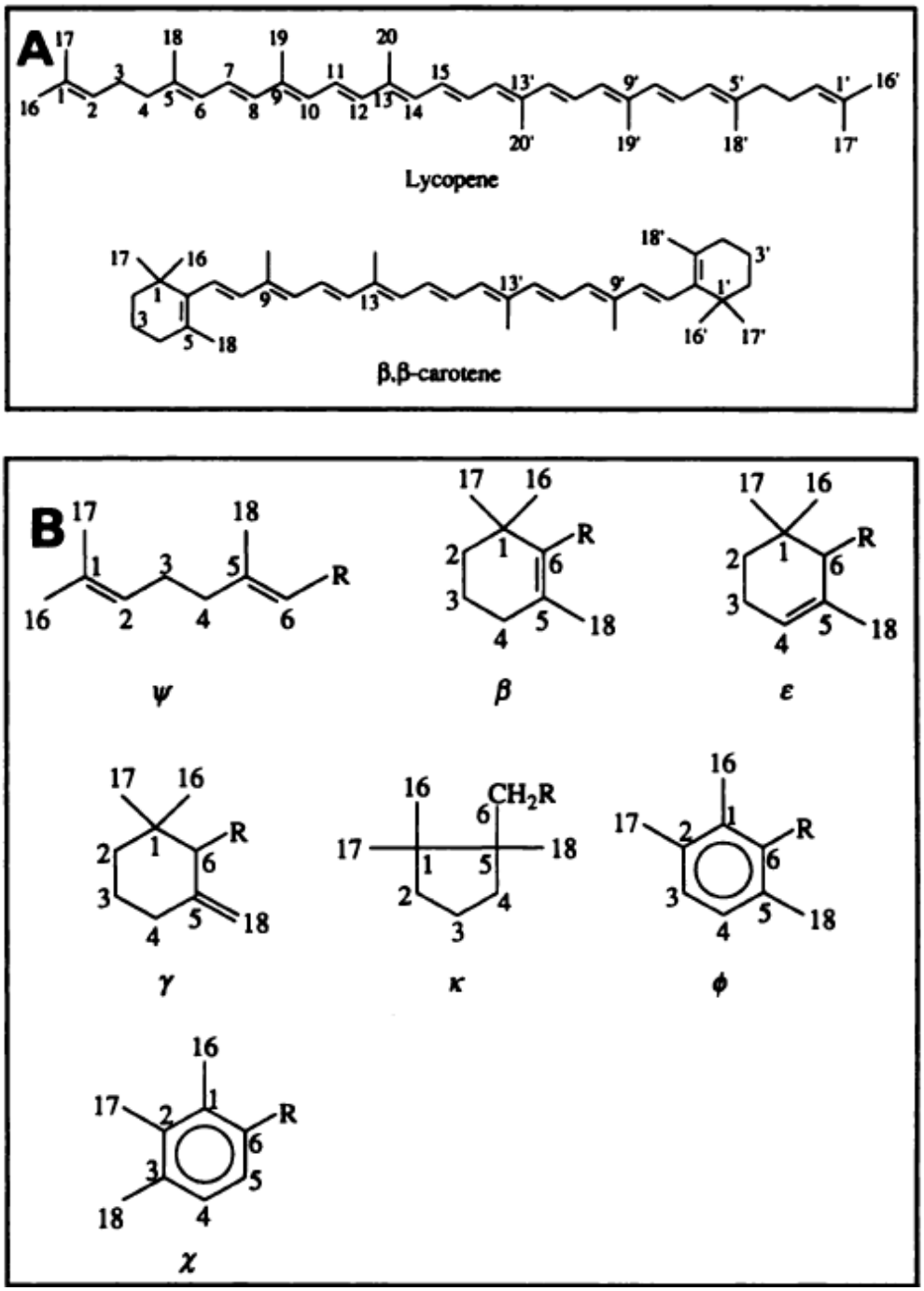

Figure 4. Structure of carotenoids A. Overview of the structure and numbering scheme of acyclic and dicyclic carotenoids; B. The seven different end groups found in carotenoids (Britton, 1995).

Table 1. Prefixes used in the nomenclature of carotenoids, corresponding to the end groups from Figure 4B.

Type	Prefix	Formula	Structure
Acyclic	ψ	C_9H_{15}	**III**
Cyclohexene	β, ε	C_9H_{15}	**IV, V**
Methylenecyclohexane	γ	C_9H_{15}	**VI**
Cyclopentane	κ	C_9H_{17}	**VII**
Aryl	ϕ, χ	C_9H_{11}	**VIII, I**

1.2.2 Importance of carotenoids

Carotenoids are often thought of as the pigments in leaves, fruits, vegetables and flowers. Carotenoids absorb light maximally between 460 nm and 550 nm and thus appear red, orange, or yellow in colour, to the human eye. The carotenoid's colour is often masked by the green chlorophyll pigments in leaves, but as these decrease during the senescence stage, carotenoids are left responsible for the beautiful colours of autumn leaves (Figure 5). The distinctive colouration that carotenoid accumulation gives to fruits and flowers is responsible for attracting pollinators and favouring seed dispersal. However, it is important to remember that dietary carotenoids accumulate in a variety of other organisms, such as animals, fish, birds, insects and microorganisms (Britton, 1995). Carotenoids in animals were found to establish sexual behaviour, reproduction and avoidance of predation or parasitism, whereas fish and birds accumulating these important isoprenoids increase their immune system and advertise health (McGraw, 2006; McGraw and Klasing, 2006).

Maybe the best known derivative of carotenoids is vitamin A, a product of a mono-oxygenase type cleavage of the carotenoids, restricted to compounds containing a β -ring end group, such as β-carotene and β-cryptoxanthin. For humans, dietary carotenoids with provitamin A activity prevent deficiency related diseases, such as blindness, and promote human health by their antioxidant activity, as immunostimulants or photoprotectants (Cazzonelli, 2011). There have been a number of studies into the beneficial effects of these compounds (reviewed in Fraser and Bramley, 2004; Voutilainen *et al*., 2006; Mayer *et al*., 2008) in cancer, cardiovascular, age related eye diseases (Johnson *et al.*, 1995; Johnson, 2004) and the prevention of cognitive decline (Johnson, 2010; Figure 5). Lycopene, the major carotenoid from tomato fruit, was demonstrated to have effects in reducing the risk of cancer and cardiovascular diseases (Hadley *et al.*, 2002) and offer protection against macular degeneration, the leading cause of age-related blindness (Krinsky and Yeum, 2003). Astaxanthin, one of the most commercially valuable carotenoids, is thought to be a potential therapeutic agent for treating cardiovascular disease and prostate cancer (Fassett and Coombes, 2011). Lutein, one of the most stable to heat

carotenoids, and zeaxanthin, are the predominant carotenoids found in potato tubers. They are thought to play a key role in preventing advanced macular degeneration, by protecting photoreceptor cells from light generated oxygen radicals (Schalch, 1992). Moreover, lutein is also believed to help reduce lung cancer (Khachik *et al.*, 1992).

Carotenoids are essential pigments for photosynthetic organisms, (Cogdell and Frank, 1987), fulfilling two major roles in photosynthesis, as accessory light harvesting pigments and photoprotectants against harmful oxygen molecules.

The capturing of light for photosynthesis by plants is made *via* light-harvesting complexes (LHCs), composed of proteins in association chlorophylls and with carotenoids such as neoxanthin, violaxanthin and lutein (Muller *et al.*, 2001). In their role as accessory light harvesting pigments, carotenoids absorb light in the spectral region in which the sun irradiates maximally, from 400 to 500 nm, thus extending the range of wavelengths over which light can drive photosynthesis. Carotenoids then transfer this energy to chlorophyll molecules, as part of the primary photochemical events of photosynthesis (Polivka and Frank, 2010).

Secondly, carotenoids are potent quenchers of singlet molecular oxygen [O_2 ($^1\Delta_g$)] generated in solar light-induced photooxidative stress conditions (Terao *et al.*, 2011). As plants absorb more light energy than they can use in photosynthesis, it is necessary for them to quench the singlet-excited chlorophylls and harmlessly dissipate any excess excitation energy as heat, through the protective non-photochemical quenching mechanisms or NPQ (Muller *et al.*, 2001). Carotenoids function as photoprotectants, crucial for oxygenic photosynthesis, as shown by a study on the lethal effects of inhibitors of carotenoid biosynthesis in plants (Bramley *et al*., 1993).

Moreover, the importance of xanthophylls for photosynthesis and the normal development of the plant is evident in several NPQ and carotenoid-impaired mutants, which have bleaching, delayed greening, *viviparous* and semi-lethal phenotypes (Niyogi, 1999; Pogson *et al*., 2005; Bailey and Grossman, 2008; Alboresi *et al*., 2011).

The oxidative cleavage of carotenoids produces apocarotenoids, such as vitamin A but also plant growth regulators such as abscisic acid (ABA), a hormone found to be mediating plant responses to environmental stresses (Schwartz *et al*., 1997) and the branching inhibition phytohormones, strigolactones (SLs; Section 1.3.4). Other apocarotenoid derived signalling molecules are blumenin and mycorradicin, with roles in controlling the beneficial arbuscule turnover during arbuscular mycorrhizal (AM) fungi symbiosis and starting the hyphal branching in the rhizosphere (Figure 5; Akiyama *et al.*, 2005; Walter *et al.*, 2010).

Also, there is a multitude of compounds responsible for enhancing the flavour and aroma of flowers and fruits, all derived from the cleavage of carotenoids (Figure 5; Auldridge *et al*., 2006a). Currently, there are several apocarotenoids synthesized in the nutraceuticals industry, to be used in a range of cosmetics foods or food additives, for poultry, livestock, fish and crustaceans (reviewed in Del Campo *et al.*, 2007). An example of an apocarotenoid used as a food additive is bixin (annatto), a red-coloured, di-carboxylic monomethyl ester apocarotenoid, derived from *Bixa orellana*. Also, saffron-derived carotenoids have a high antioxidant capacity that makes them relevant for human health (Verma and Bordia, 1998). Other carotenoid-derived volatiles (α- and β-ionone) are predominant nor-isoprenoids found in the mature stigma tissue, components of aroma and taste of flowers and fruits (Goff and Klee, 2006).

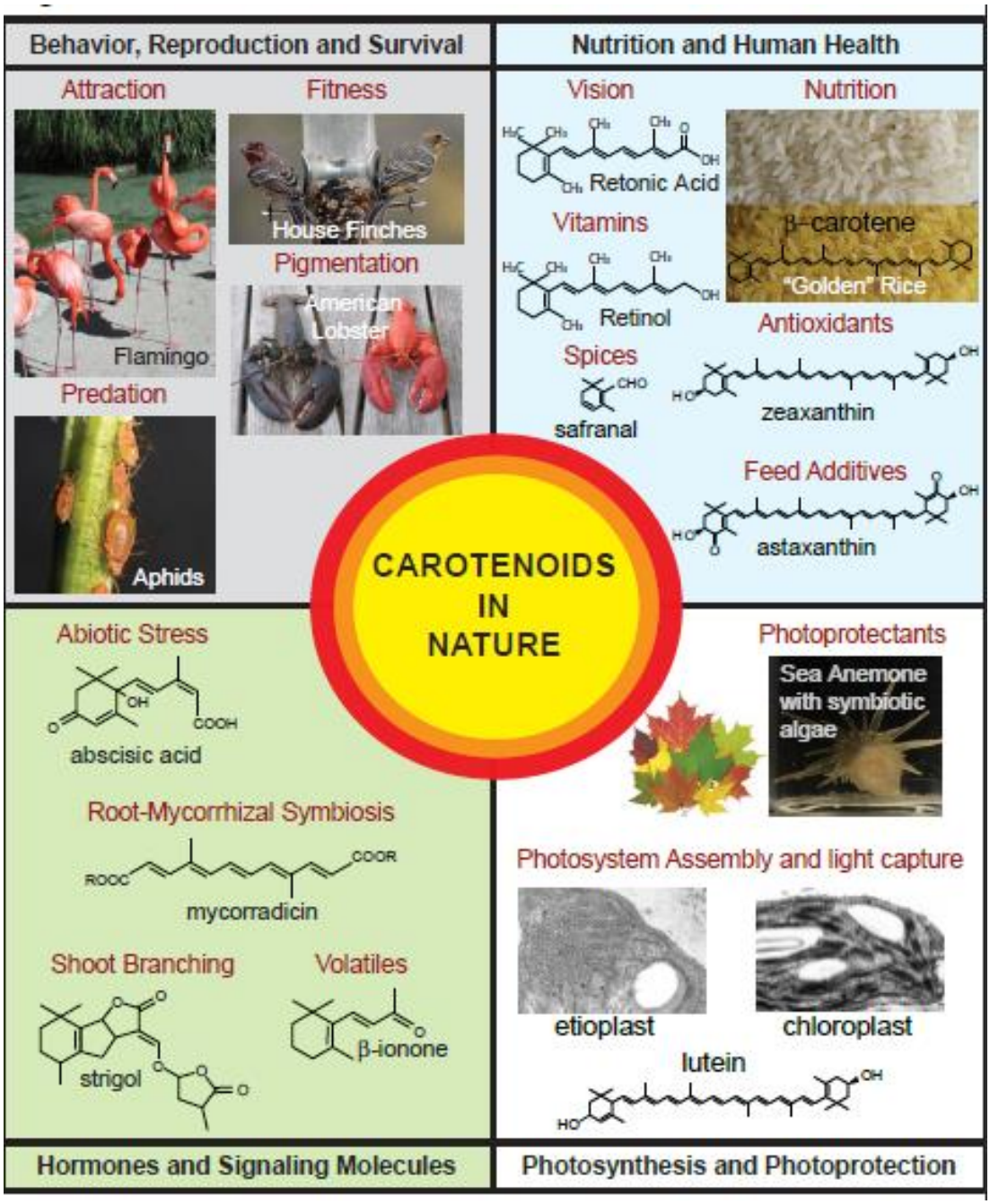

Figure 5. The function and importance of carotenoids. The important roles that carotenoids play in (1) promoting animal behaviour, reproduction and survival (2) improving nutrition and human health (3) assembly of photosystems, light capture and photoprotection and (4) providing substrates for the biosynthesis of plant growth regulators and other signalling molecules (Cazzonelli, 2011).

1.2.3 Carotenoids in potato tubers-natural variation and content

The flesh of potato tubers can range from white (as in *Solanum tuberosum* cv. Pentland Javelin) to cream/yellow (*Solanum tuberosum* cv. Desiree) or even yellow/orange (as in *Solanum tuberosum* Phureja), depending on the type and levels of carotenoid pigments (Iwanzik *et al*., 1983; Breithaupt and Bamedi, 2002). In the white fleshed cultivars and breeding lines, the total carotenoid content ranges from 50 to 100 µg 100 g FW^{-1}. The yellow flesh cultivars of potato can contain up to 270 µg 100 g FW^{-1} of carotenoid contents (Brown *et al*., 2006). The main carotenoids of *Solanum tuberosum* tubers are xanthophylls such as violaxanthin, antheraxanthin, lutein and zeaxanthin (Nesterenko and Sink, 2003). The provitamin A precursors such as β-carotene and β-cryptoxanthin represent minor components of commonly cultivated potato flesh.

The carotenoid content in yellow or white flesh in potato tubers is known to be strongly influenced by an allele at the *Y* locus (Brown *et al.*, 1993), mapped to chromosome 3 of potato (Bonierbale *et al*., 1988). There is evidence that *CrtRb2* corresponds to the *Y* locus (Brown *et al.*, 2006; Kloosterman *et al.*, 2010), but other genes such as *PSY* may also impact on the yellow flesh trait (Thorup *et al.*, 2000).

1.3 Regulation of carotenoid content in storage organs

Carotenoids are essential compounds for all plants, insects and animals, fulfilling crucial roles in the overall fitness and survival of these organisms (Section 1.2.2). Considering the importance of manipulating carotenoid content, the regulation of its accumulation has generated substantial interest in the past years, with significant progress being continuously made (reviewed by Cazzonelli *et al*., 2009b).

The enzymes involved in carotenogenesis are located within the plastid (Kreuz *et al.*, 1982; Lutkebrinkhaus *et al.*, 1982), encoded by nuclear genes (Hirschberg, 2001), with the pre-proteins being post-translationally targeted to the plastids and processed there. This aspect of carotenoid biosynthesis makes its regulation especially complex. Also, it is thought that the levels of carotenoids from fruits and flowers are regulated in a distinct way from carotenoids in green tissues, which serve important roles as structural pigments in photosynthesis (Alberte and Andersen, 1986). It was established that expression of carotenoid genes is dependent on the species investigated (Romer *et al.*, 1993) and the developmental stage (Bugos *et al.*, 1999). Moreover, environmental factors were shown to have an effect on carotenogenesis (Bouvier *et al.*, 1996; Audran *et al.*, 1998; Steinbrenner and Linden, 2001).

Numerous studies have provided evidence for the idea of a metabolic sink mechanism responsible for controlling carotenoid accumulation in plants, but there is also indication that turnover of carotenoids is modulating the levels of these pigments in storage organs (Cazzonelli *et al*., 2009b).

1.3.1 Biosynthesis of carotenoids in plants

Carotenoids are synthesized *de novo* in a variety of organisms, such as plants, fungi or bacteria (Lu and Li, 2008). Until recently, it was thought that animals are unable to synthesize carotenoids, with species such as butterflies, fish and birds only accumulating dietary carotenoids. However, a recent study by Moran and Jarvik (2010) showed that pea aphids displaying a red-green colour polymorphism possess multiple genes from the carotenoid biosynthesis pathway, enabling the red specimens to make their own carotenoids.

1.3.1.1 The production of isoprenoid derived compounds

Carotenoids are isoprenoid-types of compounds, together with tocopherols, chlorophylls, phylloquinone, gibberellins, ABA, monoterpenes and plastoquinone (Tholl and Lee, 2011). The biosynthesis of all isoprenoids is based on the production of the C5 building block, isopentenyl pyrophosphate (IPP) and its allylic isomer, dimethylallyl pyrophosphate (DMAPP).

There are two known pathways by which IPP is synthesized: the mevalonate pathway, in the cytosol, and the non-mevalonate pathway, the 2-C-methyl-D-erythritol 4-phosphate (MEP) pathway, that starts with 1-deoxy-D-xylulose 5-phosphate (DXP), in the plastids (Figure 6; reviewed in Rodriguez-Concepcion and Boronat, 2002 and Cazzonelli, 2011). In the MEP (also called the DXS) pathway, the condensation of isopentenyl diphosphate (IPP) and dimethylallyl diphosphate (DMAPP) gives rise to geranylgeranyl diphosphate (GGPP). The first steps in the MEP pathway are catalysed by 1-deoxyxylulose-5-phosphate synthase (DXS) and 1-deoxyxylulose 5-phosphate reductoisomerase (DXR).

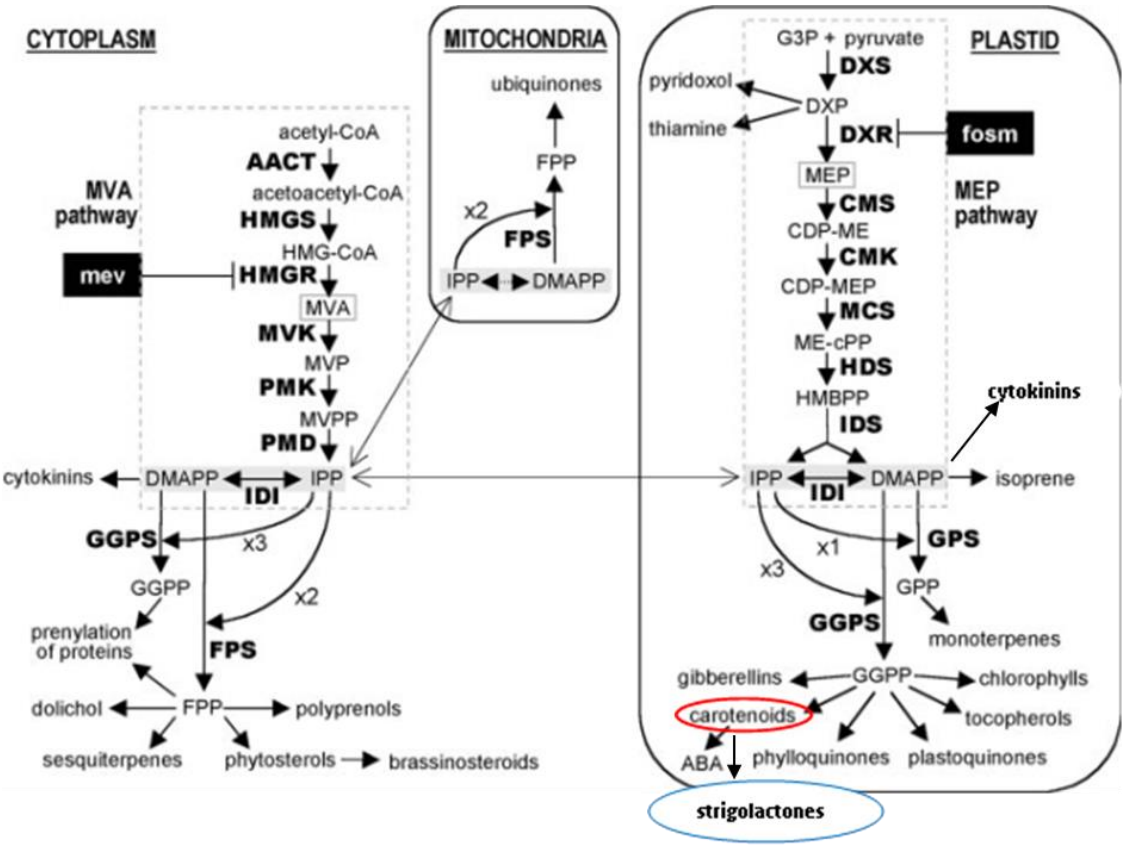

Figure 6. Isoprenoid biosynthesis pathways in the plant cell. HMG-CoA, Hydroxymethylglutaryl CoA; MVP, 5-phosphomevalonate; MVPP, 5 diphosphomevalonate; HBMPP, hydroxymethylbutenyl 4-diphosphate; FPP, farnesyl diphosphate; ABA, abscisic acid. The first intermediate specific to each pathway is boxed. AACT, acetoacetyl CoA thiolase ; HMGS, HMG-CoA synthase; HMGR, HMG-CoA reductase; MVK, MVA kinase; PMK, MVP kinase; PMD, MVPP decarboxylase; IDI, IPP isomerase; GPS, GPP synthase; FPS, FPP synthase; GGPS, GGPP synthase; DXS; DXR, DXP reductoisomerase; CDP-ME, 4-diphosphocytidyl ME; CMS, CDP-ME synthase; CMK, CDP-ME kinase; ME-cPP, 2,4-Cyclodiphosphate; MCS, ME-cPP synthase; HDS, HMBPP synthase; IDS, IPP/DMAPP synthase. The steps specifically inhibited by mevinolin (mev) and fosmidomycin (fosm) are indicated (adapted from Rodriguez-Concepcion and Boronat, 2002).

The mevalonate pathway enzymes have been well studied over the past 30 years, and several regulatory mechanisms have been uncovered (Veen and Lang, 2004). In contrast, the MEP pathway was fully elucidated only in 2002 and is less well understood in terms of both requirements and regulation (Adam *et al.*, 2002). The production of these substrates for carotenogenesis is likely to be controlled by abiotic and biotic cues, with light and circadian rhythm presumably regulating expression of many MEP and several carotenoid biosynthetic genes (for review, Cordoba *et al.*, 2009).

1.3.1.2 Carotenoid biosynthesis and regulation in plants

Although the basic biosynthetic pathway producing carotenoids is well known, the way to optimise accumulation of these compounds is not yet fully understood. The first committed step in the carotenoid biosynthesis pathway is represented by the condensation of two GGPP molecules, catalyzed by PSY. Catalysing the conversion of GGPP into phytoene, *PSY* is a nuclear-encoded small gene family consisting of *PSY1*, *PSY2* and the recently discovered *PSY3*, shown to exist in grasses (Li *et al*., 2008). This reaction gives rise to the first colourless carotenoid, 15-*cis*-phytoene (Figure 7). Phytoene is enzymatically converted into all-*trans* lycopene, the major branch point precursor for downstream carotenoids, to later form carotenes by the addition of a ε-ring or β-ring at each end of the lycopene molecule. Ring-specific hydroxylases mediate the formation of xanthophylls such as lutein and zeaxanthin (Quinlan *et al.*, 2012).

As PSY is thought to be the main rate-limiting enzyme, in many, but not all non-green tissues (Fraser *et al*., 1994; Diretto *et al*., 2007a), there has been interest in manipulation of PSY, for increased carotenoid levels (Section 1.3.2). The expression of this gene is tightly regulated by developmental cues such as high light intensity, drought, ABA, salt, temperature conditions, photoperiod, but also by post-transcriptional feedback regulation (reviewed in Cazzonelli and Pogson, 2010). It was found that *cis*-regulatory elements (box I and box IV), known for their role in light regulation of plant metabolic genes, were present in the promoters of rice *PSY1*

and *PSY2*, prone to light induction of gene expression (Cazzonelli and Pogson, 2010). Together with these light responsive *cis*-elements, a putative ABA Response Element–Coupling Element (ABRE-CE) was also identified in the promoter region of *PSY3* from rice and maize, making these two genes responsive to events associated with ABA regulation, such as drought and salt stresses (Li *et al.*, 2008; Welsch *et al.*, 2008). Recently, Toledo-Ortiz *et al*. (2010) have demonstrated that, in Arabidopsis, *PSY* is under phytochrome regulation by phytochrome-interacting factor 1 (PIF1) and other transcription factors of the PIF family, which specifically repress the gene encoding PSY.

Carotenogenesis is also subject to regulation by the *Arabidopsis thaliana* transcription factor AtRAP2.2, a member of the APETALA2 ethylene responsive family, found to moderately regulate carotenoid content *via* transcript levels of *PSY* and phytoene desaturase (*PDS*; Welsch *et al.*, 2007). Moreover, there are suggestions of feedback regulation existing in the carotenoid pathway, as Romer *et al.* (2000) obtained unexpected elevated levels of β-carotene in transgenic tomato fruits expressing a bacterial phytoene desaturase, *crtI*, from *Erwinia uredovora*.

15-*cis*-phytoene is converted into all-*trans*-lycopene, by the action of PDS, ζ-carotene isomerase (Z-ISO), ζ-carotene desaturase (ZDS) and carotenoid isomerase (CRTISO), together with a light-mediated photoisomerization (see Figure 7; Park *et al*., 2002; Isaacson *et al*., 2004; Breitenbach and Sandmann, 2005; Dong *et al*., 2007; Chen *et al*., 2010).There is evidence of PDS having a rate-limiting role in the production of 9,15,9'-tri-*cis*-ζ-carotene (ζ-carotene), as its mRNA transcript levels are up-regulated during photomorphogenesis (Welsch *et al*., 2000; Qin *et al*., 2007). Recently, it was suggested that, in the conversion of ζ-carotene to tetra-*cis*-lycopene (pro-lycopene), *Z-ISO* expression could be regulated by the dark period. In another study showing the complex regulation taking place at this level, the *ZDS* loss-of-function disturbs carotenoid accumulation and even retrograde signalling (the regulation of nuclear genes by signals originating from plastids; Pogson *et al.*, 2008),

a result explained as being due to impaired plastid development (Dong *et al*. 2007; Chen *et al*. 2010).

CRTISO, which catalyses the *cis-trans* reactions to isomerise the four *cis*-bonds introduced by the desaturases, is considered a major regulatory node in the MEP pathway (Cazzonelli *et al*., 2009b), essential for the equilibrium between *cis* and *trans* isomers (Yu *et al.*, 2011) and with a putative role in regulating the expression of PS II core proteins, in rice (Wei *et al.*, 2010). New studies have shown that carotenoid production can still occur in *crtiso* mutants, *via* photoisomerisation (Fang *et al*., 2008; Chai *et al*., 2010), putatively unravelling a crucial involvement of light in substituting the role of CRTISO action in green tissues (Cunningham and Schiff, 1985; Sandmann, 1991; Yu *et al*., 2011; Figure 7). Very interestingly, a recent study has found evidence of epigenetic regulation occurring in this step of the carotenoid biosynthesis pathway, as a protein with chromatin modifying function, the SET DOMAIN GROUP 8, was found to limit lutein production, by regulating CRTISO expression and carotenoid flux (Cazzonelli *et al*., 2009a; Figure 7).

Further along the pathway, ε-lycopene cylase (εLCY) and β-lycopene cyclase (βLCY) are responsible for the cyclisation of lycopene into the two major groups of carotenoids, the β,β- and the β,ε-carotenoids (Kim and DellaPenna, 2006). The cyclases act by introducing β- and ε-rings to lycopene, differing by the position of the double bond within the cyclohexane ring (Cunningham *et al.*, 1996), giving rise to carotenes (α- and β-carotene) and their oxygenated derivatives, the xanthophylls. The latter (lutein, zeaxanthin, antheraxanthin, violaxanthin, and neoxanthin in its 9′-*cis* rather than the all-*trans*-form) are predominantly found in the light-harvesting system (Kuhlbrandt *et al.*, 1994; Ruban *et al.*, 1994; Lee and Thornber, 1995; Takaichi and Mimuro, 1998; Croce *et al.*, 2002). In the carotenoid biosynthesis pathway, βLCY adds β-rings to lycopene, giving rise to β-carotene (β-β-carotene, precursor for zeaxanthin), whereas the action of both βLCY and εLCY leads to the formation of α-carotene (ε-β-carotene; Figure 7). Next, lutein is formed by the hydroxylation of the C3 β- and ε-rings of α-carotene by β-ring hydroxylase (CRTL-b or CrtRb) and ε-ring hydroxylase (CRTL-e; Kim and DellaPena, 2006).

The hydroxylation of β-carotene to β-cryptoxanthin and then to lutein's isomer, zeaxanthin, is carried out by β-carotene hydroxylase CRTL-b, but also known as βOH. The epoxidation of zeaxanthin to violaxanthin is catalysed by zeaxanthin epoxidase (ZEP). The de-epoxidation back to zeaxanthin is catalysed by violaxanthin de-epoxidase (VDE) (Fraser and Bramley, 2004), under high light stress (Pfundel *et al.*, 1994). It was demonstrated that the molecular relationship between βLCY and εLCY is a major factor regulating the flux through the β-ε branch, thus controlling the production of lutein, β-carotene and other xanthophyll-derived carotenoids (Yu *et al.*, 2008; Bai *et al.*, 2009). The ratio of the most abundant carotenoid, lutein, to β-carotenoids is modulated by εLCY, with any variation in its expression and/or activity controlling levels of lutein (Cuttriss *et al.*, 2007; Harjes *et al.*, 2008; Cazzonelli *et al.*, 2009a; Howitt *et al.*, 2009).

The final step in β-β branch of the carotenoid biosynthesis is the conversion of violaxanthin to neoxanthin by neoxanthin synthase (NXS; Al-Babili *et al.*, 2000). It is worth mentioning that there are many different types of xanthophyll-derived carotenoids, specific for certain plant tissues, such as the highly valued ketocarotenoids astaxanthin, capsanthin, capsorubin and canthaxanthin. For review of their biosynthesis, please refer to Giuliano *et al.* (2008) and Jackson *et al.* (2008). The regulation of xanthophyll biosynthesis was shown to influence photosystem assembly for light harvesting, photoprotection and impact on the plant response to conditions of stress (Pogson *et al.*, 1998; Dall'Osto *et al.*, 2006). A study by Woitsch and Romer (2003) found that white-light illumination generally induced expression of the three xanthophyll biosynthetic genes investigated, βOH, ZEP and VDE, during de-etiolation of seedlings of tobacco (*Nicotiana tabacum* L. cv. Samsun). Also, genes from the light transduction pathway, *LeHY5* and *LeCOP1LIKE*, from *high pigment 1* (*hp1*) and *hp2* tomato mutants, have been implicated in the regulation of carotenoid biosynthesis, positively and negatively modulating the pigmentation of tomato fruits (Liu *et al.*, 2004).

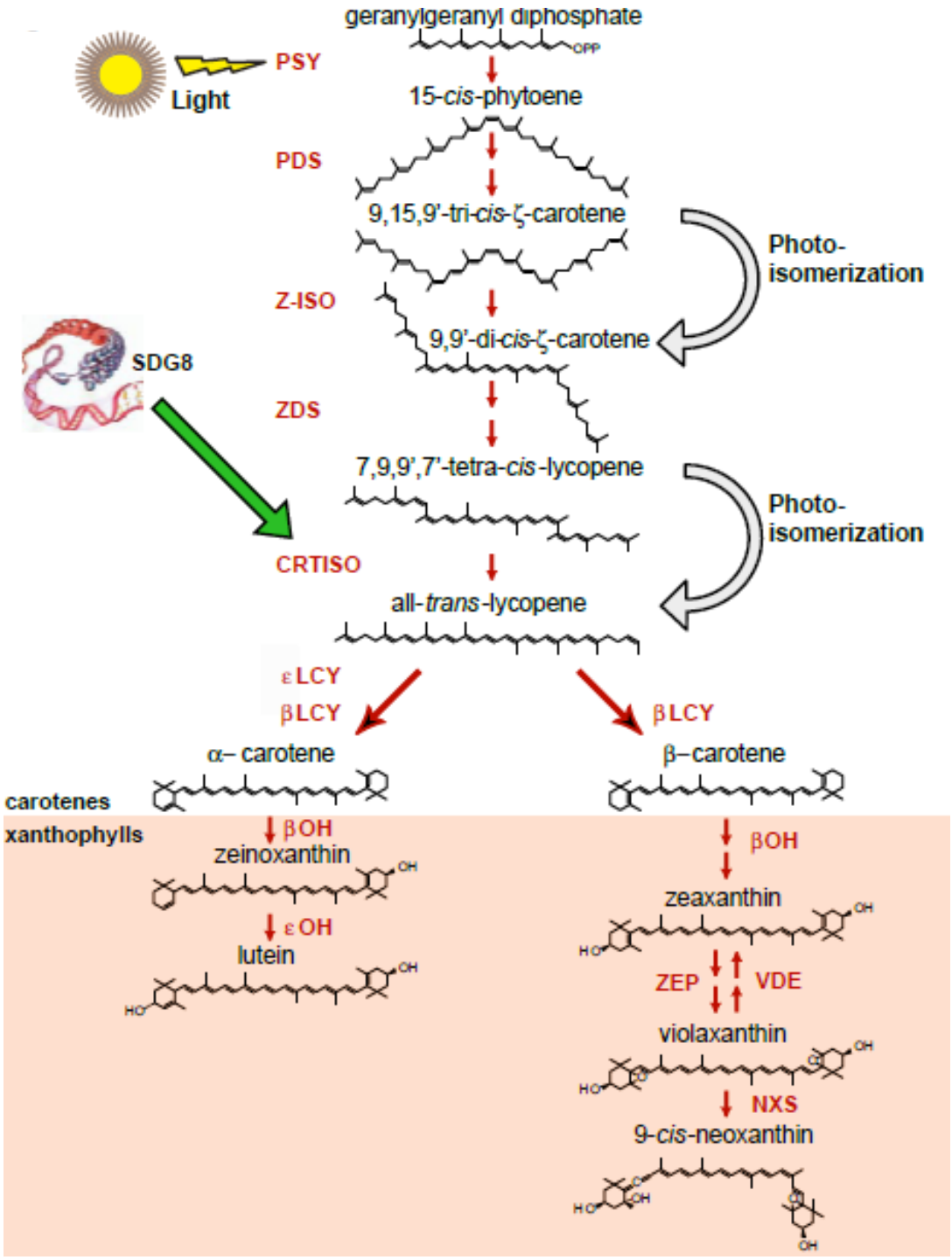

Figure 7. Overview of the carotenoid biosynthesis and regulation mechanisms in Arabidopsis. The light responsive enzyme, PSY catalyses the first committed step in the synthesis by converting GGPP to phytoene, representing a major regulatory step. The isomerisation of tetra-*cis*-lycopene (pro-lycopene) to lycopene requires the carotenoid isomerase (CRTISO) and light-mediated photoisomerisation. Modification of chromatin surrounding the *CRTISO* locus by the histone lysine methyltransferase, SET DOMAIN GROUP8 (SDG8), is rate limiting for lutein

production. Finally, lycopene undergoes modifications by εLCY and βLCY to produce α- and β-carotene respectively. The carotenes serve as substrates for the production of xanthophylls including lutein, violaxanthin and neoxanthin. The xanthophyll cycle (interconversion between zeaxanthin, antheraxanthin and violaxanthin) is responsive to light and important in photoprotection. PDS, phytoene desaturase, ZDS, ζ-carotene desaturase; Z-ISO, ζ-carotene isomerase, βOH, β-hydroxylase; εOH, ε-hydroxylase, NXS, neoxanthin synthase; VDE, violaxanthin de-epoxidase; ZEP, zeaxanthin epoxidase (adapted from Cazzonelli, 2011).

1.3.2 Manipulation of carotenoid content

Bio-fortified crops with increased bioavailable concentrations of carotenoids are being developed for consumers through traditional plant breeding or genetic manipulation (Mayer *et al.*, 2008). Studies have attempted to elevate the levels of carotenoids in potato tubers by using existing germplasm resources (Brown, 2008; Kobayashi *et al.*, 2008). For example, tubers with elevated amounts of lutein-5,6-epoxide and lutein and decreased zeaxanthin were obtained from a hybrid population, a cross between *Solanum phureja* and *Solanum stenotomum*, by Lu *et al.* (2001).

There are many studies which have successfully increased carotenoid levels in crop plants by genetic engineering. The ectopic expression of genes in a mini-carotenoid biosynthetic pathway in rice constitutes the best known example of enhancing the nutritional value of staple crops. The first ‘Golden Rice’ over-expressed PSY from daffodil (Ye *et al.*, 2000), but it was later found that a higher β-carotene content was obtained when PSY from maize was overexpressed, together with CrtI, from *Erwinia uredovora* (Paine *et al*., 2005). The accumulation of β-carotene in the endosperm of ‘Golden Rice 2’ increased to a level considered sufficient to provide most of the recommended dietary allowance of vitamin A for children consuming an average amount of rice daily (Paine *et al.*, 2005).

Efforts to constitutively express *PSY1* in tomato had serious pleiotropic results, such as dwarf plants and co-suppression of the gene in ripening fruits (Fray *et al.*, 1995). These effects were credited to a diversion of the GGPP pool from gibberellins to carotenoids. Fraser *et al.* (2002) successfully engineered a high carotenoid–containing tomato fruit in which these detrimental pleiotropic effects were alleviated, by expressing a bacterial phytoene synthase (*CrtB*) in a fruit-specific manner. Also in tomato fruits, another study by D'Ambrosio *et al.* (2004) successfully enhanced accumulation of β-carotene by expressing the LCY-B transgene to produce transgenic tomato plants whose fruits contained high amounts of β-carotene as a result of the almost complete cyclisation of lycopene, named the 'Orange tomatoes'.

The carotenoid pathway was also engineered to produce carotenoids in seeds, normally devoid of these compounds. In *Arabidopsis thaliana*, a study by Lindgren *et al.* (2003) succeeded in expressing the *AtPSY*, in a seed-specific manner, to obtain accumulation of carotenoids, ABA, and chlorophyll in seeds. Another example is the engineering of carotenoids in oil seeds of canola, by over-expressing *PSY* to elevate total carotenoid content up to 43-50 fold more than controls (Shewmaker *et al.*, 1999).

Several studies have over-expressed genes from the carotenoid pathway in potato tubers. Ducreux *et al.* (2005) successfully expressed *crtB* in both cream (*Solanum tuberosum* cv. Desiree) and yellow (*Solanum phureja*) flesh tubers, resulting in an increase of up to 78 µg carotenoid g^{-1} DW in total carotenoid content, in the most affected transgenic line. Morris *et al.* (2006b) overexpressed DXS, the enzyme responsible for the formation of IPP (Estevez *et al.*, 2001), in potato tubers, obtaining an increase in phytoene and, very interestingly, a significantly elongated tuber and early sprouting phenotype. Also in 2006(a), another study by Morris *et al.* engineered *Solanum phureja* and *Solanum tuberosum* tubers to express an algal ketolase gene, *bkt1*, resulting in increased accumulation of ketolutein and astaxanthin. Another study into silencing of εLCY in tuber tissue, carried out by Diretto *et al.* (2006) had as a result the upregulation of β-carotene levels in potato

tubers, up to 14-fold when compared to controls. Diretto *et al*. (2007a) engineered the 'Golden Potato' by over-expressing *CrtB* in tubers, together with the bacterial phytoene desaturase/isomerase *CrtI* and β-cyclase, *CrtY*, using a tuber specific promoter. This bacterial mini-pathway facilitated the increase in total carotenoids by 19.7-fold, obtaining high β-carotene levels.

1.3.3 Carotenoid storage in plants

Plastids are organelles found in cells of all higher and lower plants, including algae. They carry out a variety of functions vital for the organism's growth, according to the type of cell in which they reside (Pyke, 1999). The result of an endosymbiosis event (reviewed in Cavalier Smith, 2000), chloroplasts have transferred most of their genes to the cell nucleus. The chloroplast genome contains rarely over 200 genes, whereas its proteome is estimated to be made of 3500 to 4000 polypeptides (Race *et al*., 1999).

The accumulation of carotenoids occurs in the differentiated plastids of flowers, fruits, seeds and roots, with storage in chloroplasts (green plastids with photosynthetic role) and chromoplasts (coloured plastids), as well as amyloplasts (starch-storing plastids), leucoplasts (colourless plastids), etioplasts (dark grown chloroplasts) and elaioplasts (lipid–storing plastids, routinely found in seed; Figure 8; reviewed in Cazzonelli and Pogson, 2010). In order to store carotenoids, a lipophilic environment is required within the membranes of plastids, turning these organelles into sinks for carotenoid deposition.

Chromoplasts accumulating carotenoids synthesise them as a membrane-bound product, followed by deposition of the pigments into the lipid-bilayer. However, in order to limit any alteration of the physico-chemical properties of membrane, it is thought that the cells develop new sites for carotenoid storage in the stroma, but information is still scarce. The newly formed sites, in the form of lipid globules (plastoglobules) and specialized proteins, direct the organization of fibrillar carotenoid-containing structures (Deruere *et al.*, 1994) or crystals (reviewed in Camara *et al.*, 1995).

The regulation of carotenoid accumulation and storage was found to be influenced by a wide range of factors. Despite research concerning the chromoplast differentiation pathway in ripening fruits of *Solanaceae* and *Citrus* species (Mayfield and Huff, 1986; Lawrence *et al.*, 1997), the molecular genetic mechanisms controlling this process are yet poorly understood.

The esterification of carotenoids is one of the important processes considered to impact on the sequestration of these pigments into chromoplasts. The formation of carotenoids during ripening processes in the cells involves the progressive esterification of xanthophylls with fatty acids, producing a multitude of non-esterified carotenoids and their corresponding mono and diesters (Mínguez-Mosquera and Hornero-Méndez, 1994). This facilitates the incorporation of the more lipophilic carotenoids into the membrane and plastoglobule structures (Hornero-Méndez and Mínguez-Mosquera, 2000). Studies have previously documented the importance of esterification for carotenoid sequestration into the chromoplasts of peppers (Mínguez-Mosquera and Hornero-Méndez, 1994; Hornero-Méndez and Mínguez-Mosquera, 2000). Also, research has shown that a high proportion of carotenoids are esterified in the development of petals from flowers of marigold and *Eustoma* (Moehs *et al*., 2001; Nakayama *et al*., 2006).

It is known that carotenoid levels are modulated by the activity of carotenoid biosynthetic genes. However, recent studies have investigated the sub-cellular localisation of carotenoid biosynthetic enzymes in several species, adding much needed information to our understanding of it. The different localisations of carotenoid biosynthetic enzymes depend on the type of plastid which accumulates it.

In Narcissus, PSY was found in two forms, with different solubility. The insoluble membrane-bound form is highly active, whereas the soluble form is only active when supplemented with galactolipids (Schledz *et al*., 1996). By using import assays into pea chloroplasts, it was shown that the Arabidopsis PSY and the tomato PSY1 associate peripherally to the thylakoid membrane (Bonk *et al*., 1997; Fraser *et al*., 2000). In tomato and pepper chromoplasts, PSY was shown to be integrated into a high molecular mass complex of *ca*. 200 kDa, that also contains the IDI and GGDD enzymes (Camara, 1993; Fraser *et al*., 2000).

There are two types of carotenoid hydroxylases found in plants. The first is the non-heme di-iron enzymes BCH or HYD type, resembling the bacteriae crtZ and the cyanobacteriae CrtR-B enzymes (such as CrtRb2) that catalyse the hydroxylation of β rings. The second is the CYP97 type, the cytochrome P450 enzymes, that catalyse the hydroxylation of both β and ε rings (reviewed in Ruiz-Sola and Rodriguez-Concepcion, 2012). The three Arabidopsis CYP97 proteins have been shown to accumulate in chloroplast membranes (Joyard *et al*., 2009; Ferro *et al*., 2010). Until recently, there was some evidence to suggest the accumulation of BCH1 and BCH2 in the envelope or thylakoid membranes of chloroplasts (Cunningham and Gantt, 1998), but with no experimental data to further document their sub-plastidial localisation. Recently, Quinlan *et al*. (2012) tested the localisation of the both HYD and CYP97-types of hydroxylases. By using pea chloroplast import studies, they confirmed predictions that HYD4 localises in the membrane fraction as an integral protein. Furthermore, by testing three Arabidopsis CYP97 proteins, Quinlan *et al*. (2012) concluded these were only peripherally associated with membranes.

In 1994, Misawa *et al*. documented the localisation of PSY from ripe tomato fruits in the stroma of chromoplasts. The work of Welsch *et al*. (2000) in leaves of white mustard (*Sinapis alba* L.) presented data supporting the localisation of the endogenous PSY in the thylakoid membrane fraction of cotyledon chloroplasts. Another study by Li *et al.* (2008) reported the presence of PSY1 in the amyloplast membrane of maize endosperm cells. The study by Du *et al*. (2010) localized the rice *β-CAROTENE HYDROXYLASE* gene, *DSM2*, in the chloroplasts of leaf mesophyll cells.

Also, Thabet *et al.* (2012) have established cells from the medicinal plant, *Catharanthus roseus* (rose periwinckel) transiently transformed with a yellow fluorescent protein-fused construct, in order to obtain information on the sub-cellular localisation of GGPS. Their experiments indicated that CrGGPS is plastid-localized, within stroma and stromules. Another study by Linden *et al*. (1993) has shown that, in chloroplasts, carotenoids are found in both outer envelope membrane (OEM) and thylakoid membranes.

Plastoglobules (PGs) are lipoprotein particles with a double role as lipid biosynthesis and storage sub-compartments of thylakoid membranes in plastids (Austin *et al.*, 2006). It is known they store carotenoids (Steinmuller and Tevini, 1985; Vishnevetsky *et al*., 1999), but PGs were also shown to play a specific enzymatic role in carotenoid biosynthesis. Such an example is the proteomic analysis of PGs from chromoplasts of ripe red peppers, carried out by Ytterberg *et al.* (2006), who identified Z-carotene desaturase, lycopene β-cyclase, and two β-carotene β-hydroxylases in the PG proteome, indicating this as a site for carotenoid conversions. Also, it is thought that plastid-located carotenoids associate with binding proteins, which were found to enhance carotenoid accumulation (reviewed in Vishnevetsky *et al.*, 1999). Such an example is a protein responsible for the formation of PGs and fibrils in chromoplasts, fibrillin, believed to elevate carotenoid levels due to an increased sink effect (Simkin *et al.*, 2007).

Carotenoid production and accumulation can be modulated by the control of plastid biogenesis in plants (Giuliano *et al*., 2008; Pogson and Albrecht, 2011; for review, Cuttriss *et al*., 2007; Lu *et al.*, 2006). As demonstrated by the *high pigment* tomato mutants, *hp1* (Cookson *et al.*, 2003) and *hp3* (Galpaz *et al*., 2008). The *hp3* mutant has a mutation in the *ZEP* gene, thus reducing the amount of carotenoids downstream of zeaxanthin, a precusor of ABA, and resulting in a significant reduction in fruit size and production. This correlates with an upregulation of *FtsZ*, a gene encoding a tubulin-like protein with a role in plastid division (Osteryoung and Vierling, 1995). Cumulated, these effects give a 2-fold increase in the number of plastids and significantly greater plastid size. As a result, these mutants contain up to 35% greater levels of pigments in tomato fruits (Galpaz *et al*, 2008).

The study of the *suffulta* tomato mutant constitutes another example of plastid development influencing pigment accumulation. It was found that this mutation results in a reduced number of greatly enlarged chloroplasts in leaf and stem cells of tomato plants (Forth and Pyke, 2006). The mature green fruits of tomato were generally paler in two of the three mutant alleles investigated, with a reduction in total chlorophyll levels up to 30%. Interestingly, in red ripe tomato fruit, one allele of the mutation produced a reduction of 60% in carotenoid levels, when compared to controls (Forth and Pyke, 2006). Another relevant mutant, illustrating how plastid differentiation can control carotenoid accumulation in plants, is the cauliflower orange curd (*Or*) mutation (Li *et al.*, 2001). The naturally occurring *Or* gene mutation, initially discovered in cauliflower (*Brassica oleracea* L. var. *botrytis*), is responsible for β-carotene accumulation in normally white curd (Lu and Li, 2008). Based on these findings, a role was attributed for the *Or* gene in the differentiation process of proplastids in the shoot and inflorescence meristems into chromoplasts (reviewed in Li and van Eck, 2007; Lu *et al*., 2006).

Plastid differentiation is interconvertible and these organelles can re-differentiate (Marano *et al.*, 1993) as seen with the change of chloroplasts into leucoplasts during petal development or etioplasts during dark treatments (Pyke and Page, 1998). In the majority of cases, chromoplasts and leucoplasts form by the re-differentiation of chloroplasts, but there have been reports of chromoplasts deriving directly from proplastids or amyloplasts (Marano *et al*., 1993). In a recent study, Horner *et al.* (2007) showed that amyloplasts from tobacco floral nectaries undergo changes in form and function, as they begin to accumulate carotenoids. The starch from the nectary is broken down and replaced by osmiophilic bodies, which contain needle-like carotenoid crystals of β-carotene.

It is widely known that potato tuber amyloplasts are responsible for storing vast amounts of starch grains, but there is little information on the type of plastid able to also accumulate the carotenoids that the plant produces in these storage organs. Visualisation by electron microscopy of pigmented tuber flesh failed to identify, up to date, any carotenoid storing structures (M. Taylor, unpublished), as documented with the carotenoid crystals from carrot (*Daucus carota*) root (Frey-Wyssling and Schwegler, 1965).

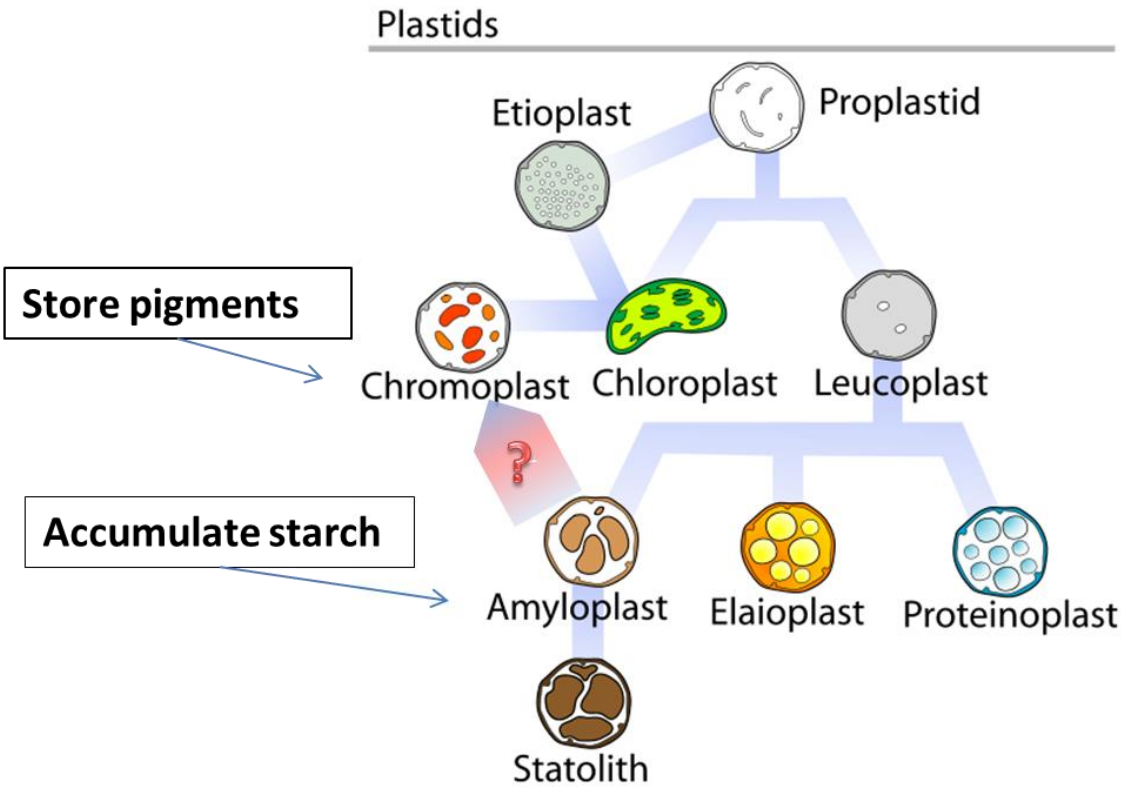

Figure 8. Types of plastids and their inter-conversion. All plastids differentiate from the colourless pluripotent progenitor-proplastid. Dependent on their type, proplastids have roles in photosynthesis (chloroplasts), storage of products like starch (amyloplasts) and gravitropism sensing (statoliths), accumulation of synthesis of fatty acids (elaioplasts) or coloured pigments (chromoplasts). Shaded bars between the types of plastids signify the relations of differentiation and interconversion. It is unclear if amyloplasts can evolve into chromoplasts by accumulating pigments. Adapted figure from source: http://en.wikipedia.org/wiki/File:Plastids_types_en.svg, accessed March 2012.

1.3.4 Degradation of carotenoids

As discussed in Section 1.3.2, manipulation of the carotenoid biosynthesis pathway can lead to enhanced accumulation in storage organs. However, new research has raised the question of how degradation or turnover of different carotenoids can constitute another mechanism regulating the levels of these pigments in crop plants. The levels of carotenoids in plants are dictated by the balance between their rate of synthesis and catabolism (Cuttriss *et al*., 2011). Investigation of these two processes in a recent study on $^{14}CO_2$ uptake showed rapid synthesis and, subsequently, degradation of carotenoids (Beisel *et al*., 2010).

As mentioned in Section 1.2.2., carotenoids serve as substrates for the production of compounds for the flavour and aroma of flowers and foods, such as β-cyclocitral, β-ionone, geranial, geranyl acetone, theaspirone, α-damascenone and β-damascenone (Bezman *et al*., 2005), but also of phytohormones and other signalling molecules in plants (reviewed in Cazzonelli, 2011). The first evidence of the degradation of carotenoids originated from independent studies by Olson (1964), Goodman and Huang (1965), Olson and Hayaishi (1965), when isolation of crude enzyme fractions from rat intestines and liver led them to report the enzymatic cleavage of β-carotene. Next, a study into viviparous maize seeds led to the identification of the *viviparous 14* (*VP14*) gene. This was shown to cleave 9-*cis*-epoxycarotenoids, the first committed step in ABA biosynthesis (Tan *et al*., 1997). From then on, homology based analysis on the *VP14* aided the identification of many apocarotenoid producing enzymes, known as carotenoid cleavage dioxygenases (CCDs).

An ancient gene family, the *CCD*s are found in bacteria, plants and animals (for review, see Kloer and Schulz, 2006). They have several common characteristics: they are metal proteins containing a Fe^{2+} atom, thought to be crucial for their catalytic activity (Redmond *et al.*, 2001), have four conserved histidines - possibly coordinating iron binding and a conserved C-terminus peptide sequence (Auldridge *et al*., 2006b). In Arabidopsis, there are nine members of the *CCD* family (*AtCCD1*,

AtCCD4, *AtCCD7*, *AtCCD8* and the 9-*cis*-epoxycarotenoid dioxygenases-*NCED2*, *NCED*3, *NCED5*, *NCED6* and *NCED9*). The NCED sub-family of enzymes are specific for 9-*cis*-epoxy carotenoids, such as 9′-*cis*-neoxanthin and 9-*cis*-violaxanthin, and includes the VP14 enzyme.

The *CCD* genes were shown to be responsible for the cleavage of *trans*-carotenoids, with some degree of promiscuity for their substrate selection. The plant NCEDs cleave the 11,12 double bonds of *cis*-carotenoids and CCD1 and CCD7 enzymes cleave the 9,10 double bonds of their respective carotenoid substrates (Auldridge *et al*., 2006b). The CCD1 enzyme from *Arabidopsis thaliana* (Schwartz *et al*., 2001) catalyses the cleavage of all *trans* and 9-*cis* epoxycarotenoids, resulting in the generation of apocarotenoid derived plant volatiles. In recent work, it was demonstrated that CCD1 also cleaves the 5′6′ and 7′8′ double bonds of lycopene and monocyclic carotenoids (Vogel *et al*., 2008; Huang *et al*., 2009b).

Another enzyme from the *CCD* gene family, cleaving apocarotenoids at the 9'10' position, CCD4 was shown to have two isoforms in chrysanthemum, *CmCCD4a* and *CmCCD4b*, with differential expression levels in stem and petals (Ohmiya *et al*., 2006). Following a study by Huang *et al*. (2009a), CCD4 failed to cleave both linear and hydroxyl group-containing carotenoids. Thus, it is now argued that CCD4 can only cleave non polar carotenoids, such as β-carotene (Rubio Moraga *et al*., 2009).

Research into the regulation of carotenoid accumulation by turnover has demonstrated close connection between these two mechanisms. The RNA interference (RNAi) silencing of *CmCCD4a* determined the transition from white to yellow coloured chrysanthemum petals (Ohmiya *et al*., 2006). Also, in avocado leaves, Foerster *et al*. (2009) found that changes in the equilibrium of biosynthesis/degradation of carotenoids constitute a mechanism for long-term adjustment of the carotenoid levels in these plant organs. Recently, a study by

Campbell *et al.* (2010) found elevated expression of the potato *CCD4* gene in mature tubers from white-fleshed cultivars, when compared with yellow-fleshed tubers.

Experiments studying long-distance signals in mutants that exhibited increased branching or tillering suggested that other factors in addition to auxins and CKs might also be involved in controlling bud outgrowth. Examples include the *Arabidopsis thaliana* (L.) *Heynh* (Arabidopsis) *more axillary growth* (*max*), pea (*Pisum sativum*) *ramosus* (*rms*), petunia (*Petunia hybrida*) *decreased apical dominance* (*dad*) and rice (*Oryza sativa*) *high tillering dwarf* (*htd*) mutants (Beveridge *et al.*, 1994; Napoli, 1996; Morris *et al.*, 2001; Stirnberg *et al.*, 2002; Sorefan *et al.*, 2003; Zou *et al.*, 2005; Simons *et al.*, 2007; Shimizu-Sato *et al.*, 2009). Studying these mutants led to the identification of SLs as carotenoid-derived plant hormones with a major role in determining axillary bud outgrowth (Gomez-Roldan *et al.*, 2008; Umehara *et al.*, 2008; reviewed in Dun *et al.*, 2009; Domagalska and Leyser, 2011; Gong *et al.*, 2012). There have been orthologs of the *max* mutants found in species such as petunia, pea, rice (Arite *et al.*, 2007), tomato (Vogel *et al.*, 2010; Kohlen *et al.*, 2012), kiwi fruit (*Actinidia chinensis*; Ledger *et al.*, 2010) and chrysanthemum (Liang *et al.*, 2010).

Although SLs are compounds long known for their role as germination stimulants (Cook *et al*. 1966; Cook *et al*., 1972,) and more recently, as pre-symbiotic branching factors for arbuscular mycorrhiza (Akiyama *et al*., 2005), it was lately shown that SLs are derived from carotenoids, through oxidative cleavage catalysed by CCDs. Overall, this suggests that the flux of carbon passing through the carotenoid biosynthetic pathway not only controls the supply of carotenoids in storage organs, but also regulates the generation of regulatory metabolites.

1.4 Aims of the present study

Recently, the use of molecular, genetic, biochemical and genomic approaches has enabled researchers to identify and characterize a nearly complete set of the genes and enzymes involved in carotenoid biosynthesis (Gong *et al.*, 2012). This has provided additional tools for manipulating the carotenoid content and composition in plants. These advances have motivated significant progress in the metabolic engineering of carotenogenesis, with studies successfully enhancing accumulation (Li and van Eck, 2007), developing novel compounds (Ralley *et al.*, 2004) and redirecting metabolite flux (Zhu *et al.*, 2008; reviewed in a number of excellent studies: Sandmann *et al*., 2006; Giuliano *et al*., 2008; Fraser and Bramley, 2009). However, the regulation of carotenoid biosynthesis is a complex process, not yet fully understood, despite the significant progress made over the last decade of carotenoid-related research.

The present study proposes two main strategies to investigate the regulation of carotenoid accumulation in potato tubers. The first strategy aimed to identify the sub-cellular localisation of key carotenoid biosynthetic enzymes, in the attempt to establish if this is one of the many factors that could influence the accumulation of carotenoids in potato tubers. The tagging of proteins with fluorescent markers such as the GFP from the jellyfish *Aequorea victoria* and red fluorescence protein RFP from *Discosoma striata* has been used for some time as a method that enabled researchers to visualize non pigmented plastids in plants (reviewed by Chiu *et al.*, 1996). For this purpose, CrtRb2 (β-carotene hydroxylase 2) and PSY were chosen to be fluorescently tagged and for their accumulation into a specific sub-cellular compartment of potato tuber cells to be established.

PSY1 and *PSY2* encode key enzymes in the carotenoid biosynthesis pathway in tomatoes, with PSY1 acting as a fruit and flower specific enzyme and PSY2 a green tissue isoform (Fraser *et al.*, 1994). Santos *et al.* (2005) has shown that the lack of phytoene synthesis is the step which limits the carotenoid pathway in white carrot

roots. The expression levels of βOH transcripts are also considered critical for carotenoid accumulation, as a study by D'Ambrosio *et al.* (2004) found a direct correlation between elevated xanthophyll levels and increased transcripts of this gene, in chloroplast and chromoplast containing tissues of hemizygous transgenic plants. Moreover, results from microarray data by Ducreux *et al.* (2008) have shown up-regulated expression of both *CrtRb2* and *PSY2* in carotenoid rich *Phureja* tubers.

Secondly, the degradation of carotenoids was addressed as a potential regulator of accumulation. Microarray experiments in potato have clearly shown enhanced expression of *CCD4* in white-fleshed potato tubers, with much lower expression levels in carotenoid accumulating yellow-fleshed potato tubers (Ducreux *et al.*, 2008). Recently, a study by Campbell *et al.* (2010) showed that, together with 2- to 5-fold increase in the levels of carotenoids in tubers, the down-regulation of *CCD4* led to a heat sprouting phenotype and formation of elongated shape chain tubers, implicating the CCD4 as a factor in tuber heat responses. The aim of the present study was to uncover the role of *CCD*8, another important member of the *CCD* gene family, in carotenoid accumulation and potato metabolism, by analysis and characterisation of transgenic *CCD8*-RNAi potato plants.

Chapter 2 Materials and Methods

2.1 Plasmids

2.1.2 pGENTR1a

pGENTR1a (3858 base pairs-bp; Figure 9) is a Gateway® system entry clone with attL1 and attL2 recombination sites, modified from the dual selection pENTR1a vector (Invitrogen, UK) by Sean Chapman (The James Hutton Institute-JHI, UK). The plasmid contains chloramphenicol and gentamycin resistance genes for selection in bacteria. Gateway vectors, such as pGENTR1a, contain the *ccdB* cytotoxic gene, a lethal gene that targets DNA gyrase, ensuring that the plasmid containing it cannot be propagated in standard *Escherichia coli* (*E.coli*) strains (Section 2.2.7 for details). The *ccdB* gene can be replaced by any DNA fragment cloned into the plasmid, a feature most useful for cloning purposes, as only cells containing a recombinant DNA give rise to viable clones in standard *E.coli* cells.

2.1.3 pGEM-T-Easy

pGEM®-T Easy (Promega, UK) are linear vectors with single 3′-terminus thymine overhangs at both termini, for convenient T/A cloning (Section 2.5.1). This high copy number plasmid contains T7 and SP6 RNA polymerase promoters, bordering a multi cloning site (MCS) with the α-peptide coding region of β-galactosidase for the blue/white visual screening of colonies. The plasmid contains a gene for ampicillin resistance in bacteria. Vector map is available at http://www.promega.com/products/pcr/pcr-cloning/pgem_t-easy-vector-systems/.

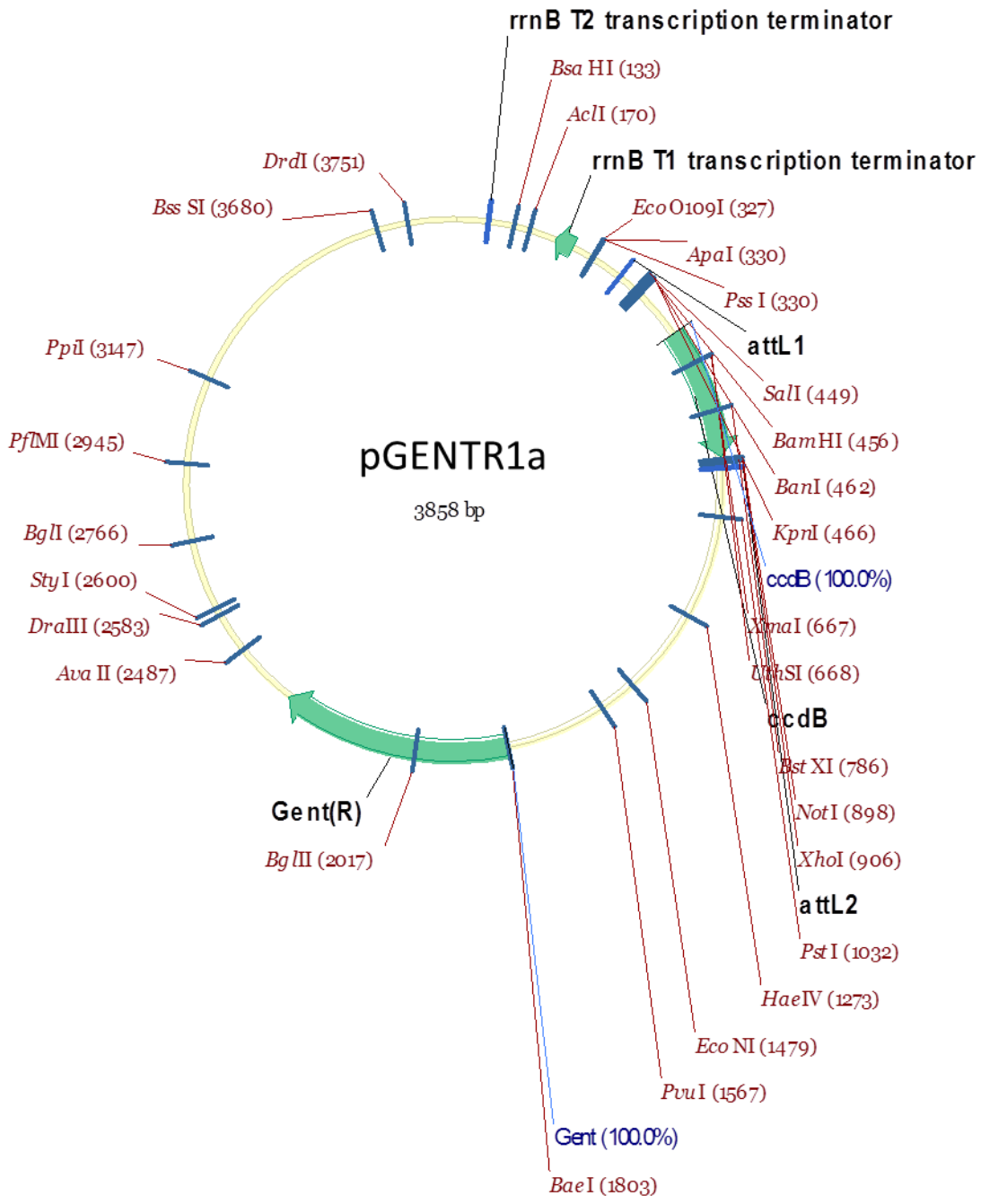

Figure 9. pGENTR1a vector map

2.1.4 pK7FWG2

Agrobacterium tumefaciens is known for its capacity to transfer a particular DNA segment (T-DNA) of its tumor-inducing (Ti) plasmid into the nucleus of infected plant cells (Zupan and Zambryski, 1995). The binary system of transfer and insertion of genes into the plant genome is based on these characteristics of *Agrobacterium*. Two separate plasmids are necessary in this binary system (Hooykaas and Schilperoort, 1992). First is a wide-host-range small replicon plasmid, containing the DNA fragment of interest, replacing the T-DNA, together with an origin of replication (*ori*), T-DNA borders and selection markers for bacteria. Second is a helper Ti plasmid, harbored in *Agrobacterium* cells, lacking the entire T-DNA region but containing an intact *virulence* (*vir*) region. For transformation (Section 2.3.2), the recombinant small replicon is transferred via bacterial conjugation or direct transfer to *Agrobacterium*, harboring a helper Ti plasmid (Tinland *et al.*, 1994), using the appropriate bacterial strains from Section 2.2. Plant cells are co-cultivated with *Agrobacterium*, to allow transfer of recombinant T-DNA into the plant genome and then grown under antibiotic selection.

pK7FWG2 is a binary destination clone designed to create a protein with a C-terminal fusion to GFP in the Gateway system (Figure 10). Available from Flanders Interuniversity Institute for Biotechnology (VIB, Ghent, Belgium), this vector is a 11880 bp binary plasmid with kanamycin and spectinomycin resistance genes for *in planta* and bacterial selection. It also contains the *ccdB* cytotoxic gene (Section 2.1.1 for details on this gene), so propagation of this vector can only be made using the DB3.1 competent cells (Section 2.2.7). The presence of attR1 and attR2 λ phage derived-recombination sites in the pK7FWG2 sequence facilitates transfer into this destination vector of the DNA fragments cloned into the pGENTR1a plasmid, by the Gateway reaction described in Sections 2.1.1 and 2.5.3. For further reference on this vector, refer to Karimi *et al.* (2002).

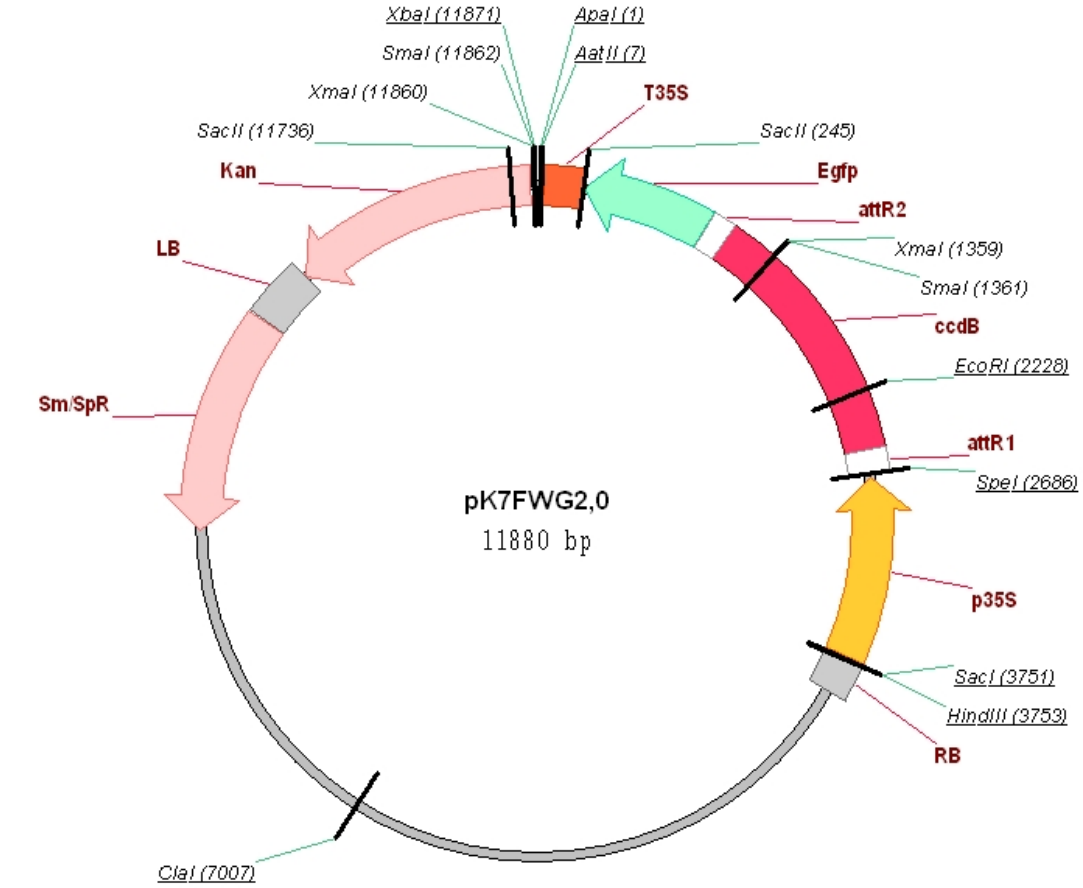

Figure 10. pK7FWG2 vector map

2.1.5 pK7RWG2

pK7RWG2 (11866 bp) is a destination vector, part of the Gateway cloning system, very similar to pK7FWG2 (Figure 11 for vector map), with a C-terminal fusion to RFP. For further reference, refer to Voinnet *et al*. (1999) and Karimi *et al*. (2002).

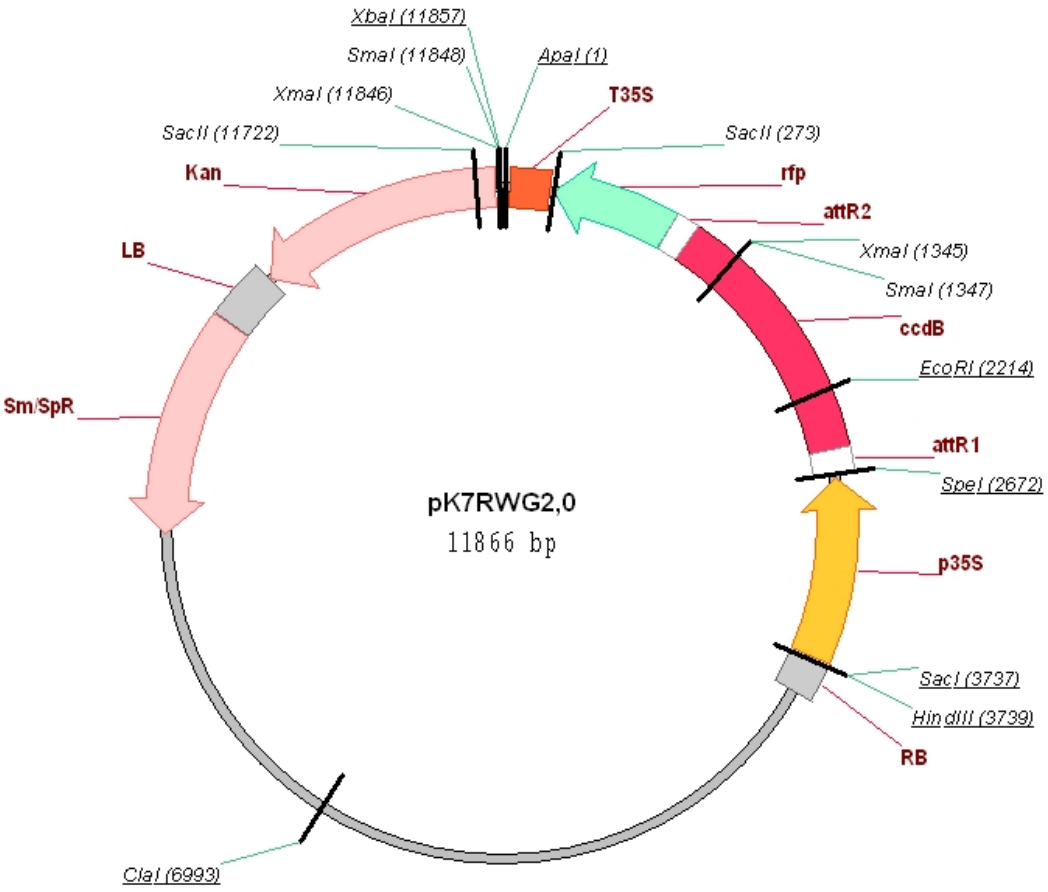

Figure 11. pK7RWG2 vector map

2.1.6 pP19K

Previous work in transient expression of proteins *via Agrobacterium*-mediated infection has established that post-transcriptional gene silencing (PTGS) is a limiting factor (Voinnet *et al.*, 1999). However, by mixing cultures carrying a standard binary expression vector for a suppressor of gene silencing with a binary expression vector for the gene of interest, the levels of expression can be highly increased. pP19K helper plasmid expresses the p19 protein from tomato bushy stunt virus (TBSV), demonstrated to be a PTGS suppressor (Voinnet *et al.*, 1999), under the control of the *Cauliflower Mosaic Virus* (*CaMV 35S*) constitutive promoter. This was kindly provided by Sean Chapman (JHI, UK) and used in combination with *Agrobacterium* cultures (Section 2.2.5), containing plasmids for transient expression.

2.1.7 pGreen mGFP 5ER 3'OCS

The pGreen mGFP 5ER 3′OCS (octopine synthase terminator) is a small (3 kb) Ti binary plasmid, based on the pGreen vector (Hellens *et al.*, 2000), but engineered by Petra Boevink (JHI, UK) to target the GFP signal to the endoplasmic reticulum (vector map and details at http://www.pgreen.ac.uk). The plasmid replicates to high copy numbers in *E. coli*, but replication in *Agrobacterium tumefaciens* requires the helper plasmid pSOUP (Section 2.2.6). The vector was used as a positive control in the confocal microscopy experiments, to check the transient expression of tagged proteins in mesophyll cells.

2.1.8 pHELLSGate 8

A hairpin RNAi silencing vector with the *ccdB* gene (Section 2.1.1 for details on this gene), pHellsgate 8 is able to accept inserts from Gateway™ entry vectors containing the gene of interest, flanked by *att*L in a single Gateway specific reaction (system obtained from Invitrogen, UK). For reference, see Helliwell *et al.* (2002).

2.2 Bacterial strains

2.2.1 *E. coli* DH5α

A strain of recombination-deficient suppressing cells, *E. coli* DH5α (Invitrogen, UK) is commonly used for the propagation of plasmids. Following transformation, the blue/white screening of colonies on plates containing (5-bromo-4-chloro-3-indoyl-β-D-galactopyranoside) X-gal or Bluo-gal can be used to detect cells containing recombinant plasmid and making use of the *lacZ*ΔM15's α-complementation of the β-galactosidase gene. These cells have been used for transformation of ligation reactions (Section 2.11.5 for details) and propagation of plasmid DNA from Section 2.1.2.

2.2.2 OneShot® TOP10 Electrocomp™ *E. coli*

Electro-competent *E. coli* cells, One Shot® TOP10 Electrocomp™ provide high efficiency cloning and propagation for high-copy plasmids, yielding more than 1×10^8 transformations μg^{-1} monomer pUC19 with non-saturating amounts (50 pg) of DNA. These cells also enable blue/white screening of colonies as detailed in the section above. The cells were supplied by Invitrogen, UK and used to transform ligations involving vectors from Sections 2.1.3 and 2.1.4.

2.2.3 ElectroMAX™ DH10B™

ElectroMAX™ DH10B™ (Invitrogen, UK) are electro-competent *E. coli* cells used for the transformation of ligation reactions (Section 2.3.2 for protocol) involving plasmids from Sections 2.1.1, as they enable efficient cloning of both prokaryotic and eukaryotic genomic DNA. They are equivalent to the cells described in the section above.

2.2.4 ElectroMAX™ *Agrobacterium tumefaciens* LBA4404

ElectroMAX™ *Agrobacterium tumefaciens LBA4404* cells are transformed by electroporation (Section 2.3.2), a method used to introduce polar molecules into a host cell through the cell membrane. These cells contain virulence functions

necessary for the transgression of the T-DNA region of binary transformation vectors into plants (Section 2.1.3 for details). The cells were purchased from Invitrogen, UK and used for transformation of plasmids from Section 2.1.4, designed for stable transformation of potato (Sections 2.7.3 to 2.7.7 for details on this method).

2.2.5 AGL1/pBBR1MCS1_ Vir G_{NS4D}

The AGL1/pBBR1MCS1_Vir G_{NS4D} electro-competent cells were kindly provided by Alison Roberts (JHI, UK). This *Agrobacterium tumefaciens* strain contains a helper plasmid with the carbenicillin resistance gene and an extra plasmid containing the virulence gene *G*, designed to elevate *vir* gene expression. The cells were used to transform (Section 2.3.2 for protocol) plasmid DNA from Sections 2.1.3 to 2.1.6 and express it transiently as detailed in Sections 2.7.1 to 2.7.2.

2.2.6 AGL1 pSOUP

These *Agrobacterium tumefaciens* electro-competent cells contain the pSOUP helper plasmid necessary for the replication functions of the pGreen plasmid (Section 2.1.6). Further information on the pGreen/pSoup system can be found at http://www.pgreen.ac.uk. For the transformation protocol, refer to Section 2.3.2.

2.2.7 DB3.1 *E. coli*

Library efficiency DB3.1™ competent cells (Invitrogen, UK) are recommended for the propagation of plasmids containing the *ccdB* cytotoxic gene. They contain the *gyr*A462 allele which renders the strain resistant to the toxic effects of this lethal gene (Section 2.1.1 for details). The DB3.1 competent cells were used for propagation of the Gateway plasmids from Sections 2.1.1, 2.1.3, 2.1.4 and 2.1.7. The transformation procedure is detailed in Section 2.3.1.

2.2.8 Preservation of bacterial cultures

Bacterial cultures of *E. coli* were grown overnight in Luria Bertani (LB) medium, supplemented with the appropriate antibiotics, at 37ºC, with gentle shaking. The

Agrobacterium tumefaciens strains were cultivated for two to three days, in similar medium with antibiotics, at 28ºC. Glycerol stocks were made by mixing 650 µl of the grown culture with 350 µl 50% glycerol (w/v), inverting several times and snap freezing the tubes in liquid nitrogen, before storing at -80ºC until required.

2.3 Transformation of competent cells

2.3.1 Transformation of competent *E. coli* by heat shock

For transformation of ligations, 2 to 5 µl un-purified reaction was mixed with 200 µl of competent *E. coli*, thawed on ice, followed by gentle pipetting to mix. The reaction was incubated on ice for 20 min and then transferred to a water bath at 42ºC for 60 s, before placing it on ice for 5 min. A 900 µl aliquot of SOC medium (Section 2.4.1) was quickly added to the transformation, with gentle mixing. The samples were incubated at 37ºC for one hour, with shaking at 225 rpm. Lastly, the mixture was plated on LB agar medium, with the suitable antibiotics to allow growth of the transformed plasmids.

2.3.2 Transformation of competent *E.coli* and *Agrobacterium* by electroporation

The transformation of electro-competent cells made use of a Bio-Rad electroporator MicroPulser, following the manufacturer's protocol for *E. coli* and *Agrobacterium* cells. A 40 µl aliquot of electro-competent cells was thawed on ice for five minutes and 1 to 2 µl of a ligation mixture or the relevant plasmid was added. After gentle pipetting, the mix was placed into a pre-chilled electroporation cuvette (Bio-Rad; 0.2 cm electrode gap) and transferred to the cuvette chamber of the electroporator. A pulse controller was used in addition to the standard protocol for electroporation, applying the following conditions: resistance 200 Ω; voltage 25 kV; capacitance 25 µF. A 900 µl aliquot of SOC medium (Section 2.4.1) was quickly added to the sample cells, which were then placed on an orbital shaker at 225 rpm, 37ºC for *E.coli* or 28ºC *Agrobacterium*, for one hour. The samples were plated onto LB agar medium, with relevant antibiotics selection.

2.4 Culture media and antibiotics

2.4.1 Bacterial culture media

Both Luria Bertani (LB) and SOC media were autoclaved and stored at room temperature (LB) or -20ºC (SOC).

Luria-Bertani (LB) medium:	
Tryptone	1.0% (w/v)
NaCl	1.0% (w/v)
Yeast extract	0.5% (w/v)
$MgSO_4.7H_20$	0.1% (w/v)

SOC medium:	
Tryptone	2.0% (w/v)
Glucose	20 mM
NaCl	10 mM
Yeast extract	0.5% (w/v)
MgCl	10 mM
KCl	2.5 mM

2.4.2 Tissue culture media

Murashige and Skoog (MS) medium was autoclaved and stored at room temperature until required. Each HB medium was freshly prepared by adding filter sterilized supplements, mixed thoroughly and stored at -20ºC.

MS-20 (Murashige and Skoog):	
2% (w/v)	Sucrose
0.5% (w/v)	Murashige and Skoog basal medium and vitamins (Melford)
0.8% (w/v)	Agar (Melford)
The pH was adjusted to 5.8 with 1 M NaOH.	

MS-30 (Murashige and Skoog):

Identical to MS-20 medium but with 3% (w/v) Sucrose

HB1 medium (MS-30 plus the following supplements):

0.02 mg l^{-1}	Gibberellic acid (GA_3)
0.2 mg l^{-1}	α-napthalene acetic acid (NAA)
2.5 mg l^{-1}	Zeatin riboside (ZR)

pH adjusted to 5.8 with 1 M NaOH.

HB2 medium (MS-30 plus the following supplements):

0.02 mg l^{-1}	Gibberellic acid (GA_3)
0.02 mg l^{-1}	α-napthalene acetic acid (NAA)
2.0 mg l^{-1}	Zeatin riboside (ZR)

pH adjusted to 5.8 with 1 M NaOH

2.4.3 Buffers

The agro-inoculation buffer was prepared fresh on the day, filter sterilized and kept on ice. Buffer A was filter sterilized and stored at room temperature. The RNA extraction buffer was made fresh on the day, from autoclaved stock solutions. The sprout release assay (SRA) buffer was prepared fresh on the day, and filter sterilized. The rest of the buffers were kept at -4°C.

Agro-inoculation buffer:

0.01M MgCl

0.01M MES buffer, pH 5.6

15 μM Acetosyringone

Buffer A for application of GR24 in the sprout release assay (Section 2.7.8):

4% PEG 1450

25% Ethanol

0.05% Acetone

2 X Ligation buffer (Promega):

30 mM Tris.HCl, pH 7.8

10 mM $MgCl_2$

10 mM DTT

1 mM ATP

10 X Buffer *PfuUltraII*:

200 mM Tris-HCl (pH 8.8 at 25°C)

100 mM $(NH_4)_2SO_4$

100 mM KC1

1% Triton X-100

1 mg ml^{-1} BSA

20 mM $MgSO_4$

RNA Extraction buffer:

50 mM Tris-HCl, pH 8.0

50 mM LiCl

5 mM EDTA

0.5 % SDS (w/v)

Sterile distilled water (SDW)

10 X Formaldehyde agarose gel buffer:

200 mM 3-[N-morpholino] propanesulfonic acid (MOPS) (free acid)

50 mM Sodium acetate

10 mM EDTA

pH to 7.0 with NaOH

RNA loading buffer:

0.55 % (w/v) Bromophenol blue
0.8 mM EDTA
0.23 M Formaldehyde
4 % (v/v) Glycerol
6 % (v/v) Formamide
0.8 % Formaldehyde Agarose gel buffer

SRA buffer:

20 mm MES
300 mM Mannitol
5 mM Ascorbic acid
pH adjusted to 6.5 using KOH

2.4.4 Antibiotics

Several types of antibiotics were used in this study, for selection purposes (Table 2). If not otherwise stated, the antibiotics were prepared with SDW and filter sterilized.

Table 2. Concentration of stock and working solutions of antibiotics. The type of antibiotic used was determined by the resistance genes on the plasmid for which selection was made (Sections 2.1 and 2.2). Cefotaxime has a broad spectrum of activity against Gram positive and negative bacteria and was used to block the division of *Agrobacterium*.

Antibiotic type	Concentration required			Concentration of the stock (mg ml^{-1})	Solvent used
	For *E. coli* (µg ml^{-1})	For *A.tumefaciens* (µg ml^{-1})	For plant selection (µg ml^{-1})		
Ampicillin	50-100	-		100	H_2O
Cefotaxime	-	250		125	H_2O
Chloramphenicol	50	-		100	MeOH
Gentamycin	15	-		50	H_2O
Kanamycin	100	100	50	100	H_2O
Rifampicin	-	100		50	MeOH
Spectinomycin	50-100	100		100	H_2O

2.4.5 Hormones

Concentration of hormones used in the sprout release assay (Section 2.7.8):

GR24	2.5 µM
6-benzylaminopurine (BAP)	50 µM
Giberellic $acid_3$ (GA_3)	50 µM

2.4.6 Fluorescent dye staining

The 3,3′-Dihexyloxacarbocyanine iodide ($DiOC_6$) fluorescent dye (Sigma Aldrich) was used to stain transgenic and control tuber tissue (Section 2.8.2). The lipophilic cationic properties of this dye, originally designed for mitochondria staining (Pringle *et al.*, 1989; Weisman *et al.*, 1990), make possible imaging of the nuclear envelope and endoplasmic reticulum, if the dye concentration is increased (Koning *et al.*, 1993). In time, the dye is incorporated into additional cellular membranes and hence $DiOC_6$ fluorescent dye was used to stain amyloplast membrane of potato cells. Soluble in dimethylsulphoxide (DMSO) and very sensitive to light, this dye was diluted to a stock of 1 to 2 mg ml^{-1}, with a working solution of 1 to 2 µg ml^{-1} in water. The wavelength used for excitation was 488 nm and the emission spectrum was collected from 505 to 530 nm, as detailed in Section 2.8.1.

2.5 Cloning systems

2.5.1 T/A cloning system

DNA fragments of interest were cloned into pGEM-T Easy vectors according to Promega's instructions. This type of vector contains a single thymidine base at the 3′ terminus that prevents the re-circularisation of its linearized form. For A/T cloning, PCR products were tagged by *Taq* polymerase with single 5′ adenosine overhangs, compatible with the 3′ thymidine bases present on the pGEM-T Easy vector (http://www.invitrogen.com/site/us/en/home/Products-and-Services/Applications/Cloning/PCR-cloning/ta-cloning.html?ICID=cvc-pcrcloning-c2t1 for details). The presence of several enzyme restriction sites on the MCS site permits the easy release of the cloned gene fragments. The ligation reactions were performed as in Section 2.11.5, followed by transformation into competent *E.coli* (Section 2.3.1).

As the MCS of the pGEM-T Easy vector is located within the α-peptide coding region for the enzyme β-galactosidase, the insertional deactivation of the enzyme allows identification of the recombinant clones by blue-white color selection on plates containing X-gal (32 μg ml^{-1}) and isopropyl- β-D-thiogalactopyranoside (IPTG; 32 μg ml^{-1}).

2.5.2 pGENTR1a cloning

Cloning of PCR products into pGENTR1a was necessary in order to introduce the desired gene fragments into the destination vectors by Gateway cloning (Section 2.5.3). The PCR products were released from the pGEM-T Easy vector by restriction digest and gel purified as detailed in Section 2.11.4, together with similarly digested 0.5 μg of pGENTR1a. The vector was dephosphorylated, as described in Section 2.11.6. The ligation reaction was performed as in Section 2.11.5, with overnight incubation at 4ºC. Transformation of the resulting plasmids was made into One Shot Top 10 electro-competent cells (Invitrogen, UK), as described in Section 2.3.2.

2.5.3 Gateway cloning system

The Gateway cloning system (Invitrogen, UK) is based on the presence of λ phage recombination sites in an entry clone such as pGENTR1a, containing the gene of interest and a destination vector (in this study, pK7FWG2 and pK7RWG2). The two plasmids recombine in the presence of an enzyme, specifically the LR Clonase (Invitrogen, UK), to give a final vector into which the gene of interest is cloned. The procedure was carried out as stated in the supplier's instructions, using 120 to 150 ng μl^{-1} of entry vector. After one hour incubation at 25ºC and inactivation of the reaction by proteinase K treatment, the resulting plasmids were transformed into electro-competent *E.coli* cells, as described in Section 2.3.2, using spectinomycin LB agar plates for selection of transformants.

2.6 Plant material

2.6.1 Potato

Seed tubers of potato cv. Desiree and Craig's Royal were kindly provided by Ralph Wilson (JHI, UK). Leaves from six to seven-week-old plants were infected with *Agrobacterium* inoculum, in the transient expression experiments (Section 2.7.2). Stable transformation of potato (detailed in Sections 2.7.3 to 2.7.7) used stocks of similar aged tissue culture grown potato plants, obtained from the Science and Advice for Scottish Agriculture (SASA, http://sasa.gov.uk).

2.6.2 Nicotiana benthamiana

Seed of *Nicotiana benthamiana* Domin. was obtained from virus-free stocks maintained at The James Hutton Institute. Leaves from six to eight-week-old healthy plants were used for agro-infiltration in the transient expression experiment (Section 2.7.2).

2.6.3 Growth conditions

The potato plants were obtained from seed tubers planted in 30 cm diameter pots containing a compost mix of: 85 % (v/v) Irish moss peat; 7 % (v/v) Pavoir sand; 7 % (v/v) Perlite; 0.2 % (w/v) limestone (magnesium); 0.2 % (w/v) limestone (calcium); 0.1 % (w/v) Sincrostart base fertilizer (William Sinclair, Lincoln, UK); 0.1 % (w/v) Celcote wetting agent (LBS Horticulture, Lancashire, UK) 0.15 % (w/v) Osmocote mini controlled release fertilizer (Scotts, Humberside, UK) and 0.03 % (w/v) Intercept insecticide (Bayer CropScience, UK). The *Nicotiana benthamiana* plants were sown in the same compost as potato plants, but in 10 cm diameter pots. Growth was maintained in a glasshouse with a daytime temperature of 20ºC and night time of 15ºC. The light intensity varied between 400 and 1000 µmol m^{-2} s^{-1} with a mean day length of 16 hours.

2.6.4 Maintaining stocks

For stable transformation of potato (Sections 2.7.3 to 2.7.7), a stock of *Solanum tuberosum* L. cv. Desiree was maintained by sub-culturing internodes from five to six weeks old tissue culture plantlets onto fresh MS-20 medium (Section 2.4.2). Growth conditions were 18 to 22ºC under artificial lighting (16 h light 8 h dark cycle 100 µmol m^{-2} s^{-1}). Plants were sub-cultured every three to four weeks by transferring actively growing apices to new medium.

2.6.5 Production of microtubers

Single nodes originating from one-month-old, tissue-culture-grown potato plantlets, were excised from the lower stem of the plants. Eight explants were then transferred onto the solidified MS-20 medium and supplemented with the respective chemicals, depending on the treatment applied (Section 2.4.5). After sealing the plates with Nescofilm, a sterile scalpel was used to make a side vent, covered with Micropore tape. The explants were grown in total darkness at 20ºC for four weeks, with monitoring at regular intervals.

2.6.6 Harvesting material

Potato tubers for microscopy were harvested from developing potato plants, grown as in Section 2.6.3. For extraction of nucleic acids, tap water washed potato material such as leaf, stem, root, stolons and tubers, was quickly dried and snap-frozen in liquid nitrogen, followed by storage at -80ºC until analysis.

2.7 Protocols

2.7.1 Bacterial cultures for transient inoculation

The expression clones from Section 4.2.1 were electroporated (Section 2.3.2) into *Agrobacterium tumefaciens* AGL1 cells, with the *vir G* expression enhancer (Cho and Winans, 2005). Also, the pP19K helper plasmid (Section 2.1.5), was transformed into AGL1/vir G cells. The control used for all transient experiments, expressing GFP, was the pGreen mGFP5ER (Section 2.1.6), transformed by electroporation into AGL1/ pSoup cells (Section 2.2.6). After selection of transformants on plates with LB medium and the corresponding antibiotics, liquid cultures of these constructs were initiated from single colonies. The cultures were then grown at 37ºC overnight, in the case of *E. coli* and at 28ºC for two to three days, for *Agrobacterium* cells. On the day of inoculation, the liquid cultures were pelleted by centrifugation at 2000 × *g* for 15 min and re-suspended in freshly prepared agro-inoculation buffer (Section 2.4.3), to an OD_{600} of 0.3-0.6, where 0.1 is equal to 1×10^{x6} cells ml^{-1}.

2.7.2 Leaf inoculation of *Nicotiana benthamiana* and potato

The *Agrobacterium* cultures for transient transformation (Section 2.2.5) were re-suspended in infiltration medium (Section 2.4.3) as mentioned above, to give suspensions with a concentration of OD_{600}~ 0.1-0.2. The pP19K/AGL1/pVirG cells were mixed in with suspensions of similar concentration, containing the gene of interest into a pK7RWG2 or pK7FWG2/AGL1/pVirG plasmid, to give a final OD_{600} of 0.1. The cultures were inoculated into wounded *Nicotiana benthamiana* and potato mature leaves, by using a sterile plastic syringe, according to the method described by Bendahmane *et al.* (2000). For analysis, the infected leaves were collected at 2, 3 and 4 days post inoculation (dpi) and imaged on a confocal laser scanning microscope-CLSM (Section 2.8.1 for details).

2.7.3 Tissue culture techniques for stable transformation of potato

The tissue culture practices were carried out in a laminar air flow cabinet cleaned with 70% (v/v) ethanol, to ensure sterile conditions. The growth media and antibiotics used were filter sterilized and all pipette tips and handling material were sterilised by autoclaving.

2.7.4 Explants for transformation

Internodes originating from five to six weeks old potato plantlets cv. Desiree were cultured into a high-hormone solution (MS-30, 10 μg ml^{-1} NAA, 10 μg ml^{-1} zeatin riboside) overnight, prior to transformation.

2.7.5 *Agrobacterium* for transformation

Liquid cultures were initiated for each construct transformed (Section 2.3) into *Agrobacterium* cells. Single colonies were inoculated into 5 ml Luria Bertani (LB) medium supplemented with kanamycin and rifampicin (100 μg ml^{-1}) and then grown overnight at 28ºC, with 150 rpm shaking. Subsequently, 1 ml of this overnight culture was grown into 50 ml LB medium containing 50 mg l^{-1} kanamycin monosulphate, as above, until an optimal OD_{600} of 0.1-0.2 was reached. Then, cells of *Agrobacterium* culture were centrifuged at 1500 x *g* for ten minutes, the supernatant removed and the pellet re-suspended in 5 ml MS-20.

2.7.6 Co-cultivation

A numer of 150 to 200 potato explants from cv. Desiree, together with 1 ml of the transformed *Agrobacterium*, were cultured for one hour at 28ºC, with gentle shaking (50 rpm). Once removed, the explants were then blotted dry on sterile filter paper and grown on HB1 medium (Section 2.4.2) under low light conditions (15 μmol m^2. s^{-1} photosynthetic photon flux density) at 18 to 22ºC. After 24 h, the co-cultivated explants were transferred onto fresh HB1 regeneration medium, supplemented with 500 μg ml^{-1} cefotaxime.

2.7.7 Selection and regeneration of independent transgenic lines

The explants were removed from the HB1 medium containing cefotaxime after 14 days and sub-cultured onto HB2CK plates (HB2 medium containing 100 µg ml^{-1} kanamycin and 250 µg ml^{-1} cefotaxime), every two weeks. Once shoots originating from the regenerated calli formed, they were excised and further grown onto MS-20CK selection medium (MS-20 containing 100 µg ml^{-1} kanamycin and 250 µg ml^{-1} cefotaxime). Only the shoots which rooted directly from the base cut end were considered to be putative transgenic plants. Moreover, they were subjected to two rounds of selection on regeneration medium supplemented with antibiotics. Finally, the surviving shoots were moved onto fresh MS-20 medium for four to six weeks before being grown in the glasshouse.

2.7.8 Sprout release assay

For the sprout release experiment, potato tubers stored at 4ºC for three to four months were selected. The required numbers of transgenic and control potato tubers were carefully washed with tap water, ensuring not to dislodge any eyes. After a further rinse in sterile distilled water, the material was dried using tissue paper. Next, pieces of potato containing one eye, mostly from the superior part of the tuber, were excised using a cork borer size 2 and then cut to give cores of 5 mm in length. The respective buds were washed three times for 15 min in SRA buffer (Section 2.4.3), with gentle agitation, and rinsed in sterile distilled water for an extra 15 min. After drying the tuber discs on sterile filter paper, the material was incubated in 30 ml of the appropriate solution for 5 min, with gentle shaking. Meanwhile, Petri dishes with water soaked sterile filter paper were prepared. After a gentle drying of the tuber discs with sterile filter paper, the tuber cores were carefully placed in the previously prepared dishes, followed by an application of 10 µl of 2.5 µM GR24 in Buffer A (Section 2.4.3) or a Buffer A for the control, and left to dry for 5 min. The plates were sealed with Nescofilm, covered with aluminium foil and kept in the dark, at room temperature. Bud movement and sprout growth was monitored once daily for 7 to 10 days.

2.8 Microscopy

2.8.1 Confocal imaging Leica SP2

The precise localisation of the proteins of interest, tagged with GFP/RFP in the transformed leaf or tuber material, was investigated on an upright CLSM (Leica Microsystems Ltd, UK), equipped with a TCS-SP2 scanning head and Argon and Krypton lasers. For CLSM purposes, cells were imaged with a 63x/1.2 Planapo objective and recorded at 1024 x 1024 pixels per image. The captured images were analysed with the TCS SP software, provided by the manufacturing company (Leica Microsystems, Heidelberg, Germany) and assigned false-colouring: green for GFP and $DiOC_6$ fluorescence, magenta for RFP, blue for chlorophyll auto-fluorescence. The fluorescent molecules used for microscopy are detailed in Table 3.

2.8.2 Confocal imaging Zeiss LSM710

Potato tuber tissue and sap, prepared as detailed in Section 2.8.3 was imaged on a Zeiss LSM710 system (Zeiss Jena, Germany), fitted on an upright Axio Imager Z2 microscope and a Zeiss AxioCam HRc camera; cells were imaged using a C-Apochromat 63 x/1.2W Corr objective and recorded at 1024 x 1024 pixels per image. Once captured, the images were analysed with the Zen2010 software (Zeiss Jena, Germany) and assigned false-colouring, as in Section 2.8.1.

Table 3. Characterisation of the fluorescent molecules used for confocal imaging. The GFP and RFP fluorescent emission came from proteins of interest, which were tagged at the C-terminus with these proteins. The $DiOC_6$ dye stains mitochondria, endoplasmic reticulum and other membranes in the cell. Chlorophyll auto-fluorescence was detected in leaf tissues.

Fluorescent molecule	Excitation maximum λ (wavelength) nm	Emission spectrum λ (wavelength) nm	Observations
GFP	488	510-532	Fusion protein, green fluorescence
RFP	563	600-644	Fusion protein, red fluorescence
$DiOC_6$	488	505-530	Carbocyanine iodide dye, green fluorescence
Chlorophyll	488	620-720	Based on its auto-fluorescence properties; red/far red fluorescence

2.8.3 Preparation of tuber tissue and fluorescent dye staining of amyloplasts

Tuber tissue from developing transgenic and control potato was cut into sections of 200 to 250 µm thickness, by using a 752M vibroslice from Campden Instruments Ltd, UK. The tissue was placed in SDW and briefly rinsed. Then, the tuber slices were incubated into $DiOC_6$ staining dye (purchased from Sigma Aldrich), diluted in water to a working concentration of 1 to 2 µg ml^{-1}, for two to three hours before imaging on the SP2 platform, as detailed in Section 2.8.1.

2.8.4 Bright field imaging Leica stereomicroscope

Whole tuber buds and transversal sections were imaged under a Leica MZFLIII stereo-microscope, equipped with a Leica DC500 digital camera.

2.8.5 Image processing and 3D

Confocal and bright field images were processed to decrease saturation and increase sharpness by adjusting light levels, using the Adobe Photoshop 6.0 software (Adobe Systems Inc., San Jose, CA, USA). Volume rendering and 3D models were constructed using the IMARIS software (Bitplane, Zurich).

2.9 Extraction of nucleic acids

2.9.1 Promega Miniprep extraction of DNA from plasmids

LB medium (5ml), containing the appropriate antibiotic for each of the plasmids/*E.coli* strains, was inoculated from a single colony and grown overnight at 37ºC. Then, plasmid DNA was extracted using the Wizard Plus SV Miniprep DNA Purification System (Promega), following the manufacturer's protocol. The extraction procedure is based on the principle that DNA binds to silica in the presence of chaotropic salts. Once cells or tissue have been disrupted and the plasmid released, the DNA binds to the silica membrane of the SV columns. Then, 100 µl of nuclease-free water was used to elute the purified DNA from the spin column.

2.9.2 Isolation of genomic DNA from fresh tissue

Two to three young leaves from potato plants, weighing between 0.1 to 0.15 g, were placed in 1.5 ml Eppendorf tubes, snap frozen in liquid nitrogen and ground to a powder. For isolation of the DNA, the Aqua Genomic Kit from MoBiTech, UK, was used, following the manufacturer's instructions: (http://www.mobitec.de/de/products/bio/06_dna_prot_tools/aquagenomic.html).

2.9.3 Isolation of RNA from freeze dried tissue

Freeze dried powdered tissue (1 to 2 g) was mixed in a sterile RNase free 50 ml Sorvall tube with 7 ml of hot (preheated at 80ºC) RNA extraction buffer (Section 2.4.3), supplemented with 50% (v/v) phenol and vortexed vigorously. Then, 10 ml of SDW and 16 ml of chloroform:isoamyl alcohol (24:1 v/v) were added, followed each time by a 2 min vortex. The tubes were centrifuged at 14000 x *g*, 4ºC, for 20 min. The supernatant was removed into a fresh, sterile 50 ml Sorvall tube, containing an equal volume of 4M LiCl and mixed thoroughly, before incubation at -80ºC until the next day. The sample was thawed on ice and centrifuged again at 14000 x *g*, 4ºC, for 40 minutes. After removal of the upper aqueous phase, the remaining pellet was re-suspended in a mixture of 5 ml SDW, 500 µl 3 M NaOAc, pH 5.2. Once dissolved,

15 ml 100 % ethanol were further added to the aqueous solution, followed by incubation at -80ºC for another one to two hours. After subsequent thawing, the solution was centrifuged at 14000 x *g*, 4ºC, for 40 minutes, in order to collect the precipitated RNA. The pellet obtained was washed with 10 ml ice-cold ethanol and centrifuged for an additional 40 min at 4ºC and 14000 x *g*. The ethanol was removed and the pellet dried on the bench, at room temperature, then re-suspended in 500 µl of RNase free water. Samples were kept at -20ºC for another hour, before a final centrifugation at 14000 x *g*, designed to sediment any remaining contaminants, followed by transfer of the extracted RNA to a fresh 1.5 ml Eppendorf tube. The samples were stored at -80ºC whilst awaiting analysis.

2.10 Analysis of extracted nucleic acids

2.10.1 Quantification of concentration by spectrophotometer

The concentrations of nucleic acids were routinely estimated using a NanoDrop® ND-1000 full-spectrum (220 to 750 nm) UV/Vis spectrophotometer. This apparatus measures the concentration of 1 µl of aqueous solutions of nucleic acids from its absorbance values, at a 50-fold higher concentration (3700 ng μl^{-1}) than samples measured by a standard cuvette spectrophotometer. For full details, see http://www.nanodrop.com/Library/nd-1000-v3.7-users-manual-8.5x11.pdf.

Absorbance of DNA and RNA samples was measured at 260 and 280 nm with a ratio of 1.8 accepted as 'pure' for DNA and a ratio of 2.0 'pure' for RNA. The generally accepted extinction coefficients for nucleic acids are 20 µl μg^{-1} cm^{-1} double-stranded DNA and 25 µl μg^{-1} cm^{-1} for RNA.

2.10.2 Gel electrophoresis

Agarose gels were made by mixing 0.5 to 1 g of agarose with 50 ml 1X Tris/Borate/EDTA (TBE) buffer, followed by heating on low power in a microwave oven for one to two min. The mixture was cooled to 65ºC and 1 µl of 10 mg ml^{-1} ethidium bromide was added, before casting the gel and leaving it to set for 30 min. The respective samples were loaded onto the gel, into the lanes formed by the previous insertion of a comb, and separated for 30 to 40 min by electrophoresis at 50 mA constant current, with sufficient 1X TBE buffer to cover the gel. Subsequent imaging was made under UV light, using a UVITech transiluminator (UVITech, Cambridge, UK).

2.10.3 DNA and RNA quality by gel electrophoresis

A volume of 5 µl of DNA samples, mixed with 1 µl of Lambda DNA/Hind III marker solution (Promega, UK) was separated on 1% and 2% agarose gels. A similar volume of total RNA samples was mixed with 1 µl of RNA loading buffer (Section 2.4.3) and denatured by heating to 70ºC for 10 min, prior to loading on the gel and imaging as stated above.

2.11 Enzymatic interactions with nucleic acids

2.11.1 Polymerase chain reactions

The polymerase chain reaction (PCR) was performed using two types of polymerases. The non-proof reading Go*Taq* Flexi DNA polymerase (Promega) was used for routine PCR reactions, where information on presence/absence/length in bp of a certain DNA fragment was needed. The total reaction volume of 50 µl contained 2 units (U) of Promega Go*Taq* DNA polymerase and 10 µl of the proprietary Green Go*Taq*® Reaction Buffer, together with 10 to 50 ng of template genomic DNA. Also, a set of gene-specific forward and reverse primers (concentration of 0.4 µM) were used, together with all four deoxynucleotides (dNTPs), at a concentration of 200 µM. The PCR fragments were generated using the following thermal cycling conditions: 3 min denaturation at 95ºC followed by 25 to 40 cycles of 95ºC for 30 s, 30 to 60 s at the appropriate melting temperature (Tm), which was typically between 3 to 5ºC below primer melting point, and a 60 s 72ºC extension time per 1kb of expected amplicon. Negative and, when possible, positive controls were employed for each PCR reaction.

The *PfuUltra™ II* Fusion HS DNA polymerase (Stratagene, Agilent Technologies), known for its high fidelity in DNA synthesis, was employed for amplification of fragments of interest designed to be cloned into vectors, for stable plant transformation (Sections 2.7.3 to 2.7.7). The polymerase has 3′ to 5′ exonuclease proof reading activity that enables the polymerase to correct nucleotide mis-incorporation errors, making it suitable for cloning applications (for details, http://www.genex.cl/stock/600670.pdf). In a final volume of 50 µl, 40.5 µl of distilled water was mixed with 5 µl 10x *PfuUltraII* reaction buffer (Section 2.4.3), 0.5 µl of dNTPs mix (25 mM each), 1 µl DNA template (100 ng μl^{-1}), 1 µl of the respective primers (each 10 mM) and 1 µl of the *PfuUltra™* II Fusion HS DNA polymerase. The amplification conditions were the following: 2 min denaturation at 95ºC followed by 15 to 30 cycles of 95ºC for 30 s, 30 to 60 s at the appropriate Tm (typically 3 to 5ºC below primer melting point), 15 s at 72ºC extension time, per 1kb of expected amplicon, together with a final step of 72ºC for 3 min.

2.11.2 Design of PCR and sequencing primers

Gene specific PCR primers were designed using the Vector NTI software (Invitrogen, UK), ckecking for primer dimers and hairpin formation. The sequences of the primers used are found in Sections 3.2.1 to 3.2.2, 4.2.1, 5.2.1 to 5.2.3.

2.11.3 Endonuclease restriction enzyme digest of DNA

The DNA to be digested (1 to 2 µg) was mixed gently with an optimal buffer, recommended by the restriction enzyme's manufacturer, in a 10-fold excess (between 10 to 20 units). Then, 1µl or 1 U of the enzyme was added to the reaction, followed by incubation at 37ºC for 2 to 3 hours. The digested DNA was imaged as detailed in Section 2.10.2.

2.11.4 DNA recovery from an agarose gel

Both restriction digested vector and DNA fragments were electrophoretically separated on agarose gels and cut out under blue light illumination. The QIAEX II gel extraction kit (Qiagen) was used for purification of the restriction fragments, as detailed in the manufacturer's protocols. Elution was made in 20 to 50 µl of SDW, storing the samples at 4ºC until ligation.

2.11.5 DNA ligation

The principle of ligating DNA fragments into a linearised plasmid makes use of the formation of new phosphodiester bonds between the phosphate residues at the 5' termini and the adjacent 3'-hydroxyl residues (Sambrook *et al.*, 1989). Molar ratios of 3:1, 1:1 and 1:3 insert to vector were used for all ligations. Vector DNA and the fragments to be inserted, in various molar ratios (1:3, 1:1 and 3:1 vector to insert) together with 1 unit or 1µl of T4 ligase (Promega) and its 2X buffer (Section 2.4.3) were mixed to a final volume of 20 µl. The samples were then left at room temperature for 40 min or at 4ºC overnight, before transforming 1 to 2 µl, undiluted, into competent cells. Positive and negative controls were set up with every ligation reaction.

2.11.6 Vector DNA dephosphorylation

Re-circularisation of vector DNA during cloning is a common issue when using restriction endonucleases to generate compatible cohesive ends for ligations. Hence, SAP (Shrimp Alkaline Phosphatase, Promega) was used on the linear plasmid, as it catalyses the dephosphorylation of 5' phosphates from DNA. According to the manufacturer's protocol, 1 U of SAP μg^{-1} vector digested DNA was placed at 37ºC for 15 min in 1X SAP buffer, to a final reaction volume of 30 to 50 µl. Unlike other type of phosphatases, SAP is irreversibly and completely inactivated by incubation at 65ºC for 15 min. The reaction was centrifuged and 1 to 2 µl were used for future ligations (as detailed in Section 2.11.5).

2.11.7 Purification of PCR products

The resulting samples from PCR reactions were purified using the Wizard SV purification kit (Promega), according the manufacturer's protocol. The purpose was to remove all traces of impurities, such as enzymes, salts from buffers and primers. The Wizard SV kit functions on the principle that DNA binds to a silica membrane in the presence of chaotropic salts, hence, after the PCR product is mixed with guanidine isothiocyanate, the centrifugation step will facilitate DNA binding to the silica membrane of the column. Before elution in 50 µl SDW, the DNA was washed several times with ethanol to remove any remaining impurities.

2.11.8 DNA sequencing

Sequencing of different plasmid vector fragments and PCR products, isolated and purified as stated above, using the relevant Promega and Qiagen kits, was carried out by the Genome Services facility based at JHI, using an automated ABI 3730 capillary-based sequencer and BigDye Terminator Cycle Sequencing Kit (Applied Biosystems).

2.11.9 Ethanol precipitation of DNA

The DNA precipitation by addition of ethanol was carried out by first calculating the volume of DNA being precipitated, then adding 1/10th volume of 3 M sodium

acetate, pH 5.2 and mixing thoroughly. Then, 2.5 volumes of ice cold 70% ethanol was added, mixed thoroughly and incubated at -80ºC for at least 30 min. Samples were then centrifuged for 15 min at 14000 x *g* and the supernatant decanted. Another 1 ml of 70 % ethanol was added, the sample briefly centrifuged and the supernatant removed. The DNA pellet was left to air dry for approximately 15 min, before re-suspension in an appropriate volume of 10 mM Tris pH 7.2.

2.11.10 Purification of RNA

For purification, 100 µg of RNA from each sample was purified using the silica-membrane spin columns from the RNeasy Mini kit (Qiagen), following the manufacturer's instructions. The resulting RNA was checked for concentration and quality as described in Sections 2.10.1 and 2.10.3.

2.11.11 DNase I treatment of RNA

In order to remove contaminating genomic DNA from the final total RNA samples, a DNase I (Qiagen) treatment was applied at the time of the purification step from above, performed as detailed in the supplier's instructions.

2.11.12 cDNA synthesis

For qRT-PCR analysis, cDNA was synthesized from the respective purified RNA samples. This reverse transcription process of 5 µg of DNase I treated total RNA was carried out using Invitrogen Superscript III Reverse Transcriptase (Invitrogen Life Technologies, Carlsbad, California, USA). A mixture of 50 ng of random hexamers (pdN_6, Amersham Biosciences) was added to the RNA, along with 1 µl of 10 mM dNTP mix. The volume was made up to 13 µl using RNase free water and the samples were placed on a heating block for 5 min, at 65ºC. After at least 1 min on ice, 10 µl of 2X RT buffer, 4 µl of 25 mM $MgCl_2$, 2 µl of 100 mM DTT and 1 µl Superscript III reverse transcriptase (200 Units per µl) were added to the samples, followed by vortexing and incubating at 25ºC for 10 min. The reverse transcription reaction was allowed to proceed by incubation at 50ºC, for 50 min. Then, the enzyme was deactivated by incubation at 85ºC for 5 min.

2.11.13 Universal probe system based qRT-PCR

A quantity of 25 ng of first strand cDNA, synthesized as stated in Section 2.11.12, was used as template for qRT-PCR. The Universal Probe Library-UPL (http://www.roche-applied-science.com/sis/rtpcr/upl/ezhome.html), a system that employs an online assay design software and 165 pre-validated, real-time PCR probes, is designed to avoid non-specific signal from related sequences and primer dimers. In short, the sequence of the gene of interest was introduced in the assay designer tool, resulting in the design of a set of primers spanning the probe. These were manually checked as in Section 2.11.2. Next, the sets of primers for both the gene of interest and the internal control gene, *ELONGATION FACTOR 1α* (*EF-1α*; Long *et al.*, 2010) were validated in an experiment using the software built-in method for standard curve design. The standard qRT-PCR reaction of 25 µl contained 1 X FastStart *Taq*Man® Probe Master, 0.2 µM gene specific primers and 0.1 µM probe. The samples were amplified using a StepOnePlus Real-Time PCR system thermal cycling block from Applied Biosystems. Thermal cycling conditions were: 10 min denaturation at 95ºC followed by 40 cycles of 15 s at 95ºC, 1 min at 60ºC. All reactions were carried out in triplicate. The values obtained were interpreted in a relative quantitative manner, using the ΔΔCT method (Livak, 1997)

2.12 Biochemical analysis

2.12.1 Carotenoid extraction from tissue plants

Carotenoid extractions were all performed under subdued artificial light conditions, in order to prevent changes in the carotenoid composition of the samples. Between 1 to 2 g of freeze dried plant tissue, harvested as in Section 2.6.6 and ground into a fine powder, was mixed in a 15 ml polypropylene tube with approximately 500 mg of a mixture (1:1:1) of acid washed sand (for cell disruption), sodium bicarbonate (to neutralize degrading acids) and anhydrous sodium sulphate (to remove any residual moisture). A volume of 5 ml 100% acetone was added to the tubes, followed by one hour on a Stuart SB2 Fixed Speed Rotator (Bibby Scientific Ltd, UK). Samples were then centrifuged at 4ºC for 5 min at 4500 x *g* and the supernatant passed through a 0.2 µm Whatman anotop-10 filter, into a fresh 15 ml graduated polypropylene tube. A note was taken of the volume obtained and a 1 ml aliquot was used for spectrophotometric estimation of the carotenoids, as detailed in Section 2.12.3. To finish, the samples were dried down under a gentle stream of oxygen-free nitrogen (BOC gasses) and stored at -80ºC prior to HPLC analysis.

2.12.2 Saponification procedure of carotenoid esters

In general, the carotenoids with naturally occurring hydroxycarotenoids (i.e. lutein, zeaxanthin, β-cryptoxanthin) and violaxanthin (an epoxycarotenoid) are esterified with straight chain fatty acids such as lauric, myristic, and palmitic acids, making them difficult to separate chromatographically. Hence, these samples are customarily saponified to remove the fatty acids and liberate the parent carotenoids (Khachik *et al.*, 1991). Dried carotenoid extracts, obtained as in Section 2.12.1, were re-suspended in 5 ml of methanolic potassium hydroxide (10 % w/v in 100 % methanol). After transfer into 20 ml glass quick-fit tubes, the samples were kept overnight at 4ºC under nitrogen, in the dark. Next, 10 ml of degassed diethyl ether was added along with enough saturated NaCl to form two layers (typically 5 ml). The upper layer was transferred into a fresh 20 ml glass tube and washed with 10 ml SDW. The sample formed two layers, with the top aqueous phase being removed

into a new 15 ml graduated polypropylene tube and dried under a gentle stream of oxygen-free nitrogen (Britton, 1985).

2.12.3 Total carotenoid content

The total carotenoid content was estimated by spectrophotometry, as detailed by previous studies (Schiedt and Liaaen-Jensen, 1995). For calculations, the following formula was applied, where *x* - represents the amount in g of carotenoids; *y* - the amount in ml of solution in which x is found; *E* - the extinction coefficient of a particular carotenoid (assuming a value of 2500 M^{-1} cm^{-1} for total carotenoid estimation); *x* gives an absorbance A_{450nm}, so assuming an one cm path cuvette, we have:

$$x = A_{450nm} \times y / (E \times 100)$$

2.12.4 Analysis of strigolactone content in potato root tissue

For extraction of strigolactone from root tissues, potato plants were grown under control and phosphate starvation conditions, as described by Lopez-Raez *et al*. (2008) for tomato, making use of an aeroponics system from http://nutriculture.com/index.htm,. Once harvested, tissue was frozen in liquid nitrogen and freeze dried. The procedure of extraction was carried out as detailed by Lopez-Raez *et al*. (2008). The combined dried fractions were resuspended into 250 µl of acetonitrile:water (25:75 v/v) and filtered through Minisart SRP4 0.45 µm filters (Sartorius, Goettingen, Germany), before the analysis on the High Performance Liquid Chromatography-Mass Spectrometry (HPLC-MS-MS), as in Lopez-Raez *et al.* (2008).

2.12.5 HPLC

The carotenoid standards required for HPLC analysis were acquired from www.carotenature.com. Compounds such as β-carotene, β-cryptoxanthin, lutein, zeaxanthin, neoxanthin and violaxanthin were aliquoted and stored at -80ºC, in the dark. The HPLC separation of carotenoids was carried out by using a Phenomenex

Spherisorb ODS-2 5 µm 250 × 4.6 mm reverse phase C_{18} column and a binary solvent gradient of 0 to 40% Solvent B (0-20 min), 40 to 60% Sovent B (20-25 min), 60 to 100% Sovent B (25-26 min), 100% Solvent B (26-35 min), 100–0% B (35-36 min) at a flow rate of 1 ml min^{-1} (A= acetonitrile/water 9:1 (v/v); B= 100 % ethyl acetate). The column was allowed to re-equilibrate in 100% A for 10 min between injections. Peak responses were detected using a variable UV-Vis detector set at 450 nm on a Gynkotek UVD340 detector using Dionex Chromeleon software version 6.60. The remainder of the HPLC equipment consisted of a Dionex UltiMate 3000 autosampler and a Gykotek p580-A LPG pump. For calculations, each of the carotenoid concentrations was obtained by comparison of their relative proportions, as reflected by the integrated HPLC peak areas, to the total carotenoid content determined by spectrophotometry, detailed in Section 2.12.3.

2.12.6 Chlorophyll extractions

In order to accurately measure the chlorophyll content of potato leaves, a DMSO mediated extraction and subsequent measurement of the sample's absorbance on a spectrophotometer was carried out, adapted from Barnes *et al.* (1992). For this study, whole leaves from 4 to 6 biological replicates of potato plants were used, grown as in Section 2.6.3. A size 10 cork borer was used to create leaf discs, while avoiding the midrib. The discs were then weighed and a measurement of the relative chlorophyll was made. Using a scalpel blade, the leaf discs were cut into small pieces and inserted into a 7 ml brown vial. Next, 5 ml of DMSO was added, followed by brief mix and then incubation in the dark, at room temperature, for 24 h. The supernatant was transferred into a cuvette, for spectrophotometric quantification. Three technical replicates of the absorbance were made, measuring two absorbance values for each sample, A_{649nm} and A_{665nm}. Then, the following formulas were employed:

$$\text{Chlorophyll a}_{conc} = 12.19 \times A_{665nm} - 3.45 \times A_{649nm}$$

$$\text{Chlorophyll b}_{conc} = 21.99 \times A_{649nm}\ 5.32 \times A_{665nm}$$

$$\text{Total chlorophyll}_{conc} = \text{Chlorophyll a} + \text{Chlorophyll b}$$

2.13 Statistical analysis

Throughout the thesis, analysis of the significance level was applied to data sets collected from three biological replicates. The results were analysed using Student's *t* significance tests, in Windows Excel 2010.Where necessary, analysis of variance was carried out using GenStat 14th Edition software (VSN Interantional Ltd).

Chapter 3 The role of the potato *CCD8* gene in stolon and tuber development

3.1 Introduction

Phytohormones such as ABA (Zeevaart and Creelman, 1988) or strigolactones (SLs), a newly found class of branching inhibitors (Gomez-Roldan *et al*., 2008; Umehara *et al*., 2008) are derived from carotenoid precursors (Section 1.3.4). Currently, it is thought that CCD7 catalyses the 9, 10 cleavage of β-carotene to produce 10′-apo-β carotenal and β-ionone, followed by CCD8 action, which catalyses the cleavage of 10′-apo-β-carotenal, to produce 13-apo-β-carotenone. The Arabidopsis MAX1 enzyme, a cytochrome P450 (Sorefan *et al*., 2003) and MAX2, a leucine rich repeat F-box protein (Stirnberg *et al*., 2002) together with the rice *DWARF27* (*D27*) gene (Lin *et al*., 2009) are also involved in the biosynthesis and signalling of SLs, but the complex biochemical pathway and their mode of action remains to be fully resolved.

Recently, Alder *et al*. (2012) brought further information onto the role of D27, showing that the enzyme is a β-carotene isomerase, catalysing the conversion of all-*trans*-β-carotene into 9-*cis*-β-carotene. This product is further cleaved by CCD7 into a 9-*cis*–configured aldehyde. Subsequently, CCD8 adds three oxygen molecules to 9-*cis*-β-apo-10′-carotenal, thus changing its arrangement. Alder *et al*. (2012) argued that these reactions give rise to carlactone, a chemical with biological activities similar to strigolactone.

In recent years, significant progress has been made in our understanding of the interaction between SLs and other phytohormones in modulating shoot branching. The relationship between auxin and SLs (reviewed in Leyser, 2008; Beveridge and Kyozuka, 2010; Xie *et al*., 2010; Dun *et al*., 2012) is currently under debate and explained by two alternative models of action: the canalisation and the second messenger hypotheses. The canalisation model proposes that SLs act by reducing the accumulation of PIN-FORMED (PIN) auxin efflux carrier protein on the plasma membrane. This reduction would then prevent polar auxin transport (PAT) out of the bud into the main stem and result in inactive axillary buds (Prusinkiewicz *et al*.,

2009). In contrast, the second messenger model supports the direct action of SLs in the axillary bud, inhibiting their activation and subsequent growth by an auxin-transport-independent mechanism (Brewer *et al*., 2009). Cytokinin was proposed as a candidate for the second messenger signal (Palni *et al*., 1988; Li *et al*., 1995). However, bud break was found to precede increases in cytokinin levels (Turnbull *et al*., 1997), suggesting that CKs are not primarily responsible for bud outgrowth.

There is great interest in investigating the effects of the *CCD* gene family in plants, not only due to the role of CCDs in producing SLs, but also due to the possibility of gaining insight on important factors for the carotenoid metabolic engineering efforts. In *Arabidopsis thaliana* seeds, maize endosperm, strawberry fruit (*Fragaria x ananassa*) and *Chrysanthemum morifolium* flowers, silencing of the *CCD1*/*4* genes resulted in accumulation of carotenoids in these tissues (Auldridge *et al*., 2006a; Ohmiya *et al*., 2006; Garcia-Limones *et al*., 2008; Vallabhaneni *et al*., 2010). In grape (*Vitis vinifera*), Mathieu *et al.* (2005) reported elevated carotenoid levels by silencing the *VvCCD1*.

Recent studies in grape (Floss and Walter, 2009) and in rice (*Oryza sativa*) endosperm (Ilg *et al*., 2010) did not confirm these previous findings, following reduced *CCD1* expression. Moreover, they showed that apocarotenoids and not carotenoids are the substrate of *CCD1* action *in planta* (Floss and Walter, 2009; Ilg *et al*., 2010). Down-regulation of *CCD7* and/or *CCD8* expression in tomato (Vogel *et al.*, 2010; Kohlen *et al.*, 2012), kiwi fruit (Ledger *et al*., 2010) and *Chrysanthemum* flowers (Liang *et al*., 2010) resulted in above ground phenotypes with increased stem branching, but made no connection between total carotenoid levels and expression of the *CCD7* and *CCD8* genes. However, it is still possible that the carotenoid pool size is determined, at least in part, by the activity of CCDs.

In potato, tubers develop from stolons, a type of diageotropic shoot or stem with strongly elongated internodes that usually originate from basal stem nodes (Struik, 2007). The number and size distribution of tubers are traits of critical economic importance and are strongly influenced by the degree of stolon branching (Celis-Gamboa *et al.*, 2003). Additionally, the activation status of tuber apical and axillary buds impacts on important traits such as tuberisation, dormancy and sprout number. These aspects of the tuber life-cycle are probably orchestrated by a complex interplay of phytohormones, but the role of SLs has just started to be investigated in more detail. Taking into account the importance of *CCD* genes in carotenoid turnover and SL biosynthesis, it was considered timely to investigate the factors controlling carotenoid accumulation in potato tubers by RNAi-mediated silencing of the potato *CCD8* gene. The resulting transgenic lines were analysed over two growing seasons in 2010 and 2011.

3.2 Results

3.2.1 Identification and characterisation of the potato *CCD8* gene

A sequence similarity search of the DFCI Potato Gene Index (http://compbio.dfci.harvard.edu/cgi-bin/tgi/gimain.pl?gudb=potato) failed to identify a potato EST with sequence similarity to published *CCD8* sequences. In order to identify the potato *CCD8* gene homologue, a tBLASTx search (Altschul *et al.*, 1990) of an early release of the potato genome was carried out using the *Arabidopsis thaliana* transcript sequence (AT4G32810.1; work performed by Wayne Morris, JHI, UK).

The first potato genome sequence to be reported was for a doubled monoploid potato clone, DM1-3 516R44 (subsequently referred to as DM). The reduced heterozygosity of DM monoploid enabled assembly of the genomic shotgun sequence (The Potato Genome Sequencing Consortium, 2011), whereas this is still in progress for a diploid clone, RH89-039-16 (RH), also being sequenced. Examination of the RNAseq data for the doubled monoploid DM potato (publicly available on the potato genome browser http://potatogenomics.plantbiology.msu.edu/index.html) indicated that the

CCD8-specific transcript was expressed at very low levels in the DM potato type, compared with the diploid line RH89-039-16 (RH) of cultivated potato. Subsequent comparison of the Desiree cDNA sequence with the tomato sequence available from the Sol Genomics Network website (http://solgenomics.net/) revealed a high degree of sequence identity (96.3%) with the tomato *CCD8* sequence (transcript number Solyc08g066650.2.1; work carried out by work performed by Mark Taylor and Wayne Morris, JHI, UK). In order to obtain the full length cDNA sequence from Desiree, 5′ and 3′ sequences were amplified from root cDNA using primers based on the tomato transcript sequence (work by Wayne Morris, JHI, UK; Table 4).

Table 4. Primer sequences based on the tomato transcript sequence, used to amplify *CCD8* gene from potato root

Primer name	Primer sequence
PF 5′ CCD8	5′- TCACCATACTCTCAAATTCTCTCAA-3′
PR 5′ CCD8	5′- GAGAGTAATTTGGCCATGTCACC-3′
PF 3′ CCD8	5′- GGAGAATTAGAAGCAGCATTGG-3′
PR-3′ CCD8	5′- GCTATTTCAAAAACTGGAAAATTTAG-3′

The complete potato *CCD8* (*StCCD8*) gene was predicted to be 4497 nt and have 6 exons (Figure 12A). The coding sequence of the potato *CCD8* gene is 1816 bp. As part of the characterisation of the potato *CCD8* gene, a sequence alignment was carried out, using the tomato (SlCCD8) and petunia (PhCCD8) protein sequences (Appendix 1). A phylogenetic tree was generated using the CCD8 proteins sequences from a variety of plant species (Figure 12B). This analysis confirmed the taxonomy predictions, as StCCD8 clustered together with SlCCD8 and PhCCD8, in a well-supported sub-clade. Surprisingly, AtCCD8 clustered together with CCD8s of maize, rice and sorghum, separately from the dicots, in a result similar to Kohlen *et al.* (2012).

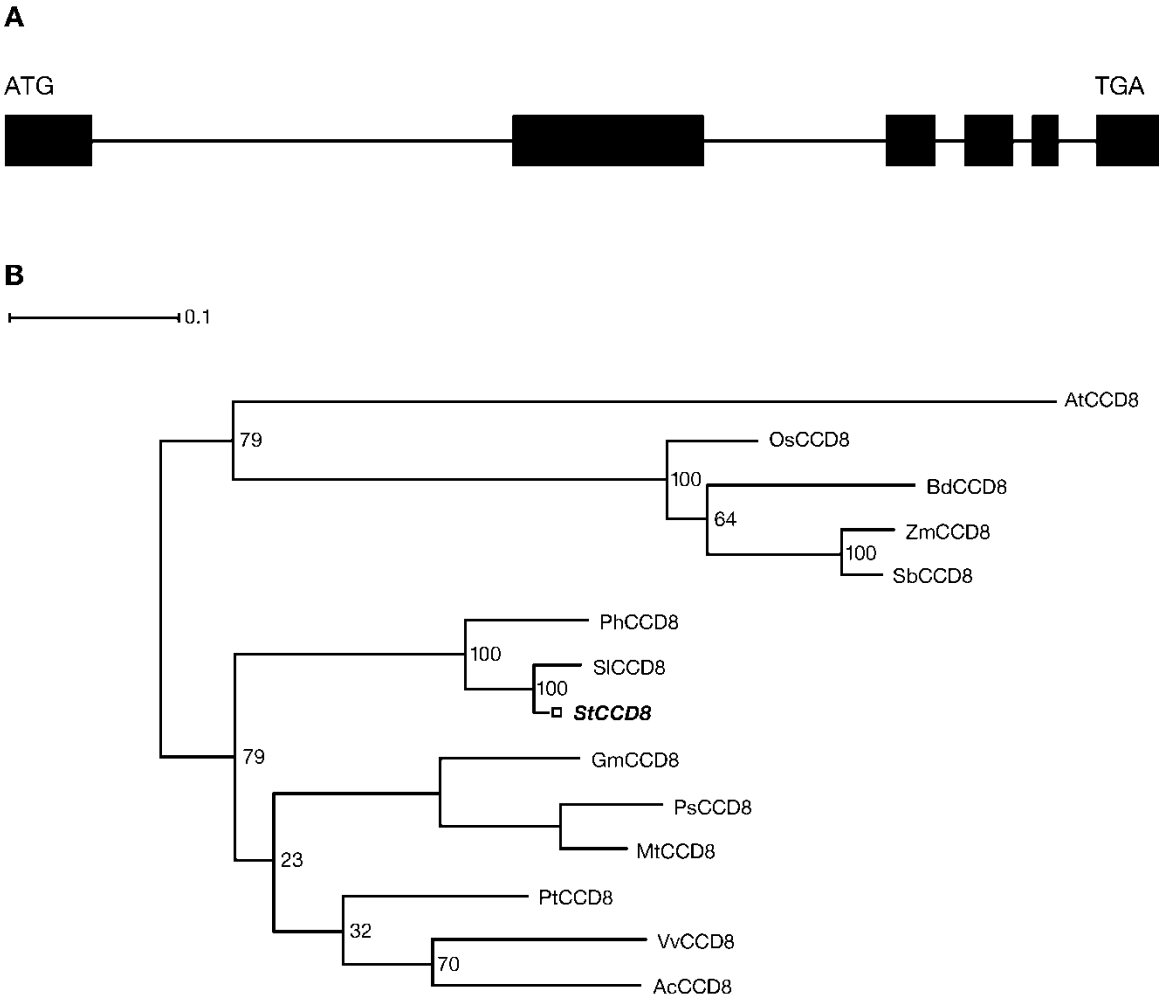

Figure 12. Characterisation of *CCD8* gene from potato. A. The postulated exon/intron structure for the *StCCD8* gene (4497 nt), where exon 1 is 340 nt, exon 2 is 745 nt, exon 3 is 192 nt, exon 4 is190 nt, exon 5 is 104 nt, exon 6 is245 nt, intron 1 is 1640 nt, intron 2 is 712, intron 3 is 112 intron 4 is 73 nt, intron 5 is 146 nt. B. Maximum likelihood phylogeny of known *CCD8* orthologs, generated using TOPALi; the protein's label signifies the species the protein originated from: Ac, *Actinidia chinensis*; At, *Arabidopsis thaliana*; Bd, *Brachypodium distanchyon*; Gm, *Glycine max*; Mt, *Medicago truncatula*; Os, *Oryza sativa*; Ph, *Petunia hybrida*; Ps, *Pisum sativum*; Pt, *Populus trichocarpa*; Sb, *Sorghum bicolor*; Sl, *Solanum lycopersicum*; St, *Solanum tuberosum*; Vv, *Vitis vinifera*; Zm, *Zea mays*.; *AcCCD8* (GU206812.1), *AtCCD8* (AT4G32810), *BdCCD8* (LOC100831734), *GmCCD8* (LOC100814148), *MtCCD8* (Medtr3g127920), *OsCCD8* (Os01g0746400), *PhCCD8* (AY743219), *PsCCD8* (AY557342), *PtCCD8* (POPTRDRAFT_561749), *SbCCD8* (Sb03g034400), *VvCCD8* (LOC100250765), *ZmCCD8* (GRMZM2G446858); Branch lengths are drawn to scale, with the scale bar showing the number of amino acid changes.

3.2.2 Down-regulation of the potato *CCD8* gene results in severe phenotypic effects

In order to investigate the role of the potato *CCD8* gene, an RNAi silencing construct was engineered to down-regulated the expression of this gene in potato plants. A 530 bp sequence of the *CCD8* cDNA (Appendix 2) was sub-cloned into the pDONR201 by a BP clonase reaction. The *CCD8* sequence was then introduced into the pHellsgate8 vector (Helliwell *et al*., 2002) under the control of a *CaMV 35S* promoter, *via* Gateway cloning, as described in Section 2.5.3. The resulting *CCD8*-RNAi construct was transformed by electroporation into *Agrobacterium tumefaciens* strain LBA4404 and used for *Agrobacterium* mediated transformation of the cream-fleshed cv. Desiree, as presented in Sections 2.7.3 to 2.7.7. Vector engineering and production of the transgenic plants was carried out by Laurence Ducreux, JHI, UK.

General phenotypic observations suggested that, in the 20 independent transgenic potato lines obtained, there was a gradient of severity in the effects observed. Two transgenic lines presenting a severe phenotype, when compared to wild type potato, were selected for further analysis. Plantlets from tissue culture were grown for four weeks before transplantation in the glasshouse. Each independent transformation line had three potato plants cultivated in a random block design, as to reduce the effects of the environment. Growth of the putative transgenic plants in the glasshouse was under the conditions detailed in Section 2.6.3. Two transgenic lines presenting a severe phenotype, when compared to wild type potato, were selected for further analysis (lines 1, 8). These lines exhibited similar phenotypes and line 1 was used consistently throughout the experiments described in this study. *CCD8*-RNAi lines 17 and 21, considered to be less affected by the CCD8 silencing, as deducted by visual observations of the degree of branching, were considered useful for inclusion in some experiments.

The effect of transformation with the RNAi construct on gene expression was determined by qRT-PCR in tubers, roots and stems of potato plants. Design of the primer and probe sequences was carried out by submitting the *CCD8* sequence to the online tool from Roche (UK), but omitting the 530 bp used for generating the RNAi hairpin (Table 5).

The *CCD8* transgene expression in the RNAi silencing construct was driven by the constitutive *CaMV 35S* promoter. RNAi lines 17 and 1, plus controls-empty vector transformant (EV) and potato cv. Desiree were analysed at developing (60 days) and mature (90 days) stages, with the plants grown from seed tubers. Quantitative RT-PCR analysis of root, stem and tuber of the *CCD8*-RNAi plants showed reduced accumulation of the CCD8 specific transcript, as expected. The *CCD8* gene transcript levels were found to be significantly down-regulated (up to 10-fold less than in controls) in all three tissues analysed, both at developing and mature stage (Figure 13A-C; Figure 14A-C).

Table 5. Primer and probe sequences used for qRT-PCR of the *CCD8* gene in *CCD8*-RNAi potato plants.

UPL Primer /probe name	**UPL Primer /probe sequence**
Primer Forward *Ef1-α*	5′-CTTGACGCTCTTGACCAGATT-3′
Primer Reverse *Ef1-α*	5′-GAAGACGGAGGGGTTTGTCT-3′
Primer Forward *CCD8*	5′-AGCATTTGTGCATGTTATGTGTAA-3′
Primer Reverse *CCD8*	5′-GGCACTTCTACACTTGCAACAA-3′
Probe 117 *Ef1-α*	5′-AGCCCAAG-3′
Probe 59 *CCD8*	5′-CAGTGGCA-3′

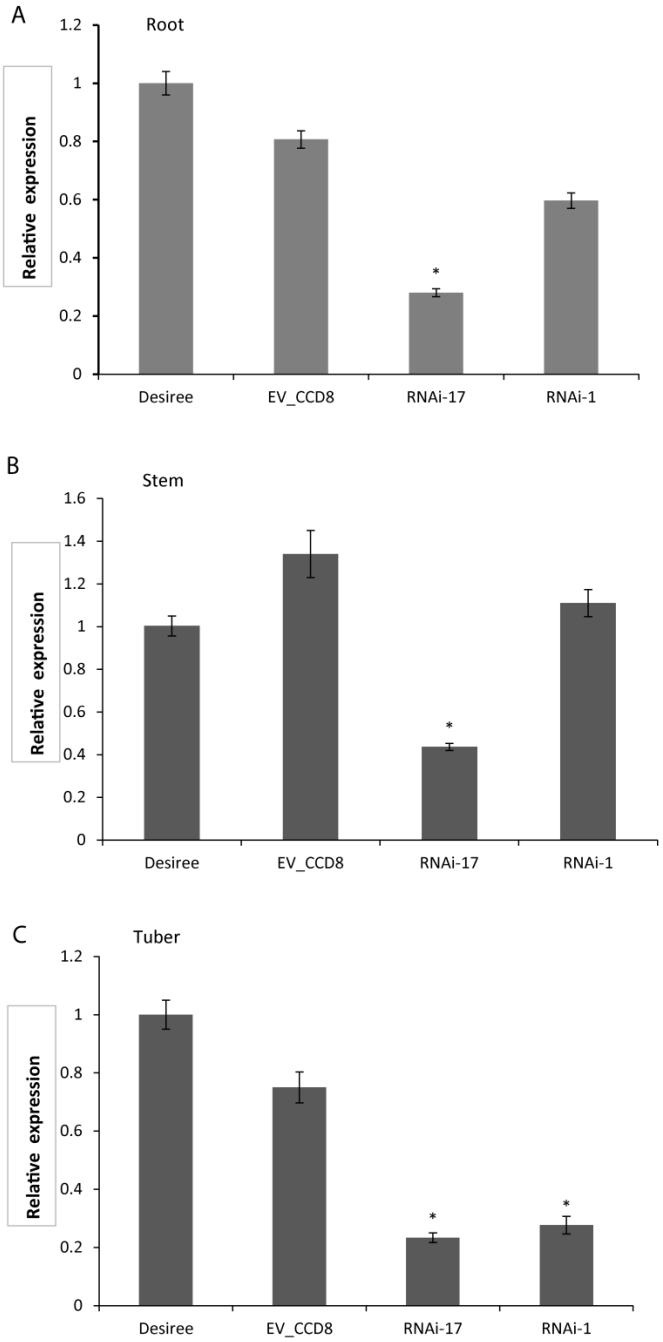

Figure 13. *CCD8* expression levels in tissue of developing (60-day-old) *CCD8*-RNAi lines. Root (A), stem (B) and tuber (C) was sampled from potato plants grown from tubers. Values are means of triplicate assays ± SE (standard error), based on three biological replicates (n=3), expressed relative to the value in wild type samples. Statistical differences from the wild type control were calculated with Student's one-tailed t test, assuming unequal variance. An asterisk was added where there was a significant difference between the calculated (P <0.05) values for RNAi lines and controls.

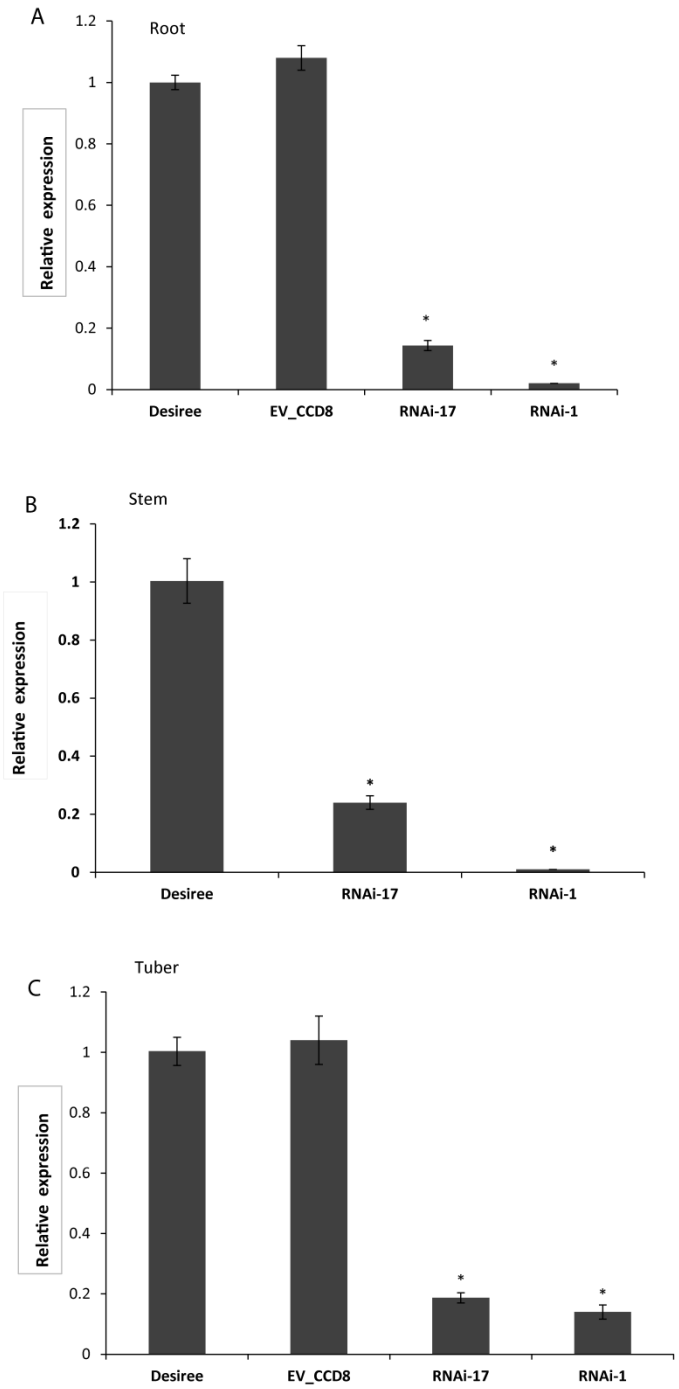

Figure 14. *CCD8* expression levels in tissue of developing (90-day-old) *CCD8*-RNAi lines. Root (A), stem (B) and tuber (C) was sampled from potato plants grown from tubers. Values are means of triplicate assays ± SE (standard error), based on three biological replicates (n=3), expressed relative to the value in wild type samples. Statistical differences from the wild type control were calculated with Student's one-tailed t test, assuming unequal variance. An asterisk was added where there was a significant difference between the calculated (P <0.05) values for RNAi lines and controls.

Phenotypic differences between the wild type and *CCD8*-RNAi potato were visible early in the development of the plants. Nodes of the transgenic potato gave rise to shoots (Figure 15A), which continued to grow into numerous lateral stems. Below ground, few stolons were observed as instead of normal diageotropic growth, stolons tended to emerge and form new shoots. As shown in Figure 15B, the *CCD8*-RNAi plants increase in the number of main stems and lateral branches gave a 'bushy' phenotype to the potato plants, observed early into the development. As the plants matured, it was also observed that the RNAi lines presented a reduction in plant height (data not shown). Measurements confirmed that the transgenic potato lines had a significant increase in the number of main and lateral stems (Figure 15C) and a reduction in plant height (Figure 15D). Although control plants produced flowers, no floral organs were formed in the *CCD8*-RNAi lines.

Visual observations based on the paler green colour of the transgenic *CCD8*-RNAi leaves suggested that these plants had less chlorophyll than controls (Figure 16A). This was confirmed by a DMSO based total chlorophyll extraction (performed as described in Section 2.12.5), which showed lower levels of chlorophyll in the leaf of *CCD8*-RNAi plants, when compared with controls (Figure 16B).

Also, the nodes from the lower stem of transgenic potato plants were seen to develop miniature tubers (Figure 17). These 'aerial tubers' produced shoots, not only from the apical bud, but also from lateral ones, indicating a perturbation of apical dominance.

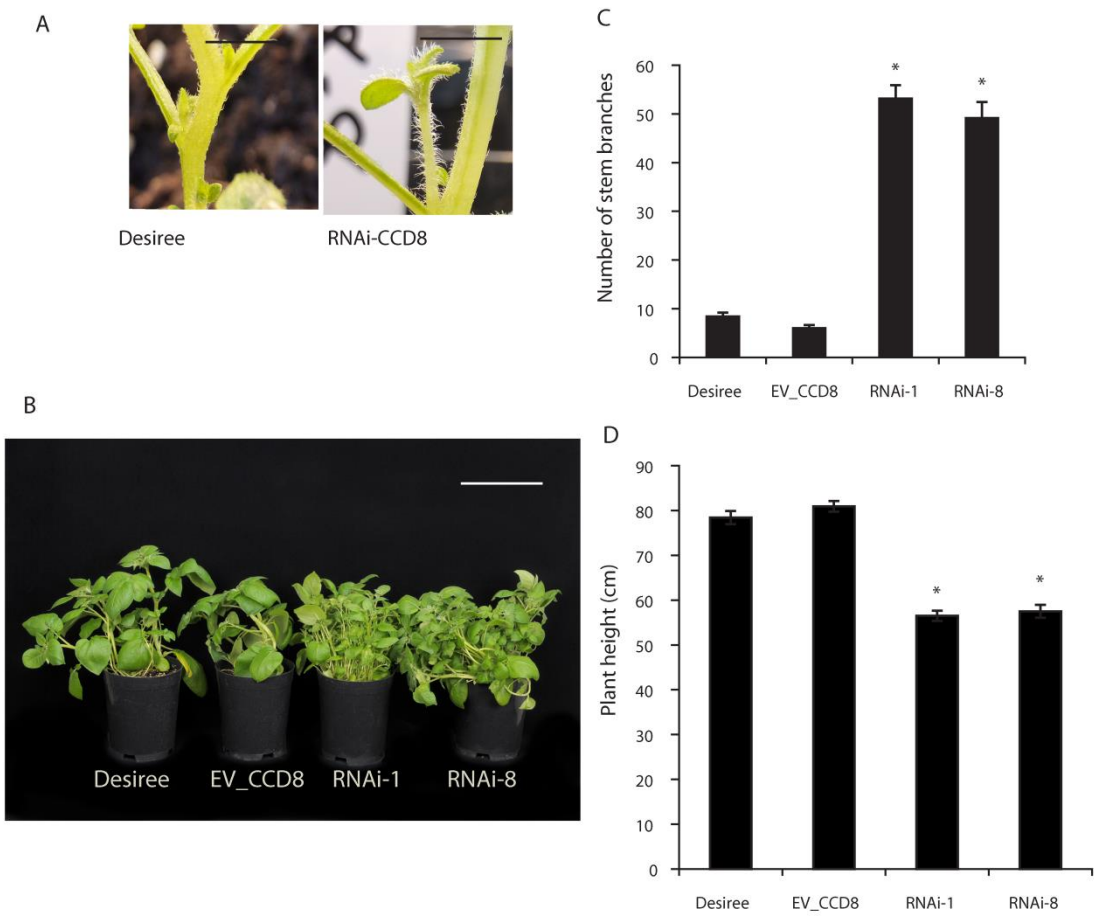

Figure 15. Potato *CCD8*-RNAi branching phenotype. A. Outgrowth of the RNAi nodal stem buds into shoots, early in development, *versus* wild type controls. B. Comparison of number of main and lateral stems between the controls (potato cv. Desiree and EV_CCD8) and RNAi potato lines 1 and 8. C. Distribution of number of stem branches and plant height in *CCD8*-RNAi potato lines compared to controls (wild type cv. Desiree) and EV_CCD8 potato. Scale bars= 1cm (A), 20 cm (B). Values are based on analysis of 60-day-old plants, grown from tissue culture stem cuttings, where n=14. Error bars indicate ± SE (standard error). Statistical differences from the wild type control were calculated with Student's one-tailed t test, assuming unequal variance. An asterisk was added where there was a significant difference between the calculated (P <0.05) values for RNAi lines and controls.

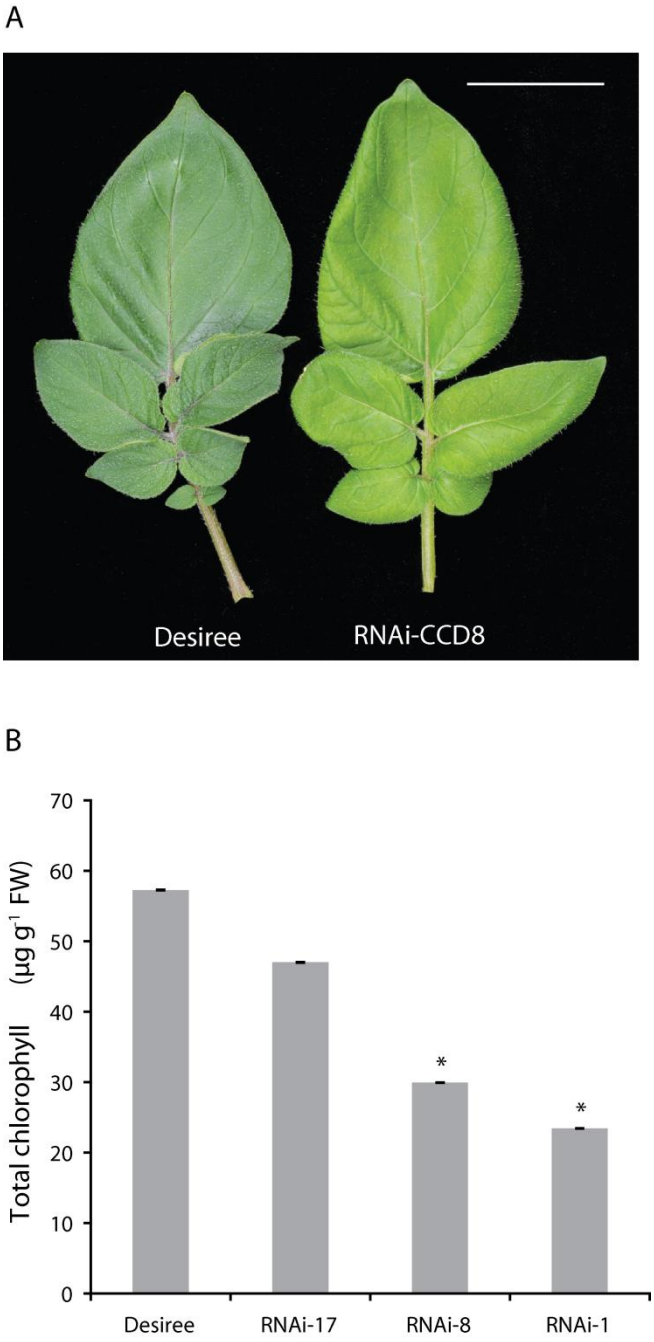

Figure 16. Chlorophyll content in *CCD8*–RNAi plants. A. Comparison of leaf colour from transgenic and control potato cv. Desiree plants. B. Total chlorophyll content in leaf tissue of Desiree and *CCD8*-RNAi lines of potato plants. Samples were obtained from leaf discs taken from the 3rd node of the main stem of 60-day-old plants grown from tubers. Scale bar= 5 cm. Values are means of triplicate assays ± SE, using tissue sampled from 4 independent biological replicates. Statistical differences from the wild type control were calculated with Student's one-tailed *t* test, assuming unequal variance. An asterisk was added where there was a significant difference between the calculated (P <0.05) values for RNAi lines and controls.

Figure 17. Formation of 'aerial' tubers on the lower nodes of the stems of CCD8-RNAi potato plants, with new shoots developing from the apical and lateral tuber buds.

Underground, the RNAi plants produced few stolons, with new tubers forming from sessile buds derived from mother tubers, as seen in Figure 18A-B. Intriguingly, when exposed to light, the newly formed tubers produced shoots. Moreover, the fully underground tubers manifested an outgrowth of the lateral buds, leading to an elongated and knobbly tuber, not seen in control plants (Figure 18C-D). At maturity, the resulting tubers were elongated, similar in shape to *Solanum phureja* DM potatoes (Figure 19). Also, in pot experiments, the tuber yield of the *CCD8*-RNAi potato plants was up to 3-fold lower than the control's, with a high number of small size tubers (up to 2.9-fold more) formed by the transgenics (Figure 20).

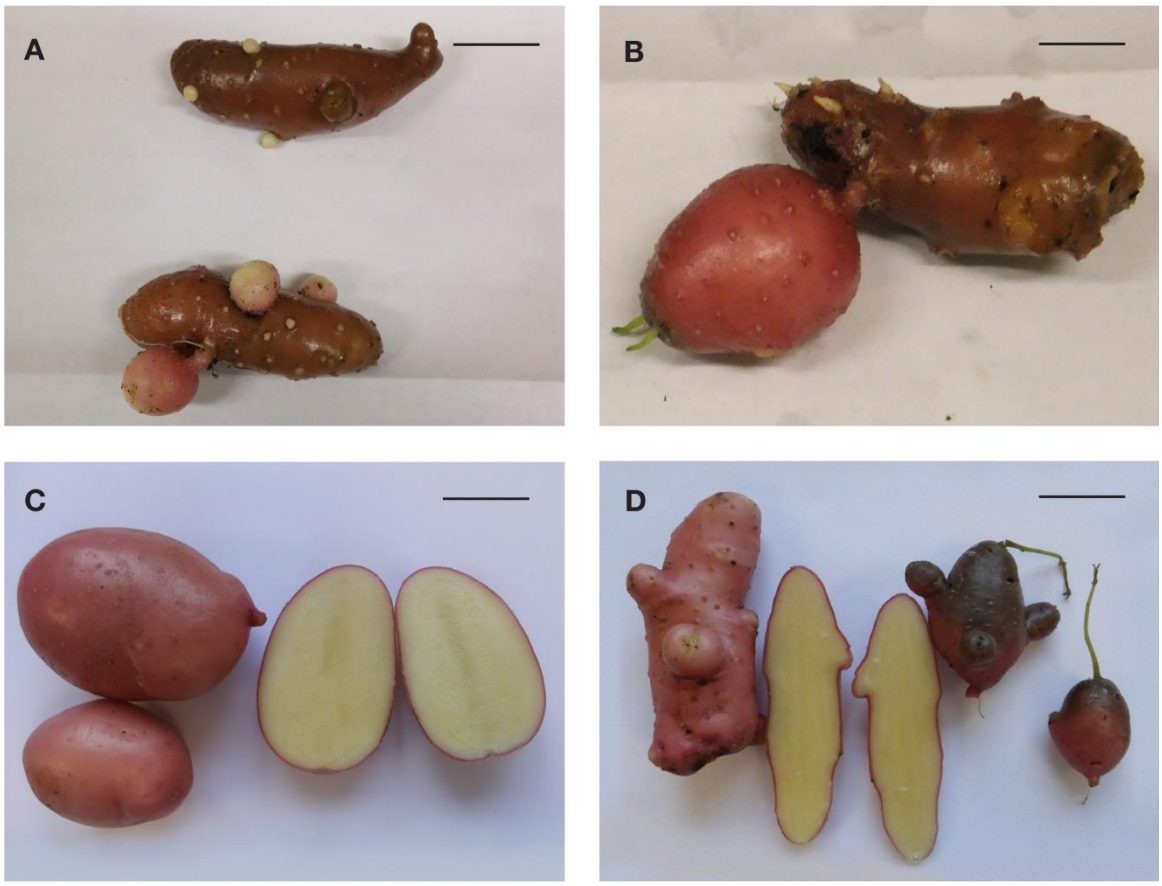

Figure 18. Phenotype of *CCD8*-RNAi potato tubers. A, B. Formation of new tubers directly from mother tubers. C. Mature tubers of potato cv. Desiree**.** D. *CCD8*-RNAi mature tubers showing outgrowth of lateral buds (present in fully underground tubers) and premature shooting of the apical buds, encountered in light exposed tubers. Scale bars= 3 cm (A), 4 cm (B), 6 cm (C-D).

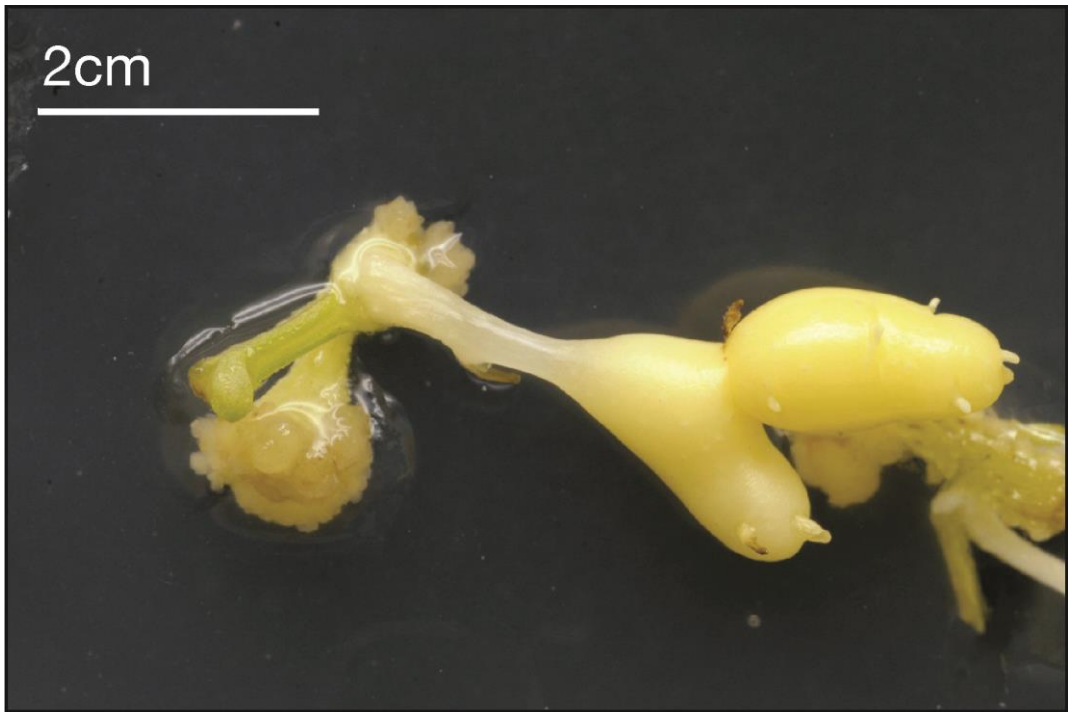

Figure 19. Phenotype of DM tubers grown in vitro from node stem cuttings, as described in Section 2.6.5.

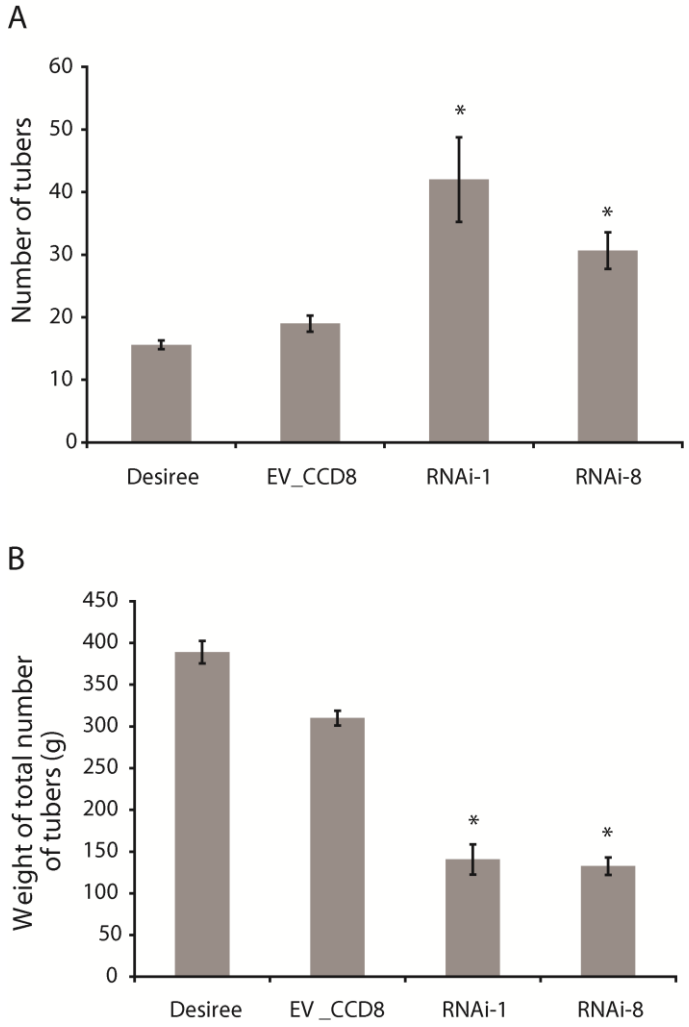

Figure 20. Distribution of number and yield (g) based on the fresh weight of potato tubers in *CCD8*-RNAi potato lines, compared to controls (wild type cv. Desiree) and EV_CCD8 potato. Values are based on analysis of 60-day-old plants grown from tissue culture stem cuttings, on 14 biological replicates (n=14). Error bars indicate ± SE (standard error). Statistical differences from the wild type control were calculated with Student's one-tailed t test, assuming unequal variance. An asterisk was added where there was a significant difference between the calculated (P <0.05) values for RNAi lines and controls.

Studies have previously reported increases in total carotenoid levels when expression of genes from the *CCD* family was silenced or reduced (Auldrige *et al*., 2006a; Vallabhaneni *et al*., 2010; Garcia-Limones *et al*., 2008; Ohmiya *et al*. 2006, Campbell *et al*., 2010). To establish if the *CCD8* gene can influence carotenoid accumulation in potato tubers, the total carotenoid content was determined spectrophotometrically in root and developing/mature tuber tissue, as described in Section 2.12.3. In developing tubers, total carotenoid levels were significantly increased in the *CCD8*-RNAi lines, as confirmed by data from two growing seasons (Figure 21A; Figure 22A). However, analysis of mature tuber and root tissue failed to reliably suggest any significant difference between the total carotenoid levels of RNAi transgenic potato plants and controls (Figure 21B; Figure 22B-C). Analysis by HPLC (performed as in Section 2.12.4) of the carotenoid composition of saponified and non-saponified tissue extracts, in samples from two selected RNAi lines, did not show any difference between the major carotenoids accumulating in the *CCD8*-RNAi lines and control samples. Running of samples and collection of data from the HPLC equipment was carried out by Raymond Campbell, JHI, UK (data not shown).

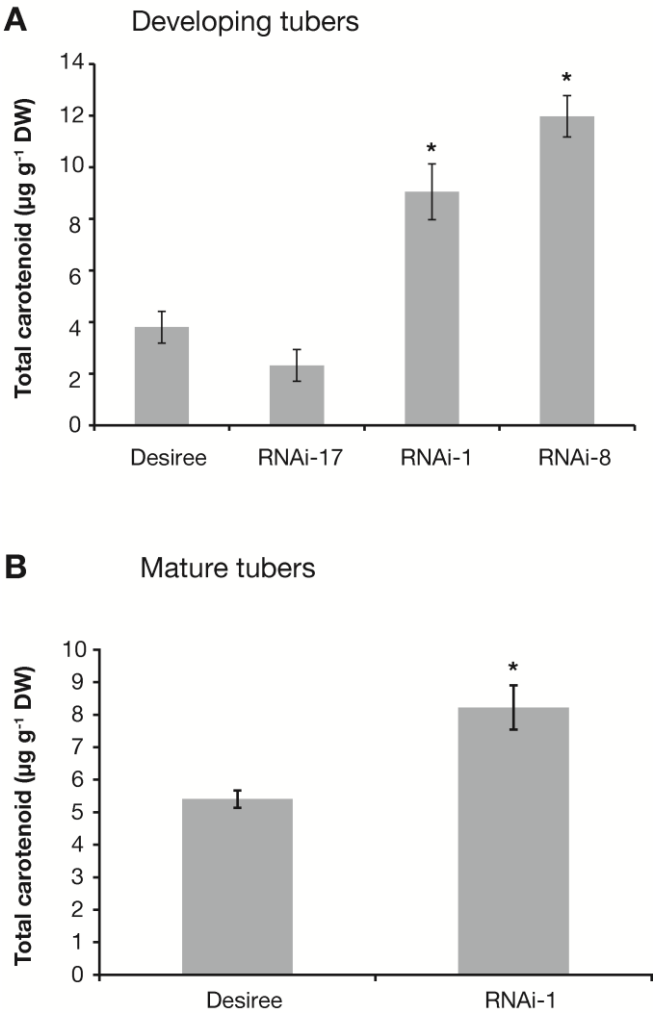

Figure 21. Total carotenoid content of control and *CCD8*-RNAi plants in the second season of growth. Developing (A) and mature (B) potato tuber tissue, grown from tissue culture stem cuttings, where n=3 (biological replicates). Error bars indicate ± SE (standard error). Statistical differences from the wild type control were calculated with Student's one-tailed *t* test, assuming unequal variance. An asterisk was added where there was a significant difference between the calculated (P <0.05) values for RNAi lines and controls.

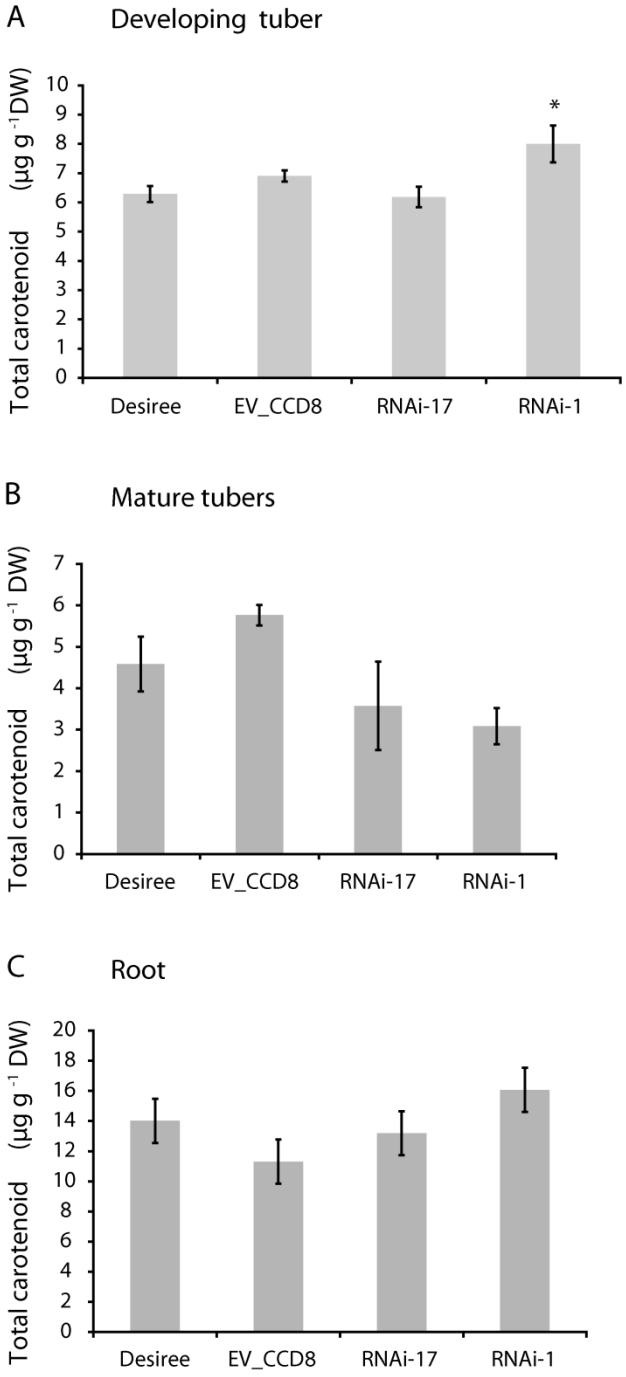

Figure 22. Total carotenoid content in developing (A), mature (B) tuber and root (C) tissue of *CCD8*-RNAi potato plants, in the first season of growth. Values are based on analysis of 60 (developing) and 90 (mature) day-old plants grown from tissue culture stem cuttings, where *n*=3 (biological replicates). Error bars indicate ± SE (standard error). Statistical differences from the wild type control were calculated with Student's one-tailed *t* test, assuming unequal variance. An asterisk was added where there was a significant difference between the calculated (P <0.05) values for RNAi lines and controls.

3.2.3 The *CCD8* phenotype is due to reduced strigolactone levels in *CCD8*-RNAi lines

In most plants, the synthesis of SLs is thought to take place in the root and possibly the lower part of the stem (reviewed by Dun *et al*., 2009). This was consistent with the expression data of *CCD8* in potato cv. Desiree (analysis carried out by Laurence Ducreux, JHI, UK). The highest expression of the *CCD8* gene was in root tissues, but it was also observed to a significant level in stolons. SLs are normally present in plants in minute amounts and hence, very difficult to quantify (Jamil *et al*., 2010). Thus, to measure the SLs levels in tissues, the plants are grown under phosphate starvation conditions, known to facilitate production and/or exudation of this phytohormone (Yoneyama *et al*., 2007).

To obtain information on the capacity of the *CCD8*-RNAi plants to produce strigolactones, the levels of these phytohormones were investigated in roots of control and RNAi transgenic potato plants (as described in Section 2.12.4; growth of plants, extractions, running of samples and data collection carried out by Wouter Kohlen and Efstathios Roumeliotis, Wageningen Universitat - WUR, Netherlands). Previously, in potato roots, orobanchol and orobanchyl acetate were the only strigolactones detected (Roumeliotis *et al*., 2012). In this study, orobanchol was the only strigolactone present at levels that could be quantified accurately. As seen in Figure 23A, the removal of phosphate from the nutrient solution increased the levels of orobanchol in control potato plants. This was not the case for the *CCD8*-RNAi plants, found to have significantly lower levels of orobanchol throughout the experiment.

A complementation experiment was devised to confirm that the observed phenotype was due to reduced SL levels. For this, tubers were produced *in vitro* from EV and RNAi nodal cuttings of potato stem (as described in Section 2.6.5). In the absence of added SL, the RNAi tubers from RNAi line 1 exhibited a distinct stolon branching phenotype, which was absent from EV control and RNAi line 17 (Figure 23B).

Compared with controls, stolons from RNAi line 1 grew extremely rapidly and were highly branched. Inclusion of the synthetic GR24, in concentration of 10 ng μl^{-1}, in the solid tuberisation medium, resulted in a severe decrease in the extent of stolon growth and degree of branching (Figure 23B), indicating that the phenotype of the *CCD8*-RNAi transgenic potato line 1 was due to lowered levels of SL.

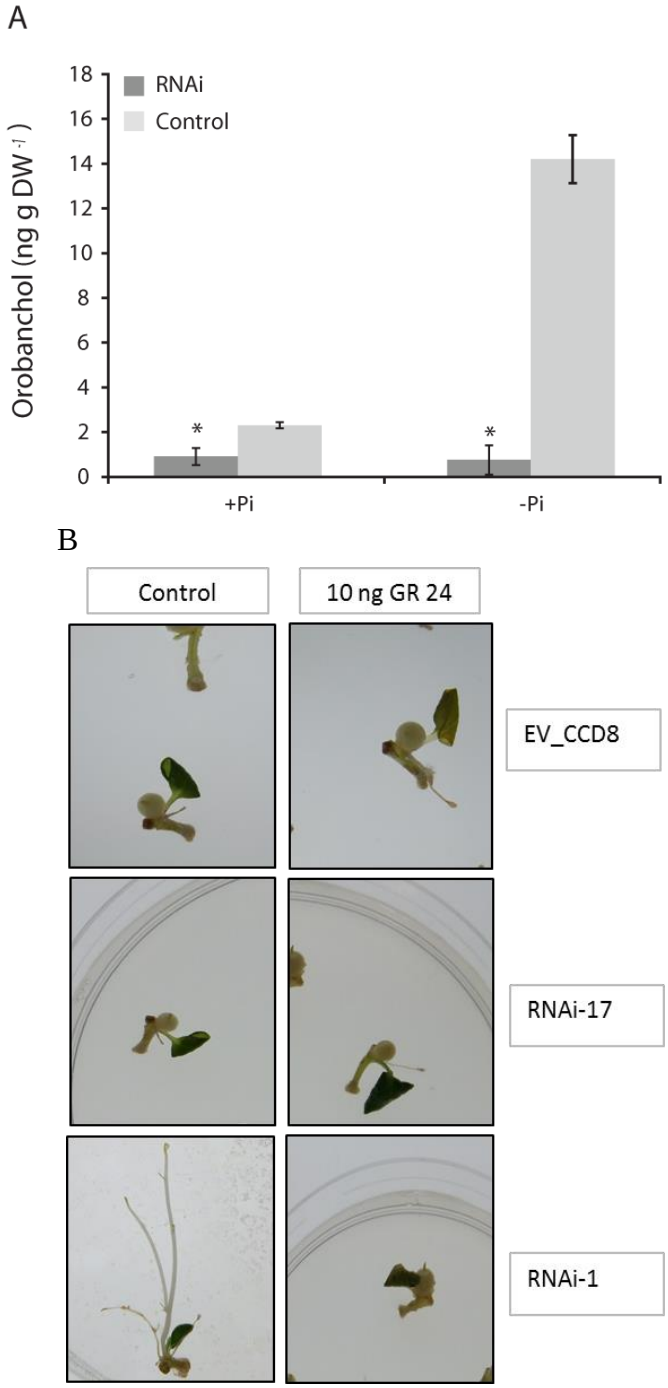

Figure 23. Phenotype of *CCD8*-RNAi plants is due to lack of SLs. A. Analysis of orobanchol content in roots of control (Desiree) and transgenic *CCD8*-RNAi potato plants, grown under normal conditions (+Pi) and phosphate starvation (-Pi), where *n*=6. Statistical differences from the wild type control were calculated with Student's one-tailed *t* test, assuming unequal variance. An asterisk was added where there was a significant difference between the calculated (P <0.05) values for RNAi lines and controls. B. Effect of GR 24 application on the branching of stolons from microtubers of *CCD8*-RNAi lines 17, 1 and control. The data is based on one independent experiment, where *n*=24 for each treatment, per line.

3.2.4 Strigolactone-*CCD8* mediated effects on tuber bud dormancy

SLs play an important part in the reduction of bud outgrowth, either on their own (Brewer *et al*., 2009) or in combination with auxin, as reported by Crawford *et al*. (2010) and Liang *et al*. (2010). Mature tubers from *CCD8*-RNAi and potato cv. Desiree, stored in darkness at room temperature, were monitored for sprouting behaviour, up to 12 weeks after harvest. Visual observation of the *CCD8* RNAi mature tubers indicated an accelerated pattern of sprouting, when compared to Desiree tubers. *CCD8*-RNAi potato tubers had sprouts up to 3 mm in length (Figure 24). Thus, it was considered worthwhile to investigate the effect of *CCD8* down-regulation on tuber bud dormancy.

A convenient system for investigating tuber bud growth is the sprout release assay, described by Hartmann *et al*. (2011). According to this technique, the formation of sprouts is observed in buds excised from potato tubers. In this study, tubers were harvested from control and RNAi potato plants about 12 weeks old. The tubers were stored in darkness at 4ºC for two weeks, before setting up the sprout release assay with tuber buds, as described in Section 2.7.8. Monitoring the total percentage of sprout formation in control solution did not demonstrate any significant difference between RNAi lines and control (Figure 25A). Also, application of GR24 suggested a slight inhibition in sprout formation at similar levels in transgenic and wild type tuber buds (Figure 25B). However, it was observed that in the water (and Buffer A, as described in Section 2.7.8) treatment, the *CCD8*-RNAi lines formed bud sprouts from day 2, much quicker than wild type buds, which showed sprouts from day 4.

Cytokinin and gibberellin are considered sprout growth promoting hormones (Suttle, 2004; Beveridge and Kyozuka, 2010), so the tuber discs were treated with synthetic cytokinin (6-benylaminopurine-BAP) and gibberellin (GA_3) to establish how SLs affect the action of these growth regulators in potato buds. In wild type potato, tuber buds formed high numbers of sprouts after 7 days of treatment with BAP (up to

42%; Figure 25C) or GA_3 (100%; Figure 25D), confirming previous reports (Hartmann *et al*., 2011). In RNAi buds, BAP treatment elicited a strong sprouting response, inhibited by GR24 application (Figure 25E). The sprout-inducing effect of GA_3 on tuber buds was reduced by addition of GR24 to the treatment (Figure 25F). Surprisingly, the RNAi transgenic lines were much less responsive than controls to GA_3 treatment, up to 40% sprouting, compared to up to 100% in wild type (Figure 25D). This suggested a decreased sensitivity to GA_3, but not cytokinin in the *CCD8*-RNAi transgenic potato.

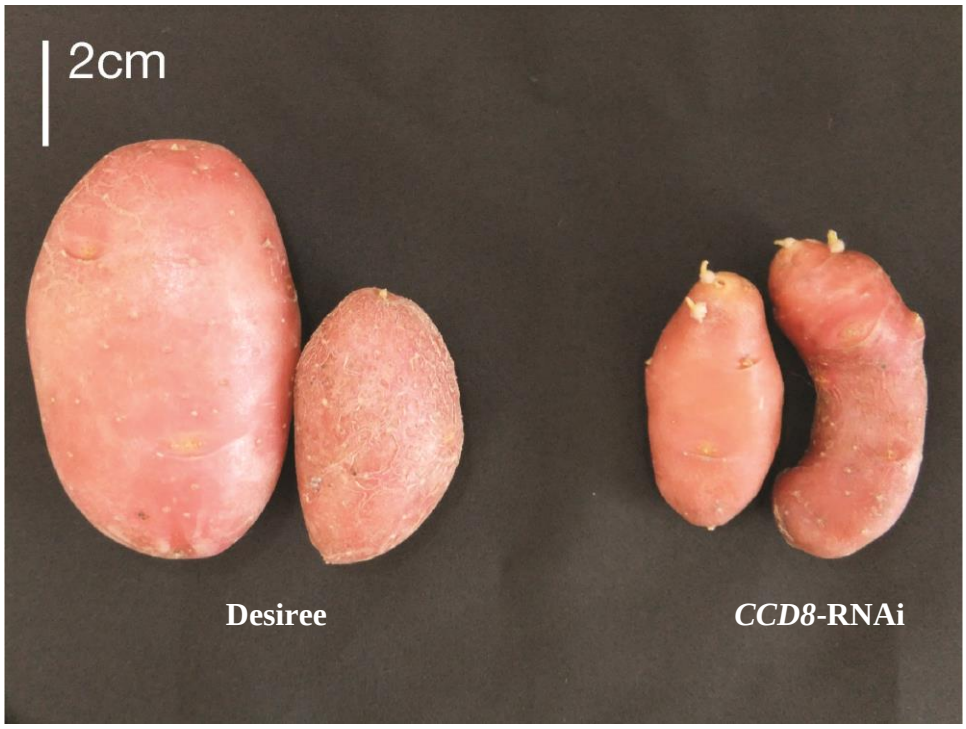

Figure 24. Comparison of sprouting behaviour of the *CCD8*-RNAi potato tubers, *versus* potato cv. Desiree, at 3 months after harvest. The RNAi tubers show increased level of sprouting, with sprouts up to 3 mm in length.

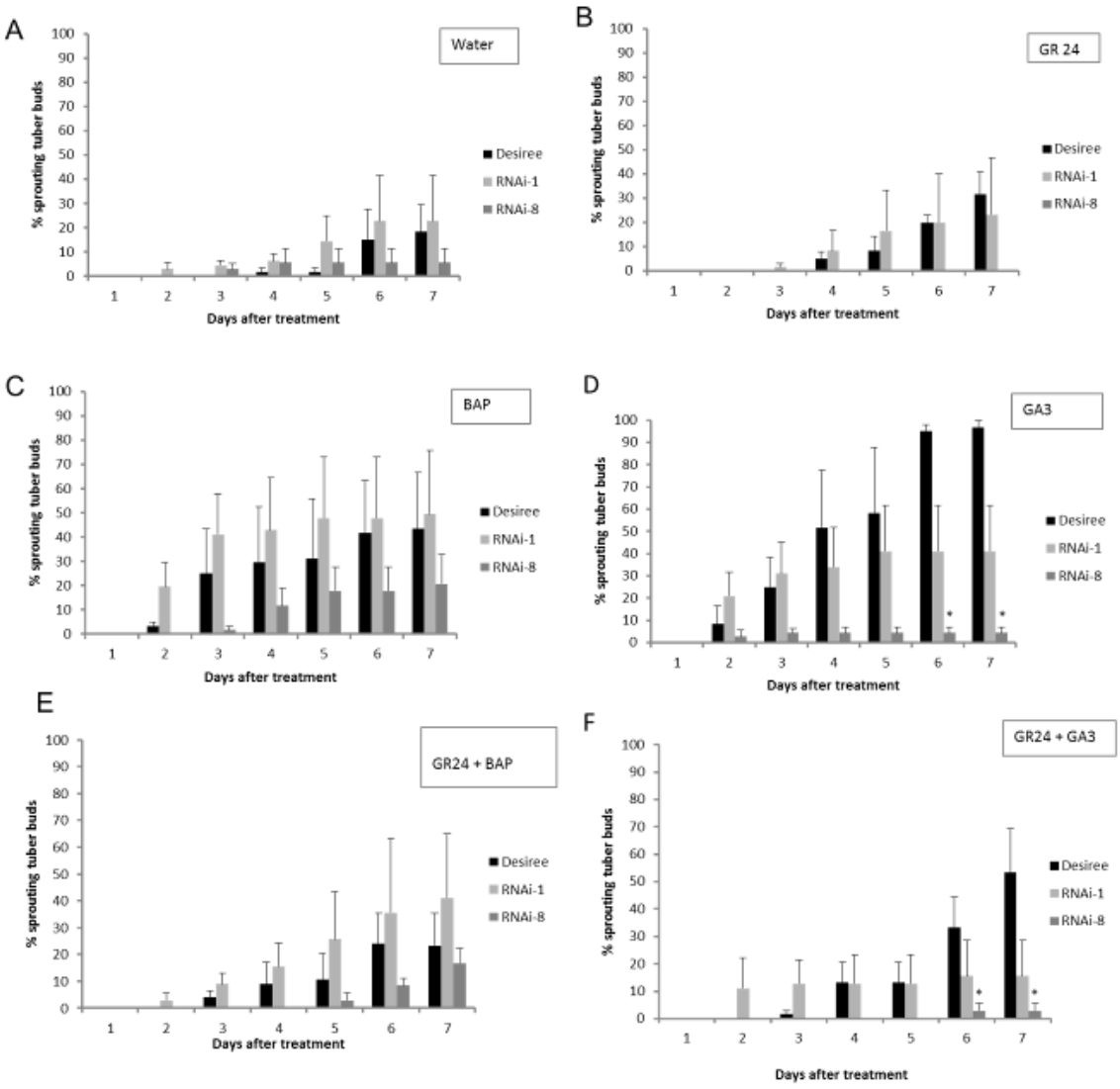

Figure 25. Sprouting of the Desiree and *CCD8*-RNAi potato lines in water (control solution, described in Section 2.7.8; A), under application of synthetic strigolactone-GR24, 2.5 µM (B), of sprout inducing synthetic cytokinin–benylaminopurine, 50 µM (BAP; C) and gibberellin, 50 µM (GA_3; D) and in combination with synthetic SL, GR24 (2.5 µM; E-F). The sprouting behaviour of tuber discs from control and RNAi potato lines was monitored over 7 days. Tissue was sampled from mature tubers stored at 4ºC for 10 days after harvest. Values are means of three independent experiments, where each n=20 (biological replicates). Statistical differences from the wild type control were calculated with Student's one-tailed t test, assuming unequal variance. An asterisk was added where there was a significant difference between the calculated (P <0.05) values for RNAi lines and controls. Error bars represent ±SE (standard error).

In order to further investigate the results obtained from the sprout release assay (Figure 25) and establish if any interactions exist between the different hormone treatments and the diverse genotypes (lines), the data was subjected to analysis of variance in Genstat 14th Edition. The results showed that there is a significant relationship between the lines and treatment and possibly the lines and the day of sprouting (Table 6).

Table 6. Analysis of variance on the interaction between treatments, lines and days of the data from obtained in the sprout release assay (presented in Figure 25); d.f, degrees of freedom; s. s., sum of squares; m. s., mean square; v.r., variance ratio. The F pr. (corresponding probability) value here is less than 0.001 (<.001), so the relationship is significant at a 0.1% level of significance.

TREATMENTS line*treatment*day
COVARIATE "No Covariate"

Variate	**buds**				
Source of variation	d.f.	s.s.	m.s.	v.r.	F pr.
line	2	21238.7	10619.3	27.45	<.001
treatment	5	25837.3	5167.5	13.36	<.001
day	6	34249.8	5708.3	14.76	<.001
line.treatment	10	14060.9	1406.1	3.64	<.001
line.day	12	12942.2	1078.5	2.79	0.001
treatment.day	30	7708.2	256.9	0.66	0.91
line.treatment.day	60	11371.4	189.5	0.49	0.999
Residual	252	97475.1	386.8		
Total	377	224884			

Next, qRT-PCR analysis was performed as described in Section 2.11.13, using sprouting and non-sprouting tuber buds of potato cv. Desiree. Preliminary data (not shown) suggested that the *CCD8* transcript, detected in non-sprouting buds at 0h after water treatment, was then absent when transcript from 3 and 6 days was analysed. Interestingly, when a sprout inducing treatment was applied, containing 50 µM GA_3 and BAP, it was not possible to detect the *CCD8* gene transcript even at 0h after treatment. This data seem to suggest an immediate down regulation of CCD8 expression by these treatments, but further qRT-PCR analysis is needed.

3.3 Discussion

Studies from many plant species have shown that SLs inhibit the outgrowth of axillary lateral buds or meristems, thereby regulating shoot branching patterns. The effects of SL manipulation in different plant species are important due to their control over the morphology and overall ecological fitness of plants (Aarssen, 1995). The SL biochemical pathway shows that key steps are catalysed by CCD7 and CCD8, although the pathway remains to be fully elucidated. In this study, transgenic *CCD8*-RNAi potato plants were characterised. The phenotypes exhibited by the RNAi lines were complex and gave new insights into the roles of SLs, particularly over aspects of the potato tuber life cycle.

The effects of *CCD8* down-regulation are assumed to be due to a reduced level of strigolactone biosynthesis. In potato roots, the only strigolactone that could be detected was orobanchol. Under phosphate starvation, there was a large stimulation in the content of orobanchol in roots only in wild type cv. Desiree (*ca*. 6-fold) and not in the RNAi line tested. This supports the view that the *CCD8* lines were compromised in SL biosynthesis. Further evidence that the RNAi phenotypic effects were due to reduced SL content came from a complementation experiment with *in vitro* microtubers. Here, the synthetic strigolactone GR24, when added to the *in vitro* tuberisation medium, reversed the accelerated and highly branched stolon growth effects seen in RNAi microtubers from RNAi line 1.

A distinct feature of the *CCD8*-RNAi lines was the growth habit of stolons. The diageotropic nature of stolon growth was completely lost in the *CCD8*-RNAi lines, so that instead of growing horizontally from the mainstem, stolons emerged to produce above-ground stems. This implies that strigolactone production in the stolons is necessary for maintenance of the diageotropic growth. Previously, it has been demonstrated that SLs are able to modulate local auxin levels and that the net result of SL action is dependent on the auxin status of the plant (Ruyter-Spira *et al*.,

2011). It is possible that the tightly balanced auxin-strigolactone interaction is the basis for the mechanism of diageotropic stolon growth and disruption of the level of SL can therefore have a major effect on this aspect of growth.

Possibly due to the lack of underground stolons, a high level of aerial tuber formation was observed in the *CCD8*-RNAi lines. The buds from the aerial tubers exhibited a low degree of dormancy and produced sprouts as the aerial tubers were developing, not only from the apical bud but also from axillary buds, indicating a lack of apical dominance in the aerial tubers. It has recently been demonstrated that potato tubers exhibit apical dominance behaviour that is very similar to that of other stems (Teper-Bamnolker *et al*., 2012). Shoot apical dominance and branching regulation is thought to involve three long-range hormonal signals, auxin, SLs and cytokinins, although the details of their interaction remain to be clarified in detail. Evidently, perturbation of *CCD8* expression and by implication, strigolactone level, has a dramatic effect on tuber apical dominance. Interestingly, the degree of tuber sprouting appeared to be influenced by exposure to light. This was observed in aerial tubers, where both apical and axillary tuber buds exhibited little dormancy, but also in tubers that formed below ground and were exposed to light, which rapidly commenced growth.

Although the increased sprouting in the light may suggests an increased sensitivity to light of *CCD8*-RNAi lines, in general, a reduction of SLs or SL signalling is associated with reduced light signalling. In Arabidopsis, it has been demonstrated that there is an interaction between light and SL responses (Tsuchiya and McCourt, 2010). Strigolactones regulate the nuclear localization of the CONSTITUTIVE PHOTOMORPHOGENESIS1 (COP1) ubiquitin ligase, which in part determines the levels of light regulators such as the Arabidopsis transcription factor LONG HYPOCOTYL 5 (HY5). The current study provides further evidence of an interaction between light and SLs.

Recently, it has been demonstrated that TEOSINTE BRANCHED1, CYCLOIDEA and PCF (TCP) transcription factors act downstream of SLs to control shoot branching (Braun *et al*., 2012). In potato, a *TCP* gene termed St*TCP*-1 is expressed at high levels in endo-dormant tuber apical buds, but on dormancy release, expression of the *TCP* gene was not detectable (Faivre-Rampant *et al*., 2004). Similarly, in potato sprouts, *TCP* expression levels in apically repressed axillary buds were relatively high compared with the expression level in the apical bud. Expression of the potato *CCD8* gene was high in dormant buds but its expression level rapidly decreased on treatment with hormones known to cause release from dormancy (Faivre-Rampant *et al*., 2004). This pattern of expression is consistent with a role for SLs in regulation of *TCP* expression, which in turn may control activation status of the meristem. Interestingly, as the *CCD8*-RNAi tubers exhibited a lower degree of tuber dormancy compared with parental controls and EV lines, it would be worthwhile that further research should investigate the levels of *TCP* in such dormant tuber buds.

The results in this study suggest an interaction between SLs levels and bud sensitivity to GAs. GR24 treatment inhibited tuber sprout growth and the inhibition could not be overcome by either GA_3 or BAP treatment, providing evidence of SL acting downstream of these other phytohormones. There are very few studies documenting an involvement of GAs in controlling apical dominance. Early research showed a role for GA in promoting auxin-derived inhibition of bud growth in decapitated plants of pea (Jacobs and Case, 1965; Scott *et al*., 1967). There are also two reports on a negative correlation between bioactive GA_1 levels and branching, as seen in *Citrus* and *Chrysanthemum* transgenic plants (Fagoaga *et al*., 2007; Miao *et al*., 2010). Interestingly, it was recently proposed that gibberellin could change bud sensitivity to application of synthetic SLs, as seen in dwarf pea plants with low GA_1 (Luisi *et al*., 2011).

Measurements of the total carotenoid levels in tissues of *CCD8*-RNAi plants showed a significant increase in developing tubers, confirmed over two growing seasons. However, data for mature tubers and root of transgenic potato failed to reliably suggest such a change in carotenoid levels. A very recent study on the effects of *CCD8* down-regulation in tomato did not report any changes in total carotenoid levels in transgenic plants (Kohlen *et al*., 2012). However, the study found a relationship between the reduced expression of *CCD8* and tomato reproductive phenotypes such as smaller flowers, fruits, as well as fewer and smaller seeds per fruit.

Overall, the present study brings forth evidence to sustain a role of SLs in not only dictating the architecture of potato plants, but also in maintaining tuber bud dormancy. The *CCD8*-RNAi plants, deficient in SL biosynthesis, produced tubers that sprouted earlier than controls. Comparison of the degree of sprouting in whole tubers of CCD8-RNAi *versus* data from the sprout release assay indicated some variation of this phenomenon amongst the lines (line 8 sprouted less than line 1), but this might results from the nature of the assay, involving excision and wounding of the tissues. The application of a synthetic strigolactone was sufficient to reduce the effects of gibberellin and cytokinin treatment. Morever, the RNAi tuber buds showed a diminished response to application of GA_3 sprout inducing treatment. The newly found relationship between SL and GA requires further investigation. Hence, studying in more detail the dynamics of the SL-GA mode of action could potentially provide valuable insight over new branching-controlling factors and their interaction with other phytohormones.

Chapter 4 Study on the sub-cellular localisation of CrtRb2 and PSY2 in *Nicotiana benthamiana* and potato leaves

4.1 Introduction

In order to enhance the carotenoid content of plant-derived food, the carotenoid biosynthetic pathway has been subject to genetic engineering over the past decade (reviewed in Fraser and Bramley, 2009; Section 1.3.2), with rudimentary rate-limiting enzymes having been over-expressed, multiple steps in pathways engineered (Diretto *et al*., 2007a), new products or pathways introduced (Ralley *et al*., 2004; Morris *et al*., 2006) and precursors diverted (Kovacs *et al*., 2007). Despite the fundamental reactions involved in carotenoid formation having been established, complex interactions regulate the formation and catabolism of carotenoids, with different groups of these compounds being formed at different stages of plant development, in various tissues and compartments of plant cells (Section 1.3.3).

The import of the carotenoid biosynthetic proteins into plastids is mediated by a specific translocation complex in which folding, oligomeric assembly, membrane insertion and, in chloroplasts, further translocation take place (reviewed in Soll and Schleiff, 2004; Li and Chiu, 2010). The translocation of nuclear-encoded proteins across membranes is vital for the successful completion of the many metabolic functions performed by plastids (Soll and Schleiff, 2004). Import into the correct organelle depends on the amino or N-terminus cleavable sequences (known as ‘transit peptides’; Lee *et al*., 2008).

A key issue in carotenoid metabolic engineering is how the products are stored within the plant, impacting on the amount of product produced and its stability. Despite taking their name from carrot, a crop plant that accumulates high levels of carotenoids in the root, the carotenoid pigments are seldom encountered at high levels in underground storage organs such as tubers and roots and potato tubers generally containing low levels of carotenoids (Section 1.2.3). There is a lack of information on the site of synthesis and accumulation of carotenoids in potato tubers, as no obvious chromoplasts can be seen in potato tubers (Taylor, unpublished).

'Molecular imaging' has brought us the necessary tools to obtain valuable insight into the sub-cellular signals regulating processes in organelles (Zorov *et al*., 2004). The use of fluorescent probes, such as GFP and RFP, enable the visualisation of tagged proteins when agro-infiltrated into plant tissues. This can help to localise proteins at a sub-cellular level. Methods such as the electroporation of protoplasts, particle-mediated DNA delivery (biolistics), polyethylene glycol-mediated DNA uptake and *Agrobacterium*-mediated transformation (agro-infiltration) can serve to introduce purified plasmid DNA into cells (Kokkirala *et al*., 2010). The applicability of transient expression systems has even been extended to develop high throughput streamlined and systematic methods of cloning GFP-ORF fusions, to assess their sub-cellular localisation in Arabidopsis cells (Koroleva *et al*., 2005).

This chapter describes the engineering and transient expression of the genes encoding two carotenoid biosynthetic enzymes, CrtRb2 and PSY2, into mesophyll cells of *Nicotiana benthamiana* and potato leaves. The results presented here help establish the functionality *in vivo* of the engineered proteins and the targeting of the fluorescently tagged CrtRb2 and PSY2 proteins in *Nicotiana bethamiana* and potato mesophyll cells, before expressing the two proteins of interest in potato tuber tissue (described in Chapter 5).

4.2 Results

4.2.1 Generation of constructs for localisation studies in leaves

A study comparing the expression patterns of the major genes encoding the enzymes of the carotenoid pathway (Morris *et al.*, 2004) cloned from a high carotenoid potato *Solanum phureja* DB375\1 library the cDNA encoding the *PSY* and *CrtRb2* genes. The sequences were found to be 96%, in the case of *PSY2* (Fraser *et al*., 1994) and 97%, for the *CrtRb2* identical to their tomato homologues. The sequences cloned by Morris *et al*. (2004) were introduced into Gateway binary vectors (reviewed by Karimi *et al.*, 2002), and used in sub-cellular localisation studies, to determine the site of synthesis of carotenoids in potato tubers (experiments described in Chapter 5). The translocation of cytosolically-made proteins into their respective compartments requires signals to correctly target and transfer the precursor proteins (Bionda *et al*., 2010). *In silico* analysis of the N-termini of the CrtRb2 and PSY2 proteins, using the Chloro P program (Emanuelsson *et al*., 1999; http://www.cbs.dtu.dk) strongly suggested the proteins were targeted to chloroplasts. Based on the output from this software, both proteins were predicted to have a chloroplast targeting peptide (Table 7).

Table 7. Summary of the output from ChloroP prediction software. The higher the Score, the neural network output score on which the cTP/non-cTP assignment is based, the more certain is the network that this sequence contains an N-terminal chloroplast transit peptide (cTP). The prediction cTP/no cTP is based solely on this score. cTP tells whether or not this is predicted as a cTP-containing sequence; "Y" means that the sequence is predicted to contain a cTP; "-" means that is predicted not to contain a cTP. The CS-score is the MEME scoring matrix score for the suggested cleavage site. cTP-length is the predicted length of the presequence

Query name	Length (AAs)	Score	cTP	CS score	cTP length
CrtRb2	338	0.547	Y	1.951	59
PSY2	439	0.548	Y	5.638	48

However, *in silico* predictions require experimental verification to remove the possibility of errors (Koroleva *et al*., 2005). Thus, fusions of full length cDNAs encoding *PSY2* and *CrtRb2* with RFP or GFP at the carboxy terminus were constructed as shown in Figure 27. The carboxy terminus was chosen as to avoid impairing the import of the constructs into the plastids, by attaching the fluorescent tag to the transit peptide, which is located at the amino-terminus. To ensure transcription of the fluorescent tag for the two proteins, the stop codon from both gene sequences was removed (Appendix 3 for the complete coding sequences, showing the nucleotides encoding for the stop codons in bold).

Briefly, both the *CrtRb2* and *PSY2* genes were PCR amplified using the PFU II Ultra polymerase (Stratagene, UK; protocol described in Section 2.11.1) with primers containing restriction sites at the 3′ and 5′ ends (Table 8). The entry clone-pGENTR1a (Section 2.1.1), together with the purified PCR products (as described in Section 2.11.7) were double digested with *Sal I* and *Xho I* (Promega, UK) in the recommended buffer for 3 h (following the method in Section 2.11.3). After a 15 min 65˚C heat deactivation of the enzymes and SAP treatment of the vector DNA (Section 2.11.6), the ligation reaction was set up in a ratio of 1:3 vector to insert, using the Speed Ligase kit (Promega; protocol described in Section 2.11.5). The ligation plasmid was then electroporated into TOP 10 electro-competent cells (Invitrogen; method detailed in Section 2.3.2) and grown on gentamycin 50 µg ml^{-1} LB plates at 37˚C, overnight.

The entry clones obtained, P-pGEN (containing the *PSY2* gene) and B-pGEN (containing the *CrtRb2* gene) were digested with *Hpa I*, as detailed in Section 2.11.3, to confirm insertion of the transgenes in the correct orientation (Figure 26). Based on this result, the clones with a correct orientation were sequenced to obtain further confirmation on the sequence of the start codon and fluorescence tag. This procedure was performed by the James Hutton DNA Sequencing Service, using a 48 capillary ABI3730 machine (http://www.hutton.ac.uk/research/facilities/genome-technology/sequencing).

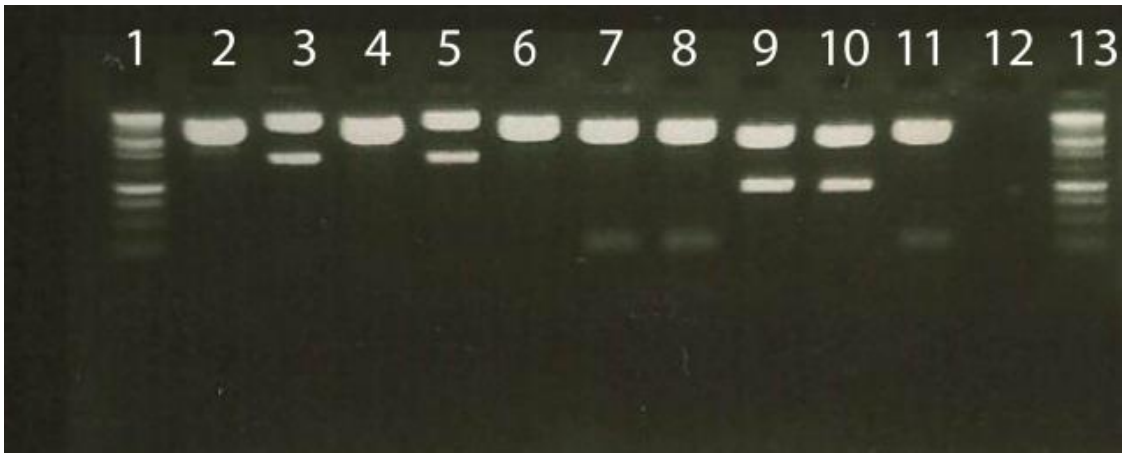

Figure 26. Agarose gel of restriction enzyme digest with *Hpa I* of the P-pGEN and B-pGEN entry clones. Lane 1 and 13, 10 kb ladder (Promega, UK); lane 2 to 6, PSY-pGEN; lane 7 to 11, B-pGEN; lane 12, no template control. The plasmids containing the transgenes *PSY2* and *CrtRb2* in a correct orientation, as identified based on the predicted lengths of the resulting bands, were lanes 2, 4, 6 for *PSY2* and 7, 8, 11 for *CrtRb2.*

Next, the P-pGEN and B-pGEN plasmids were used in four independent LR Gateway reactions (as described in Section 2.5.3) with the pK7FWG2 (Section 2.1.3) and pK7RWG2 (Section 2.1.4) vectors. The Gateway recombination reaction gave rise to a new series of binary vectors with *PSY2* (P-pK7F, P-pK7R) and *CrtRb2* (B-pK7F, B-pK7R) fluorescently tagged at the C-terminus (Figure 27) and under the control of the *Cauliflower Mosaic Virus 35S* (*CaMV 35S*) promoter.

In order to test the sub-cellular localisation of *PSY2* and *CrtRb2* proteins, the P-pK7F, P-pK7R, B-pK7F and B-pK7R plasmids were transiently expressed in *Nicotiana benthamiana* and potato leaves (Figure 28 for an overview of the method). The expression clones containing the two genes of interest were electroporated into *Agrobacterium tumefaciens* AGL1 cells (Sections 2.2.5 to 2.2.6), with and without

the *vir G* expression enhancer (method described in Section 2.3.2). Also, the pP19K helper plasmid (Section 2.1.6) was transformed into AGL1/vir G cells. The control used for this assay was the pGreen mGFP 5ER 3'OCS plasmid (Section 2.1.7). The liquid cultures of these constructs in *Agrobacterium* cells were prepared and agro-inoculated into *Nicotiana benthamiana* and potato leaves as described in Sections 2.7.1 to 2.7.2.

Table 8. Primer sequences for cloning of full length *CrtRb2* and *PSY2* into pGENTR1a.

Primer name	Sequence
Primer Forward *CrtRb2*	5′-AAA AGT CGA CAA AAT GGC GGC CGG AAT-3′
Primer Reverse *CrtRb2*	5′-AAA ACT CGA GCC TAA TAA TCC CTT AGA AAT TTT A-3′
Primer Forward *PSY2*	5′-AAA AGT CGA AAT GTC TGT TGC TTT GTT GTG-3′
Primer Reverse *PSY2*	5′-AAA ACT CGA GCC TGT CTT TGC TAG TGG GGA A-3′

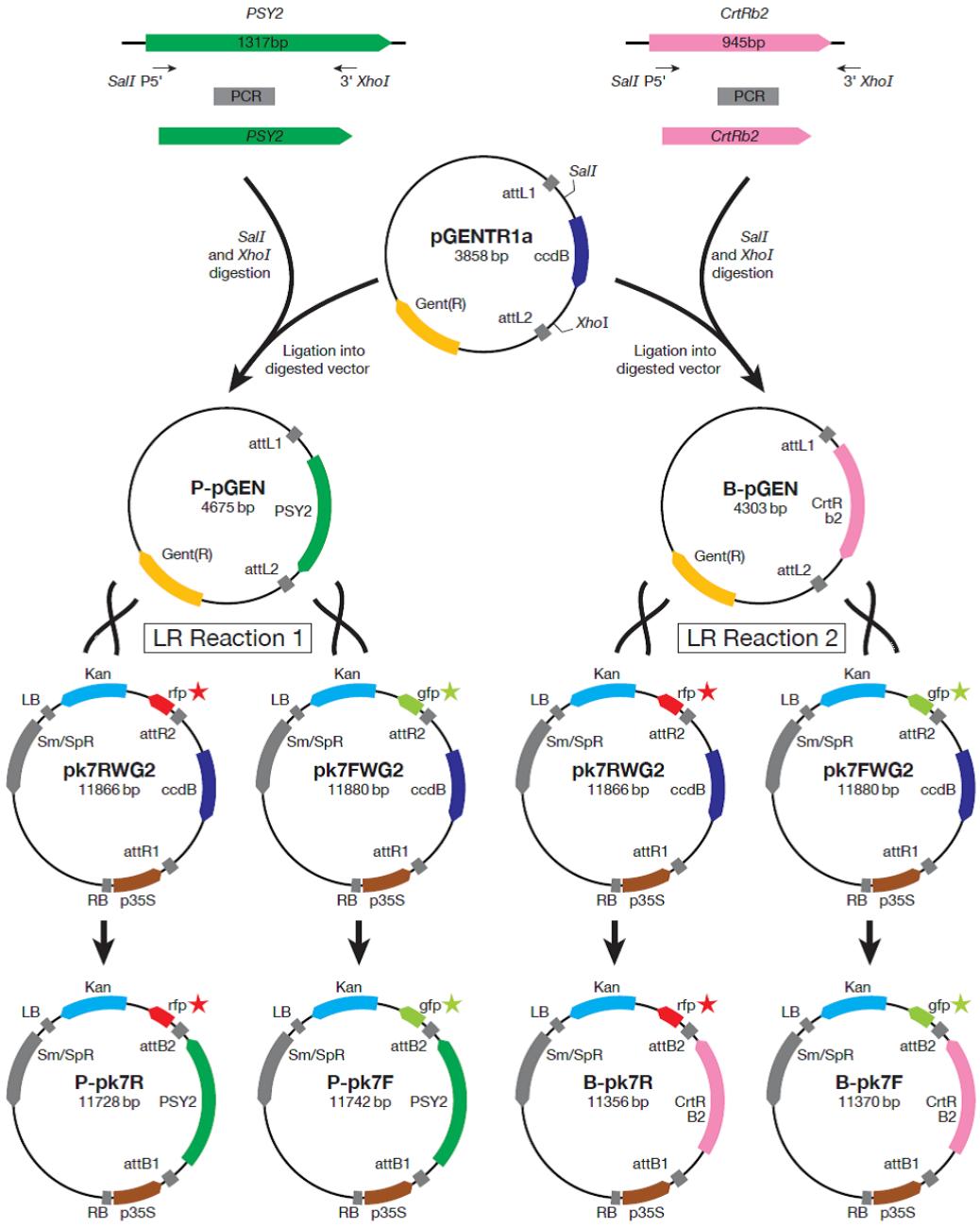

Figure 27. The strategy used for cloning the full length coding sequences of *PSY2* and *CrtRb2* genes into the pK7RWG2 and pK7FWG2 Gateway binary vectors. Abbreviations: PCR, polymerase chain reaction; LR reaction, Gateway reaction, mediated by LR Clonase (Invitrogen, UK); P-pGEN-*PSY2*, containing the pGENTR1a plasmid; B-pGEN-*CrtRb2*, containing the pGENTR1a plasmid; P-pK7R-*PSY2*, containing pK7RWG2 plasmid; P-pK7F-*PSY2*, containing pK7FWG2 plasmid; B-pK7R-*CrtRb2*, containing pK7RWG2 plasmid; B-pK7F-*CrtRb2*, containing pK7FWG2 plasmid; RB, right border; LB, left border; Kan, Kanamycin resistance genes; Sm/SpR, Streptomycin/Spectinomycin resistance genes; p35S, *Cauliflower Mosaic Virus 35S* promoter.

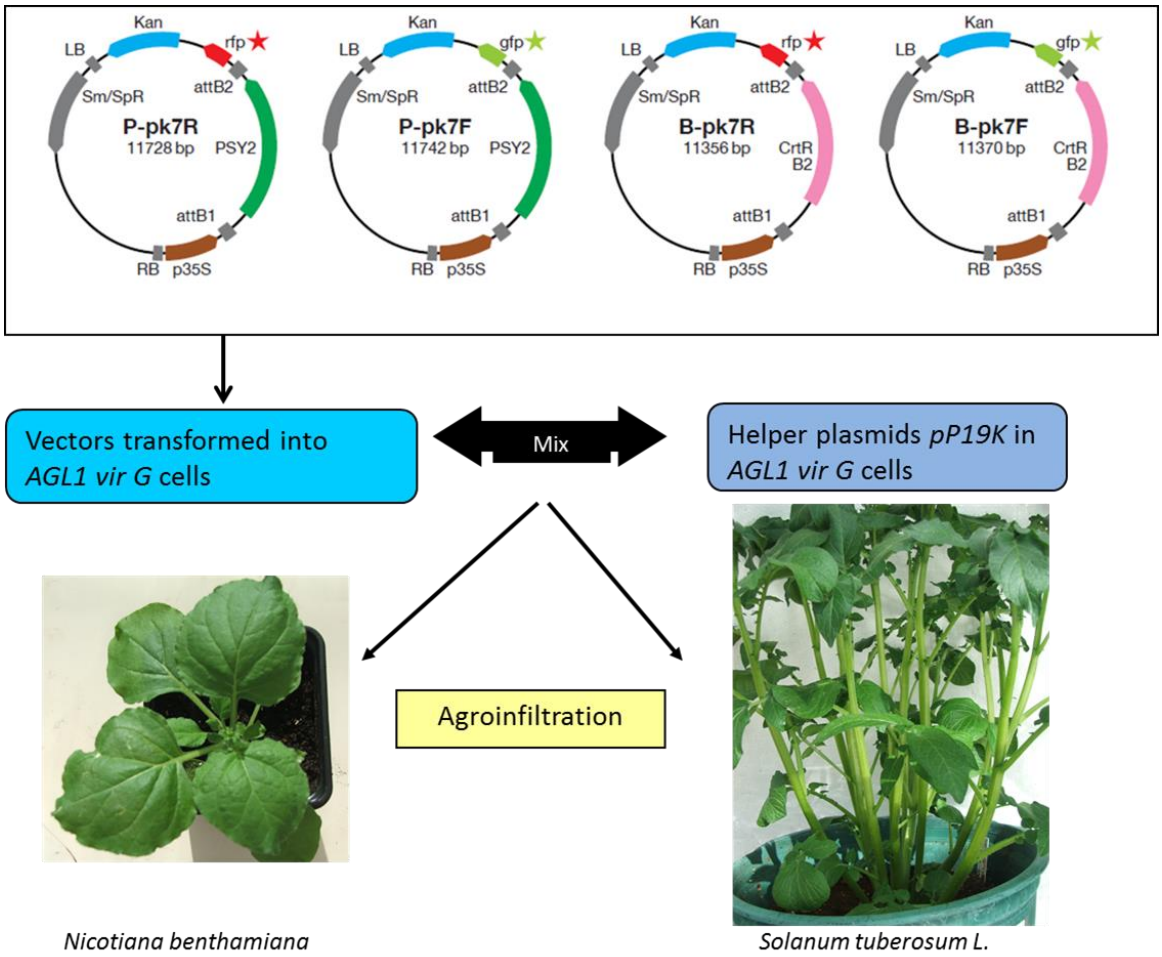

Figure 28. Overview of the method employed for transient expression of *PSY2* and *CrtRb2*-containing plasmids into leaves. The P-pK7R, P-pK7F, B-pK7R, and B-pK7F constructs were expressed in leaves of *Nicotiana benthamiana* and potato (*Solanum tuberosum* L.). For the detailed protocol of the agro-infiltration procedure, Sections 2.7.1 to 2.7.2.

4.2.2 Transient expression of the full length *CrtRb2* and *PSY2* in *Nicotiana benthamiana* and potato cv. Desiree mesophyll cells reveals different patterns of localisation

Constructs carrying fusions of full length cDNAs encoding PSY2 and CrtRb2 with RFP or GFP at the 3′ termini were transiently expressed in fully expanded *N. benthamiana* leaves, using an agro-infiltration approach, as described in Sections 2.7.1 to 2.7.2. Imaging was carried out as described in Sections 2.8.1 to 2.8.2. The analysis of the images obtained was carried out using the software provided by the manufacturing company. Images were processed using the Adobe Photoshop 6.0 software (Adobe Systems), as detailed in Section 2.8.5.

Both GFP-tagged CrtRb2 and PSY-2 proteins (green signal) are localised in the chloroplasts (indicated by blue false-colouring of chlorophyll auto-fluorescence) of the leaf mesophyll cells, but each has a different sub-organellar localisation. The CrtRb2-GFP signal (Figure 29A) is located throughout the stroma of the chloroplasts (shown in Figure 29B, marked by the chlorophyll auto-fluorescence). This is highlighted by the presence of a stromule, as seen in Figures 29A, C. The PSY2-GFP signal (Figure 29D) was detected as concentrated foci in the chloroplasts (Figure 29E-F). The agro-inoculation of *N. benthamiana* leaves with both PSY-2-GFP (Figure 29G) and CrtRB2-RFP (Figure 29H) constructs, showed their localisation was stable, even when they were co-expressed in the same chloroplast (Figure 29I).

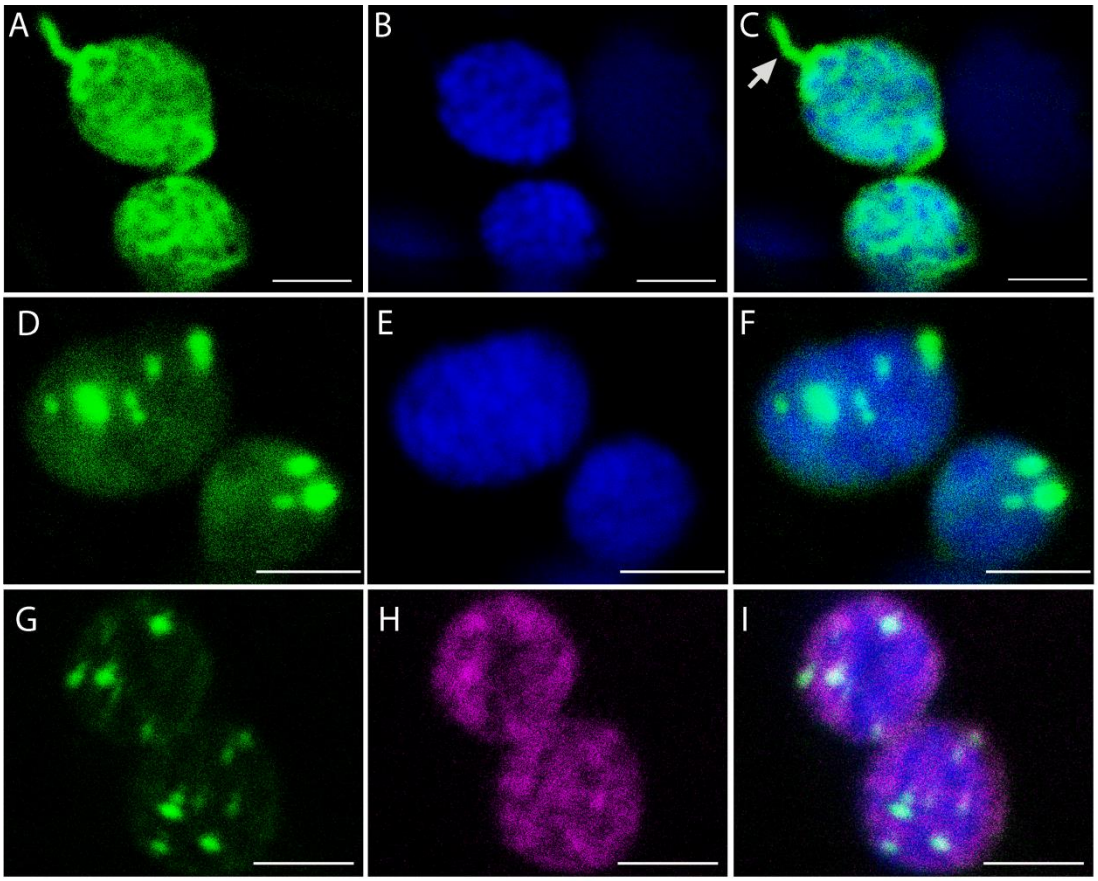

Figure 29. Transient expression of tagged CrtRb2 and PSY2 in *Nicotiana benthamiana* leaf chloroplasts. The full length sequence of CrtRb2-GFP (A) localised into the stroma of chloroplasts, but not the auto-fluorescent, chlorophyll-containing thylakoids (B), being particularly noticeable in a stromule (arrow; A, C). In contrast, the PSY2-GFP (D) fusion protein was detected as concentrated foci in the chloroplasts (E-F). Co-infection of the mesophyll cells with PSY2-GFP (G) and CrtRb2-RFP (H) did not alter their localisation pattern in chloroplasts (I). Bars=5 μm.

As information concerning the site of accumulation of two key biosynthetic enzymes at a sub-organellar level, in storage organs such as tubers, is scarce, it was considered necessary to obtain more insight into their precise location in chloroplasts. Thus, IMARIS software (Bitplane, Zurich) was used for volume rendering and 3D analysis of the images obtained by confocal microscopy. Previous studies have successfully shown that IMARIS can make use of the parameters captured together with the confocally-taken images and give 3D representations of the observed signals (Fei, 2002; Sugawara *et al*., 2005; Andlauer and Sigrist, 2012). This in-depth analysis confirmed localisation of both proteins inside the leaf chloroplasts and highlighted previous observations on the difference in the sub-organellar localisation pattern between CrtRb2 and PSY2 proteins. The CrtRb2-GFP signal was found into the stroma, whereas the PSY2-GFP signal was observed to accumulate in punctuated spots or speckles, inside the chloroplasts (Figure 30).

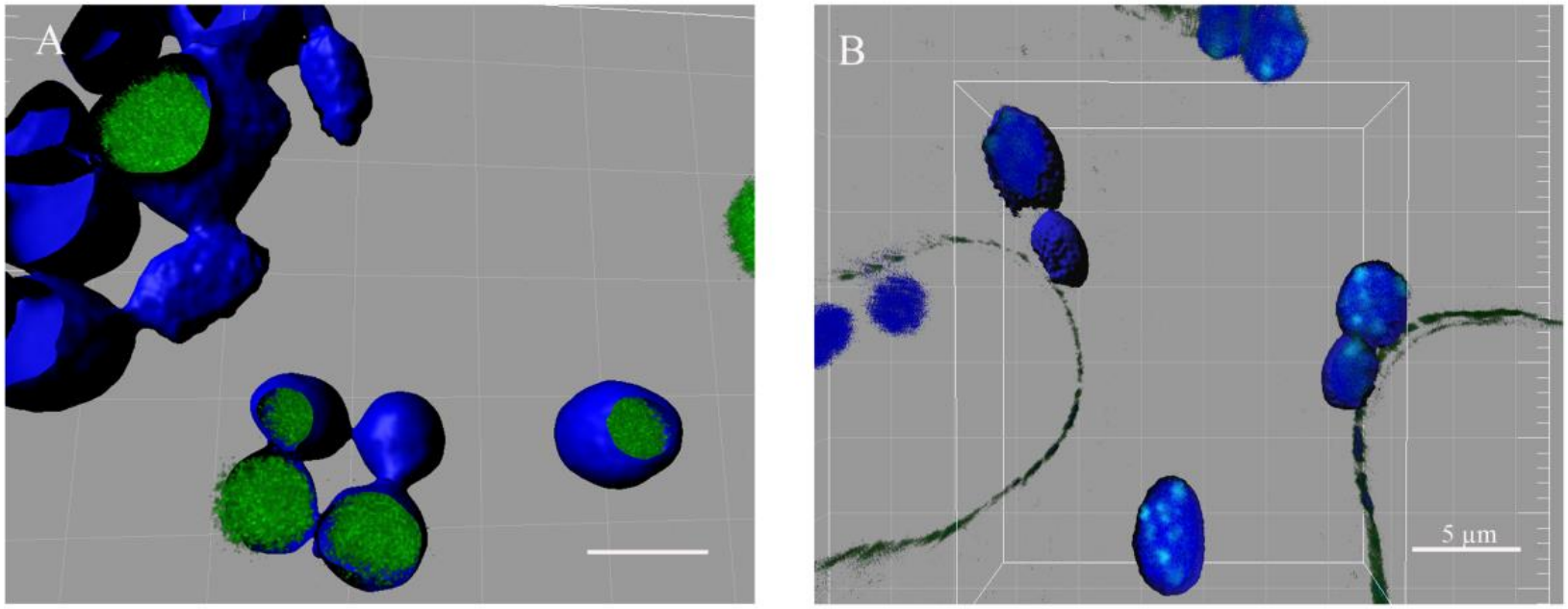

Figure 30. Representation in IMARIS of 3D visualisation based on confocal images of chloroplasts expressing CrtRb2-GFP (A) and PSY2-GFP (B) fusion proteins. The chlorophyll autofluorescence, designated by the blue false-colouring, serves to mark the contour of the chloroplasts, into which the GFP signal (green colour) was detected. Bars=5 µm.

Although *N. benthamiana* is an excellent model system for transient expression studies, it was considered necessary to confirm the localisation pattern of CrtRb2 and PSY fusions by expressing the constructs in the mesophyll of potato leaves. Probably due to the potato leaf morphology, characterized by less air space between the mesophyll cells than *N. benthamiana*, agro-infiltration of potato leaves did not generally lead to such high transient expression levels.

Based on the methodology described in the study of Bhaskar *et al.* (2009), who reported the transient expression of fluorescently tagged proteins in leaves of several potato cultivars, and using potato leaves of a suitable size and developmental stage (of 7 to 10 cm in diameter, from 6 week-old-plants), it was possible to achieve good levels of transient expression of CrtRb2 and PSY2 in potato mesophyll cells. These results confirmed previous findings from *N. benthamiana* mesophyll cells, demonstrating the same differential localisation pattern of CrtRb2 and PSY2 in potato cv. Desiree leaves, as CrtRb2 was detected as a stromal signal (Figure 31A), whereas PSY localised as concentrated foci into plastids (Figure 31B).

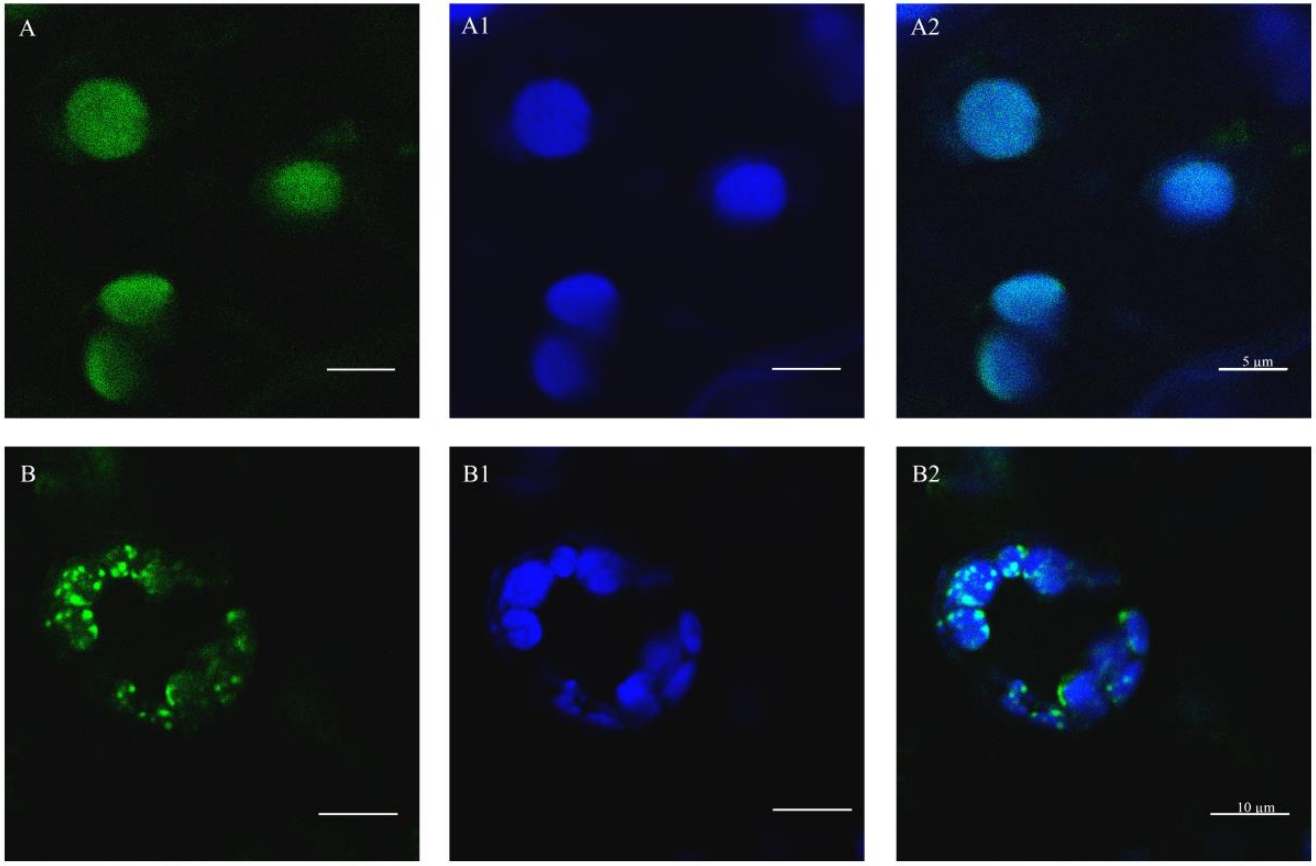

Figure 31. Transient expression of tagged CrtRb2 and PSY2 in potato leaf chloroplasts. The full length sequence of CrtRb2-GFP (A) localised into the stroma of chloroplasts, but not the auto-fluorescent, chlorophyll-containing thylakoids (A1). Merge (A2). In contrast, the PSY2-GFP (B) fusion protein was detected as concentrated foci in the chloroplasts (B-B1). Merge (B2). Bars=5 µm (A) and 10 µm (B).

4.2.3 The transit peptides of *CrtRb2* and *PSY2* fluorescently tagged, localise identically as full length sequences in *Nicotiana benthamiana* and potato cv. Desiree leaves

The ChloroP-predicted lengths of the N-terminus presequences (annotated as transit peptides) of *CrtRb2* and *PSY2* were 59 and 48 amino acids in length (shown as bold amino acid residues in Appendix 4). Bionda *et al.* (2010) suggested the required length for efficient translocation of proteins into chloroplast is 60 or more amino acids, but previous work by Misawa *et al*. (1994) reported the size of the ripe tomato fruit PSY transit peptide to be *ca.* 80 amino acid residues. To confirm that the fusion of the fluorescent probes to CrtRb2 and PSY2 proteins did not result in changed patterns of localisation, the predicted transit peptides of both proteins were fused to fluorescent proteins and transiently expressed in mesophyll cells of *Nicotiana benthamiana* and potato leaves. Hence, both the first 60 and 80 amino acids from potato CrtRb2 and PSY2 proteins were used to generate fusion-variants of these transit peptides with RFP or GFP at the carboxy termini, similar to the strategy detailed in Figure 27.

Investigation of the *in vivo* localisation pattern of CrtRb2 and PSY2 transit peptides, GFP/RFP tagged, showed similar results to the previous experiments, in which the full length coding sequence of CrtRb2 and PSY2 was transiently expressed in mesophyll cells of *N. benthamiana* and potato leaves. The CrtRb2-GFP signal for the 60 amino acid variants (Figure 32A) showed accumulation in the stroma of leaf chloroplasts (marked by the chlorophyll auto-fluorescence, in Figure 32A1). The 60 amino acid version of the PSY2 protein, GFP tagged (Figure 32B), localised as concentrated foci in the plastids (Figure 32B1). These results are similar to the ones obtained in previous experiments with the full length sequences of *CrtRb2* and *PSY2*.

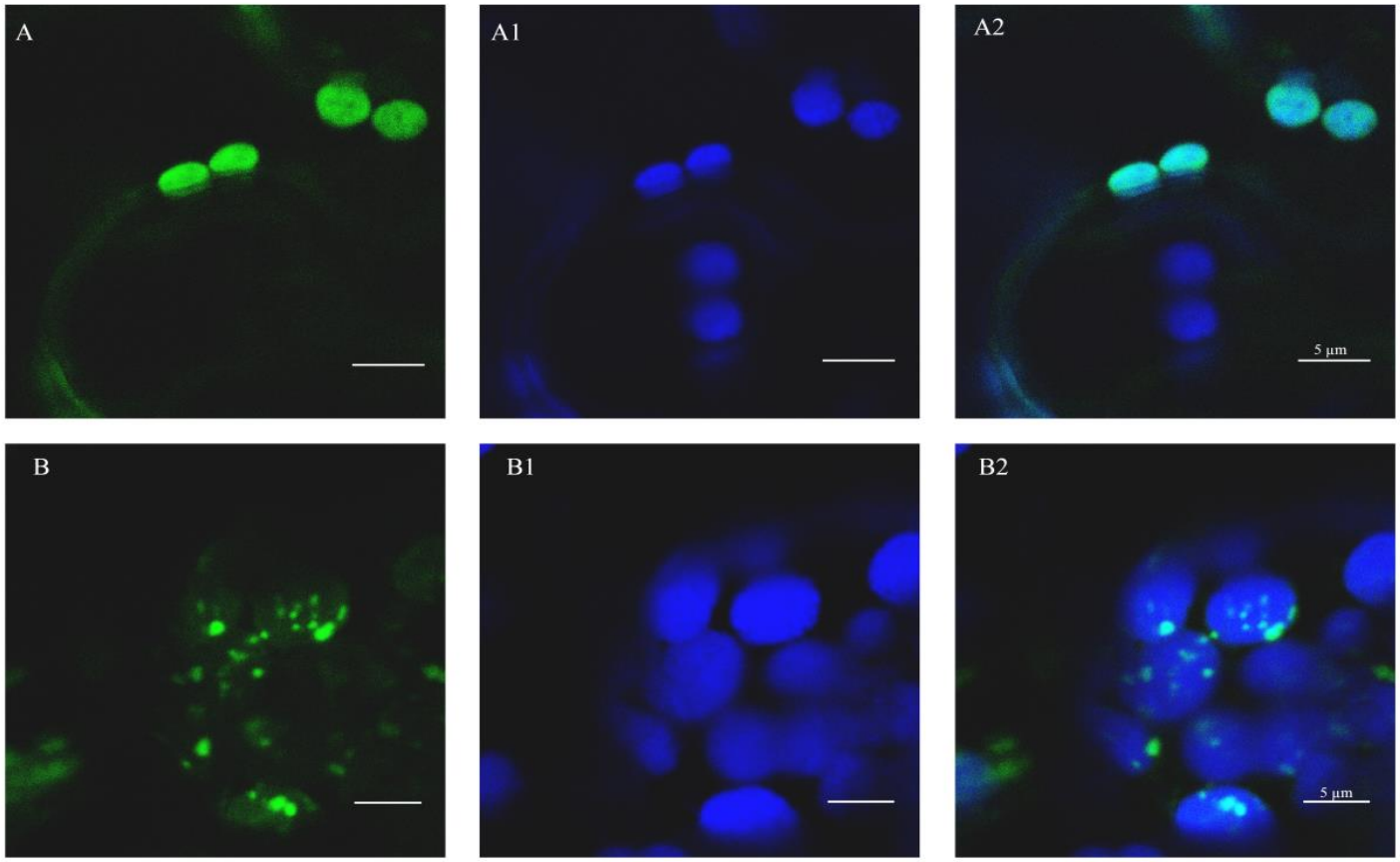

Figure 32. Transient expression of transit peptide of CrtRb2 and PSY2 in *Nicotiana benthamiana* leaf chloroplasts. CrtRb2-GFP (A) and PSY2-GFP (B) transit peptide fusion proteins, at 3 dpi. A1 to B1, Chlorophyll auto-fluorescence. The chloroplasts from A1, lacking a GFP signal, are most probably situated in another mesophyll cell, not yet infected by the *Agrobacterium*. A2 to B2, Merge of the GFP and the chlorophyll auto-fluorescence channels. Bars=5 µm.

4.2.4 Efforts to transiently express *CrtRb2* and *PSY2* into potato tubers

The agro-infiltration of fluorescently tagged proteins into plant tissues offers many advantages for the study of gene function and attempts to extend it from leaves to other tissues such as tomato fruits has proved possible (Orzaez *et al*., 2006). Hence, the transient expression of *CrtRb2* and *PSY2* genes was attempted in tuber tissues, by several methods.

In a procedure similar to the agro-infiltration of leaves, *Agrobacterium* cells expressing CrtRb2 and PSY2 were re-suspended in agro-infiltration buffer (prepared as in Section 2.4.3) and the injection of the plasmid-containing buffer solution (Section 2.7.2) was attempted into potato tubers. Another method used to transiently express CrtRb2 and PSY2 into tubers was based on the "Sonication-Assisted *Agrobacterium*-mediated Transformation" (SAAT) developed by Trick and Finer (1997). Hence, applying the SAAT principle of subjecting the plant tissue to brief periods of ultrasound in the presence of *Agrobacterium* (Trick and Finer, 1997), tuber slices (1 to 2 cm in thickness) were mixed with 20 ml of diluted (OD_{600} 0.1–0.5) *Agrobacterium* and sonicated for 0 to 300 s (as detailed by Liu *et al*., 2005). Vacuum infiltration of the constructs, assisted by sonication of the infiltration solution and/or tuber cells, based on experiments by Liu *et al.* (2005), was also attempted.

Despite the variety of methods used, efforts to transiently express *CrtRb2* and *PSY2* in potato tubers proved unsuccessful, as verified by confocal microscopy. In order to gain insight into the localisation of these key biosynthetic enzymes in potato tubers, an *Agrobacterium*-mediated stable transformation of potato stem cuttings was adopted (detailed in Sections 2.7.3 to 2.7.7), with the results of this approach presented in Chapter 5.

4.3 Discussion

The clarification of the *in vivo* localisation of enzymes is crucial for an improved understanding of their biological roles. By developing accessible methods of verifying the sub-cellular localisation of proteins, such as the transient expression systems, it is possible to gain insight into the localisation pattern of important pathway enzymes in plant cells.

The results presented in this chapter describe the engineering of constructs expressing two key carotenoid biosynthetic enzymes, fused to fluorescent tags, and their localisation into mesophyll cells. The transient expression of the *CrtRb2* and *PSY2* proteins in leaves of *Nicotiana benthamiana* gave high levels of expression, facilitating the sub-cellular localisation of these enzymes. The benefits of using fluorescently tagged enzymes to study localisation of carotenoid biosynthetic enzymes have been reviewed recently (Shumskaya *et al*., 2012). Also, other studies have extensively used tagging of enzymes with fluorescent proteins, keeping the gene products with the tags still active (Koroleva *et al*., 2005; Forth and Pyke, 2006; Verweij *et al*., 2008; Kokkirala *et al*., 2010; Shaw and Gray, 2011). Moreover, it is known that PSY accumulates to low levels and the sensitivity of the confocal microscopy approach enables detection that could possibly be missed using proteomic approaches.

However, over-expression of the pathway genes could conceivably perturb the system and thus observations are from tissues that are already subject to metabolic engineering. In leaves of both *Nicotiana benthamiana* and potato, identical localisations of the tagged proteins were observed with the tagged full-length cDNA and the tagged transit peptide, but also with these sequences alone. Clearly, in the latter case, no increase in carotenoid accumulation could be accounting for the observed localisation patterns. Additionally, co-expression studies demonstrated the same localisations in cells that over-express the CrtRb2 and PSY2 enzymes simultaneously.

The agro-infiltration and expression of the CtrRb2 and PSY2 constructs in potato leaves posed some difficulty. This was also valid for attempts to transiently express these plasmids into cells of potato tubers. The efficiency of transient expression can vary from host to host and some plant species seem recalcitrant to the technique. Despite a lack of clarity over the causes for the differences in efficiency, it is thought that structural factors, such as the compact nature of the tissues or the vein pattern, play an important role, together with the bacteria-host compatibility (Wroblewski *et al*., 2005). In the present study, despite lacking comparative data between cultivars to confirm that the developmental stage of the infiltrated leaves influenced transient expression, it was observed that the expression of the CrtRb2 and PSY2-containing constructs was successful when young, less compact leaves of potato were used.

The analysis of fluorescently-tagged CrtRb2 and PSY2 carotenoid biosynthetic enzymes, transiently expressed in mesophyll cells of *Nicotiana benthamiana* and potato, confirmed *in silico* predictions of their accumulation into plastids. The expression of both the full length coding sequence and the transit peptide of *CrtRb2* produced images in which the enzyme was shown to accumulate inside the chloroplasts. The investigations carried out using the confocal microscope gave new insight into this enzyme's sub-organellar localisation in chloroplasts. The images imply the accumulation of CrtRb2 in the stroma fraction of the plastids, a result further supported by the image in which the CrtRb2-GFP signal is present in a stromule, a stroma-filled tubule (Figure 29A-C). Stromules were thought, until recently, to allow communication between plastids and other cell compartments (Kohlen *et al*., 2000). However, Schattat *et al.* (2012) brought solid evidence against this theory, using colour differences to distinguish between the fusion and non-fusion events of similar organelles.

Analysis of the images captured and subsequent processing in IMARIS confirmed this conclusion. Hence, the 3D model of the chloroplasts, constructed based on the data files associated with the *in vivo* expression of CrtRb2-GFP, showed that this enzyme localises into the stroma of the plastids. Transiently expressing the full

length coding sequence and the transit peptide of *PSY2* in mesophyll cells of *Nicotiana benthamiana* and potato also gave consistent results regarding the localisation of PSY. The enzyme was apparent as concentrated foci or 'activity centres' at the chloroplast level. Analysis in IMARIS of the images taken of CrtRb2-GFP and PSY2-GFP expressing chloroplasts confirmed that both signals were being imported inside these organelles. In the literature, there is a strong indication of a plastidial pattern of localisation for both *CrtRb2* and *PSY* (Section 1.3.3).

However, there was a consistent difference in the compartmentalisation of the CrtRb2 and PSY2 enzymes in chloroplasts of the mesophyll cells, as shown throughout the study. The investigation of the fate after import of carotenoid biosynthetic enzymes such as the *Sinapis alba* GGPS, *Narcissus pseudonarcissus* PSY, PDS and LYC showed that differential fates and different membrane association mechanisms exist for the individual enzymes (Bonk *et al*., 1997). Previously, it was shown that, in the chromoplasts from *Narcissus pseudonarcissus*, PSY and PDS occur in two distinct forms, one soluble and inactive, the other membrane-bound and active (Schledz *et al*., 1996; Al-Babili *et al*., 1996). Based on results from protein import assays carried out in pea chloroplasts, Bonk *et al*. (1997) suggested there are three fates that carotenoid biosynthetic enzymes can have upon import. Firstly, enzymes can remain in an uncomplexed form in the chloroplast stroma, as in the case of GGPS. Secondly, they can transiently form complexes with chaperone molecules such as Cpn60 and associate rapidly and quantitatively to the thylakoid membranes, a fate that PSY is prone to adopt. Thirdly, enzymes can remain soluble after import, associating with Cpn60 to form high molecular mass complexes.

As lipid-containing structures, primarily attached to the thylakoid membranes (Rey *et al*., 2000), PGs emerge as a possible active site of carotenoid conversion in chromoplasts, as suggested by reports on the detection of carotenoid biosynthetic enzymes in the proteome of bell pepper (*Capsicum annuum* L.) chromoplasts (Siddique *et al*., 2006) and of pepper PGs (Ytterberg *et al*., 2006). Based on these results, new roles are being suggested for PGs, implying a functional metabolic link between the inner envelope and thylakoid membranes.

PSY was reported to be strongly associated with membranes, in its active form (Schledz *et al*., 1996). Welsch *et al*. (2000) reported that PSY localised in the thylakoid membrane of mature chloroplasts, based on immunoblot analysis with PSY antiserum. Recently, an Arabidopsis zinc finger protein, VAR3 (At5g17790), proved to interact with CCD4, was localized to the chloroplasts as punctuated spots (Naested *et al*., 2004), very similar to the pattern of localisation encountered in the case of PSY2 in the mesophyll cells. Based on identification of CCD4 into the proteome of chloroplast PGs, Ytterberg *et al*. (2006) claimed these spots could represent plastoglobules. This brings forth evidence to support the hypothesis that the build-up of PSY2 in 'concentrated foci', as confirmed by 3D volume rendering in IMARIS software, signals the accumulation of this carotenoid biosynthetic enzyme into PGs.

By expressing the predicted transit peptides of CtrRb2 and PSY2 in mesophyll cells, it was possible to observe an identical pattern of localisation as the full length sequences. Interestingly, by imaging and further processing in IMARIS the information associated with the expression of CtrRb2 and PSY2 in chloroplasts, a differential pattern of localisation of these proteins was observed. The CrtRb2 enzyme accumulated in the stroma, whereas PSY2 localised in punctuated spots, both inside the chloroplasts. Based on these findings, it is possible to infer that distinct compartmentalisation rules exist to discriminate between enzymes with important regulatory roles in the carotenoid biosynthetic pathway.

Chapter 5 Investigation of stably expressed CrtRb2 and PSY2 in potato cv. Desiree tuber tissue

5.1 Introduction

The expression of carotenoid biosynthetic genes is known to dictate the levels of carotenoids in plants, but studies have recently shown that other factors can also influence the accumulation of these pigments throughout plant life (reviewed in Cazzonelli and Pogson, 2010).

Ducreux *et al.* (2005) found that transgenic lines expressing the highest levels of *CrtB* in the tuber, both at the transcript and protein levels, did not accumulate the highest content of tuber carotenoid. Also, Li *et al.* (2006) showed that the increase in β-carotene observed in the yellow *Or* cauliflower curd is not due to higher biosynthesis levels in these mutant plants. Another study by Clotault *et al.* (2008) reported expression of carotenogenesis-related genes in white carrot root, devoid of carotenoids. Factors such as plastid biogenesis and inter-conversion are also thought to influence the differential accumulation of carotenoids in plants (Egea *et al*., 2010). Also, very recently, it has been shown that in maize leaves different PSY isozymes target to different sub-organellar localisations (Shumskaya *et al*., 2012). In this study, small variations in target peptide sequences appear to be sufficient to influence the different localisations.

The activity of carotenoid biosynthetic enzymes is thought to be determined by their membrane association, with many such enzymes (including PSY) known to require a membrane context for their activity. Either *via* membrane attachment or spanning domains or by interacting with other anchor-like proteins, that possess such domains, the carotenoid enzymes can associate to membranes and fulfil their role in biosynthesis. Ruiz-Sola and Rodriguez-Concepcion (2012) proposed a hypothetical model for multi-enzyme complexes functioning in the biosynthesis of carotenoids in Arabidopsis plants. According to it, the protein complexes, associated to the chloroplast envelope membrane, catalyse the production of phytoene from IPP and DMPP (formed by IDI, GGDS and PSY), phytoene into lycopene (PDS, Z-ISO, ZDS and CRTISO), phytoene into β-carotene (PDS, Z-ISO, ZDS, CRTISO and LCYB)

and lycopene into lutein (LCYE, LCYB and CYP97s). Then, individual enzymes, associated with either the envelope or thylakoid membranes, would convert β-carotene into β,β-xanthophylls.

However, little is known about the sub-organellar localisation of key carotenoid biosynthetic enzymes in potato tubers. In the present study, this issue was investigated as a potential factor in influencing the total carotenoid levels in plant storage organs. In Chapter 4, the transient expression of CrtRb2 and PSY2 in mesophyll cells revealed different pattern of localisation of these two enzymes in the chloroplasts. Attempts to transiently express these genes of interest, fluorescently tagged, into potato tubers, were unsuccessful (Section 4.2.4). Hence, fusions of potato *CrtRb2* and *PSY2* with RFP were engineered and stably expressed in tubers. Non-invasive confocal microscopy in combination with 3D volume rendering of the observed structures enabled the localisation of the RFP-tagged biosynthetic enzymes within the potato tuber to be determined.

5.2 Results

5.2.1 Engineering of constructs for stable expression of *CrtRb2* and *PSY2* in potato tuber tissue

In order to achieve expression of the *CrtRb2* and *PSY2* into these storage organs, an *Agrobacterium* mediated-stable transformation approach of potato cv. Desiree internodes was used. To safeguard against any developmental phenotypes, as reported by Fray *et al*. (1995) and Busch *et al*. (2002) and to ensure presence of the targeted CrtRb2 and PSY2 proteins in the tubers, it was necessary to express the two genes of interest under the tuber-specific *B33*-patatin promoter. Hence, the previously engineered binary vectors expressing CrtRb2 and PSY2 under the constitutive promoter *CaMV 35S* promoter (Section 4.2.1) were modified for this purpose. The *CaMV 35S* sequence was replaced by the *B33*-patatin promoter sequence (Figure 33 for an overview of the cloning strategy).

Briefly, the 1.7 kb sequence of the *B33* promoter was amplified in a PCR reaction (Section 2.11.1) from the B33-pBIN19 plasmid, kindly provided by Sophia Sonnewald (Erlangen-Nuremberg University, Germany), using primers with *Spe* I and *Pme* I restriction sites at the 5′ and 3′ ends (Table 9). The resulting PCR product was cloned by T/A cloning into pGEM-T-Easy (as in Section 2.5.1) and sequenced. The B33 in pGEM-T-Easy construct was doubly digested with *Spe* I and *Pme* I restriction enzymes. The P-pK7R and B-pK7R binary vectors, obtained in Section 4.2.1, were also doubly digested with *Spe* I and *Pme* I restriction enzymes, as in Section 2.11.3, to release the *CaMV 35S* promoter that was driving expression of the transgenes. Then, the vectors were treated with SAP (Section 2.11.6). The B33-patatin sequence, with *Spe* I and *Pme* I restriction sites at 3′ and 5′ ends, was then ligated into the digested and treated P-pK7R and B-pK7R vectors, as in Section 2.11.5. Following this ligation reaction, new expression clones were obtained, containing the *PSY2* and *CrtRb2* transgenes with expression under the control of the B33-patatin promoter, designated P-B33-pK7R and B-B33-pK7R (Figure 33).

Table 9. Primer sequences B33-patatin cloning strategy

Primer name	Primer sequence
Primer Forward *B33* (*Pme* I sites)	5′AAAA GTT TAA AC AGCTTATGTTGCCATATAGAGTAGT 3′
Primer Reverse *B33* (*Spe* I sites)	5′AAAA A CTA GTGGTGCTTTGAGCATATAACAAGC 3′

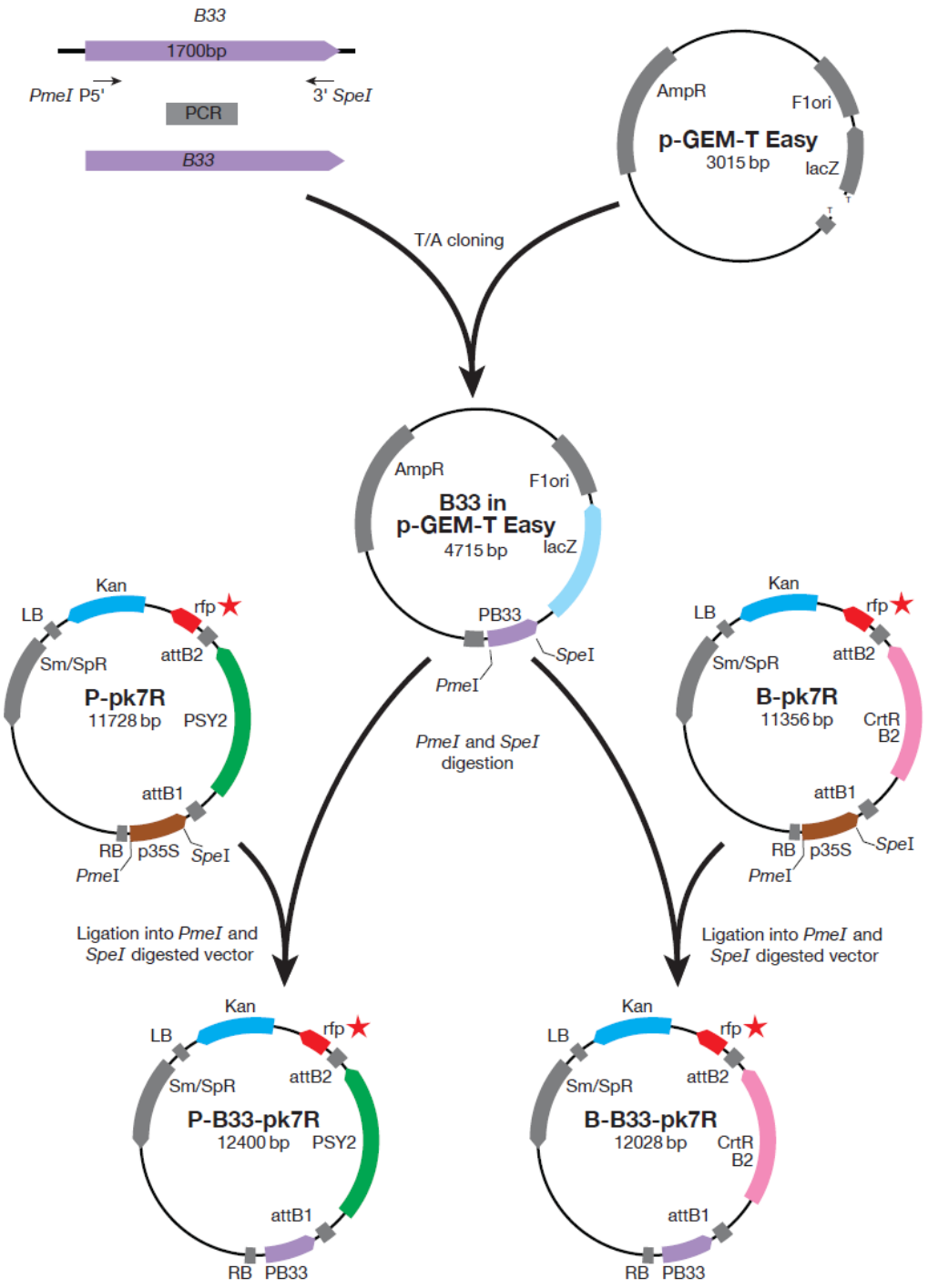

Figure 33. Cloning strategy for over-expression of *PSY2* and *CrtRb2* under B33-patatin tuber specific promoter. The strategy used for modifying the P-pK7R and B-pK7R vectors, obtained in Section 4.2.1, to express the full length coding sequences of *PSY2* and *CrtRb2* genes into the pK7RWG2 and pK7FWG2 Gateway binary vectors under the B33-patatin tuber specific promoter. Abbreviations: PCR, polymerase chain reaction; AmpR, Ampicillin resistance genes; F1 *ori*, origin of replication; lac Z-βeta-galactosidase; PB33, patatin B33 promoter; P-pK7R-*PSY2*, containing pK7RWG2 plasmid; B-pK7R-*CrtRb2*, containing pK7RWG2 plasmid; RB, right border; LB, left border; Kan, Kanamycin resistance genes; Sm/SpR,

Streptomycin/ Spectinomycin resistance genes; p35S, *Cauliflower Mosaic Virus 35S* promoter; P-B33-pK7R- and B-B33-pK7R-*CrtRb2*, *PSY2*/CrtRb2 containing pK7RWG2 plasmid, under control of the B33 patatin promoter.

5.2.2 Generation of transgenic potato plants, over-expressing the *CrtRb2* and *PSY2* transgenes

The B-B33-pK7R and P-B33-pK7R expression clones were transformed into *Agrobacterium tumefaciens* strain LBA4404 using the methods detailed in Section 2.3.2. A total of 19 transgenic lines over-expressing *PSY2* were obtained from 500 internode explants, representing a transformation efficiency of 3.8%. In the case of *CrtRb2* transgenics, 4 lines were obtained from 200 internode explants, representing a transformation efficiency of 2%. The plantlets obtained from tissue culture were grown in sterile conditions for four to six weeks before transferring them to the glasshouse (Figure 34 for image of callus to shoots; growth conditions as in Section 2.6.3). Each putative transgenic line was represented in the glasshouse by three potato plants.

Visual inspection of the transgenic potato plants did not show any apparent phenotypic changes, when compared with the control plants, EV lines and the control plants cv. Desiree. However, by harvesting developing and mature tubers at approximately 12 and 16 weeks after planting, it was observed that the tuber flesh throughout the *PSY2* potato lines had a yellow colour (Figure 35). This was present to a lesser extent for potato tubers from the *CrtRb2* lines, as determined by visual observations of the tuber flesh from transformant lines.

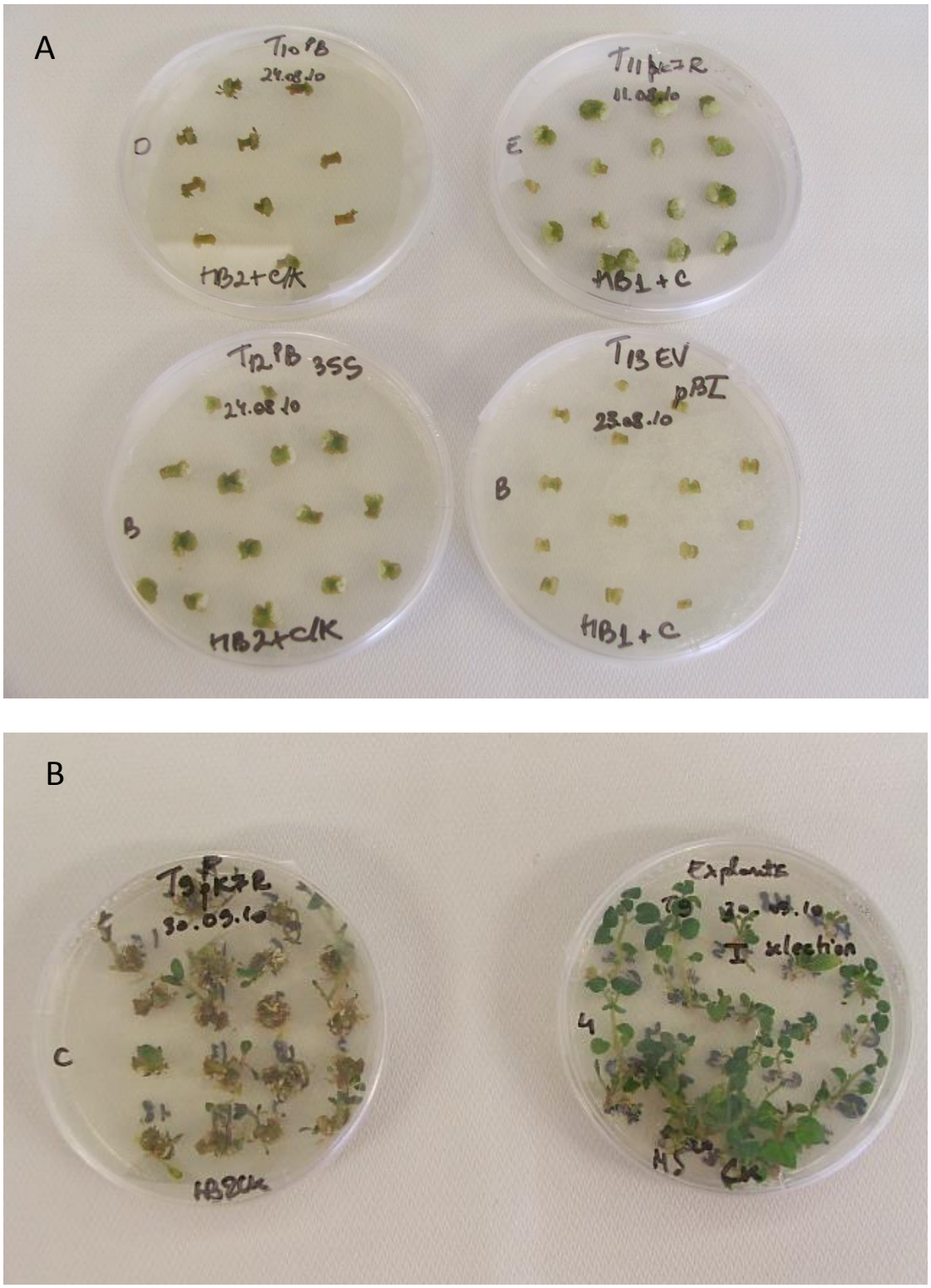

Figure 34. The cultivation of transformed internode explants of HB2 medium with selection, as detailed in Sections 2.7.3 to 2.7.7. A, Four to five week-old internodes, now forming visible calli. B, Formation of shoots from the calli (left), as observed just before excision and re-rooting on fresh MS-30 medium with antibiotic selection (right) to ensure growth of only transformed shoots.

Figure 35. Comparison of tuber flesh from control potato cv. Desiree and transgenic potato over-expressing the *PSY2* transgene under control of the *B33*-patatin tuber specific promoter. Image is representative for the lines obtained by transformation of the B33:PSY2 construct.

5.2.3 Analysis of transcript levels in *CrtRb2* and *PSY2* transgenic potato lines

The transcript levels of the *CrtRb2* and *PSY2* genes were measured in transgenic tuber tissue over two growing seasons, by employing qRT-PCR assays (UPL system, Roche, UK; https://www.roche-applied-science.com/sis/rtpcr/upl/). The primer and probe sequences suitable for RT-PCR were obtained by submitting the full length sequences of the *CrtRb2* and *PSY2* to the UPL online design tool (Table 10). The transcript levels of both *CrtRb2* and *PSY2* were determined against expression levels of the control gene *EF1-α*, employing the ΔΔct method (Livak, 1997). Total RNA, extracted from stolons and mature tubers of *CrtRb2* and *PSY2* transgenic lines and controls-potato cv. Desiree and EV transformant, was used to generate cDNA, as described in Section 2.11.12., followed by qRT-PCR analysis, performed as in Section 2.11.13.

QRT-PCR analysis was performed on tuber and stolon tissue harvested from transgenic potato lines obtained from tissue culture grown plantlets (Figure 36A-B). In the case of *CrtRb2* transgenic potato, all four over-expressing lines examined showed a significant increase in transcript levels in both tuber and stolons (Figure 36A). The expression of *PSY2* was significantly increased in stolons in the four lines analysed, but not in the tuber tissues of the transgenic potato lines (Figure 36B).

Analysis of the transcript levels in tissue harvested from *CrtRb2* and *PSY2* transgenic plants grown from tubers, in the second season of cultivation, also showed increased transgene expression. These target genes were found to be increased by 10-fold in the case of *CrtRb2* transgenic line K1 and by 6-fold in tubers from *PSY2* over-expressing potato line R5 (Figure 37A-B).

Table 10. Primer and probe sequences as designed in the Roche UPL assay online tool, used for qRT-PCR analysis.

UPL Primer /probe name	UPL Primer /probe sequence
Primer Forward Ef1-α	5′-CTTGACGCTCTTGACCAGATT-3′
Primer Reverse Ef1-α	5'-GAAGACGGAGGGGTTTGTCT-3'
Primer Forward CrtRb2	5′-TGAGATGAACGACGTTTTCG-3′
Primer Reverse CrtRb2	5′-GAAGAAACCGTATGAAAGAAGAGC-3′
Primer Forward PSY2	5′-TCTGGGCAATATATGTGTGGTG-3′
Primer Reverse PSY2	5′-GATGCATTAGGGCCATCAAC-3′
Probe 117 Ef1-α	5′-AGCCCAAG-3′
Probe 150 CrtRb2	5′-TGCTGTTC-3′
Probe 136 PSY2	5′-TGATGAGC-3′

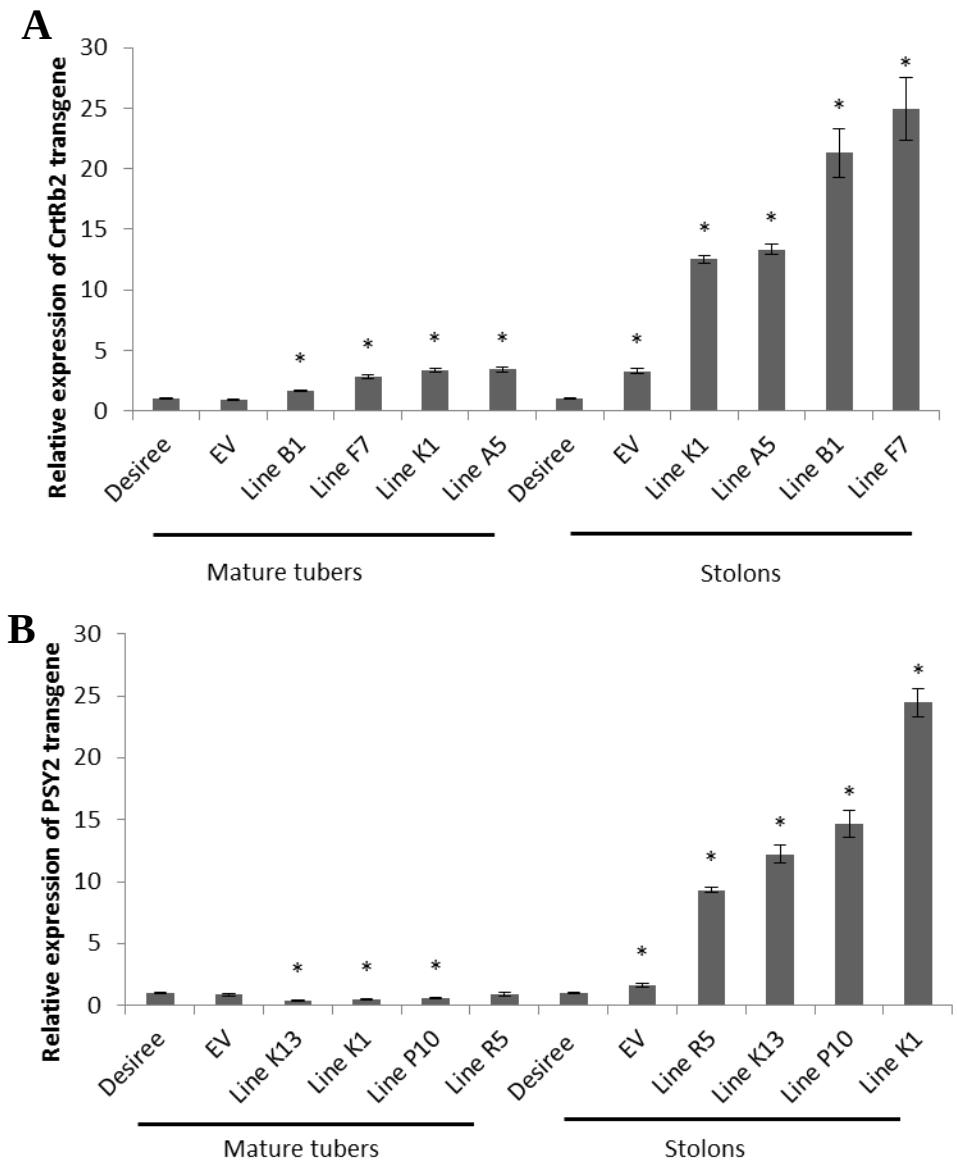

Figure 36. Expression levels in tubers and stolons of transgenic potato lines grown from tissue culture plantlets, in the first season of growth. A, CrtRb2 and B, PSY2 over-expressing lines of transgenic tuber and stolon tissue, compared to controls-wild type potato cv. Desiree and EV. Values are means of triplicate assays ± SE (standard error), based on one biological replicate, expressed relative to the value in wild type tuber and stolons. The material was grown from tissue culture stem cuttings, as described in Section 2.6.3. Statistical differences from the wild type control were calculated with Student's one-tailed *t* test, assuming unequal variance. An asterisk was added where there was a significant difference between the calculated (P <0.05) values for transgenic lines and controls.

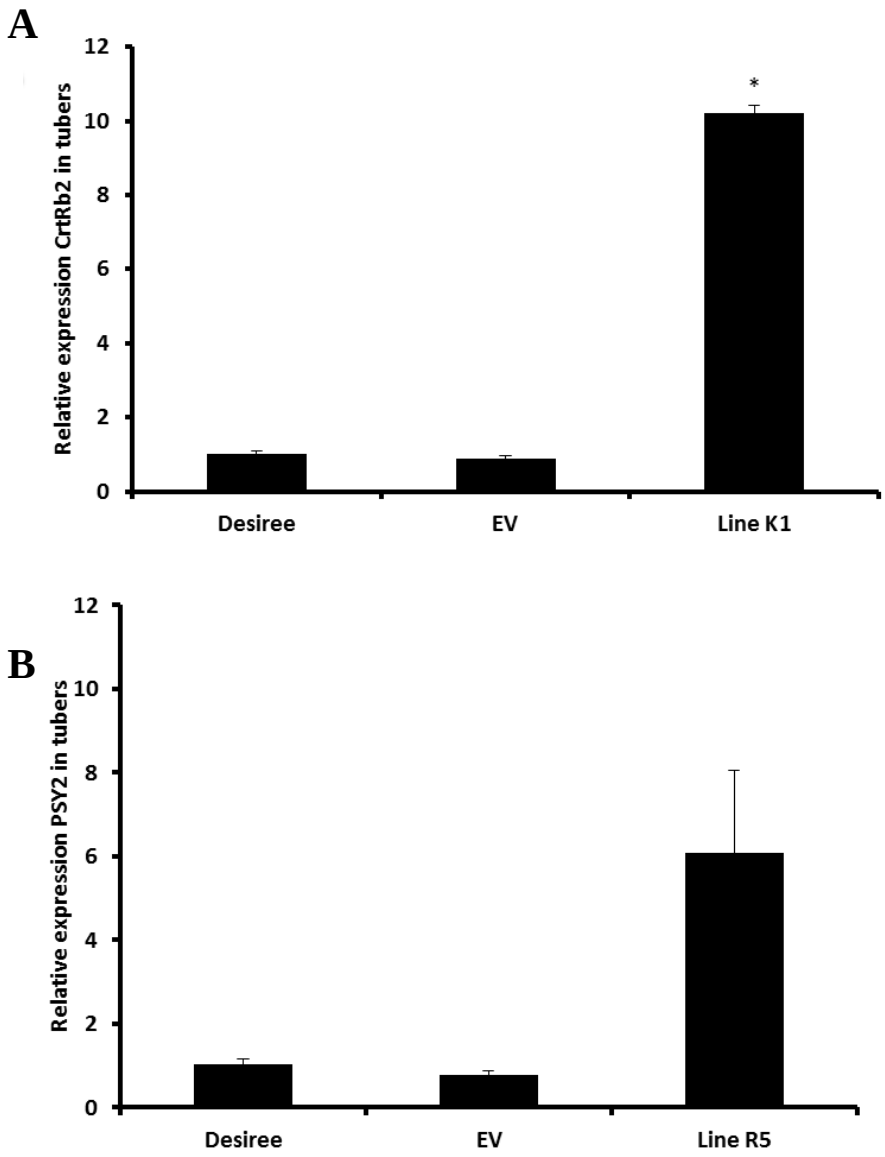

Figure 37. Expression levels in tubers of transgenic potato lines grown from tissue culture plantlets, in the second season of growth. A-CrtRb2 and B-PSY2 over-expressing lines of transgenic potato tissue, compared to controls, wild type potato cv. Desiree and EV. Values are means of triplicate assays ± SE (standard error), based on three biological replicates, expressed relative to the value in wild type tubers. The material was grown from tubers, as described in Section 2.6.3. Statistical differences from the wild type control were calculated with Student's one-tailed *t* test, assuming unequal variance. An asterisk was added where there was a significant difference between the calculated (P <0.05) values for transgenic lines and controls.

5.2.4 Measurements of total carotenoid content in *CrtRb2* and *PSY2* transgenic potato lines

Measurements of total tuber carotenoid content of both *CrtRb2* and *PSY2* over-expressing potato lines were determined spectrophotometrically (Section 2.12.1 for the described protocol), throughout two growing seasons.

In the first season of cultivation, an increase of up to 5-fold (24 µg g^{-1} DW) in the tuber total carotenoid content was observed throughout the 15 *PSY2* over-expressing lines analysed, when compared to controls (potato cv. Desiree, 3.5 µg g^{-1} DW; Figure 38A). The *CrtRb2* transformant lines also showed increases of up to 3-fold in the total carotenoid present in tubers (Figure 38B). Analysis of tuber tissue from over-expressing lines, during a second season of growth, demonstrated that the total carotenoid level was higher in both transgenic lines, when compared to wild type cv. Desiree. Despite a lower increase in total carotenoids than the one observed in the first season of growth, levels were up to 7 µg g^{-1} DW in the case of *CrtRb2* line K1 and reached 10 µg g^{-1} DW for *PSY2* line R5, an up to 2-fold increase for this transgenic line (Figure 39).

The identification of the individual carotenoids from tuber extracts was carried out using HPLC analysis, as described in Section 2.12.2., on saponified and non-saponified samples (running of samples and collection of data from HPLC by Ray Campbell, JHI, UK). Data on the carotenoid profiles in tubers of *CrtRb2* and *PSY2* and transgenic lines, during the second season of growth, showed in *PSY2* line R5 statistically significant increased β-carotene levels (Table 11). There was also indication of increased violaxanthin, antheraxanthin, lutein in *PSY2* line R5 and violaxanthin in *CrtRb2* line K1, but this data was not statistically significant (Table 11).

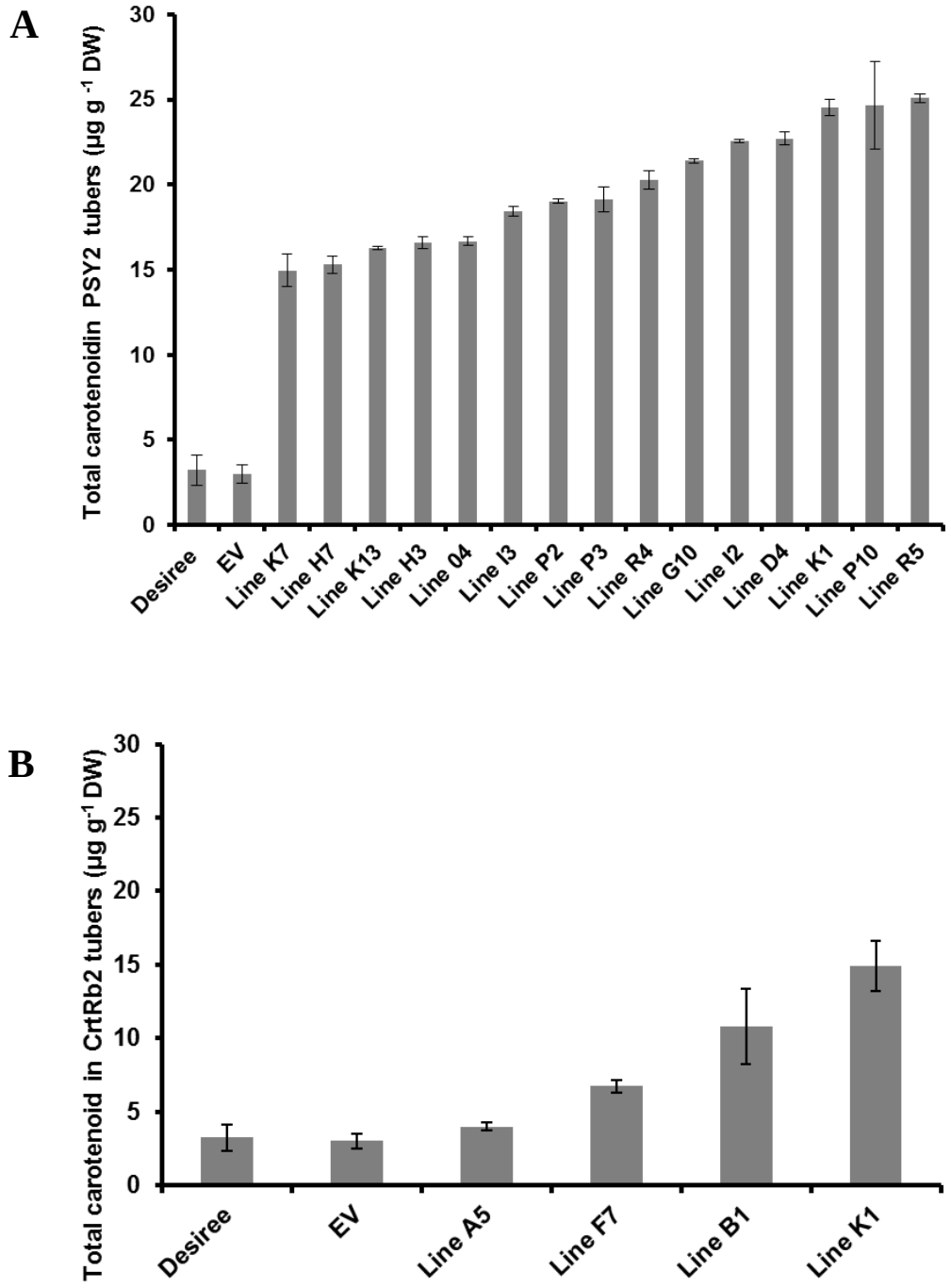

Figure 38. Total carotenoid content of transgenic potato tubers in the first season of cultivation. Comparison of values of control (Desiree and EV) and *CrtRb2* (A) and *PSY2* (B) transgenic lines. Values are the mean of two technical replicates of one biological replicate, based on analysis of tubers harvested from 90 day-old (mature) plants, grown from tissue culture stem cuttings, as described in Section 2.6.3. Error bars indicate ± the range.

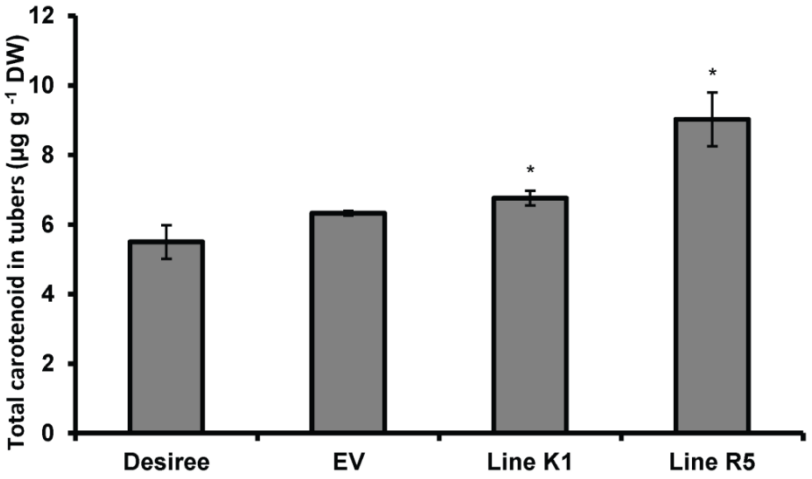

Figure 39. Total carotenoid content of transgenic potato tubers in the second season of cultivation. Comparison of control (Desiree and EV) and *CrtRb2* line K1 and *PSY2* line R5 plants. Values are based on analysis of tubers harvested from 90 days old (mature) plants, grown from tubers, based on three biological replicates, grown as described in Section 2.6.3. Error bars indicate ± SE (standard error). Statistical differences from the wild type control were calculated with Student's one-tailed *t* test, assuming unequal variance. An asterisk was added where there was a significant difference between the calculated (P <0.05) values for transgenic lines and controls.

Table 11. Carotenoid composition of tuber tissue of *CrtRb2* and *PSY2* over-expressing lines, compared to control potato cv. Desiree, in the second season of growth.Values (µg g^{-1} DW) are based on the mean of 2 to 3 biological replicates, analysis carried out in duplicate, ± SE (standard error). Statistical differences from the wild type control were calculated with Student's one-tailed *t* test, assuming unequal variance. An asterisk was added where there was a significant difference between the calculated (*P* <0.05) values for transgenic lines and controls. Abbreviations: Neo, neoxanthin isomers; Vio, violaxanthin isomers; Ant, antheraxanthin isomers; Lut, lutein; Zea, zeaxathin; βeta, β-carotene; Total, total carotenoid concentration (µg g^{-1} DW).

Line	Neo	Vio	Ant	Lut	Zea	βeta	Total
Wild type	0.7 ±0.08	2.24 ±0.59	0.75 ±0.2	1.56 ±0.3	0.12 ±0.08	0.01	5.42 ±0.7
CrtRb2 Line K1	0.95 ±0.06	4.45 ±0.5	0.38 ±0.04	0.74 ±0.02	0.06 ±0.01	0	6.59 ±0.4
PSY2 Line R5	0.59 ±0.06	3.78 ±0.9	1.16 ±0.13	3.31 ±0.9	0.14 ±0.03	0.07±0.01*	9.08 ±1.2*

5.2.5 Sub-cellular localisation of CrtRb2 and PSY2 protein fusions in potato tuber tissue

Tuber tissue from developing and mature tubers of *CrtRb2* and *PSY2* over-expressing lines was used in confocal fluorescence microscopy analysis, to determine the localisation of the RFP-tagged carotenoid biosynthetic enzymes. The tuber samples to be analysed were cut in 150 to 200 µM thick slices, as detailed in Section 2.8.3 using these or the resulting sap for imaging. The preparation and imaging protocols are described in Section 2.8.1. Confocal microscopy analysis was carried out on several tubers from each selected transgenic line, over three growing seasons. For each construct, consistency of the localisation patterns was observed in tubers from three seasons of growth, emphasising the reproducibility of the experiments and the stability of the observed subcellular accumulation.

As with the data from transient expression studies in leaf, the localisation of the CrtRb2 and PSY2 fusion proteins was in plastids. The imaging of tuber tissue over-expressing the *CrtRb2* and *PSY2* transgenes, RFP tagged, showed accumulation of these enzymes in the amyloplasts of parenchyma cells (Figure 40).

5.2.6 3D volume rendering of RFP-tagged proteins in potato tuber tissue

Images of bright-field and RFP fluorescence in amyloplasts of transgenic potato were obtained (Figure 38A-B), following the detection of the $DiOC_6$ staining, as to mark the amyloplast membrane boundaries. Such data made it possible to employ the IMARIS software for 3D volume rendering and subsequent visualisation of the $DiOC_6$ and RFP fluorescence in amyloplasts. Thus, differences in the pattern of localisation of the two enzymes inside the amyloplasts were emphasised by this type of analysis. The CrtRb2::RFP signal was present in vesicle-like membrane-bound structures, successfully stained by the $DiOC_6$, whereas the RFP-tagged PSY2 was found to be located in the amyloplasts'stroma (Figure 41).

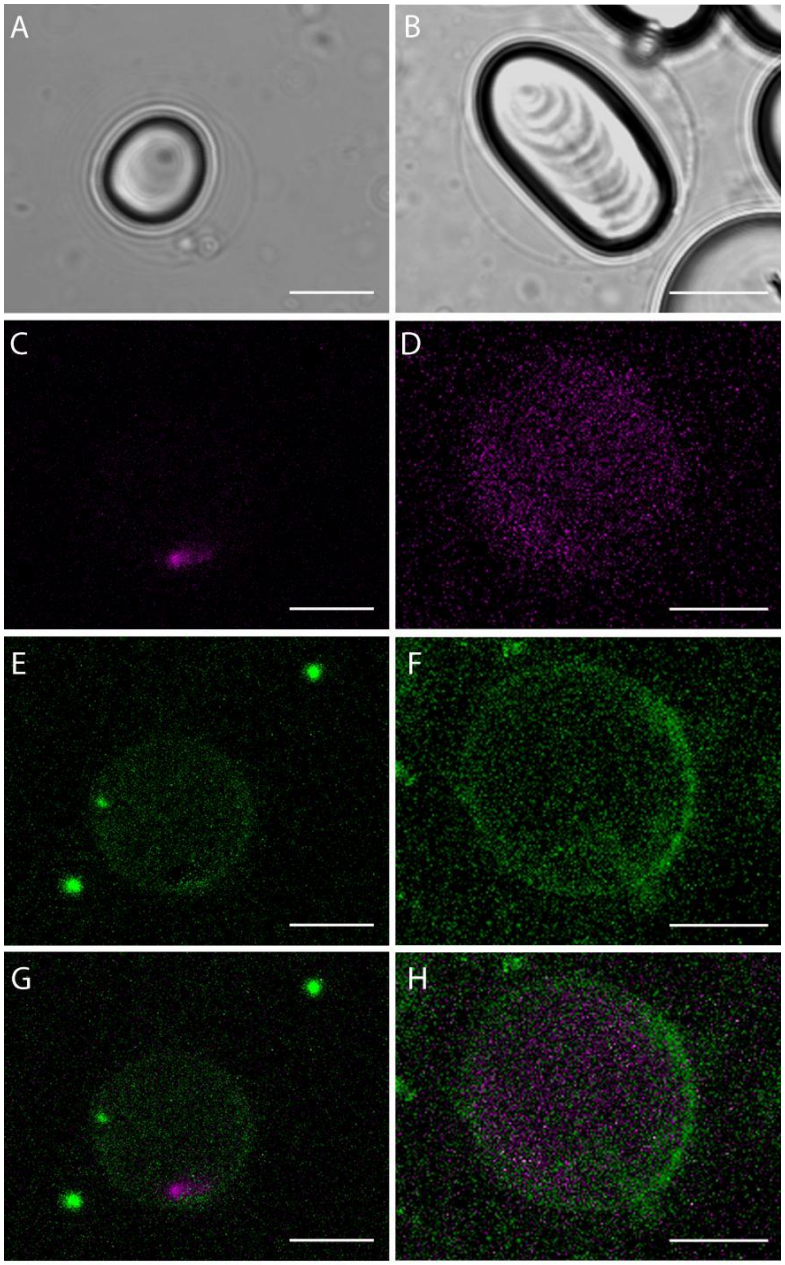

Figure 40. Stable expression of CrtRb2-RFP and PSY2-RFP fusion proteins in potato transgenic lines. Intact amyloplasts from transgenic potato lines overexpressing CrtRb2 (A, C, E, G) and PSY2 (B, D, F, H) are presented. Pseudo bright-field images show a starch grain surrounded by the amyloplast membrane (A, B). The CrtRb2-RFP fusion protein was localised in small vesicle-like, membrane bound formations (C) with the amyloplast membrane indicated by staining with DiOC6 (E). PSY2-RFP fusion protein was stromal (D), again bounded by a DiOC6-stained membrane (F). Images C-H are single confocal sections with the overlay images illustrated in G and H. Bars=20 μm (A, C, E, G) and 40 μm (B, D, F, H).

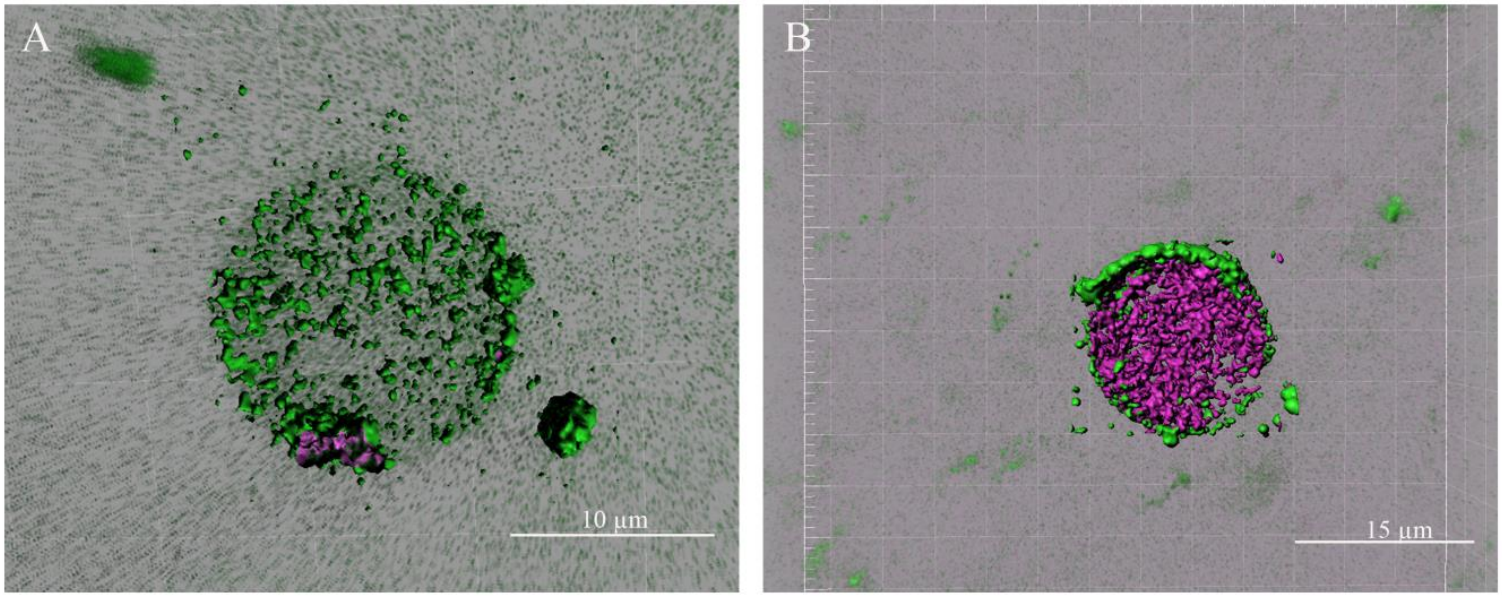

Figure 41. Representation in IMARIS of 3D visualisation based on confocal images of amyloplasts expressing CrtRb2-RFP and PSY2-RFP fusion proteins. The 3D visualisation is based on the complete z-stacks of these confocal images of the CrtRb2-RFP (A) and PSY2-RFP (B) fusion proteins confirmed previous observations. Green channel, $DiOC_6$ staining of the membranes. Magenta, RFP. Bars=10 µm (A) and 15 µm (B).

5.3 Discussion

In the present study, the sub-cellular localisation of key enzymes in the carotenoid biosynthesis pathway in potato tubers was investigated, as a possible factor influencing attempts to engineer carotenoid content in storage organs. In tubers, where it was not possible to use transient expression approaches, introduction of the tagged enzymes resulted in elevated carotenoid levels. Whilst this demonstrates that the over-expressed enzymes were functional, it is not possible to rule out that the observed localisations are in response to the increased throughput in the carotenoid pathway. Indeed, increased levels of the rate-limiting enzymes of carotenoid biosynthetic enzymes might drive plastid structural changes needed to provide a sink for the hydrophobic pathway products, as suggested by Shumskaya *et al*. (2012).

Studies have used the GFP-tagging of proteins into organelles for gaining information about their localisation. This has revolutionised our understanding of changes in the numbers, sizes and morphologies of non-photosynthetic plastids (Hibberd *et al*., 1998; Waters *et al*., 2004; Natesan *et al*., 2005). Tagging plastids with green fluorescent protein has provided a very sensitive method to visualise non-pigmented plastids in plants (reviewed by Chiu *et al*., 1996; Hanson and Kohler, 2001). Also, the observed localisations in tubers were consistently observed in samples from several transgenic lines, grown through three seasons.

Considering previous reports on the optimisation of potato transformation (Tavazza *et al.,* 1989), the transformation efficiency with *CrtRb2* and *PSY2* genes, performed on potato cv. Desiree stem cuttings was relatively low. Interestingly, differences between the levels of gene expression and total carotenoid levels in both *CrtRb2* and *PSY2* over-expressing potato lines were observed, from one season of growth to the other. There was previous evidence of the developmental signals and the external environmental stimuli influencing carotenoid levels (reviewed in Hirschberg, 2001). Recently, it was shown that secondary metabolites accumulating in tubers, including carotenoids, are subject to the collective environmental influences, even under

conditions of minimal stress (Payyavula *et al*., 2012). Moreover, Toledo-Ortiz *et al*. (2010) have demonstrated that, in Arabidopsis, *PSY* is under phytochrome regulation, by the direct binding of PIF4 to a G-box sequence in this gene's promoter. Analysis of *CrtRb2* and *PSY2* gene sequences showed that the potato *PSY2* has two G-boxes within 1.5 kb of the transcription start site, whereas none are present in the *CrtRb2* promoter. Thus, it is possible that the seasonal variation from one season of growth to the other could account for the differences observed in the analysis of the *CrtRb2* and *PSY2* transgenic potato lines.

The accumulation of carotenoids is known to be greatly influenced by not only enzyme activities, but also by the type of plastid and its storage capacity (von Lintig *et al*., 1997; Welsch *et al*., 2000; Ghassemian *et al*., 2006). It is thought that the conversion of chloroplasts into chromoplasts triggers the formation of larger PGs and/or carotenoid-sequestering structures of different shapes, permitting the deposition of high levels of carotenoids in a matrix of lipoproteins (Deruere *et al*., 1994; Vishnevetsky *et al*., 1999; Simkin *et al*., 2007; reviewed in Walter and Strack, 2011).

Current literature does not document the presence of distinct chromoplasts in the tissue of carotenoid-accumulating, yellow-fleshed potato tubers. An early study, based on biochemical separation techniques, argued that potato tuber carotenoids accumulated in the amyloplast envelope membrane (Fishwick and Wright, 1980). Confocal microscopy of RFP-tagged *CrtRb2* and *PSY2* enzymes in tubers facilitated the identification of amyloplasts as the site for accumulation of these two carotenoid biosynthetic enzymes. Staining of the amyloplast membrane with $DiOC_6$ offered the possibility to thus mark the observed structures and to perform 3D visualisation analysis in IMARIS. The resulting images showed that *CrtRb2* was detected in membrane-bound vesicle-type structures, whereas *PSY2* is targeted to the stroma of amyloplasts.

The accumulation pattern of CrtRb2 into small vesicular structures (approximately 2-3 µM in diameter), contained by mature amyloplasts, suggested that new vesicles may form during the accumulation of carotenoids. Studies on the deposition of other pigments such as anthocyanins, based on observations from light and EM microscopy, have found that these pigments are seldom uniformly distributed in the lumen of vacuoles (reviewed in Grotewold and Davies, 2008). Hence, in a large number of plant species, anthocyanins were reported to accumulate in discrete sub-vacuolar structures, known as anthocyanic vacuolar inclusions (AVIs). Interestingly, a study in *Polygonum cupsidatum* (Japanese knotweed) observed 'intravacuolar spherical bodies' inside the vacuole, even in the absence of anthocyanins, stained by neutral red (NR), which then accumulated pigments when anthocyanin formation was induced (Kubo *et al*., 1995).

Another hypothesis was that CrtRb2 localised into PGs. The possibility that these CrtRb2-containing structures were PGs was further considered. PGs, reported to be 0.5 to 1 µM in size, consist of an outer polar lipid monolayer (Brehelin and Kessler, 2008) and should not be fluorescently-stained by $DiOC_6$, a lipid bilayer-specific dye. Based on the 3D volume-rendering of the lipophilic dye-stained structures, it was demonstrated that the vesicles presented a lipid bilayer-membrane. This conclusion, together with the observed vesicles being above the PG-reported size (*ca.* 2-3 µM in diameter) led to rejection of this hypothesis.

The present study suggests that the sub-organellar compartmentalisation of carotenoid biosynthetic enzymes may provide another tier for the control of carotenoid production and that different constraints may operate in different tissues, as observed by the localisation of these genes in leaves and tubers of potato. Taking into account such factors could improve our understanding of the regulatory mechanisms dictating metabolite accumulation in plant storage organs.

Chapter 6 General discussion

6.1 General discussion

In the current economic climate and with the world population projected to reach 10 billion by 2050, food security is an acute concern. As food production *per* capita has declined in over 70 developing countries (Langmore, 1992), there are great pressures placed on our arable land, energy and biological resources, to supply nutritious foods in a sustainable manner. The turn of the century has found us with 1 to 2 billion malnourished humans, as declared by World Bank and the United Nations, making this the era with the largest number of hungry humans ever recorded in history (Pimentel and Giampietro, 1994).

Under-nourishment often brings deficiency related diseases. Humans cannot synthesize *de novo* carotenoids, so we rely on our diet to supply it. A lack in vitamin A is often responsible for child (and maternal) mortality and it is estimated that a 23–34% reduction in preschool mortality can be expected from supplying vitamin A (The State of the World's Children, UNICEF, www.un.org/en/mdg/ summit 2010, accessed August 2011). Hence, there have been numerous studies to enhance pro-vitamin A carotenoid levels in crop plants, either by traditional breeding or genetic engineering techniques (Section 1.3.2).

The carotenoid biosynthetic pathway has been the subject of research for several decades, but lately, reports have added great detail to what was previously known about the factors dictating carotenoid production and storage in plants (reviewed in Ruiz-Sola and Rodriguez-Concepcion, 2012). Considering the importance of carotenoids in plant and human life, it is essential to continuously improve our present understanding of the complex interactions regulating the accumulation of these pigments in cells. The present study used a combination of molecular and cell imaging techniques to investigate how both the turnover and the sub-cellular localisation of carotenoids can influence their levels in potato tubers.

In the first part of the study, the effects of silencing *CCD8*, a carotenoid cleavage dioxygenase, in potato cv. Desiree, were analysed. Consistent with reports from other studies on the effects of silencing *CCD* genes in crop plants (Section 1.3.4), it was demonstrated that the *CCD8*-RNAi transgenic potato plants had significantly increased the number of main and lateral branches.

Recently, there have been reports on the roles of *CCD* genes in processes other than strigolactone biosynthesis. Walter *et al*. (2010) found that *CCD7* is involved in the production of mycorradicin in mycotrophic plants such as tomato. SLs were demonstrated to also co-regulate root system architecture (Kapulnik *et al*., 2011; Ruyter-Spira *et al*., 2011). Kohlen *et al*. (2012) brought evidence of the involvement of *CCD8* in regulating multiple processes relevant for plant physiology - such as fruit set and rhizosphere signalling, and showing that a small reduction in the exudation of SLs can significantly reduce the infection by parasitic weed, without severely compromising AM symbiosis or apical dominance.

The characterisation of the transgenic *CCD8*-RNAi plants highlighted the impact of *CCD8* not only in branching, but also in fundamental processes for potato/plant life such as tuber formation and dormancy. In the most severely affected transgenic *CCD8*-RNAi lines, there was a lack of stolon formation. The complementation with the synthetic strigolactone, GR24 (Section 3.2.3) and the measurement of SLs levels-represented by orobanchol-in potato roots, confirmed that the reduced capacity of the *CCD8*-RNAi plants to produce SLs causes the branching of stolons in potato explants. Moreover, the results obtained following the application of hormones brought new evidence of the interaction of SLs and GAs, a relationship that is just starting to be documented. Also, as observed in the sprout release assays, sprouting of excised tuber buds occurred earlier in the *CCD8*-RNAi lines, when compared to the controls.

A recent study by Roumeliotis *et al.* (2012) investigated the relationship between auxin, SLs and tuber formation. These workers firstly measured IAA concentrations

in three potato stem parts and found that IAA levels are 10- to 50-fold higher than in Arabidopsis (Mashiguchi *et al*., 2011) and that they followed a gradient of levels, with the highest concentration at the base of the stem. Next, using ^{14}C-labelled IAA assays, they showed that IAA is transported from the stolon tip to basal parts of the stolons. Importantly, inhibition of the auxin transport triggered a release of dormancy of axillary stolon buds and an increase in the number of tubers (Roumeliotis *et al*., 2012), a similar effect to the one observed in the case of the tubers from the *CCD8*-RNAi plants. In the same study, Roumeliotis *et al*. (2012) applied GR24 on the basal part of stolon explants, which provoked a reduction in the tuber number. These findings illustrated the strong inhibitory effect of GR24 on stolon axillary bud outgrowth and are consistent with the data from the SRA assays, where application of GR24 together with sprout-inducing hormones such as GA_3 in the sprout release assays (Section 3.2.4) significantly reduced sprouting of the tuber buds.

Tuber induction and formation is clearly regulated by a multitude of interactions and SLs, together with other hormones, sucrose, and a recently identified FT-orthologue (Navarro *et al*., 2011) all have vital roles to play in these processes. As a point for further research, it would be interesting to optimise a protocol in order to permit the accurate identification and quantification of SL levels in extracts of potato buds during dormancy transition phases, thus bringing further information on the role of this phytohormone in tuber dormancy.

In the second part of the present study, the sub-cellular localisation of two carotenoid enzymes, CrtRb2 and PSY2, was investigated. The expression of fluorescently tagged proteins in leaves and tubers of potato plants was previously used in another study by Muñoz *et al*. (2008), to confirm by confocal microscopy the plastidial localisation of two ADP-sugar pyrophosphatases. Expression of the CrtRb2 and PSY2 proteins, fluorescently tagged, in leaves and subsequently, tubers of potato, provided information about the compartmentalisation of carotenoid enzymes in storage organs and more explicitly, in the amyloplasts of potato tubers. Moreover, by using 3D volume rendering software, it was possible to visualise the targeting of the

proteins into specific vesicle-like structures. This result provided images based on the *in vivo* localisation pattern of CrtRb2 and PSY2, not previously obtained by other studies, using traditional methods of determining the localisation of enzymes, such as import studies. The existence of pigment-sequestering structures was firstly documented by Pecket and Small (1980), who described a type of spherical intravacuolar membrane-bound vesicle, called anthocyanoplasts. Interestingly, Nozzolillo and Ishikura (1988) observed cytoplasmic membranous vesicles by studying the seedlings of red radish and *Prunus* callus. These formations, filled with anthocyanin pigments, fused to form large anthocyanin-containing bodies. Despite that these formations were vacuolar, it may be plausible that such a phenomenon can also occur with the vesicles containing CrtRb2 and PSY2, detected in the over-expressing transgenic potato lines.

Staining of tuber tissue from the CrtRb2 transgenic lines with $DiOC_6$ confirmed that the structures observed within the amyloplasts were membrane-bound. However, pigment-storing vesicles lacking a membrane have also been reported. Thus, in sweet potato cells, the 'intravacuolar pigmented globules' (cyanoplasts) reported by Nozue *et al*. (1993) appeared to lack a membrane, but their formation required the VP24 metallo-protease, which co-localised with the pigments (Nozue *et al*., 1997; Xu *et al*., 2000; Xu *et al*., 2001; Nozue *et al*., 2003).

Following the observation of the vesicle-like structures in CrtRb2 transgenic potato, it would be very interesting to know if these exist prior to the expression of the transgene or if their formation is triggered by the metabolic engineering of potato with carotenoid-producing enzymes. No such vesicles were detected in wild type tuber tissue, cv. Desiree, but this was possibly due to the limitations of image resolution. Taking into consideration these findings, there is scope in further investigating the dynamics between vesicle formation and expression of key carotenoid biosynthetic enzymes.

The data presented in this report clearly shows a spatial separation of two key enzymes of carotenoid biosynthesis in both leaves and tubers. Interestingly, in leaves

of both *Nicotiana benthamiana* and potato, CrtRb2 appeared throughout the stroma, whereas PSY2 was localised in distinct foci. These localisations were found in multiple transgenic lines. The transit peptides alone appeared to direct the transgenic protein to the same localisation, suggesting that these localisations were not due to artefactual pertubations of the biosynthetic protein localisation machinery. Conversely, in stably transformed tubers, CrtRb2 appeared in discrete foci and PSY2 was localised throughout the stroma of the amyloplast.

Currently, it is only possible to speculate about the reasons and implications for these localisations. As different plastid types can contain diverse biosynthetic enzymes, thus producing various carotenoids, stored in unique sub-plastidial structures, it is to be expected that the localisation of any multi-protein complexes formed would vary amongst them (Ruiz-Sola and Rodriguez-Concepcion, 2012). In general, the PSY enzyme is thought to localise in the chloroplasts (DellaPenna and Pogson, 2006), but its localisation within this organelle can vary amongst plant species (Qin *et al*., 2011). Also, ZDS, LCYB, BCH1 and BCH2 were found to be present in the plastoglobule proteome of pepper fruit chromoplasts, but not in that of Arabidopsis chloroplasts (Vidi *et al*., 2006; Ytterberg *et al*., 2006).

Very recently, a study by Shumskaya *et al*. (2012) reported differential localisation of PSY isozymes, connecting it to their activity and type. Transiently expressing PSYs from maize, rice and Arabidopsis in protoplasts, it was found that rice and maize PSY2 and PSY3, together with AtPSY, were present as speckles on protoplasts, the workers later confirming the enzymes to be targeted to PGs. Interestingly, this was found not to be the case for rice and maize PSY1, which was observed as homogenously filling plastids, thus suggesting a stromal, soluble localisation of this isoform.

As detailed in Section 1.2.2, carotenoids have important roles in the photosynthesis of plants and algae, and, therefore, the genes that direct the biosynthesis of carotenoids in these organisms are also regulated by light (von Lintig *et al*., 1997; Simkin *et al*., 2003; Woitsch and Römer, 2003). The *hp1* and *hp2* mutations encode the tomato orthologs of two negative regulators of light-mediated gene expression, the UV-damaged DNA binding protein 1 (DDB1) and the de-etiolated-1 (DET1) factor, (Liu *et al*., 2004), leading in the *hp2* tomato plants to the production and accumulation of high amounts of carotenoids (Mustilli *et al*., 1999).

A ZEP-deficient Arabidopsis mutant, *aba1*, was shown to have increased numbers of chloroplasts *per* cell (Rock *et al*., 1992) and a change in its carotenoid profile (Rock and Zeevaart, 1991). The *hp3* mutation in the ZEP gene, which converts zeaxanthin to violaxanthin, causes the leaves of the mutant to lack violaxanthin and neoxanthin and leads to a 75% reduction in ABA content (Galpaz *et al*., 2008), correlated with an increased accumulation (30% more) of carotenoids in tomato mature fruit. These findings suggest involvement of ABA in the production of carotenoids, but could also prove consequences of a changed carotenoid production pathway or the pool of downstream, derived-apocarotenoids.

Interestingly, Zhang *et al*. (2012) reported that carotenoid accumulation was induced by blue light treatment, but was not affected by red light treatment in the three citrus varieties. In the same study, application of ABA treatment indicated that this hormone induced its own biosynthesis at the transcriptional level, resulting in decreases in carotenoid content.

There is increasing interest into researching the roles of carotenoid-storing or carotenoid-associated formations, such as PGs, in modulating plant metabolism, especially as it is thought that enhanced expression of PGs-associated enzymes provokes physical changes in the site of carotenoid sequestration. It was previously shown that by over-expressing the tocopherol cyclase VTE1, a proliferation of PGs together with an increased level of tocopherols was obtained (Vidi *et al.*, 2006; Zbierzak *et al.*, 2010). Recently, Shumskaya *et al*. (2012) also reported that over-

expression of PSY1, with a naturally occurring sequence variation, induced the formation of plastoglobular fibrils, an effect which disappeared when the PSY active site was mutated. Taken together, these findings suggest that the increased levels of rate-controlling PG-located vitamin E and carotenoid biosynthetic enzymes might drive plastid structural changes, which are necessary in order to provide a sink for the accumulation of compounds such as tocopherols and carotenoids. Hence, in order to ensure that the metabolic engineering efforts of the carotenoid pathway have predictable outcomes, it is necessary to consider the importance of the sub-cellular localisation of carotenoid enzymes to certain regions of the plastids and of the morphological transitions and physical changes occurring in the cells by over-expression of the pathway enzymes.

References

Aarssen LW (1995) Hypotheses for the evolution of apical dominance in plants-Implications for the interpretation of overcompensation. Oikos **74:** 149-156.

Adam P, Hecht S, Eisenreich WG, Kaiser J, Grawert T, Arigoni D, Bacher A, Rohdich F (2002) Biosynthesis of terpenes: Studies on 1-hydroxy-2-methyl-2-(E)-butenyl 4-diphosphate reductase. Proceedings of the National Academy of Sciences of the United States of America **99:** 12108-12113.

Akiyama K, Matsuzaki K, Hayashi H (2005) Plant sesquiterpenes induce hyphal branching in arbuscular mycorrhizal fungi. Nature **435:** 824-827.

Al-Babili S, Hugueney P, Schledz M, Welsch R, Frohnmeyer H, Laule O, Beyer P (2000) Identification of a novel gene coding for *neoxanthin synthase* from *Solanum tuberosum*. FEBS Letters **485:** 168-172.

Al-Babili S, VonLintig J, Haubruck H, Beyer P (1996) A novel, soluble form of phytoene desaturase from *Narcissus pseudonarcissus* chromoplasts is Hsp70-complexed and competent for flavinylation, membrane association and enzymatic activation. The Plant Journal **9:** 601-612.

Alberte RS, Andersen RA (1986) Antheraxanthin, a light harvesting carotenoid foubd in a chromophyte alga. Plant Physiology **80:** 583-587.

Alboresi A, Dall'Osto L, Aprile A, Carillo P, Roncaglia E, Cattivelli L, Bassi R (2011) Reactive oxygen species and transcript analysis upon excess light treatment in wild-type Arabidopsis thaliana vs a photosensitive mutant lacking zeaxanthin and lutein. BMC Plant Biology **11:** 62.

Alder A, Jamil M, Marzorati M, Bruno M, Vermathen M, Bigler P, Ghisla S, Bouwmeester H, Beyer P, Al-Babili S (2012) The path from beta-carotene to carlactone, a strigolactone-like plant hormone. Science **335:** 1348-1351.

Altschul SF, Gish W, Miller W, Myers EW, Lipman DJ (1990) Basic local alignment search tool. Journal of Molecular Biology **215:** 403-410.

Andlauer TF, Sigrist SJ (2012) Quantitative analysis of *Drosophila* larval neuromuscular junction morphology. Cold Spring Harbor Protocols **2012:** 490-493.

Andre CM, Oufir M, Guignard C, Hoffmann L, Hausman JF, Evers D, Larondelle Y (2007) Antioxidant profiling of native Andean potato tubers

(*Solanum tuberosum* L.) reveals cultivars with high levels of β-carotene, α-tocopherol, chlorogenic acid, and petanin. Journal of Agricultural and Food Chemistry **55:** 10839-10849.

Arite T, Iwata H, Ohshima K, Maekawa M, Nakajima M, Kojima M, Sakakibara H, Kyozuka J (2007) DWARF10, an RMS1/MAX4/DAD1 ortholog, controls lateral bud outgrowth in rice. Plant Journal **51:** 1019-1029.

Audran C, Borel C, Frey A, Sotta B, Meyer C, Simonneau T, Marion-Poll A (1998) Expression studies of the zeaxanthin epoxidase gene in *Nicotiana plumbaginifolia*. Plant Physiology **118:** 1021-1028.

Auldridge ME, Block A, Vogel JT, Dabney-Smith C, Mila I, Bouzayen M, Magallanes-Lundback M, DellaPenna D, McCarty DR, Klee HJ (2006a) Characterization of three members of the Arabidopsis carotenoid cleavage dioxygenase family demonstrates the divergent roles of this multifunctional enzyme family. Plant Journal **45:** 982-993.

Auldridge ME, McCarty DR, Klee HJ (2006b) Plant carotenoid cleavage oxygenases and their apocarotenoid products. Current Opinion in Plant Biology **9:** 315-321.

Austin JR, Frost E, Vidi PA, Kessler F, Staehelin LA (2006) Plastoglobules are lipoprotein subcompartments of the chloroplast that are permanently coupled to thylakoid membranes and contain biosynthetic enzymes. Plant Cell **18:** 1693-1703.

Bai L, Kim EH, DellaPenna D, Brutnell TP (2009) Novel lycopene epsilon cyclase activities in maize revealed through perturbation of carotenoid biosynthesis. Plant Journal **59:** 588-599.

Bailey S, Grossman A (2008) Photoprotection in cyanobacteria: regulation of light harvesting. Photochemistry and Photobiology **84:** 1410-1420.

Barnes JD, Balaguer L, Manrique E, Elvira S, Davison AW (1992) A reappraisal of the use of DMSO for the extraction and determination of chlorophylls a and b in lichens and higher plants. Environmental and Experimental Botany **32:** 85-100

Beisel KG, Jahnke S, Hofmann D, Koeppchen S, Schurr U, Matsubara S (2010) Continuous turnover of carotenes and chlorophyll a in mature leaves of

Arabidopsis revealed by $^{14}CO_2$ pulse-chase labeling. Plant Physiology **152:** 2188-2199.

Bendahmane A, Querci M, Kanyuka K, Baulcombe DC (2000) *Agrobacterium* transient expression system as a tool for the isolation of disease resistance genes: application to the Rx2 locus in potato. Plant Journal **21:** 73-81.

Berezkin VG (2001) M.S. Tswett's intellectual heritage and modern chromatography. Journal of Analytical Chemistry **56:** 587-592.

Beveridge CA, Kyozuka J (2010) New genes in the strigolactone-related shoot branching pathway. Current Opinion in Plant Biology **13:** 34-39.

Beveridge CA, Ross JJ, Murfet IC (1994) Branching mutant *rms-2* in *Pisum sativum*-grafting studies and endogenous indole-3-acetic acid levels. Plant Physiology **104:** 953-959.

BezmanY, Bilkis I, Winterhalter P, Fleischman P, Rouseff R, Baldermann S (2005). Thermal oxidation of 9'-cis-neoxanthin in a model system containing peroxyacetic acid leads to the potent odorant β-damascenone. Journal of Agricultural Food Chemistry **53:** 9199–9206.

Bhaskar PB, Venkateshwaran M, Wu L, Ane J-M, Jiang J (2009) *Agrobacterium*-mediated transient gene expression and silencing: A rapid tool for functional gene assay in potato. PLoS One **4:** Article No.: e5812.

Bionda T, Tillmann B, Simm S, Beilstein K, Ruprecht M, Schleiff E (2010) Chloroplast import signals: the length requirement for translocation *in vitro* and *in vivo*. Journal of Molecular Biology **402:** 510-523.

Bonierbale MW, Plaisted RL, Tanksley SD (1988) RFLP maps based on a common set of clones reveal modes of chromosomal evolution in potato and tomato. Genetics **120:** 1095–1103.

Bonk M, Hoffmann B, Von Lintig J, Schledz M, Al-Babili S, Hobeika E, Kleinig H, Beyer P (1997) Chloroplast import of four carotenoid biosynthetic enzymes in vitro reveals differential fates prior to membrane binding and oligomeric assembly. European Journal of Biochemistry **247:** 942-950.

Bouvier F, d'Harlingue A, Hugueney P, Marin E, Marion-Poll A, Camara B (1996) Xanthophyll biosynthesis- Cloning, expression, functional reconstitution, and regulation of β-cyclohexenyl carotenoid epoxidase from

pepper (*Capsicum annuum*). Journal of Biological Chemistry **271:** 28861-28867.

Braconnot H (1817) Examen chemique du Piment, de son principe âcre, et de celui des plantes de la famille des renonculacées (Chemical investigation of the chili pepper, of its pungent principle [constituent, component], and of that of plants of the family *Ranunculus*). *Annales de Chemie et de Physique* **6:** 122-131.

Bramley PM (1993) Inhibition of carotenoid biosynthesis. *In*: Young AJ, Britton G, eds, Carotenoids in Photosynthesis. Chapman and Hall, London, pp 127–159.

Braun N, de Saint Germain A, Pillot J-P, Boutet-Mercey S, Dalmais M, Antoniadi I, Li X, Maia-Grondard A, Le Signor C, Bouteiller N, et al (2012) The Pea TCP Transcription Factor PsBRC1 acts downstream of strigolactones to control shoot branching. Plant Physiology **158:** 225-238.

Brehelin C, Kessler F (2008) The Plastoglobule: A bag full of lipid biochemistry tricks. Photochemistry and Photobiology **84:** 1388-1394.

Breitenbach J, Sandmann G (2005) ζ-Carotene cis isomers as products and substrates in the plant poly-cis carotenoid biosynthetic pathway to lycopene. Planta **220:** 785-793.

Breithaupt DE, Bamedi A (2002) Carotenoids and carotenoid esters in potatoes (*Solanum tuberosum* L.): New insights into an ancient vegetable. Journal of Agricultural and Food Chemistry **50:** 7175-7181.

Brewer PB, Dun EA, Ferguson BJ, Rameau C, Beveridge CA (2009) Strigolactone acts downstream of auxin to regulate bud outgrowth in pea and Arabidopsis. Plant Physiology **150:** 482-493.

Britton G (1985) General carotenoids methods. Methods in Enzymology **111:** 113-149.

Britton G (1991) 9th International-Symposium on Carotenoids- Held in Kyoto (Japan) 20-25 May 1990- Preface. Pure and Applied Chemistry **63:** R4-R4.

Britton G (1995) Structure and properties of carotenoids in relation to function. The FASEB Journal **9:** 1551-1558.

Britton G, Liaaen-Jensen S, Pfander H (2004) Carotenoids handbook. Birkhäuser-Verlag Ag, Basel Switzerland.

Brown CR (2008) Breeding for phytonutrient enhancement of potato. American Journal of Potato Research **85:** 298-307.

Brown CR, Culley D, Yang CP, Durst R, Wrolstad R (2005) Variation of anthocyanin and carotenoid contents and associated antioxidant values in potato breeding lines. Journal of the American Society for Horticultural Science **130:** 174-180.

Brown CR, Edwards CG, Yang CP, Dean BB (1993) Orange flesh trait in potato-inheritance and carotenoid content. Journal of the American Society for Horticultural Science **118:** 145-150.

Brown CR, Kim TS, Ganga Z, Haynes K, De Jong D, Jahn M, Paran I, De Jong W (2006) Segregation of total carotenoid in high level potato germplasm and its relationship to beta-carotene hydroxylase polymorphism. American Journal of Potato Research **83:** 365-372.

Bugos RC, Chang SH, Yamamoto HY (1999) Developmental expression of violaxanthin de-epoxidase in leaves of tobacco growing under high and low light. Plant Physiology **121:** 207-213.

Burlingame B, Charrondiere R, Mouille B (2009) Food composition is fundamental to the cross-cutting initiative on biodiversity for food and nutrition. Journal of Food Composition and Analysis **22:** 361-365.

Busch M, Seuter A, Hain R (2002) Functional analysis of the early steps of carotenoid biosynthesis in tobacco. Plant Physiology **128:** 439-453.

Camara B (1993) Plant phytoene synthase complex- component enzymes, immunology and biogenesis. Methods in Enzymology **214:** 352-365.

Camara B, Hugueney P, Bouvier F, Kuntz M, Moneger R (1995) Biochemistry and molecular biology of chromoplast development. *In* KWJJ Jeon, ed., International Review of Cytology, Vol 163, pp 175-247.

Camire ME, Kubow S, Donnelly DJ (2009) Potatoes and human health. Critical Reviews in Food Science and Nutrition **49:** 823-840.

Campbell R, Ducreux LJM, Morris WL, Morris JA, Suttle JC, Ramsay G, Bryan GJ, Hedley PE, Taylor MA (2010) The metabolic and developmental roles of carotenoid cleavage dioxygenase 4 from potato. Plant Physiology **154:** 656-664.

Cavalier-Smith T (2000) Membrane heredity and early chloroplast evolution. Trends Plant Science **5:** 174–182.

Cazzonelli CI (2011) Carotenoids in nature: insights from plants and beyond. Functional Plant Biology **38:** 833-847.

Cazzonelli CI, Cuttriss AJ, Cossetto SB, Pye W, Crisp P, Whelan J, Finnegan EJ, Turnbull C, Pogson BJ (2009a) Regulation of carotenoid composition and shoot branching in Arabidopsis by a chromatin modifying histone methyltransferase, SDG8. Plant Cell **21:** 39-53.

Cazzonelli CI, Pogson BJ (2010) Source to sink: regulation of carotenoid biosynthesis in plants. Trends in Plant Science **15:** 266-274.

Cazzonelli CI, Yin K, Pogson BJ (2009b) Potential implications for epigenetic regulation of carotenoid biosynthesis during root and shoot development. Plant Signaling & Behavior **4:** 339-341.

Celis-Gamboa C, Struik PC, Jacobsen E, Visser RGF (2003) Temporal dynamics of tuber formation and related processes in a crossing population of potato (*Solanum tuberosum*). Annals of Applied Biology **143:** 175-186.

Chai C, Fang J, Liu Y, Tong H, Gong Y, Wang Y, Liu M, Wang Y, Qian Q, Cheng Z, Chu C (2010) *ZEBRA2*, encoding a carotenoid isomerase, is involved in photoprotection in rice. Plant Molecular Biology **75:** 211-221.

Chen Y, Li FQ, Wurtzel ET (2010) Isolation and characterization of the *Z-ISO* gene encoding a missing component of carotenoid biosynthesis in plants. Plant Physiology **153:** 66-79.

Chiu WL, Niwa Y, Zeng W, Hirano T, Kobayashi H, Sheen J (1996) Engineered GFP as a vital reporter in plants. Current Biology **6:** 325-330.

Cho HB, Winans SC (2005) VirA and VirG activate the Ti plasmid repABC operon, elevating plasmid copy number in response to wound-released chemical signals. Proceedings of the National Academy of Sciences of the United States of America **102:** 14843-14848.

Clotault J, Peltier D, Berruyer R, Thomas M, Briard M, Geoffriau E (2008) Expression of carotenoid biosynthesis genes during carrot root development. Journal of Experimental Botany **59:** 3563-3573.

Cogdell RJ, Frank HA (1987) How carotenoids function in photosynthetic bacteria. Biochimica et Biophysica Acta **895:** 63-79.

Cook CE, Whichard LP, Turner B, Wall ME, Egley GH (1966) Germination of witchweed (*Striga lutea* Lour.): isolation and properties of a potent stimulant. Science **154:** 1189–1190.

Cook CE, Whichard LP, Wall ME, Egley GH, Coggon P, Luhan PA (1972) Germination stimulants. II. The structure of strigol—a potent seed germination stimulant for witchweed (*Striga lutea* Lour.) Journal of American Chemistry Society **94:** 6198–6199.

Cookson PJ, Kiano JW, Shipton CA, Fraser PD, Romer S, Schuch W, Bramley PM, Pyke KA (2003) Increases in cell elongation, plastid compartment size and phytoene synthase activity underlie the phenotype of the high pigment-1 mutant of tomato. Planta **217:** 896-903

Cordoba E, Salmi M, Leon P (2009) Unravelling the regulatory mechanisms that modulate the MEP pathway in higher plants. Journal of Experimental Botany **60:** 2933-2943.

Crawford S, Shinohara N, Sieberer T, Williamson L, George G, Hepworth J, Mueller D, Domagalska MA, Leyser O (2010) Strigolactones enhance competition between shoot branches by dampening auxin transport. Development **137:** 2905-2913.

Croce R, Morosinotto T, Castelletti S, Breton J, Bassi R (2002) The Lhca antenna complexes of higher plants photosystem I. Biochimica et Biophysica Acta-Bioenergetics **1556:** 29-40.

Cunningham FX, Gantt E (1998) Genes and enzymes of carotenoid biosynthesis in plants. Annual Review of Plant Physiology and Plant Molecular Biology **49:** 557-583.

Cunningham FX, Pogson B, Sun ZR, McDonald KA, DellaPenna D, Gantt E (1996) Functional analysis of the β and ε lycopene cyclase enzymes of Arabidopsis reveals a mechanism for control of cyclic carotenoid formation. Plant Cell **8:** 1613-1626.

Cunningham FX, Schiff JA (1985) Photoisomerisation of ζ-carotene stereoisomers in cells of *Euglena gracilis* mutant and in solution. Photochemistry and Photobiology **42:** 295-307.

Cutter EG (1978) Structure and development of the potato plant. The potato crop: the scientific basis for improvement. PM Harris, Ed. Chapman and Hall, London**:** 70-152.

Cuttriss AJ, Cazzonelli CI, Wurtzel ET, Pogson BJ (2011) Carotenoids. *In* F Rebeille, R Douce, eds, Biosynthesis of Vitamins in Plants: Vitamins A, B1, B2, B3, B5, Vol 58. Academic Press Ltd-Elsevier Science Ltd, London, pp 1-36.

Cuttriss AJ, Chubb AC, Alawady A, Grimm B, Pogson BJ (2007) Regulation of lutein biosynthesis and prolamellar body formation in Arabidopsis. Functional Plant Biology **34:** 663-672.

D'Ambrosio C, Giorio G, Marino I, Merendino A, Petrozza A, Salfi L, Stigliani AL, Cellini F (2004) Virtually complete conversion of lycopene into β-carotene in fruits of tomato plants transformed with the tomato lycopene beta-cyclase (tlcy-b) cDNA. Plant Science **166:** 207-214.

Dall'Osto L, Lico C, Alric J, Giuliano G, Havaux M, Bassi R (2006) Lutein is needed for efficient chlorophyll triplet quenching in the major LHCII antenna complex of higher plants and effective photoprotection in vivo under strong light. BMC Plant Biology **6:** 32.

Davies H, Oparka K, Viola R, Wright K, Ross H (1990) Regulation of starch synthesis in potato tubers. Plant Physiology (Rockville) **93:** 24.

Del Campo JA, García-González M, Guerrero MG (2007) Outdoor cultivation of microalgae for carotenoid production: current state and perspectives. Applied Microbiology and Biotechnology **74:** 1163-1174.

DellaPenna D, Pogson BJ (2006) Vitamin synthesis in plants: Tocopherols and carotenoids. Annual Review of Plant Biology **57:** 711-738.

Deruere J, Bouvier F, Steppuhn J, Klein A, Camara B, Kuntz M (1994) Structure and expression of 2 plant genes encoding chromoplast-specific proteins - occurrence of partially spliced transcripts. Biochemical and Biophysical Research Communications **199:** 1144-1150

Deruere J, Romer S, Dharlingue A, Backhaus RA, Kuntz M, Camara B (1994) Fibril assembly and carotenoid overaccumulation in chromoplasts- a model for supramolecular lipoprotein structures. Plant Cell **6:** 119-133.

Diretto G, Al-Babili S, Tavazza R, Papacchioli V, Beyer P, Giuliano G (2007a) Metabolic engineering of potato carotenoid content through tuber-specific overexpression of a bacterial mini-pathway. PLoS One **2:** Article No.: e350.

Diretto G, Tavazza R, Welsch R, Pizzichini D, Mourgues F, Papacchioli V, Beyer P, Giuliano G (2006) Metabolic engineering of potato tuber carotenoids through tuber-specific silencing of lycopene epsilon cyclase. BMC Plant Biology **6**: 13.

Diretto G, Welsch R, Tavazza R, Mourgues F, Pizzichini D, Beyer P, Giuliano G (2007b) Silencing of beta-carotene hydroxylase increases total carotenoid and beta-carotene levels in potato tubers. BMC Plant Biology **7**: 11.

Dodds KS (1962). Classification of cultivated potatoes. *In* "The Potato and its wild relatives" (D.S. Correll, Ed.), pp. 517-539. Texas Research Foundation, Renner, Texas.

Domagalska DA, Leyser O (2011) Signal integration in the control of plant development. Nature Reviews Molecular Cell Biology **12:** 211-221.

Dong HL, Deng Y, Mu JY, Lu QT, Wang YQ, Xu YY, Chu CC, Chong K, Lu CM, Zuo JR (2007) The Arabidopsis spontaneous cell death1 gene, encoding a ζ-carotene desaturase essential for carotenoid biosynthesis, is involved in chloroplast development, photoprotection and retrograde signalling. Cell Research **17:** 458-470.

Douches DS, Maas D, Jastrzebski K, Chase RW (1996) Assessment of potato breeding progress in the USA over the last century. Crop Science **36:** 1544-1552.

Du H, Wang N, Cui F, Li X, Xiao J, Xiong L (2010) Characterization of the β-carotene hydroxylase gene DSM2 conferring drought and oxidative stress resistance by increasing xanthophylls and abscisic acid synthesis in rice. Plant Physiology **154:** 1304-1318.

Ducreux LJM, Morris WL, Hedley PE, Shepherd T, Davies HV, Millam S, Taylor MA (2005) Metabolic engineering of high carotenoid potato tubers containing enhanced levels of β-carotene and lutein. Journal of Experimental Botany **56:** 81-89

Ducreux LJM, Morris WL, Prosser IM, Morris JA, Beale MH, Wright F, Shepherd T, Bryan GJ, Hedley PE, Taylor MA (2008) Expression

profiling of potato germplasm differentiated in quality traits leads to the identification of candidate flavour and texture genes. Journal of Experimental Botany **59:** 4219-4231

Dun EA, Brewer PB, Beveridge CA (2009) Strigolactones: discovery of the elusive shoot branching hormone. Trends in Plant Science **14:** 364-372

Dun EA, de Saint Germain A, Rameau C, Beveridge CA (2012) Antagonistic action of strigolactone and cytokinin in bud outgrowth control. Plant Physiology **158:** 487-498

Egea I, Barsan C, Bian WP, Purgatto E, Latche A, Chervin C, Bouzayen M, Pech JC (2010) Chromoplast differentiation: Current status and perspectives. Plant and Cell Physiology **51:** 1601-1611

Emanuelsson O, Nielsen H, Von Heijne G (1999) ChloroP, a neural network-based method for predicting chloroplast transit peptides and their cleavage sites. Protein Science **8:** 978-984

Estevez JM, Cantero A, Reindl A, Reichler S, Leon P (2001) 1-deoxy-D-xylulose-5-phosphate synthase, a limiting enzyme for plastidic isoprenoid biosynthesis in plants. Journal of Biological Chemistry **276:** 22901-22909.

Fagoaga C, Tadeo FR, Iglesias DJ, Huerta L, Lliso I, Vidal AM, Talon M, Navarro L, García-Martínez JL, Peña L (2007) Engineering of gibberellin levels in citrus by sense and antisense overexpression of a GA 20-oxidase gene modifies plant architecture. Journal of Experimental Botany **58:** 1407-1420.

Faivre-Rampant O, Bryan GJ, Roberts AG, Milbourne D, Viola R, Taylor MA (2004) Regulated expression of a novel TCP domain transcription factor indicates an involvement in the control of meristem activation processes in *Solanum tuberosum*. Journal of Experimental Botany **55:** 951-953.

Fang J, Chai CL, Qian Q, Li CL, Tang JY, Sun L, Huang ZJ, Guo XL, Sun CH, Liu M, Zhang Y, Lu QT, Wang YQ, Lu CM, Han B, Chen F, Cheng ZK, Chu CC (2008) Mutations of genes in synthesis of the carotenoid precursors of ABA lead to pre-harvest sprouting and photo-oxidation in rice. Plant Journal **54:** 177-189.

Fassett RG, Coombes JS (2011) Astaxanthin: A potential therapeutic agent in cardiovascular disease. Marine Drugs **9:** 447-465.

Fei Y (2002) Cone neurite sprouting: an early onset abnormality of the cone photoreceptors in the retinal degeneration mouse. Molecular Vision **8:** 306-314.

Ferro M, Brugiere S, Salvi D, Seigneurin-Berny D, Court M, Moyet L, Ramus C, Miras S, Mellal M, Le Gall S, Kieffer-Jaquinod S, Bruley C, Garin J, Joyard J, Masselon C, Rolland N (2010) AT_CHLORO, a comprehensive chloroplast proteome database with subplastidial localization and curated information on envelope proteins. Molecular & Cellular Proteomics **9:** 1063-1084.

Fishwick MJ, Wright AJ (1980) Isolation and characterization of amyloplast envelope membranes from *Solanum tuberosum*. Phytochemistry **19:** 55-59.

Floss DS, Walter MH (2009) Role of carotenoid cleavage dioxygenase 1 (CCD1) in apocarotenoid biogenesis revisited. Plant Signalling & Behavior **4:** 172-175.

Förster B, Osmond CB, Pogson BJ (2009) De novo synthesis and degradation of Lx and V cycle pigments during shade and sun acclimation in avocado leaves. Plant Physiol **149:** 1179–1195.

Forth D, Pyke KA (2006) The *suffulta* mutation in tomato reveals a novel method of plastid replication during fruit ripening. Journal of Experimental Botany **57:** 1971-1979.

Fraser PD, Bramley PM (2004) The biosynthesis and nutritional uses of carotenoids. Progress in Lipid Research **43:** 228-265.

Fraser PD, Bramley PM (2009) Genetic manipulation of carotenoid content and composition in crop plants. Carotenoids, Vol. 5: Nutrition and Health, Birkhäuser, Basel**:** 99-114.

Fraser PD, Romer S, Shipton CA, Mills PB, Kiano JW, Misawa N, Drake RG, Schuch W, Bramley PM (2002) Evaluation of transgenic tomato plants expressing an additional phytoene synthase in a fruit-specific manner. Proceedings of the National Academy of Sciences of the United States of America **99:** 1092-1097.

Fraser PD, Schuch W, Bramley PM (2000) Phytoene synthase from tomato (*Lycopersicon esculentum*) chloroplasts- partial purification and biochemical properties. Planta **211:** 361-369.

Fraser PD, Truesdale MR, Bird CR, Schuch W, Bramley PM (1994) Carotenoid biosynthesis during tomato fruit development- evidence for tissue-specific gene expression. Plant Physiology 105: 405-413.

Fray RG, Wallace A, Fraser PD, Valero D, Hedden P, Bramley PM, Grierson D (1995) Constitutive expression of a fruit phytoene synthase gene in transgenic tomatoes causes dwarfism by redirecting metabolites from the gibberellin pathway. Plant Journal **8:** 693-701.

Frey-Wyssling A, Schwegler F (1965) Ultrastructure of the chromoplasts in the carrot root. Journal of Ultrastructure Research **13:** 543-559.

Galpaz N, Wang Q, Menda N, Zamir D, Hirschberg J (2008) Abscisic acid deficiency in the tomato mutant high-pigment 3 leading to increased plastid number and higher fruit lycopene content. Plant Journal **53:** 717-730.

Garcia-Limones C, Schnaebele K, Blanco-Portales R, Luz Bellido M, Luis Caballero J, Schwab W, Muñoz-Blanco J (2008) Functional characterization of FaCCD1: A carotenoid cleavage dioxygenase from strawberry involved in lutein degradation during fruit ripening. Journal of Agricultural and Food Chemistry **56:** 9277-9285.

Ghassemian M, Lutes J, Tepperman JM, Chang HS, Zhu T, Wang X, Quail PH, Lange BM (2006) Integrative analysis of transcript and metabolite profiling data sets to evaluate the regulation of biochemical pathways during photomorphogenesis. Archives of Biochemistry and Biophysics **448:** 45-59.

Giuliano G, Tavazza R, Diretto G, Beyer P, Taylor MA (2008) Metabolic engineering of carotenoid biosynthesis in plants. Trends in Biotechnology **26:** 139-145.

Goff SA, Klee HJ (2006) Plant volatile compounds: Sensory cues for health and nutritional value? Science **311:** 815-819.

Gomez-Roldan V, Fermas S, Brewer PB, Puech-Pages V, Dun EA, Pillot J-P, Letisse F, Matusova R, Danoun S, Portais J-C, Bouwmeester H, Becard G, Beveridge CA, Rameau C, Rochange SF (2008) Strigolactone inhibition of shoot branching. Nature **455:** 189-U122.

Gong L, Yang YJ, Zhou J (2012) Genes involved in the synthesis and signaling pathway of strigolactone, a shoot branching inhibitor. Biologia Plantarum **56:** 210-214.

Goodman DS, Huang HS (1965) Biosynthesis of vitamin A with rat intestinal enzymes. Science (New York, N.Y.) **149:** 879-880.

Grotewold E, Davies K (2008) Trafficking and sequestration of anthocyanins. Natural Product Communications **3:** 1251-1258.

Hadley CW, Miller EC, Schwartz SJ, Clinton SK (2002) Tomatoes, lycopene, and prostate cancer: Progress and promise. Experimental Biology and Medicine **227:** 869-880.

Hanneman RE (1989) The potato germplasm resource. American Potato Journal **66:** 655-667.

Hanson MR, Kohler RH (2001) GFP imaging: methodology and application to investigate cellular compartmentation in plants. Journal of Experimental Botany **52:** 529-539.

Harjes CE, Rocheford TR, Bai L, Brutnell TP, Kandianis CB, Sowinski SG, Stapleton AE, Vallabhaneni R, Williams M, Wurtzel ET, Yan JB, Buckler ES (2008) Natural genetic variation in lycopene epsilon cyclase tapped for maize biofortification. Science **319:** 330-333.

Hartmann A, Senning M, Hedden P, Sonnewald U, Sonnewald S (2011) Reactivation of meristem activity and aprout growth in potato tubers require both cytokinin and gibberellin. Plant Physiology **155:** 776-796.

Hawkes JG (1947) Some observations on South American potatoes. The Annals of Applied Biology **34:** 622-631.

Hawkes JG (1972) Evolution of the cultivated potato *Solanum tuberosum*. Symposia Biologica Hungarica **12**:183-88.

Hawkes JG, Francisco-Ortega J (1992) The potato in Spain during the late 16th-century. Economic Botany **46:** 86-97.

Hellens RP, Edwards EA, Leyland NR, Bean S, Mullineaux PM (2000) pGreen: a versatile and flexible binary Ti vector for *Agrobacterium*-mediated plant transformation. Plant Molecular Biology **42:** 819-832.

Helliwell CA, Wesley SV, Wielopolska AJ, Waterhouse PM (2002) High-throughput vectors for efficient gene silencing in plants. Functional Plant Biology **29:** 1217-1225.

Hibberd JM, Linley PJ, Khan MS, Gray JC (1998) Transient expression of green fluorescent protein in various plastid types following microprojectile bombardment. Plant Journal **16:** 627-632.

Hirschberg J (2001) Carotenoid biosynthesis in flowering plants. Current Opinion in Plant Biology **4:** 210-218.

Hooykaas PJJ, Schilperoort RA (1992) *Agrobacterium* and plant genetic-engineering. Plant Molecular Biology **19:** 15-38.

Horner HT, Healy RA, Ren G, Fritz D, Klyne A, Seames C, Thornburg RW (2007) Amyloplast to chromoplast conversion in developing ornamental tobacco floral nectaries provides sugar for nectar and antioxidants for protection. American Journal of Botany **94:** 12-24.

Hornero-Méndez D, Mínguez-Mosquera MI (2000) Xanthophyll esterification accompanying carotenoid overaccumulation in chromoplasts of *Capsicum annuum* ripening fruits is a constitutive process and useful for ripeness index. Journal of Biological Chemistry **48:** 1617-1622.

Howitt CA, Cavanagh CR, Bowerman AF, Cazzonelli C, Rampling L, Mimica JL, Pogson BJ (2009) Alternative splicing, activation of cryptic exons and amino acid substitutions in carotenoid biosynthetic genes are associated with lutein accumulation in wheat endosperm. Functional & Integrative Genomics **9:** 363-376.

Huang F, Molnar P, Schwab W (2009a) Cloning and functional characterization of *carotenoid cleavage dioxygenase 4* genes. Journal of Experimental Botany **60:** 3011-3022.

Huang FC, Horvath G, Molnar P, Turcsi E, Deli J, Schrader J, Sandmann G, Schmidt H, Schwab W (2009b) Substrate promiscuity of *RdCCD1*, a carotenoid cleavage oxygenase from *Rosa damascena*. Phytochemistry **70:** 457-464.

Ilg A, Yu Q, Schaub P, Beyer P, Al-Babili S (2010) Overexpression of the rice *carotenoid cleavage dioxygenase 1* gene in Golden Rice endosperm suggests apocarotenoids as substrates in planta. Planta **232:** 691-699.

Isaacson T, Ohad I, Beyer P, Hirschberg J (2004) Analysis *in vitro* of the enzyme CRTISO establishes a poly-cis-carotenoid biosynthesis pathway in plants. Plant Physiology **136:** 4246-4255.

Iwanzik W, Tevini M, Stute R, Hilbert R (1983) Carotinoidgehalt und-zusammensetzung verschiedener deutscher Kartoffelsorten und deren Bedeutung fur die Fleischfarbe der Knolle. (Carotenoid content and composition of different potato varieties and their importance for the color of the flesh of the tuber). Potato Research **26:** 149-162.

Jackson H, Braun CL, Ernst H (2008) The chemistry of novel xanthophyll carotenoids. American Journal of Cardiology **101:** 50D-57D.

Jacobs WP, Case DB (1965) Auxin transport, gibberellin, and apical dominance. Science (New York, N.Y.) **148:** 1729-1731.

Jamil M, Charnikhova T, Verstappen F, Bouwmeester H (2010). Carotenoid inhibitors reduce strigolactone production and *Striga hermonthica* infection in rice. Archives of Biochemistry and Biophysics. **504:** 123–131.

Johnson EJ (2004) A biological role of lutein. Food Reviews International **20:** 1-16.

Johnson EJ (2010) The impact of carotenoids on cognitive function in the elderly. Agro Food Industry Hi-Tech **21:** 41-43.

Johnson EJ, Suter PM, Sahyoun N, Ribayamercado JD, Russell RM (1995) Relation between β-carotene intake and plasma and adipose tissue concentrations of carotenoids and retinoids. American Journal of Clinical Nutrition **62:** 598-603.

Joyard J, Ferro M, Masselon C, Seigneurin-Berny D, Salvi D, Garin J, Rolland N (2009) Chloroplast proteomics and the compartmentation of plastidial isoprenoid biosynthetic pathways. Molecular Plant **2:** 1154-1180.

Kapulnik Y, Delaux PM, Resnick N, Mayzlish-Gati E, Wininger S, Bhattacharya C, Sejalon-Delmas N, Combier JP, Becard G, Belausov E, Beeckman T, Dor E, Hershenhorn J, Koltai H (2011) Strigolactones affect lateral root formation and root-hair elongation in Arabidopsis. Planta **233:** 209-216.

Karimi M, Inze D, Depicker A (2002) GATEWAY vectors for *Agrobacterium*-mediated plant transformation. Trends in Plant Science **7:** 193-195.

Karrer P, Ruckstuhl H (1945) Zur Frage der antagonistischen Wirkung von Vitaminen und Antivitaminen (On the question of the antagonistic effects of vitamins and anti-vitamins) Bulletin der Schweizerischen Akademie der Medizinischen Wissenschaften **1:** 236-246.

Khachik F, Beecher GR, Goli MB, Lusby WR (1991) Separation, identification, and quantification of carotenoids in fruits, vegetables and human plasma by high- performance liquid chromatography. Pure and Applied Chemistry **63:** 71-80.

Khachik F, Englert G, Daitch CE, Beecher GR, Tonucci LH, Lusby WR (1992) Isolation and structural elucidation of the geometrical isomers of lutein and zeaxanthin in extrcats from human plasma. Journal of Chromatography-Biomedical Applications **582:** 153-166.

Kim J, DellaPenna D (2006) Defining the primary route for lutein synthesis in plants: The role of *Arabidopsis* carotenoid beta-ring hydroxylase CYP97A3. Proceedings of the National Academy of Sciences of the United States of America **103:** 3474-3479.

Kloer DP, Schulz GE (2006) Structural and biological aspects of carotenoid cleavage. Cellular and Molecular Life Sciences **63:** 2291-2303.

Kloosterman B, Oortwijn M, Uitdewilligen J, America T, de Vos R, Visser RGF, Bachem CWB (2010) From QTL to candidate gene: Genetical genomics of simple and complex traits in potato using a pooling strategy. BMC Genomics **11:** 158.

Knapp S, Bohs L, Nee M, Spooner DM (2004) *Solanaceae*- a model for linking genomics with biodiversity. Comparative and Functional Genomics **5:** 285-291.

Kobayashi A, Ohara-Takada A, Tsuda S, Matsuura-Endo C, Takada N, Umemura Y, Nakao T, Yoshida T, Hayashi K, Mori M (2008) Breeding of potato variety "Inca-no-hitomi" with a very high carotenoid content. Breeding Science **58:** 77-82.

Kohler RH, Schwille P, Webb WW, Hanson MR (2000) Active protein transport through plastid tubules: velocity quantified by fluorescence correlation spectroscopy. Journal of Cell Science **113:** 3921–3930.

Kohlen W, Charnikhova T, Lammers M, Pollina T, Tóth P, Haider I, Pozo MJ, de Maagd RA, Ruyter-Spira C, Bouwmeester HJ, López-Ráez JA (2012) The tomato CAROTENOID CLEAVAGE DIOXYGENASE8 (SlCCD8) regulates rhizosphere signaling, plant architecture and affects reproductive

development through strigolactone biosynthesis. New Phytologist **196:** 535-547.

Kokkirala VR, Yonggang P, Abbagani S, Zhu Z, Umate P (2010) Subcellular localization of proteins of *Oryza sativa* L. in the model tobacco and tomato plants. Plant Signaling & Behavior **5:** 1336-1341.

Koning AJ, Lum PY, Williams JM, Wright R (1993) DiOC6 staining reveals organelle structure and dynamics in living yeast cells. Cell Motility and the Cytoskeleton **25:** 111-128.

Koroleva OA, Tomlinson ML, Leader D, Shaw P, Doonan JH (2005) High-throughput protein localization in Arabidopsis using *Agrobacterium*-mediated transient expression of GFP-ORF fusions. Plant Journal **41:** 162-174.

Kovacs K, Zhang L, Linforth RST, Whittaker B, Hayes CJ, Fray RG (2007) Redirection of carotenoid metabolism for the efficient production of taxadiene [taxa-4(5),11(12)-diene] in transgenic tomato fruit. Transgenic Research **16:** 121-126.

Kreuz K, Beyer P, Kleinig H (1982) The site of carotenogenic enzymes in chromoplasts from *Narcissus pseudonarcissus* L. Planta **154:** 66-69.

Krinsky NI, Yeum KJ (2003) Carotenoid-radical interactions. Biochemical and Biophysical Research Communications **305:** 754-760.

Kubo H, Nozue M, Kawasaki K, Yasuda H (1995) Intravacuolar spherical bodies in *Polygonum cuspidatum*. Plant and Cell Physiology **36:** 1453-1458.

Kuhlbrandt W, Wang DN, Fujiyoshi Y (1994) Atomic model of plant light-harvesting complex by electron crystallography. Nature **367:** 614-621.

Langmore J (1992) Global population growth. Development bulletin (Australian Development Studies Network) **24:** 9-10.

Lawrence SD, Cline K, Moore GA (1997) Chromoplast development in ripening tomato fruit: Identification of cDNAs for chromoplast-targeted proteins and characterization of a cDNA encoding a plastid-localized low-molecular-weight heat shock protein. Plant Molecular Biology **33:** 483-492.

Ledger SE, Janssen BJ, Karunairetnam S, Wang TC, Snowden KC (2010) Modified CAROTENOID CLEAVAGE DIOXYGENASE8 expression

correlates with altered branching in kiwifruit (*Actinidia chinensis*). New Phytologist **188:** 803-813.

Lee ALC, Thornber JP (1995) Analysis of the pigment stoichiometry of pigment-protein complexes from barley (*Hordeum-vulgare*)- the xanthophyll cycle intermediates occur mainly in the light-harvesting complexes of photosystem-I and photosystem-II. Plant Physiology **107:** 565-574.

Lee DW, Kim JK, Lee S, Choi S, Kim S, Hwang I (2008) *Arabidopsis* nuclear-encoded plastid transit peptides contain multiple sequence subgroups with distinctive chloroplast-targeting sequence motifs. Plant Cell **20:** 1603-1622.

Leyser O (2008) Strigolactones and shoot branching: A new trick for a young dog. Developmental Cell **15:** 337-338.

Livak KJ (1997) Relative quantitation of gene expression. User Bulletin No. 2: ABI PRISM 7700 Sequence Detection System. PE Applied Biosystems, Foster City, CA, USA.

Li CJ, Guevara E, Herrera J, Bangerth F (1995) Effect of apex excision and replacement by 1-naphthylacetic acid on cytokinin concentration and apical dominance in pea plants. Physiologia Plantarum **94:** 465-469.

Li FQ, Vallabhaneni R, Yu J, Rocheford T, Wurtzel ET (2008) The maize phytoene synthase gene family: Overlapping roles for carotenogenesis in endosperm, photomorphogenesis, and thermal stress tolerance. Plant Physiology **147:** 1334-1346.

Li H-M, Chiu C-C (2010) Protein transport into chloroplasts. *In* S Merchant, WR Briggs, D Ort, eds, Annual Review of Plant Biology, Vol 61, pp 157-180.

Li L, Lu S, Cosman KM, Earle ED, Garvin DF, O'Neill J (2006) β-carotene accumulation induced by the cauliflower *Or* gene is not due to an increased capacity of biosynthesis. Phytochemistry **67:** 1177-1184.

Li L, Paolillo DJ, Parthasarathy MV, DiMuzio EM, Garvin DF (2001) A novel gene mutation that confers abnormal patterns of β-carotene accumulation in cauliflower (*Brassica oleracea* var. botrytis). Plant Journal **26:** 59-67.

Li L, van Eck J (2007) Metabolic engineering of carotenoid accumulation by creating a metabolic sink. Transgenic Research **16:** 581-585.

Liang JL, Zhao LJ, Challis R, Leyser O (2010) Strigolactone regulation of shoot branching in chrysanthemum (*Dendranthema grandiflorum*). Journal of Experimental Botany **61:** 3069-3078.

Lin H, Wang R, Qian Q, Yan M, Meng X, Fu Z, Yan C, Jiang B, Su Z, Li J, Wang Y (2009) DWARF27, an iron-containing protein required for the biosynthesis of strigolactones, regulates rice tiller bud outgrowth. Plant Cell **21:** 1512-1525.

Lindgren LO, Stålberg KG, Hōglund AS (2003) Seed-specific overexpression of an endogenous *Arabidopsis* phytoene synthase gene results in delayed germination and increased levels of carotenoids, chlorophyll, and abscisic acid. Plant Physiology **132:** 779-785.

Liu YS, Roof S, Ye ZB, Barry C, van Tuinen A, Vrebalov J, Bowler C, Giovannoni J (2004) Manipulation of light signal transduction as a means of modifying fruit nutritional quality in tomato. Proceedings of the National Academy of Sciences of the United States of America **101:** 9897-9902.

Liu ZC, Park BJ, Kanno A, Kameya T (2005) The novel use of a combination of sonication and vacuum infiltration in *Agrobacterium*-mediated transformation of kidney bean (*Phaseolus vulgaris* L.) with lea gene. Molecular Breeding **16:** 189-197.

López-Ráez JA, Charnikhova T, Gómez-Roldán V. Matusova R, Kohlen W, De Vos R, Verstappen F, Puech-Pages V, Bécard G, Mulder P, Bouwmeester H (2008) Tomato strigolactones are derived from carotenoids and their biosynthesis is promoted by phosphate starvation. New Phytologist **178:** 863–874.

Long X-Y, Wang J-R, Ouellet T, Rocheleau H, Wei Y-M, Pu Z-E, Jiang Q-T, Lan X-J, Zheng Y-L (2010) Genome-wide identification and evaluation of novel internal control genes for Q-PCR based transcript normalization in wheat. Plant Molecular Biology **74:** 307-311.

Lu S, Li L (2008) Carotenoid metabolism: Biosynthesis, regulation, and beyond. Journal of Integrative Plant Biology **50:** 778-785.

Lu S, Van Eck J, Zhou X, Lopez AB, O'Halloran DM, Cosman KM, Conlin BJ, Paolillo DJ, Garvin DF, Vrebalov J, Kochian LV, Kupper H, Earle ED, Cao J, Li L (2006) The cauliflower *Or* gene encodes a DnaJ cysteine-rich

domain-containing protein that mediates high levels of beta-carotene accumulation. Plant Cell **18:** 3594-3605.

Lu WH, Haynes K, Wiley E, Clevidence B (2001) Carotenoid content and color in diploid potatoes. Journal of the American Society for Horticultural Science **126:** 722-726.

Luisi A, Lorenzi R, Sorce C (2011) Strigolactone may interact with gibberellin to control apical dominance in pea (*Pisum sativum*). Plant Growth Regulation **65:** 415-419.

Lutkebrinkhaus F, Liedvogel B, Kreuz K, Kleinig H (1982) Phytoene synthase and phytioene dehydrogenase associated with envelope membranes from spinach chloroplasts. Planta **156:** 176-180.

Marano MR, Serra EC, Orellano EG, Carrillo N (1993) The path of chromoplast development in fruits and flowers. Plant Science **94:** 1-17.

Mashiguchi K, Tanaka K, Sakai T, Sugawara S, Kawaide H, Natsume M, Hanada A, Yaeno T, Shirasu K, Yao H, McSteen P, Zhao Y, Hayashi K-I, Kamiya Y, Kasahara H (2011) The main auxin biosynthesis pathway in Arabidopsis. Proceedings of the National Academy of Sciences of the United States of America **108:** 18512-18517.

Mathieu S, Terrier N, Procureur J, Bigey F, Günata Z (2005) A carotenoid cleavage dioxygenase from *Vitis vinifera* L.: functional characterization and expression during grape berry development in relation to C-13-norisoprenoid accumulation. Journal of Experimental Botany **56:** 2721-2731.

Mayer JE, Pfeiffer WH, Beyer P (2008) Biofortified crops to alleviate micronutrient malnutrition. Current Opinion in Plant Biology **11:** 166-170.

Mayfield SP, Huff A (1986) Accumulation of chlorophyll, chloroplastic proteins, and thylakoid membranes during reversion of chromoplasts to chloroplasts in *Citrus sinensis* epicarp. Plant Physiology **81:** 30-35.

McGraw KJ (2006) Dietary carotenoids mediate a trade-off between egg quantity and quality in Japanese quail. Ethology Ecology & Evolution **18:** 247-256.

McGraw KJ, Klasing KC (2006) Carotenoids, immunity, and integumentary coloration in red junglefowl (*Gallus gallus*). Auk **123:** 1161-1171.

Miao H, Jiang B, Chen S, Zhang S, Chen F, Fang W, Teng N, Guan Z (2010) Isolation of a gibberellin 20-oxidase cDNA from and characterization of its expression in chrysanthemum. Plant Breeding **129:** 707-714.

Mínguez-Mosquera MI, Hornero-Méndez D (1994) Changes in carotenoid esterification during the fruit ripening of *Capsicum annuum* cv. *Bola*. Journal of Agricultural and Food Chemistry **42:** 640-644.

Misawa N, Truesdale MR, Sandmann G, Fraser PD, Bird C, Schuch W, Bramley PM (1994) Expression of a tomato cDNA coding for phytoene synthase in *Escherichia coli*, phytoene formation in vivo and in vitro, and functional analysis of the various truncated gene products. Journal of Biochemistry **116:** 980-985.

Moehs CP, Tian L, Osteryoung KW, DellaPenna D (2001) Analysis of carotenoid biosynthetic gene expression during marigold petal development. Plant Molecular Biology **45:** 281-293.

Moran NA, Jarvik T (2010) Lateral transfer of genes from Fungi underlies carotenoid production in aphids. Science **328:** 624-627.

Morris SE, Turnbull CGN, Murfet IC, Beveridge CA (2001) Mutational analysis of branching in pea. Evidence that *Rms1* and *Rms5* regulate the same novel signal. Plant Physiology **126:** 1205-1213.

Morris WL, Ducreux L, Griffiths DW, Stewart D, Davies HV, Taylor MA (2004) Carotenogenesis during tuber development and storage in potato. Journal of Experimental Botany **55:** 975-982.

Morris WL, Ducreux LJM, Fraser PD, Millam S, Taylor MA (2006b) Engineering ketocarotenoid biosynthesis in potato tubers. Metabolic Engineering **8:** 253-263.

Morris WL, Ducreux LJM, Hedden P, Millam S, Taylor MA (2006a) Overexpression of a bacterial 1-deoxy-D-xylulose 5-phosphate synthase gene in potato tubers perturbs the isoprenoid metabolic network: implications for the control of the tuber life cycle. Journal of Experimental Botany **57:** 3007-3018.

Muller P, Li XP, Niyogi KK (2001) Non-photochemical quenching. A response to excess light energy. Plant Physiology **125:** 1558-1566.

Muñoz FJ, Baroja-Fernández E, Ovecka M, Li J, Mitsui T, Sesma MT, Montero M, Bahaji A, Ezquer I, Pozueta-Romero J (2008) Plastidial localization of a potato 'Nudix' hydrolase of ADP-glucose linked to starch biosynthesis. Plant and Cell Physiology **49:** 1734-1746.

Mustilli AC, Fenzi F, Ciliento R, Alfano F, Bowler C (1999) Phenotype of the tomato *high pigment-2* mutant is caused by a mutation in the tomato homolog of *DEETIOLATED1*. Plant Cell **11**: 145–157.

Naested H, Holm A, Jenkins T, Nielsen HB, Harris CA, Beale MH, Andersen M, Mant A, Scheller H, Camara B, Mattsson O, Mundy J (2004) Arabidopsis *VARIEGATED 3* encodes a chloroplast targeted, zinc-finger protein required for chloroplast and palisade cell development. Journal of Cell Science **117:** 4807-4818.

Nakayama M, Miyasaka M, Maoka T, Yagi M, Fukuta N (2006) A carotenoid-derived yellow *Eustoma* screened under blue and ultraviolet lights. Journal of the Japanese Society for Horticultural Science **75:** 161-165.

Napoli C (1996) Highly branched phenotype of the petunia *dad1-1* mutant is reversed by grafting. Plant Physiology **111:** 27-37.

Natesan SKA, Sullivan JA, Gray JC (2005) Stromules: a characteristic cell-specific feature of plastid morphology. Journal of Experimental Botany **56:** 787-797.

Navarro C, Abelenda JA, Cruz-Oro E, Cuellar CA, Tamaki S, Silva J, Shimamoto K, Prat S (2011) Control of flowering and storage organ formation in potato by *FLOWERING LOCUS T*. Nature **478:** 119-U132.

Nesterenko S, Sink KC (2003) Carotenoid profiles of potato breeding lines and selected cultivars. Hortscience **38:** 1173-1177.

Niyogi KK (1999) Photoprotection revisited: Genetic and molecular approaches. Annual Review of Plant Physiology and Plant Molecular Biology **50:** 333-359.

Nozue M, Baba S, Kitamura Y, Xu WX, Kubo H, Nogawa M, Shioiri H, Kojima M (2003) VP24 found in anthocyanic vacuolar inclusions (AVIs) of sweet potato cells is a member of a metalloprotease family. Biochemical Engineering Journal **14:** 199-205.

Nozue M, Kubo H, Nishimura M, Katou A, Hattori C, Usuda N, Nagata T, Yasuda H (1993) Characterisation of intravacuolar pigmented structures in anthocyanin- containing cells of sweet potato suspension cultures. Plant and Cell Physiology **34:** 803-808.

Nozue M, Yamada K, Nakamura T, Kubo H, Kondo M, Nishimura M (1997) Expression of a vacuolar protein (VP24) in anthocyanin-producing cells of sweet potato in suspension culture. Plant Physiology **115:** 1065-1072.

Nozzolillo C, Ishikura N (1988) An investigation of the intracellular site of anthocyanoplasts using isolated protoplasts and vacuoles. Plant Cell Reports **7:** 389-392.

Ohmiya A, Kishimoto S, Aida R, Yoshioka S, Sumitomo K (2006) Carotenoid cleavage dioxygenase (CmCCD4a) contributes to white color formation in chrysanthemum petals. Plant Physiology **142:** 1193-1201.

Olson JA (1964) The effect of bile and bile salts on the uptake and cleavage of β-carotene into retinol ester (vitamin A ester) by intestinal slices. Journal of Lipid Research **5:** 402-408.

Olson JA, Hayaishi O (1965) The enzymatic cleavage of β-carotene into vitamin A by soluble enzymes of rat liver and intestine. Proceedings of the National Academy of Sciences of the United States of America **54:** 1364-1370.

Orzaez D, Mirabel S, Wieland WH, Granell A (2006) Agroinjection of tomato fruits. A tool for rapid functional analysis of transgenes directly in fruit. Plant Physiology **140:** 3-11.

Osteryoung KW, Vierling E (1995) Conserved cell and organelle division. Nature **376:** 473-474.

Paine JA, Shipton CA, Chaggar S, Howells RM, Kennedy MJ, Vernon G, Wright SY, Hinchliffe E, Adams JL, Silverstone AL, Drake R (2005) Improving the nutritional value of Golden Rice through increased pro-vitamin A content. Nature Biotechnology **23:** 482-487.

Palni LMS, Burch L, Horgan R (1988) The effect of auxin concentration on cytokinin stability and metabolism. Planta **174:** 231-234.

Park H, Kreunen SS, Cuttriss AJ, DellaPenna D, Pogson BJ (2002) Identification of the carotenoid isomerase provides insight into carotenoid biosynthesis,

prolamellar body formation, and photomorphogenesis. Plant Cell **14:** 321-332.

Payyavula RS, Navarre DA, Kuhl JC, Pantoja A, Pillai SS (2012) Differential effects of environment on potato phenylpropanoid and carotenoid expression. BMC Plant Biology **12:** 39.

Pecket RC, Small CJ (1980) Occurrence, location and development of anthocyanoplasts. Phytochemistry **19:** 2571-2576.

Pfundel EE, Renganathan M, Gilmore AM, Yamamoto HY, Dilley RA (1994) Intrathylakoid pH in isolated pea chloroplasts as probed by violaxanthin deepoxidation. Plant Physiology **106:** 1647-1658.

Pimentel D, Giampietro M (1994) Global population, food and the environment. Trends in Ecology & Evolution **9:** 239-239.

Pogson BJ, Albrecht V (2011) Genetic dissection of chloroplast biogenesis and development: An overview. Plant Physiology **155:** 1545-1551.

Pogson BJ, Niyogi KK, Bjorkman O, DellaPenna D (1998) On the respective roles of the various xanthophylls during seedling development and high light stress in Arabidopsis. *In* G. Garab Ed. *Photosynthesis: Mechanisms and Effects*, Kluwer Academic, Dordrecht, The Netherlands. Vols I-V**:** 3293-3296.

Pogson BJ, Rissler HM, Frank HA (2005) The role of carotenoids in photosystem II of higher plants. *In*: Photosystem II: The light-driven water/plastoquinone oxido-reductase in photosynthesis. Advances in photosynthesis and respiration series, Springer Wydrzynski T. and Satoh (eds), pp515-537.

Pogson BJ, Woo NS, Forster B, Small ID (2008) Plastid signalling to the nucleus and beyond. Trends in Plant Science **13:** 602-609.

Polivka T, Frank HA (2010) Molecular factors controlling photosynthetic light harvesting by carotenoids. Accounts of Chemical Research **43:** 1125-1134.

Pringle JR, Preston RA, Adams AEM, Stearns T, Drubin DG, Haarer BK, Jones EW (1989) Fluorescence microscopy methods for yeast. Methods in Cell Biology **31:** 357-435.

Prusinkiewicz P, Crawford S, Smith RS, Ljung K, Bennett T, Ongaro V, Leyser O (2009) Control of bud activation by an auxin transport switch. Proceedings

of the National Academy of Sciences of the United States of America **106:** 17431-17436.

Pyke KA (1999) Plastid division and development. Plant Cell **11:** 549-556.

Pyke KA, Page AM (1998) Plastid ontogeny during petal development in Arabidopsis. Plant Physiology **116:** 797-803.

Qin GJ, Gu HY, Ma LG, Peng YB, Deng XW, Chen ZL, Qu LJ (2007) Disruption of phytoene desaturase gene results in albino and dwarf phenotypes in Arabidopsis by impairing chlorophyll, carotenoid, and gibberellin biosynthesis. Cell Research **17:** 471-482.

Qin XQ, Coku A, Inoue K, Tian L (2011) Expression, subcellular localization, and cis-regulatory structure of duplicated phytoene synthase genes in melon (*Cucumis melo* L.). Planta **234:** 737-748.

Quinlan RF, Shumskaya M, Bradbury LM, Beltran J, Ma C, Kennelly EJ, Wurtzel ET (2012) Synergistic interactions between carotene ring hydroxylases drive lutein formation in plant carotenoid biosynthesis. Plant Physiology **160:** 204-214.

Race HL, Herrmann RG, Martin W (1999) Why have organelles retained genomes? Trends in Genetics **15:** 364–370.

Ralley L, Enfissi EMA, Misawa N, Schuch W, Bramley PM, Fraser PD (2004) Metabolic engineering of ketocarotenoid formation in higher plants. Plant Journal **39:** 477-486.

Rey P, Gillet B, Romer S, Eymery F, Massimino J, Peltier G, Kuntz M (2000) Over-expression of a pepper plastid lipid-associated protein in tobacco leads to changes in plastid ultrastructure and plant development upon stress. The Plant Journal **21:** 483-494.

Redmond TM, Gentleman S, Duncan T, Yu S, Wiggert B, Gantt E, Cunningham FX (2001) Identification, expression, and substrate specificity of a mammalian beta-carotene 15,15 '-dioxygenase. Journal of Biological Chemistry **276:** 6560-6565.

Rock CD, Heath TG, Zeevaart JAD (1992) 2-Trans-abscisic acid biosynthesis and metabolism of ABA-aldehyde and xanthoxin in wild type and the *aba* mutant of *Arabidopsis thaliana*. Journal of Experimental Botany **43:** 249-256.

Rock CD, Zeevaart JAD (1991) The *aba* mutant of *Arabidopsis thaliana* is impared in epoxy- carotenoid biosynthesis. Proceedings of the National Academy of Sciences of the United States of America **88:** 7496-7499.

Rodriguez-Concepcion M, Boronat A (2002) Elucidation of the methylerythritol phosphate pathway for isoprenoid biosynthesis in bacteria and plastids. A metabolic milestone achieved through genomics. Plant Physiology **130:** 1079-1089.

Romer S, Fraser PD, Kiano JW, Shipton CA, Misawa N, Schuch W, Bramley PM (2000) Elevation of the provitamin A content of transgenic tomato plants. Nature Biotechnology **18:** 666-669.

Romer S, Hugueney P, Bouvier F, Camara B, Kuntz M (1993) Expression of the genes encoding the early carotenoid biosynthetic enzymes in *Capsicum annuum*. Biochemical and Biophysical Research Communications **196:** 1414-1421.

Roumeliotis E, Kloosterman B, Oortwijn M, Kohlen W, Bouwmeester HJ, Visser RGF, Bachem CWB (2012) The effects of auxin and strigolactones on tuber initiation and stolon architecture in potato. Journal of Experimental Botany **63:** 4539-4547.

Ruban AV, Young AJ, Pascal AA, Horton P (1994) The effects of illumination on the xanthophyll composition of the photosystem-II light-harvesting complexes of spinach thylakoid membranes. Plant Physiology **104:** 227-234.

Rubio Moraga A, Rambla JL, Ahrazem O, Granell A, Gomez-Gomez L (2009) Metabolite and target transcript analyses during *Crocus sativus* stigma development. Phytochemistry **70:** 1009-1016.

Ruiz-Sola MA, Rodriguez-Concepcion M (2012) Carotenoid biosynthesis in Arabidopsis: a colorful pathway. The Arabidopsis book. American Society of Plant Biologists **10:** e0158-e0158.

Ruyter-Spira C, Kohlen W, Charnikhova T, van Zeijl A, van Bezouwen L, de Ruijter N, Cardoso C, Lopez-Raez JA, Matusova R, Bours R, Verstappen F, Bouwmeester H (2011) Physiological effects of the synthetic strigolactone analog GR24 on root system architecture in Arabidopsis: Another belowground role for strigolactones? Plant Physiology **155:** 721-734.

Salaman R (1985) The history and social influence of the potato, Cambridge University Press, Cambridge.

Sambrook J, Fritsch EF, Maniatis T (1989) Molecular cloning: a laboratory manual, 3rd edition. Cold Spring Harbor Laboratory Press, Cold Spring Harbor.

Sandmann G (1991) Light-dependent switch from formation of poly-*cis* carotenes to all-*trans* carotenoids in the *Scenedesmus* mutant C-6d. Archives of Microbiology **155:** 229-233.

Sandmann G, Romer S, Fraser PD (2006) Understanding carotenoid metabolism as a necessity for genetic engineering of crop plants. Metabolic Engineering **8:** 291-302

Santos CAF, Senalik D, Simon PW (2005) Path analysis suggests phytoene accumulation is the key step limiting the carotenoid pathway in white carrot roots. Genetics and Molecular Biology **28:** 287-293.

Schalch W (1992) Carotenoids in the retina– a review of their possible role in preventing or limiting damage caused by light and oxygen. Exs **62:** 280-298.

Schattat MH, **Griffiths S**, **Mathur N**, **Barton K**, **Wozny MR**, **Dunn N**, **Greenwood JS**, **Mathur J** (2012). Differential coloring reveals that plastids do not form networks for exchanging macromolecules. Plant Cell **24**: 1465-1477.

Schiedt M, Liaaen-Jensen S (1995) Isolation and analysis. *In*: Carotenoids, vol. 1-A: Isolation and Analysis (Britton G., Liaeen-Jensen S., and Pfander H., eds), Birkhauser, Basel, pp. 104–107.

Schledz M, Al-Babili S, Von Lintig J, Haubruck H, Rabbani S, Kleinig H, Beyer P (1996) Phytoene synthase from *Narcissus pseudonarcissus*: Functional expression, galactolipid requirement, topological distribution in chromoplasts and induction during flowering. Plant Journal **10:** 781-792.

Schwartz SH, Qin XQ, Zeevaart JAD (2001) Characterization of a novel carotenoid cleavage dioxygenase from plants. Journal of Biological Chemistry **276:** 25208-25211.

Schwartz SH, Tan BC, Gage DA, Zeevaart JAD, McCarty DR (1997) VP14 of maize catalyzes the carotenoid cleavage reaction of abscisic acid biosynthesis. Plant Physiology **114:** 798-798.

Scott TK, Case DB, Jacobs WP (1967) Auxin-gibberellin interaction in apical dominance. Plant Physiology **42:** 1329-1333.

Seefeldt HF, Tonning E, Thybo AK (2011) Exploratory sensory profiling of three culinary preparations of potatoes (*Solanum tuberosum* L.). Journal of the Science of Food and Agriculture **91:** 104-112.

Shaw D, Gray J (2011) Visualisation of stromules in transgenic wheat expressing a plastid-targeted yellow fluorescent protein. Planta **233:** 961-970.

Shewmaker CK, Sheehy JA, Daley M, Colburn S, Ke D (1999) Seed-specific overexpression of phytoene synthase: increase in carotenoids and other metabolic effects. Plant Journal **20:** 401-412.

Shimizu-Sato S, Tanaka M, Mori H (2009). Auxin–cytokinin interactions in the control of shoot branching. Plant Molecular Biology **69:** 429-435.

Shumskaya M, Bradbury LM, Monaco RR, Wurtzel ET (2012) Plastid localization of the key carotenoid enzyme phytoene synthase is altered by isozyme, allelic variation, and activity. Plant Cell **24:** 3725-3741.

Siddique MA, Grossmann J, Gruissem W, Baginsky S (2006) Proteome analysis of bell pepper (*Capsicum annuum* L.) chromoplasts. Plant and Cell Physiology **47:**661-673.

Simkin AJ, Gaffe J, Alcaraz JP, Carde JP, Bramley PM, Fraser PD, Kuntz M (2007) Fibrillin influence on plastid ultrastructure and pigment content in tomato fruit. Phytochemistry **68:** 1545-1556.

Simons JL, Napoli CA, Janssen BJ, Plummer KM, Snowden KC (2007) Analysis of the *DECREASED APICAL DOMINANCE* genes of petunia in the control of axillary branching. Plant Physiology **143:** 697-706.

Soll J, Schleiff E (2004) Protein import into chloroplasts. Nature Reviews Molecular Cell Biology **5:** 198-208.

Sorefan K, Booker J, Haurogne K, Goussot M, Bainbridge K, Foo E, Chatfield S, Ward S, Beveridge C, Rameau C, Leyser O (2003) *MAX4* and *RMS1* are orthologous dioxygenase-like genes that regulate shoot branching in Arabidopsis and pea. Genes & Development **17:** 1469-1474.

Spooner DM, Bamberg JB (1994) Potato genetic resources- sources of resistance and systematics. American Potato Journal **71:** 325-337.

Spooner DM, McLean K, Ramsay G, Waugh R, Bryan GJ (2005) A single domestication for potato based on multilocus amplified fragment length polymorphism genotyping. Proceedings of the National Academy of Sciences of the United States of America **102:** 14694-14699.

Steinbrenner J, Linden H (2001) Regulation of two carotenoid biosynthesis genes coding for phytoene synthase and carotenoid hydroxylase during stress-induced astaxanthin formation in the green alga *Haematococcus pluvialis*. Plant Physiology **125:** 810-817.

Steinmuller D, Tevini M (1985) Composition and function of plastoglobuli .1. Isolation and purification from chloroplasts and chromoplasts. Planta **163:** 201-207.

Stirnberg P, van de Sande K, Leyser HMO (2002) MAX1 and MAX2 control shoot lateral branching in *Arabidopsis*. Development **129:** 1131-1141.

Struik PC (2007) Above-ground and below-ground plant development. *In*: Vreugdenhil D, ed. Potato biology and biotechnology: advances and perspectives. Elsevier, 3–26.

Sugawara Y, Kamioka H, Honjo T, Tezuka K, Takano-Yamamoto T (2005) Three-dimensional reconstruction of chick calvarial osteocytes and their cell processes using confocal microscopy. Bone **36:** 877-883.

Suttle JC (2004) Physiological regulation of potato tuber dormancy. American Journal of Potato Research **81:** 253-262.

Takaichi S, Mimuro M (1998) Distribution and geometric isomerism of neoxanthin in oxygenic phototrophs: 9 '-cis, a sole molecular form. Plant and Cell Physiology **39:** 968-977

Tan BC, Schwartz SH, Zeevaart JAD, McCarty DR (1997) Genetic control of abscisic acid biosynthesis in maize. Proceedings of the National Academy of Sciences of the United States of America **94:** 12235-12240.

Tavazza R, Tavazza M, Ordas RJ, Ancora G, Benvenuto E (1989) Genetic transformation of potato (*Solanum-tuberosum*) - an efficient method to obtain transgenic plants. Plant Science **59:** 175-181.

Teper-Bamnolker P, Buskila Y, Lopesco Y, Ben-Dor S, Saad I, Holdengreber V, Belausov E, Zemach H, Ori N, Lers A, Eshel D (2012) Release of apical

dominance in potato tuber is accompanied by programmed cell death in the apical bud meristem. Plant Physiology **158:** 2053-2067.

Terao J, Minami Y, Bando N (2011) Singlet molecular oxygen-quenching activity of carotenoids: relevance to protection of the skin from photoaging. Journal of Clinical Biochemistry and Nutrition **48:** 57-62.

Thabet I, Guirimand G, Guihur A, Lanoue A, Courdavault V, Papon N, Bouzid S, Giglioli-Guivarc'h N, Simkin AJ, Clastre M (2012) Characterization and subcellular localization of geranylgeranyl diphosphate synthase from *Catharanthus roseus*. Molecular Biology Reports **39:** 3235-3243.

The Potato Genome Sequencing Consortium (2011) Genome sequence and analysis of the tuber crop potato. Nature **475**: 189–195

Tholl D, Lee S (2011) Elucidating the metabolism of plant terpene volatiles: Alternative tools for engineering plant defenses? Biological Activity of Phytochemicals **41:** 159-178.

Thorup TA, Tanyolac B, Livingstone KD, Popovsky S, Paran I, Jahn M (2000) Candidate gene analysis of organ pigmentation loci in the *Solanaceae*. Proceedings of the National Academy of Sciences of the United States of America **97:** 11192-11197.

Tinland B, Hohn B, Puchta H (1994) *Agrobacterium tumefaciens* transfers single-stranded transferred DNA (T-DNA) into the plant-cell nucleus. Proceedings of the National Academy of Sciences of the United States of America **91:** 8000-8004

Toledo-Ortiz G, Huq E, Rodriguez-Concepcion M (2010) Direct regulation of phytoene synthase gene expression and carotenoid biosynthesis by phytochrome-interacting factors. Proceedings of the National Academy of Sciences of the United States of America **107:** 11626-11631.

Trick HN, Finer JJ (1997) SAAT: sonication-assisted *Agrobacterium*-mediated transformation. Transgenic Research **6:** 329-336.

Tsuchiya Y, McCourt P (2010) Strigolactones as small molecule communicators. Molecular Biosystems **8:** 464-469.

Turnbull CGN, Raymond MAA, Dodd IC, Morris SE (1997) Rapid increases in cytokinin concentration in lateral buds of chickpea (*Cicer arietinum* L) during release of apical dominance. Planta **202:** 271-276.

Umehara M, Hanada A, Yoshida S, Akiyama K, Arite T, Takeda-Kamiya N, Magome H, Kamiya Y, Shirasu K, Yoneyama K, Kyozuka J, Yamaguchi S (2008) Inhibition of shoot branching by new terpenoid plant hormones. Nature **455:** 195-U129.

Vallabhaneni R, Bradbury LMT, Wurtzel ET (2010) The carotenoid dioxygenase gene family in maize, sorghum, and rice. Archives of Biochemistry and Biophysics **504:** 104-111

Veen M, Lang C (2004) Production of lipid compounds in the yeast *Saccharomyces cerevisiae*. Applied Microbiology and Biotechnology **63:** 635-646.

Verma SK, Bordia A (1998) Antioxidant property of Saffron in man. Indian Journal of Medical Sciences **52:** 205-207.

Verweij W, Di Sansebastiano GP, Quattrocchio F, Dalessandro G (2008) *Agrobacterium*-mediated transient expression of vacuolar GFPs in Petunia leaves and petals. Plant Biosystems **142:** 343-347.

Vidi PA, Kanwischer M, Baginsky S, Austin JR, Csucs G, Dormann P, Kessler F, Brehelin C (2006) Tocopherol cyclase (VTE1) localization and vitamin E accumulation in chloroplast plastoglobule lipoprotein particles. Journal of Biological Chemistry **281:** 11225-11234.

Vishnevetsky M, Ovadis M, Vainstein A (1999) Carotenoid sequestration in plants: the role of carotenoid-associated proteins. Trends in Plant Science **4:** 232-235.

Vogel JT, Tan B-C, McCarty DR, Klee HJ (2008) The carotenoid cleavage dioxygenase 1 enzyme has broad substrate specificity, cleaving multiple carotenoids at two different bond positions. Journal of Biological Chemistry **283:** 11364-11373.

Vogel JT, Walter MH, Giavalisco P, Lytovchenko A, Kohlen W, Charnikhova T, Simkin AJ, Goulet C, Strack D, Bouwmeester HJ, Fernie AR, Klee HJ (2010) SlCCD7 controls strigolactone biosynthesis, shoot branching and mycorrhiza-induced apocarotenoid formation in tomato. Plant Journal **61:** 300-311.

Voinnet O, Pinto YM, Baulcombe DC (1999) Suppression of gene silencing: a general strategy used by diverse DNA and RNA viruses of plants.

Proceedings of the National Acadademy of Sciences of the United States of America **96:** 14147-14152.

von Lintig J, Welsch R, Bonk M, Giuliano G, Batschauer A, Kleinig H (1997) Light-dependent regulation of carotenoid biosynthesis occurs at the level of phytoene synthase expression and is mediated by phytochrome in *Sinapis alba* and *Arabidopsis thaliana* seedlings. Plant Journal **12:** 625-634.

Voutilainen S, Nurmi T, Mursu J, Rissanen TH (2006) Carotenoids and cardiovascular health. American Journal of Clinical Nutrition **83:** 1265-1271.

Wadsworth GR, McKenzie JC (1963) The potato, with special references to its use in the United Kingdom. Nutrition Abstracts and Reviews **33:** 327-344.

Walter MH, Floss DS, Strack D (2010) Apocarotenoids: hormones, mycorrhizal metabolites and aroma volatiles. Planta (Berlin) **232:** 1-17.

Walter MH, Strack D (2011) Carotenoids and their cleavage products: Biosynthesis and functions. Natural Product Reports **28:** 663-692.

Waters MT, Fray RG, Pyke KA (2004) Stromule formation is dependent upon plastid size, plastid differentiation status and the density of plastids within the cell. Plant Journal **39:** 655-667.

Wei JL, Xu M, Zhang DB, Mi HL (2010) The role of carotenoid isomerase in maintenance of photosynthetic oxygen evolution in rice plant. Acta Biochimica et Biophysica Sinica **42:** 457-463.

Weisman LS, Emr SD, Wickner WT (1990) Mutants of *Saccharomyces cerevisiae* that block intervacuole vesicular traffic and vacuole division and segregation. Proceedings of the National Academy of Sciences of the United States of America **87:** 1076-1080.

Welsch R, Beyer P, Hugueney P, Kleinig H, von Lintig J (2000) Regulation and activation of phytoene synthase, a key enzyme in carotenoid biosynthesis, during photomorphogenesis. Planta **211:** 846-854.

Welsch R, Maass D, Voegel T, DellaPenna D, Beyer P (2007) Transcription factor RAP2.2 and its interacting partner SINAT2: Stable elements in the carotenogenesis of *Arabidopsis* leaves. Plant Physiology **145:** 1073-1085.

Welsch R, Wuest F, Baer C, Al-Babili S, Beyer P (2008) A third phytoene synthase is devoted to abiotic stress-induced abscisic acid formation in rice

and defines functional diversification of phytoene synthase genes. Plant Physiology **147:** 367-380.

Willstatter R (1933) A chemist's retrospects and perspectives. Science (New York, N.Y.) **78:** 271-274.

Woitsch S, Romer S (2003) Expression of xanthophyll biosynthetic genes during light-dependent chloroplast differentiation. Plant Physiology **132:** 1508-1517.

Wroblewski T, Tomczak A, Michelmore R (2005) Optimization of *Agrobacterium*-mediated transient assays of gene expression in lettuce, tomato and Arabidopsis. Plant Biotechnology Journal **3:** 259–273.

Xie X, Yoneyama K, Yoneyama K (2010) The Strigolactone Story. Annual Review of Phytopathology **48:** 93-117.

Xu WX, Moriya K, Yamada K, Nishimura M, Shioiri H, Kojima M, Nozue M (2000) Detection and characterization of a 36-kDa peptide in C-terminal region of a 24-kDa vacuolar protein (VP24) precursor in anthocyanin-producing sweet potato cells in suspension culture. Plant Science **160:** 121-128.

Xu WX, Shioiri H, Kojima M, Nozue M (2001) Primary structure and expression of a 24-kD vacuolar protein (VP24) precursor in anthocyanin-producing cells of sweet potato in suspension culture. Plant Physiology **125:** 447-455.

Ye XD, Al-Babili S, Kloti A, Zhang J, Lucca P, Beyer P, Potrykus I (2000) Engineering the provitamin A (beta-carotene) biosynthetic pathway into (carotenoid-free) rice endosperm. Science **287:** 303-305.

Yoneyama K, Yoneyama K, Takeuchi Y, Sekimoto H (2007) Phosphorus deficiency in red clover promotes exudation of orobanchol, the signal for mycorrhizal symbionts and germination stimulant for root parasites. Planta **225:** 1031-1038.

Ytterberg AJ, Peltier JB, van Wijk KJ (2006) Protein profiling of plastoglobules in chloroplasts and chromoplasts. A surprising site for differential accumulation of metabolic enzymes. Plant Physiology **140:** 984-997.

Yu BY, Lydiate DJ, Young LW, Schafer UA, Hannoufa A (2008) Enhancing the carotenoid content of *Brassica napus* seeds by downregulating lycopene epsilon cyclase. Transgenic Research **17:** 573-585.

Yu QJ, Ghisla S, Hirschberg J, Mann V, Beyer P (2011) Plant carotene *cis-trans* isomerase CRTISO a new member of the far (red)- dependent flavoproteins catalysing non-redox reactions. Journal of Biological Chemistry **286:** 8666-8676.

Zbierzak AM, Kanwischer M, Wille C, Vidi P-A, Giavalisco P, Lohmann A, Briesen I, Porfirova S, Brehelin C, Kessler F, Doermann P (2010) Intersection of the tocopherol and plastoquinol metabolic pathways at the plastoglobule. Biochemical Journal **425:** 389-399.

Zeevaart JAD, Creelman RA (1988) Metabolism and physiology of abscisic acid. Annual Review of Plant Physiology and Plant Molecular Biology **39:** 439-473.

Zhang L, Ma G, Kato M, Yamawaki K, Takagi T, Kiriiwa Y, Ikoma Y, Matsumoto H, Yoshioka T, Nesumi H (2012) Regulation of carotenoid accumulation and the expression of carotenoid metabolic genes in citrus juice sacs *in vitro*. Journal of Experimental Botany **63:** 871–886.

Zhu C, Naqvi S, Breitenbach J, Sandmann G, Christou P, Capell T (2008) Combinatorial genetic transformation generates a library of metabolic phenotypes for the carotenoid pathway in maize. Proceedings of the National Academy of Sciences of the United States of America **105:** 18232-18237.

Zitnak A, Johnston GR (1970) Glycoalkaloids and bitterness in potatoes. American Potato Journal **47:** 256–260.

Zorov DB, Kobrinsky E, Juhaszova M, Sollott SJ (2004) Examining intracellular organelle function using fluorescent probes- From animalcules to quantum dots. Circulation Research **95:** 239-252.

Zou JH, Chen ZX, Zhang SY, Zhang WP, Jiang GH, Zhao XF, Zhai WX, Pan XB, Zhu LH (2005) Characterizations and fine mapping of a mutant gene for high tillering and dwarf in rice (*Oryza sativa* L.). Planta **222:** 604-612.

Zupan JR, Zambryski P (1995) Transfer of T-DNA from *Agrobacterium* to the plant cell. Plant Physiology **107:** 1041-1047.

http://www.potato2008.org/en/potato/utilization.html, accessed April 2012.

http://faostat.fao.org/site/339/default.aspx, accessed March 2012.

http://www.potato2008.org/en/world/index.html, accessed in March 2012.

http://www.potato2008.org/en/potato/water.html, accessed September, 2010.

http://cipotato.org/potato/how-potato-grows, accessed March 2012.

http://www.potato.org.uk/market-information/consumers, accessed March 2012.

http://cipotato.org/potato/nutrition, accessed April 2012.

http://www.potato2008.org/en/potato/factsheets.html, accessed April 2012.

http://en.wikipedia.org/wiki/File:Plastids_types_en.svg, accessed March 2012.

http://www.promega.com/products/pcr/pcr-cloning/pgem_t-easy-vector-systems/accessed April 2012.

http://www.invitrogen.com/site/us/en/home/Products-and-Services/Applications/Cloning/PCR-cloning/ta-cloning.html?ICID=cvc-pcrcloning-c2t1 accessed April 2012.

http://www.mobitec.de/de/products/bio/06_dna_prot_tools/aquagenomic.html accessed April 2012.

http://www.nanodrop.com/Library/nd-1000-v3.7-users-manual-8.5x11.pdf accessed April 2012.

http://www.genex.cl/stock/600670.pdf accessed April 2012.

http://www.basic.northwestern.edu/biotools/oligocalc.html accessed April 2012.

http://www.hutton.ac.uk/research/facilities/genome-technology/sequencing

http://www.roche-applied-science.com/sis/rtpcr/upl/ezhome.htmlaccessed April 2012.

http://nutriculture.com/index.htm accessed April 2012.

www.carotenature.com accessed April 2012.

https://www.roche-applied-science.com/sis/rtpcr/upl/ accessed April 2012.

www.un.org/en/mdg/ summit 2010 accessed August 2012

http://www.jalview.org/

Appendix 1.

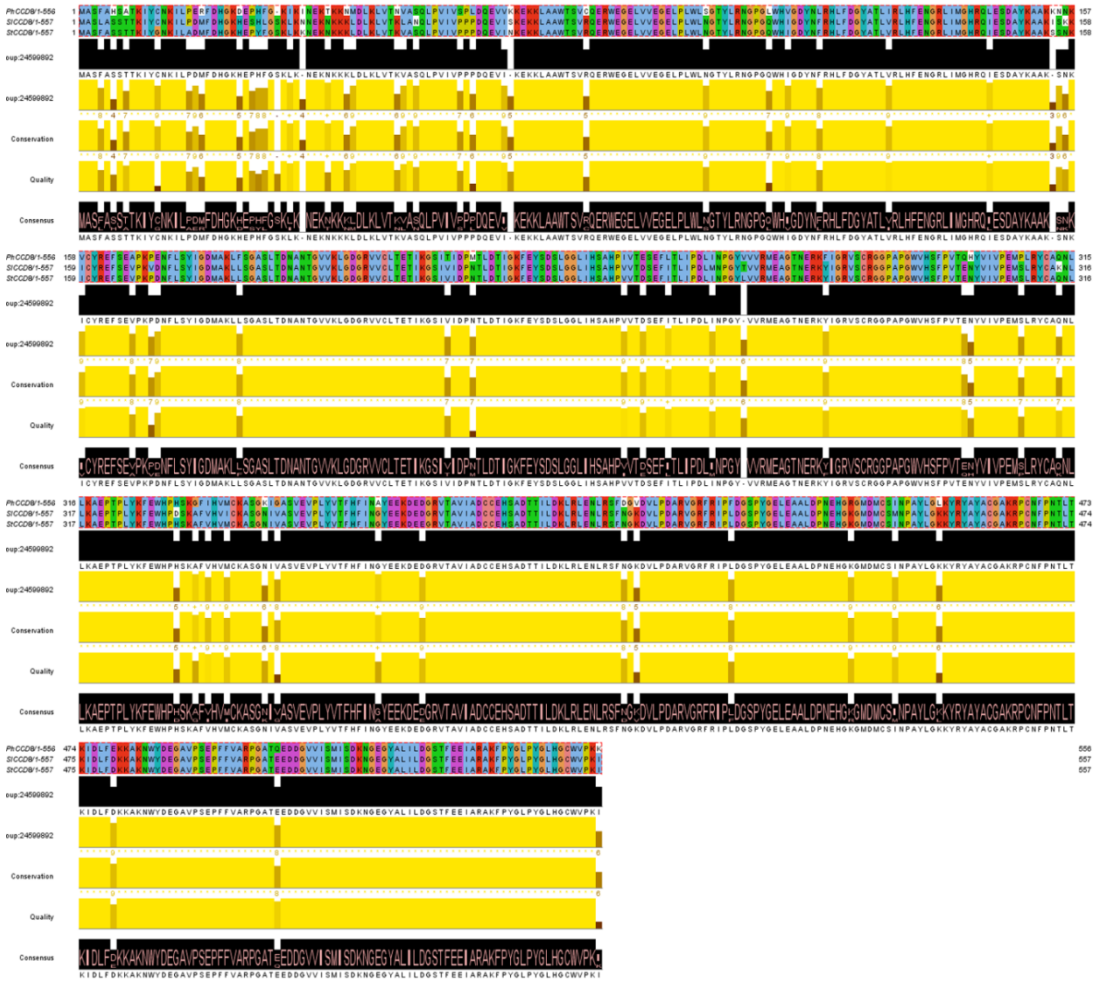

Alignment of the known and putative CCD8 protein sequences; Ph, *Petunia hybrida*; Sl, *Solanum lycopersicum*; St, *Solanum tuberosum*, using the Jalview software (http://www.jalview.org/).

Appendix 2.

> *StCCD8* RNAi hairpin sequence

TTGCAGATTGCTGTGAGCATAGCGCCGACACCACCATCCTTGATAAGCTCCGC
CTTGAGAATCTTCGCTCCTTCAACGGCAAGGATGTCTTGCCCGATGCAAGGGT
TGGAAGATTCAGAATACCATTAGATGGAAGTCCATATGGAGAATTAGAAGCAG
CATTGGACCCAAATGAACATGGAAAAGGAATGGATATGTGCAGTATTAATCCT
GCTTATTTAGGCAAGAAATACAGATATGCTTATGCTTGTGGTGCTAAGAGGCC
TTGTAATTTCCCCAACACCCTCACCAAGATTGATTTGTTTGATAAAAAGGCAA
AGAATTGGTATGATGAAGGTGCTGTGCCTTCTGAACCATTCTTTGTGGCTCGA
CCCGGTGCAACCGAGGAAGATGATGGTGTTGTAATCTCAATGATCAGTGACAA
GAATGGAGAAGGATATGCTCTAATACTGGATGGATCAACATTTGAAGAAATTG
CAAGAGCAAAATTTCCTTATGGTCTCCCCTATGGGCTACATGGTTGTTGGGTT

The 530 bp sequence of the potato *CCD8* gene introduced into the pHellsgate8 vector, to generate the *CCD8*-RNAi construct.

Appendix 3.

CrtRb2

ATGGCGGCCGGAATTTCAGCCTCCGCTGGTTCCCGAACTATTTGCCTCCGTCACAACCCG
TTTCGCGGTCCAAAATCCGCCTCAACCGCCCCGCCAGTTCTGTTCTTCTCTCCGTTAACTC
GCAATTTTGGCGCAATTTTGCTGTCTCGAAGAAAGCCGAGGTTGGCGGTTTGCTTTGTGC
TGAAGAATGAGAAATTGAATAGTACTATCCAAAGTGAGTGTGAAGTAATACAGGATCAG
ATACAAGTAGAGATTAATGAGGAGAAGAGTTTAGCTGCCTGTTGGCTGGCGGAAAAATT
GGCGAGGAAGAAATCGGAGAGGTTTACTTATCTTGTGGCGGCTGTCATGTCTAGTTTAGG
GATTACTTCTATGGCGATTTTGTCGGTTTATTACAGATTTTCATGGCAAATGGAGGGTGG
AGAAGTGCCTTTTTCTGAAATGTTAGCTACATTCACTCTCTCGTTTGGCGCTGCCGTAGGA
ATGGAGTACTGGGCGAGATGGGCTCATAGAGCACTATGGCATGCTTCTTTATGGCACATG
CACGAGTCACACCATAGACCAAGAGAAGGACCTTTTGAGATGAACGACGTTTTCGCCAT
AACGAATGCTGTTCCAGCTATAGCTCTTCTTTCATACGGTTTCTTCCATAAAGGCCTCGTC
CCTGGCCTCTGTTTCGGCGCTGGATTGGGGATCACAGTATTTGGTATGGCTTACATGTTC
GTTCACGATGGACTGGTTCATAAGAGATTCCCTGTAGGGCCTATTGCCAACGTGCCTTAC
TTTCGGAGGGTAGCTGCTGCACATCAGCTTCATCACTCGGACAAATTTGGTGTCCCATAT
GGCTTGTTCCTAGGACCTAAGGAATTGGAAGAAGTAGGAGGGCTTGAAGAGTTGGAAAA
GGAAGTCAACCGAAGGATTAAAATTTCTAAGGGATTATTA**TGA**

PSY2

ATGTCTGTTGCTTTGTTGTGGGTTGTTTCTCCGAATTCTGAGGTCTTAAATGGGACAGGAT
TCTTGGATTCAGTCCGAGAAGGGAACCGGGGTTTGGAATCATCCAGGTTCCCATCTCCGA
ATAGGAATTCGATGTGGAAAGGGAGATTCAAGAAAGGTGGGAGACAGGAGTGGAATTT
TGGGTTTTTAAATGCAGATTTGAGATATTCGTGTTTAGGAAGATCAAGAACTGAGAATGG
AAGGAGTTTTTCTGTACAGTCCAGTTTGGTGGCTAGTCCAGCTGGAGAAATGGCTGTGTC
ATCAGAGAAAAAGGTGTATGAGGTGGTATTGAAGCAGGCAGCTTTAGTGAAGAGGCATC
TGATATCTACTGAGGACATAGAAGTGAAGCCGGATATTGTTGTTCCGGGTAATTTGGTTG
TTGAGTGAAGCATATGATCGTTGTGGCGAAGTATGTGCAGAGTATGCTAAGACATTTTAC
TTAGGAACCATGCTAATGACTCCAGACAGAAGAAGAGCTATCTGGGCAATATATGTGTG
GTGCAGGAGAACTGATGAGCTTGTTGATGGCCCTAATGCATCACACATAACTCCACAAG
CTTTAGATAGGTGGGAGGCCAGGCTGGAAAGATATTTTGCAAGCGGGCGGCCATTTGAT
ATGCTTGATGCAGCTTTATCCGATACTGTTTCCAAATTTCCTGTTGATATTCAGCCATTCA
GAGATATGGTTGAAGGAATGCGTATGGACTTGTGGAAATCCAGATACAACAACTTTGAT
GAACTATATCTATATTGTTACTATGTCGCTGGTACAGTAGGATTGATGAGTGTTCCAATT
ATGGGCATTGCACCTGAATCAAAGGCAACGACAGAGAGTGTATATAACGCAGCTTTGGC
TTTAGGGATCGCAAATCAACTAACCAATATACTCAGAGATGTAGGAGAAGATGCAAGAA
GAGGAAGAGTATACTTACCTCAAGATGAATTAGCACAGGCAGGGCTCTCCGATGAAGAC
ATTTTTGCTGGAAGAGTGACTGATAAGTGGAGGATCTTTATGAAGAAGCAAATTCAGAG
GGCAAGGAAATTCTTTGATGAGGCAGAAAAAGGTGTCACAGAACTGAGCTCTGCTAGTA
GATGGCCGGTGTTGGCGTCGTTGCTGTTATATCGCAAGATACTGGACGAGATTGAAGCG
AACGACTACAACAACTTCACAAGGAGGGCTTATGTGAGCAAGCCAAAGAAGCTTCTGAC
GTTGCCCATTGCTTATGCAAGATCTCTAGTGCCCCCTAAGTCAACTTCTTCCCCACTAGCA
AAGACA**TGA**

The complete amino acid coding sequences of potato CrtRb2 (942 bp) and PSY2 (1318 bp), used in Section 4.2.1. The modified nucleotides encoding for the stop codons are shown in bold.

Appendix 4.

StCrtRb2

M A A G I S A S A G S R T I C L R H N P F R G P K S A S T A P P V L F F S P L T R N F G A I L L S R R K P R L A V C F V L K N E K L N S T I Q S E C E V I Q D Q I Q V E I N E E K S L A A C W L A E K L A R K K S E R F T Y L V A A V M S S L G I T S M A I L S V Y Y R F S W Q M E G G E V P F S E M L A T F T L S F G A A V G M E Y W A R W A H R A L W H A S L W H Met H E S H H R P R E G P F E M N D V F A I T N A V P A I A L L S Y G F F H K G L V P G L C F G A G L G I T V F G M A Y M F V H D G L V H K R F P V G P I A N V P Y F R R V A A A H Q L H H S D K F D G V P Y G L F L G P K E L E E V G G L E E L E K E V N R R I K I S K G L L

StPSY2

M S V A L L W V V S P N S E V L N G T G F L D S V R E G N R G L E S S R F P S P N R N S M W K G R F K K G G R Q E W N F G F L N A D L R Y S C L G R S R T E N G R S F S V Q S S L V A S P A G E M A V S S E K K V Y E V V L K Q A A L V K R H L I S T E D I E V K P D I V V P G N L G L L S E A Y D R C G E V C A E Y A K T F Y L G T M L M T P D R R R A I W A I Y V W C R R T D E L V D G P N A S H I T P Q A L D R W E A R L E R Y F A S G R P F D M L D A A L S D T V S K F P V D I Q P F R D M V E G M R M D L W K S R Y N N F D E L Y L Y C Y Y V A G T V G L M S V P I M G I A P E S K A T T E S V Y N A A L A L G I A N Q L T N I L R D V G E D A R R G R V Y L P Q D E L A Q A G L S D E D I F A G R V T D K W R I F M K K Q I Q R A R K F F D E A E K G V T E L S S A S R W P V L A S L L L Y R K I L D E I E A N D Y N N F T R R A Y V S K P K K L L T L P I A Y A R S L V P P K S T S S P L A K T

The ChloroP-predicted lengths of the transit peptides of *CrtRb2* and *PSY2* 59 and 48 amino acids in length, shown as bold amino acid residues.